
# WICT 2015

## Proceedings of the Workshop on Innovation on Information and Communication Technologies 2015

Institute ITACA
Information and Communication Technologies

Editors:
Dr. Carlos Fernandez-Llatas
Dra. Maria Guillen

# Committees

## Organizing Committee

- **Chair**: Maria Guillem, Universitat Politècnica de València, Spain
- Alberto Bonastre, Universitat Politècnica de València, Spain
- Jose Manuel Catala, Universitat Politècnica de València, Spain
- Montserrat Robles, Universitat Politècnica de València, Spain
- Carlos Fernández-Llatas, Universitat Politècnica de València, Spain
- Jose Mariano Dahoui, Universitat Politècnica de València, Spain
- Isidora Navarro, Universitat Politècnica de València, Spain
- Manuel Traver Salcedo, Universitat Politècnica de València, Spain

## Scientific Committee

- **Chair**: Carlos Fernandez-Llatas, Universitat Politècnica de València, Spain
- Cenk Demiroglu, Ozyegin University, Turkey
- Johan Gustav Bellika, National Center of Telemedicine, Norway
- Yigzaw Kassaye Yitbarek, University of Tromso, Norway
- Raymundo Barrales, Universidad Autónoma Metropolitana de México
- D. Frank Yong. Li, University of Agder, Norway
- Antonio Martinez, Tecnologías para la Salud y el Bienestar S.A., Spain
- Jose Carlos Campelo, Universitat Politècnica de València, Spain
- Juan Vicente Capella, Universitat Politècnica de València, Spain
- Antonio Mocholí, Universitat Politècnica de València, Spain
- Sara Blanc, Universitat Politècnica de València, Spain
- Carlos Baraza, Universitat Politècnica de València, Spain
- Joaquin Gracia, Universitat Politècnica de València, Spain
- David De Andres, Universitat Politècnica de València, Spain
- Ricardo Mercado, Universitat Politècnica de València, Spain
- Miguel Rodrigo Bort, Universitat Politècnica de València, Spain
- Alejandro Liberos, Universitat Politècnica de València, Spain
- Jorge Pedrón, Universitat Politècnica de València, Spain
- Lenin Lemus, Universitat Politècnica de València, Spain
- Vicente Traver, Universitat Politècnica de València, Spain
- Pilar Sala, Universitat Politècnica de València, Spain
- Alvaro Martinez, Universitat Politècnica de València, Spain
- Jose Luis Bayo, Universitat Politècnica de València, Spain
- Juan Miguel García-Gomez, Universitat Politècnica de València, Spain
- Miguel Angel Rodriguez-Hernandez, Universitat Politècnica de València, Spain
- Elena Bernal-Mor, Universitat Politècnica de València, Spain
- Diego Felipe Pacheco-Páramo, Universitat Politècnica de València, Spain
- Julian Camilo Romero-Chavarro, Universitat Politècnica de València, Spain
- Diego Boscá Tomás, Universitat Politècnica de València, Spain
- Luis Tello-Oquendo, Universitat Politècnica de València, Spain
- Israel Leyva-Mayorga, Universitat Politècnica de València, Spain
- Julian Romero, Universitat Politècnica de València, Spain
- Gema Ibañez, Universitat Politècnica de València, Spain
- Pedro Yuste, Universitat Politècnica de València, Spain

*Table of Contents*

# Hardware-in-the-loop Simulation for Wireless Acoustic Modems Design

S. Blanc[1], S. Masud[2]

[1] Institute for the Applications of Advanced Information and Communication Technologies (ITACA), Universitat Politècnica de València, Spain
sablacla@disca.upv.es
http://ucert.upv.es/
[2] Electronics and Embedded Systems Cluster, Lahore University of Management Sciences, Pakistan
smasud@lums.edu.pk

**Abstract.** Underwater communication systems design can be clearly improved by Hardware-In-The-Loop (HWIL) simulation. While tests in the sea are complex and expensive, this paper presents a low cost method to bring the channel propagation water effect in the lab testing. The implementation has been carried out in a System-On-Chip platform which flexibility allows closing the simulation loop in an all-in-one architecture.

## 1 Introduction

Acoustic communication in underwater sensor networks design is challenging due to effects of the underwater channel on the transmitted signal such as multipath, Doppler shifts, absorption, among others [1]. The underwater channel variability is high while communication is expected to be reliable enough to deal with worst-case channel conditions. However, testing in real scenarios is complicated. Currently, models that reproduce the effects of the underwater channel are preferred during early stages of the design. Only in an advance prototyping stage, the design is eventually tested in real conditions. Alternatively, water tanks or small marine crafts are cheap and accessible to verify prototyping against multipath and Doppler effects but unfortunately these resources cannot afford the whole underwater channel complexity. What it should be desirable is the testing of the system under design into the ocean at an early stage but under the controlled environment of the laboratory. To bring the ocean into the laboratory is not possible, but it is feasible to bring either a numerical model or a passive acoustics recording reproduction in the hardware simulation loop. In other words: to carry out a Hardware-in-the-loop (HWIL) simulation.

HWIL is a technique for development of complex real-time embedded control systems that enhances the quality and reliability of the prototype testing. The simulation provides an effective platform by adding the complexity of the plant under control to the test. This idea has been successfully translated into complex embedded systems [2], air simulation systems [3] or radio frequency simulation systems [4]. The same way, the underwater channel effects on the acoustic signal can be added to the hardware simulation.

Among literature, much research has been done in underwater acoustic propagation models [5], [6], [7], [8], [9]. In wireless sensor network design, propagation models provide information about the received signal attending to different sound-speed depth profiles or fields and absorbing boundaries and that should be worthily useful to



C.Fernandez-Llatas and M.Guillen (Ed.):
Workshop on Innovation on
Information and Communication Technologies
(ITACA-WIICT 2015)

ISBN 978-84-608-4139-5

hardware simulation testing. Moreover, propagation models can be widened including additional signal processing features expected on the modem but not available in an early stage. Thus, the integration of the model-processed signals in the loop can lead to a low-cost and rapid prototyping.

The purpose of this paper is to describe the integration of a propagation model in the hardware loop and implementation details carried out on a system-on-chip to perform as waveform generator.

Mayor contributions of this paper include the hardware architecture necessary to provide signals that contain the channel propagation effects to the HWIL simulation. The rest of the paper is organized as follows. Section 2 describes the generation of reference signals to the HWIL process. Section 3 presents a waveform hardware architecture overview and section 4 describes the whole hardware simulation loop. Section 5 concludes the paper.

## 2 Reference Signals

Simple underwater propagation models are based on Thorp theory [10] while currently many researches accept the ray-tracing technique, which is the best one to represent the propagation of acoustic signals for frequencies from 50 Hz to 1 MHz. In 1987, Porter and Bucket presented the BELLHOP algorithm, an implementation of the ray-tracing technique that has evolved to its most recent version in 2010 [5]. The advantage of being a highly accepted algorithm [11] is its translation into numerical models such as Octave or MATLAB and discrete models such as NS-3 and OPNET.

Fig. 1 illustrates the block diagram that integrates a modem signal processing steps and the channel model. The numerical model has been implemented in MATLAB following the specifications of the acoustic ITACA modem described in [12]. This numerical model integrates a dynamic underwater channel response. W(t) output is defined in expression (1) and contains both the transmitted sequence S(t) and the propagation effect ε(t) where t is the sample period.

$$W(t) = S(t) + \varepsilon(t) \tag{1}$$

A whole simulation sequence starts by the bit chain codification, pass through W(t) file and follows the reception steps to finish comparing the received payload with the expected payload. On the other hand, a half simulation starts with the real recorded waveform R(t) till the payload comparison. Both branches lead to intermediate files, as for example W'(t) with data processed after signal amplification and filtering.

Fig. 2 shows a short extract of the output file that contains W(t) results. First column set the relative sampled time and the second column contains the signal voltage. Thus, given both axis: time and voltage W(t) is plotted.

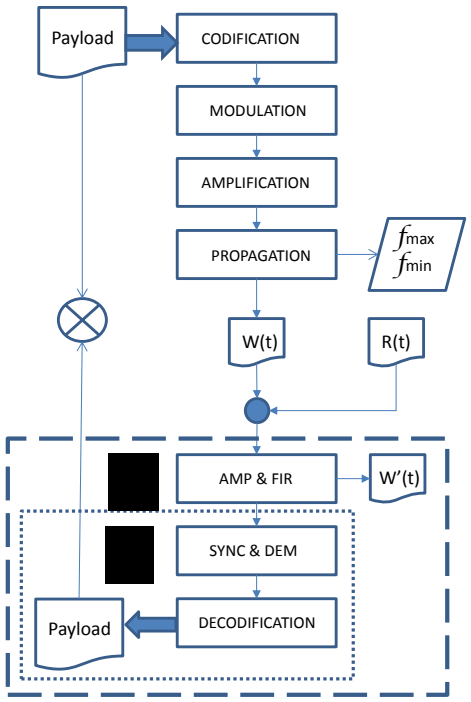


**Fig. 1.** Block diagram implemented to obtain the waveform

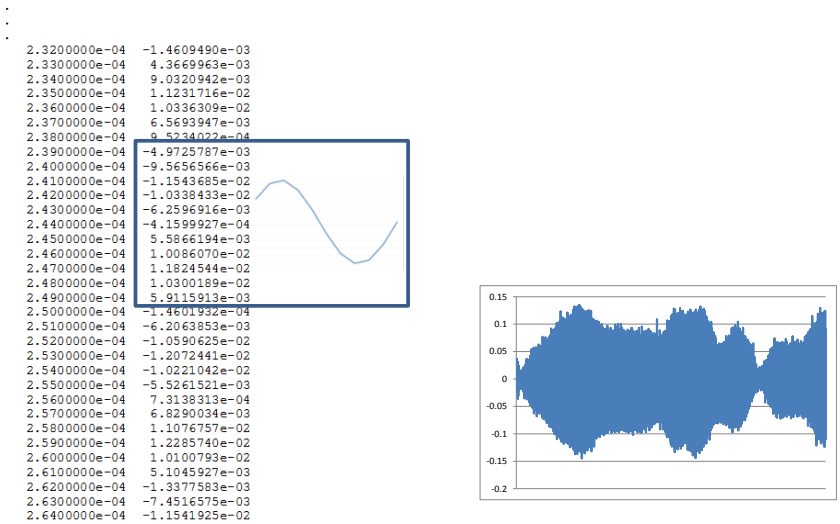


**Fig. 2.** W(t) file fragment example: relative time and signal sampled voltage (left); Signal recording fragment in a small craft marine (P.D. Pobla de Farnals) (Rx-Tx 1m depth; 10m distance; 85kHz carrier frequency) (right)

Fig. 2 shows a plotted example of R(t). Real signals captures by passive acoustic devices are of actual interest to guarantee that system results are comparable with the

real expected behavior at sea campaigns. Moreover, Fig. 2 shows a constant sample period. Thus data can be simplified into the sample frequency and the array of voltage values observed at each 1µs. Sample frequency should be adapted to the test requirements because there is not a unique neither best suitable value.

W(t), R(t) or W'(t) contain similar profiles useful to the HWIL simulation. Thus, A or B squares in Fig. 1 are removed and substituted by hardware as shown in Fig. 4 where the voltage values array is processed and downloaded into the waveform generation hardware. W(t), R(t) or W'(t) files that already contain the channel propagation effects on the transferred signal need to be turned into a hardware model useful for HWIL simulations. In Fig. 3, the waveform hardware architecture integrates the waveform hardware model downloaded and upgraded by the HW download process hosted in computer.

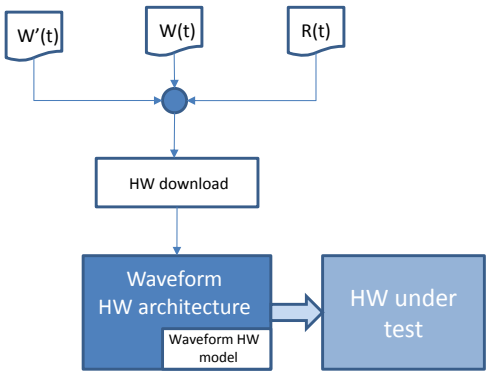


**Fig. 3.** W(t), R(t) and W'(t): Waveform HW architecture inputs

## 3 Waveform Hardware Architecture

The waveform hardware architecture is supported by a programmable device and it is divided into three main blocks: a waveform processor, a memory and an analog computing engine. Blocks are connected by the bus interface represented in Fig. 4. Thus, the waveform processor is the bus master and at the same time it is a command interpreter, a data bridge and a sample frequency regulator.

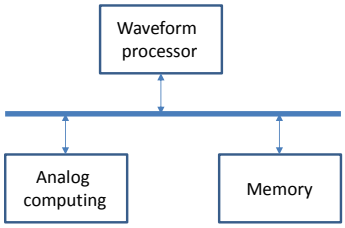


**Fig. 4.** Waveform hardware architecture blocks

The analog computing consists of a one-bit sigma-delta digital-to-analog converter and analog front-end block while the memory block is the voltage storage data.

This structure has been implemented in a cSoC device that contains a hard embedded microcontroller subsystem based on Cortex™- M3, a programmable analog circuit and a flash FPGA [13]. Three steps are needed for waveform generation (Fig. 5). First-

ly, in green, new information request. Secondly, in red, data download; and thirdly, in orange, send the stored sample values to the Sample Sequencing Engine (SSE) byte register, writing the DAC 24 bits data to the phase accumulator and updates the 1-bit DAC output accordingly in a loop. The analog signal is defined between 0 and 2.56V.

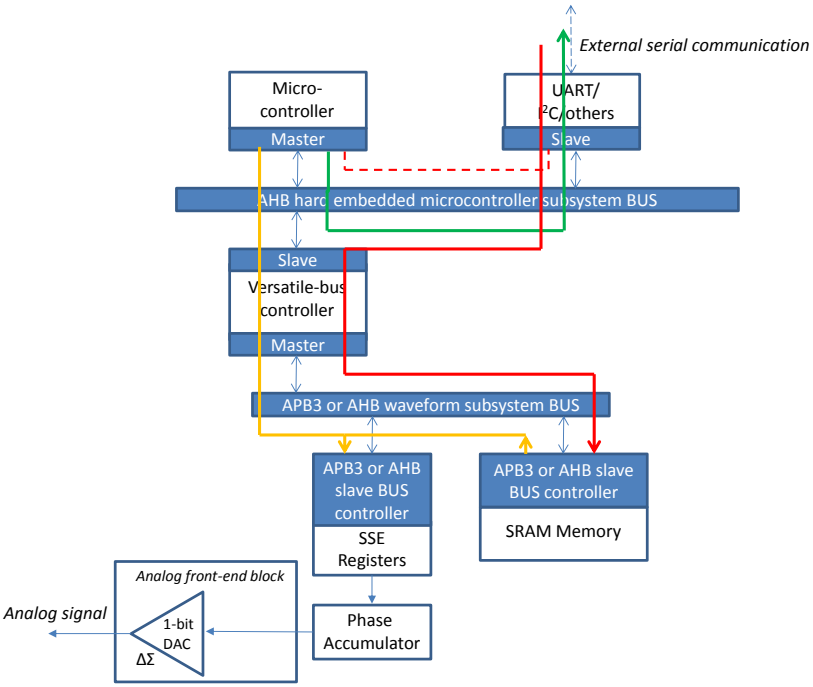


**Fig. 5.** Waveform generation steps

## 4 All-In-One Architecture

In order to enhance fast developments of suitable communication protocol as well as improvements in signal processing, the design of acoustic modems with processing capabilities can be carried out within platforms that admit both real communication tests and simulated loads. In this way, open architectures are a flexible solution for the research community to make adding, upgrading and swapping components easy. Moreover, the recent growth of system on chip (SoC) with hard processor will undoubtedly help to this fast development.

Thus, in a first stage, blocks in Fig. 3 that correspond to the waveform hardware architecture and the hardware under test have been developed in a unique cSOC device. The hardware under test module input is connected with the analog signal in Fig. 5 allowing a waveform simulation process. The connection is shown in Fig. 6 that represents a dual-core architecture.

On the one hand, the Sample Sequencing Engine (SSE) is managed by the µWave-Controller master that reads a new voltage value per cycle from memory to be loaded into SSE registers. On the other hand, the µ-Controller Cortex M3 manages the ADC process configuring the Post-Processing Unit. After digital conversion, PPE results are transformed into inputs to other modem components such as correlators or demodulators. The versatile design of a cSoC allows dual configurations of the hard system to

be integrated as master as well as slave but in different buses. Fig. 6 shows two squares (A and B) with components designed on the FPGA while components out of these squares are hard system on chip built structures.

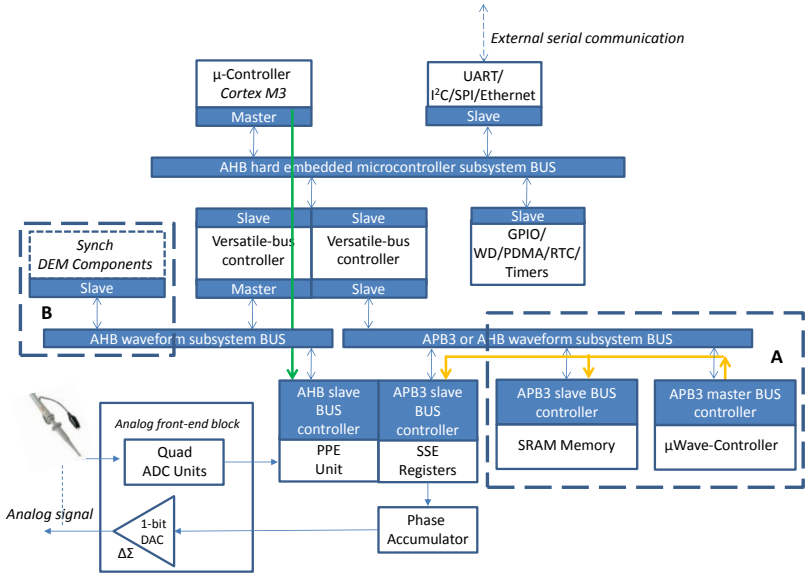


**Fig. 6.** Dual-core integration

Fig. 7 shows the digital conversion method. ADC block sets the interruption flag over a pre-conFig.d voltage threshold. The conversion is adjusted to the digital signal rising edge allowing the calculus of the input signal frequency.

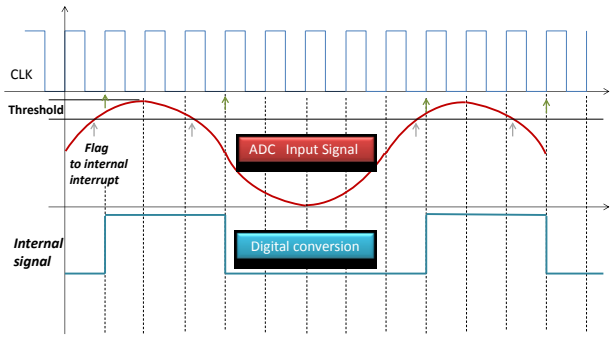


**Fig. 7.** Digital signal generated based on voltage threshold detection

## 5 Simulation and Discussion

Currently, SoC hard systems have burst into the market recently. Their capabilities are still limited thought their architectural potential could stand them up in future till DSP performance capabilities. However, these systems show at present relevant speed limits. Such is the case of the SoC platform used for the experiments [13]. SDD sample time is fixed set to 10µs. This is the updating phase accumulator time (see Fig. 5).

Thus, W(t) minimum sample time must be set over 10µs.
The W'(t) signal in Fig. 8 (A) corresponds to the LMS output generated following the processes described in Fig. 1. Examples (B) and (C) show oscilloscope captures from the DAC output signal corresponding to '1' expected [-20, +20] mV and '0' expected [-50, +50] mV. Vpp is correctly adjusted while the output voltage has been modified above 0V. The signal presents a discrete shape that implies up to 10µs (SDD sample time) delay to pass certain threshold compared with the real signal.

To carry out the AD conversion, threshold was set to 50mV. In case of B inputs in Fig. 8 no interruption occurs while in case of C, Fig. 9 shows a statement of time schedule. Loop outputs are adequate as expected.

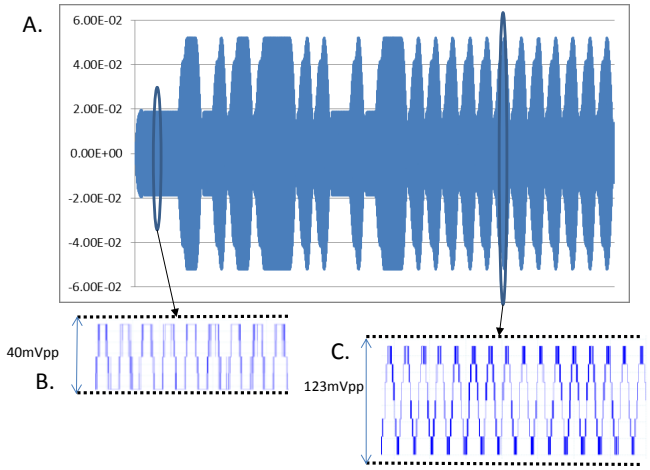


**Fi. 8.** W'(10µs): Oscilloscope view

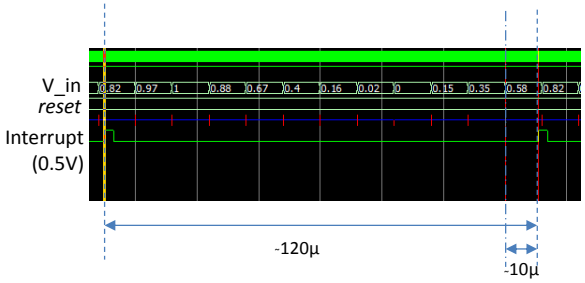


**Fig. 9.** ADC simulation view

## 6 Conclusions

Underwater modem design is still in need of low cost and feasible resources to enhance simulation processes with the whole complexity of the propagation water channel. Experiments carried out in sea waters are expensive and complicated. Simple methods are necessary that include the underwater channel in the simulation loop.

Although this problem has been solved in software simulation, this paper presents a method which novelty consists in the lodging of the propagation channel effects over the transmitted signal into the hardware simulation process.

The paper describes a simple architecture to generate a signal based on passive acoustic records or numerically modeling. One-bit sigma-delta digital-to-analog conversion has been tested with suitable results, while some performance speed limits exist but just dependent on the development platform.

Hardware loop is closed to prove the whole simulation process with analog to digital conversion all in one device. Results show the feasibility of the method.

## References


1. E.M. Sozer, M. Stojanovic, and J.G. Proakis, "Underwater acoustic networks"," IEEE J. Oceanic Engineering, vol. 25, no. 1, pp. 72-83, Jan. 2000
2. W. Kim, B. Lee, K. Kim, T. Yang, S. Kim, "A real-time HWIL simulation control system architecture for implementing evaluation environment of complex embedded systems", 13th International Conference on Advanced Communication Technology (ICACT), pp. 254-259, 2011.
3. Raytheon's Modeling and Simulation: Supporting all phases of system development, test and training; available in http://www.raytheon.com/news/technology_today/archive/2013_i1.pdf; accessed in May 2015.
4. L. Carter, J. Dyal, S. Doshi, R. Bagrodia, "Underwater Acoustic Modeling and Simulation", Military Communications Conference, pp. 1-8, 2008.
5. M. Porter. The BELLHOP manual and user's guide: Preliminary draft. Available in: http://oalib.hlsresearch.com/Rays/HLS-2010-1. pdf, (30/04/2015).
6. L.M. Wolff, E. Szczepanski, S. Badri-Hoeher, " Acoustic underwater channel and network simulator", Proceedings of the 2012 OCEANS Conference.
7. C.A. Clark, K.B. Smith, " An efficient normal mode solution to wave propagation prediction", IEEE Journal of Oceanic Engineering, 33(4):462–476,2008.
8. W. Jinjin, C. Ping, Y. Dong, "An underwater acoustic channel simulator for UUV communication performance testing", Proceedings of the 2010 IEEE International Conference on Information and Automation, pages 2286–2290, June, 2010.
9. A.P. Rosenberg, D. Chizhik, Q. Zhang, "High frequency rough surface parabolic equation modeling for underwater acoustic communications", IEEE Military Communications Conference (MILCOM) 2009, pp. 6, October, 2009.
10. W.H. Thorp, "Analytic description of the low-frequency attenuation coefficient", The Journal of the Acoustical Society of America, 42(1):270, 1967.
11. J. Llor, M. P. Malumbres. "Underwater Wireless Sensor Networks: How Do Acoustic Propagation Models Impact the Performance of Higher-Level Protocols", Sensors 12 (2), pp. 1312_1335. issn: 1424-8220, January 2012.
12. A. Sánchez, S. Blanc, P. Yuste, A. Perles, J.J. Serrano, "An ultra-low power and flexible acoustic modem design to develop energy-efficient underwater sensor networks". Sensors 12 (6), pp. 6837-6856, June 2012.
13. SmartFusion; web available in http://www.microsemi.com/products/fpga-soc/design-resources/dev-kits/smart-fusion-development-kits; accessed in May 2015.

# An eHealth Portal to prevent depression in the University Community through emotional virtual agents

Sabina Asensio-Cuesta[1], Adrián Bresó[1], Cristóbal Miralles[2], Juan Miguel García[1], Montserrat Robles[1]

[1] Instituto de Aplicaciones de las Tecnologías de la Información y de las Comunicaciones Avanzadas (ITACA), Universidad Politècnica de València, Camino de Vera s/n, 46022 Valencia, España
[2] Departamento de Organización de Empresas Universidad Politècnica de València, Camino de Vera s/n, 46022 Valencia, España

**Abstract.** The World Health Organization (WHO) expects that depression will become the first disability cause in 2030. Therefore, depression prevention strategies are required. This paper presents an eHealth Portal proposal project. Project aim is to develop an interactive web-based platform that assists University Community to prevent depression disorders through emotional virtual agents (virtual doctor). The environment chosen to evaluate the eHealth Portal is the Universitat Politècnica de Valencia's University Community. In that context, depression affects student, lecturers and administrative employees. Project motivation contributes The Spanish Network of Healthy Universities' main strategic lines. Due to the complexity of the project an interdisciplinary collaborative work group has been created.

## 1 Introduction

Current predictions indicate that by 2030 depression will be the leading cause of disease burden globally. When only the disability component is taken into consideration in the calculation of the burden of disease, mental disorders account for 25.3% and 33.5% of all years lived with a disability in low- and middle-income countries, respectively [1].

The European Study of the Epidemiology of Mental Disorders (ESEMeD) project found that 13% of Europeans will develop a major depression at some point in their life and 4% did so in the 12 months prior to the study [2]. The total number of people suffering from depression in Europe reached 21 million in 2004 [3]. In Europe 118 billion euros of which 61% are indirect costs related to sick leave. The cost in mental diseases in Europe is almost twice that of cancer [4]. While in Spain it is 5.005 million per year. In Spain depression is the second leading cause of work disability transient, only behind dysfunctions locomotors [5]. Consequently the 'Strategy on Mental Health of the National Health System' published by the Spanish Ministry of Health in 2007, has six main lines of action related to Depression: (1) promotion of mental health, prevention and eradication of social stigma; (2) health care to patients; (3)



C.Fernandez-Llatas and M.Guillen (Ed.):
Workshop on Innovation on
Information and Communication Technologies
(ITACA-WIICT 2015)

ISBN 978-84-608-4139-5

coordination between institutions, scientific societies and associations; (4) training of health personnel; (5) promoting research; and (6) information and evaluation systems [6]. Therefore depression prevention constitutes a society health challenge given the serious impact in the medium and long term, individually and as social, family and work.

There are different mechanisms to prevent depression some of them assisted by Health Information Technology (Health IT). Information technology (IT) can help individuals to change their health behaviors. This is due to its potential for dynamic and unbiased information processing enabling users to monitor their own progress and be informed about risks and opportunities specific to evolving contexts and motivations. However, in many behavior change interventions, information technology is underused by treating it as a passive medium focused on efficient transmission of information and a positive user experience [7]. In contrast, Help4Mood is an interactive user interaction thought empathic virtual agents that have a positive effect on stress management self-efficacy and enjoyment [8]. Also PREVENDEP interactively can prevent episodes of depression and suicide using an empathic virtual agent. This virtual agent tries to help users through adaptive and personalized Cognitive behavioral therapy (CBT) intervention [9], based in the self-reporting user information [10]. Moreover Maier et al. [11] have developed a prototype for patient self-management for work-related disorders. One component was an information portal for training and health literacy, which was integrated with the Semantic Web. Likewise Australian government has developed a Health Portal called 'Fighting Fit' containing a 'Mental Health On-Line' area [12]. Finally, in line with the eHealth Portal project proposed the 'Mental Health and Wellbeing Portal' is an initiative to provide the Deakin University Community with ready access to mental health related information and support [13].

This paper presents the eHealth Portal Proposal to develop an interactive web-based platform that assists University Community to self-prevent depression through emotional virtual agents. The paper describes project background, discusses the project scenario and objectives. Moreover, it outlines several implementation aspects. Finally interdisciplinary work group is presented.

## 2 Project Background

The background of the project is supported by two previous research projects:

– The European Project Help4Mood [FP7-ICT-2009-4; 248765], under which has been developed and tested the software Help4Mood. Help4Mood is based on the interaction of the user (patient) with an interactive virtual agent (see the virtual assistant in Fig 1). The software is able to identify symptoms related to major depression and propose a suitable and personalized treatment [8].

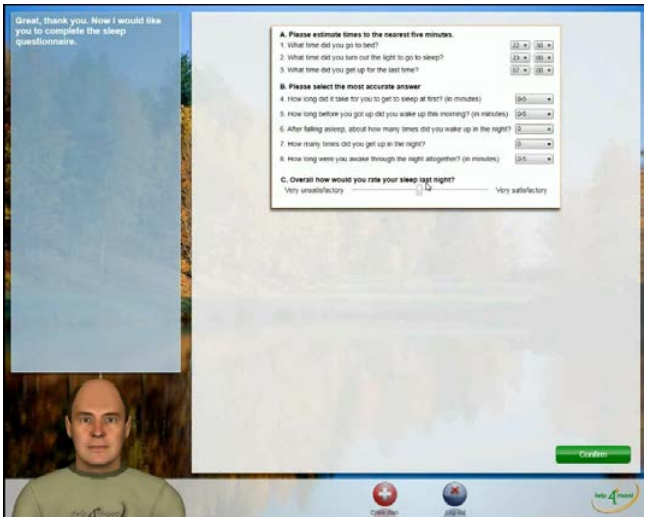


**Fig 1.** Help4Mood interface example.

– The PREVENDEP project is designed to prevent episodes of depression and suicide through continuous collection of information self-reported by the patient for identifying risk factors and providing information, suggestions and recommendations of activities that contribute to minimize risks [10] trough an intelligent virtual agent (see Fig 2).

**Fig 2.** PrevenDep interface example.

## 3 Project Scenario

In the Spanish university context the concern for health has promoted 'The Spanish Network of Healthy Universities' formed by institutions committed to health promotion in the university environment. The strategic lines of the universities Network are: university environments that promote health; the inclusion in university curricula of training in health promotion at undergraduate and postgraduate level; research on health promotion; participation and collaboration between public health agencies, community institutions and universities; services' offer and activities on campus aimed at promoting the health of the University Community. And the Network objective is the University Community (Students, Administration and Services, Lecturers and Research) and society as a whole.

Environments are defined as those places and social contexts where people develop daily activities and which interact personal and environmental, organizational factors affecting the health and well-being of those who live, work, they learn it, etc. The University meets several of the characteristics of these environments; on the one hand, it is a workplace, the other is an educational center and also is an institution of special relevance in both investigating and ensures the advancement of our society [14].

In this University Environment depression problem has been detected and its prevention has become a must to contribute to achieve the desired Healthy Universities Environment.

## 4 Objectives

The proposed eHealth Portal project aim is a Web-Based Support System to prevent depression in the University Community through emotional virtual agents. To achieve this overall objective the following specific objectives are planned:

### 4.1 Objectives regarding the identification of mood disorder symptoms related

- Definition of indicators associated with mood disorder.
- Methods development for quantifying defined indicators. Homogenization of the indicators risk levels.
- Detection questionnaires based on previous indicators and quantification.
- Standardized diagnostic questionnaires; detection depression levels, hopelessness and anxiety questionnaires [14-22].
- Programming virtual agent for interaction with the user during the identification stage symptoms.

- Programming the module responsible for planning sessions at this stage. Definition of the activation criteria and selection of appropriate questionnaires and diagnostic tests.
- Design and implementation user health status reports.

### 4.2 Objectives regarding the intervention after the identification of mood disorders

- Structured tasks definition and implementation for the mood disorder detected intervention.
- Virtual agent programming to direct adaptive and personalized intervention sessions based on Cognitive Behavioral Therapy (CBT) [9]. Regarding the managing of emotions in the virtual agent, in order to improve the human-agent interaction, the cognitive appraisal theory of emotions [23] will be apply.
- Virtual agent adaptability programming based on the evolution of the user: verbal communication (contents offered: activities / recommendations / alerts) and non-verbal communication (managing emotions).
- Virtual agent programming to give users feedback about their evolution.
- Evolution reports design and implementation for user intervention.

### 4.3 Objectives regarding software development

- Study of the actual virtual agent technologies developments in order to select the most appropriate to implement the graphical interface in the eHealth portal.
- Interactive web-based system development (see Fig 3). Anonymous user access to eliminate depression stigma problems.
- Creating a focus group at the beginning of the eHealth Portal development process to establish the outline of the portal. The focus group will have at least 6 members representing students, administrative employees and lecturers.
- Design portal usability testing. Scheduling periodic usability testing during the redesign process and software development.
- Design and usability testing (test online and personal) of the final eHealth Portal.

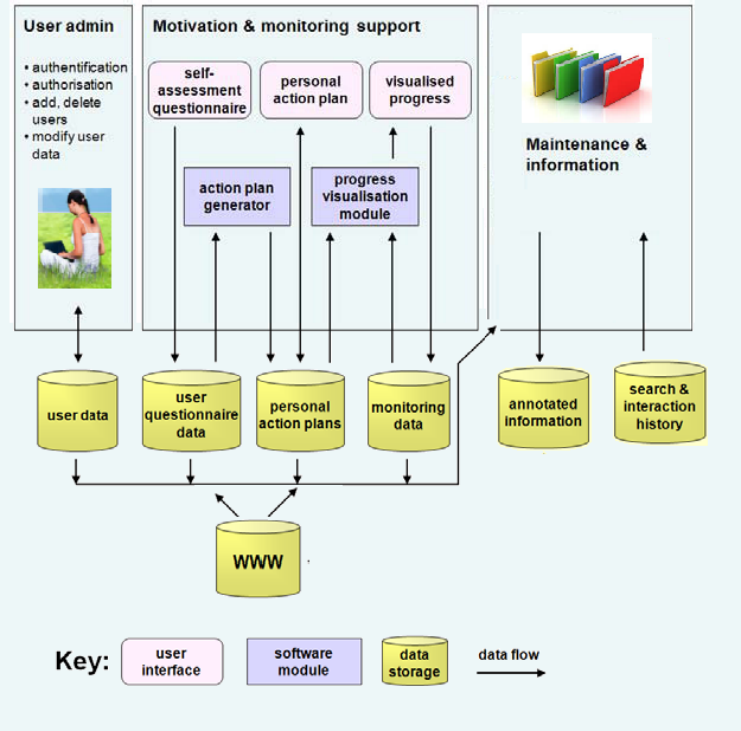


**Fig. 3.** eHelth Portal system architecture first approach (Adapted from [11])

### 4.4 Objectives regarding assessment Portal

– Final solution will be evaluated by three user groups: students, lecturers and administrative employees. Each group will consist of at least 15 volunteers who express a desire to participate in the project. Students will be from at least three different schools in their first year. Also administrative employees should represent at least three different schools. Lecturers group proposed is a temporary contract pending promotion ones.

## 4 Interdisciplinary Collaborative Work Group

Due to the complexity of the eHealth Portal project an interdisciplinary collaborative work group is required. The current project working group consists of 12 members organized as following:

- Four members (PhD in Computer Science) from Institute for the Applications of Advanced Information and Communication Technologies (ITACA). Research Group IBIME.
- A member (PhD in Computer Science) from Human-Computer Interaction and Usability from Research Center on Software Production Methods.
- Four Doctors from Occupational Health Centre at the Universitat Politècnica de València (UPV).
- A Doctor form Health Center Aldaia (Valencia, Spain)
- Two members (Psycopedagogy) from Institute of Education Sciences at the Universitat Politècnica de València (UPV). Student's orientation office.
- A member (PhD Industrial engineer) from Disabled People`s Service.

## 5 Conclusions

The eHealth Portal project presented to prevent depression in University Community is a new initiative that aims to provide the UPV University Community with ready access to mental health related information and support. eHealth Portal is an interactive tool for preventing and coping with depression that teaches self-help skills through emotional virtual agents. After eHealth Portal development phase an exhaustive evaluation phase will be performed to ensure the effectiveness of it to achieve the depression prevention target proposed. Finally eHealth Portal will be available for all university community.

## References


1. World Health Organization. Global burden of mental disorders and the need for a comprehensive, coordinated response from health and social sectors at the country level. Report EB130/9. (2011)
2. Alonso J, Angermeyer MC, Bernert S, Bruffaerts R, Brugha TS, Bryson H, et al. Prevalence of mental disorders in Europe: results from the European Study of the Epidemiology of Mental Disorders (ESEMeD) project. Acta Psychiatr Scand Suppl. (2004). 21–7.
3. Sobocki P, Jonsson B, Angst J, Rehnberg C. Cost of depression inEurope. J Ment Health Policy Econ (2006). Vol 9. 87–98
4. A. Valladares, T. Dilla, J. A. Sacristán. Depression: a social mortgage. Latest advances in knowledge. Esp minutes Psiquiatr. Actas Españolas de Psiquiatría (2009). Vol. 37(1):49-53
5. Kennedy CM, Powell J, Payne TH, Ainsworth J, Boyd A, Buchan I. Active Assistance Technology for Health-Related Behavior Change: An Interdisciplinary Review. Eysenbach G, ed. Journal of Medical Internet Research. (2012) Vol. 14(3)
6. Depresión, la segunda causa de baja por incapacidad temporal. Jano on-line y agencias, marzo 2004 (citado 25 de septiembre de 2007). Available at: http://db.doyma.es/cgi-bin/wdbcgi.exe/ doyma/press.plantilla?ident=31688 [Accessed 25 May. 2015].

7. Mental Health strategy of the National Health System. Ministry of Health and Consumer Affairs (2006). Available at: http://www.msc.es. [Accessed 25 May. 2015].
8. Jin SA. The effects of incorporating a virtual agent in a computer-aided test designed for stress management education: the mediating role of enjoyment. Computer Human Behaviour. 2010; 26(3):443–51. doi: 10.1016/j.chb.2009.12.003. [Accessed 25 May. 2015].
9. Kaltenthaler, Eva et al. (2008). Computerised cognitive behavioural therapy for depression: systematic review. In: The British Journal of Psychiatry 193.3
10. Prevendep. Sistema computacional de ayuda a la prevención de episodios de depresión y suicidio – PREVENDEP. IBIME. Available at: https://ibime.webs.upv.es/?page_id=26 [Accessed 25 May. 2015].
11 Maier E, Reimer U, Schar SG, Zimmermann PG. SEMPER: a Web-based support system for patient self-management. 2010 Presented at: 23rd Bled eConference: eTrust: Implications for the Individual, Enterprises and Society; Jun 20-23, 2010; Bled, Slovenia. Available at: http://ecenter.fov.uni-mb.si/proceedings.nsf/Proceedings/16DB5E433CFFAC33C1257757003AEB6E/$File/15_Maier.pdf [Accessed 28 May. 2014].
12. Australian Government. Department of Defense. Available at: http://www.defence.gov.au/health/healthportal/Depression .asp. [Accessed 25 May. 2015]
13. Mental Health and Wellbeing Portal. Available at: http://mental-health-wellbeing.deakin.edu.au/[Accessed 25 May. 2015]
14. Ministerio de Sanidad, Servicios Sociales e Igualdad. Red Española de Universidades Saludables. Principios, objetivos y estructuras de la red (2015). Available at: http://www.msssi.gob.es/profesionales/saludPublica/prevPromocion/promocion/UniversidadesSaludables/docs/AnexoI.pdf
15. Mental Health and Wellbeing Portal. Deakin University. Available at: http://mental-health-wellbeing.deakin.edu.au/ [Accessed 28 May. 2015]
16. Montgomery Questionnaire. Available at: http://www.juntadeandalucia.es/servicioandaluzdesalud/library/plantillas/externa.asp?pag=/contenidos/gestioncalidad/CuestEnf/PT7-DeprMontgomery.pdf [Accessed 28 May. 2015]
17. Hamilton Questionnaire. Available at: http://www.juntadeandalucia.es/servicioandaluzdesalud/library/plantillas/externa.asp?pag=/contenidos/gestioncalidad/CuestEnf/PT7_AnsHamilton.pdf [Accessed 28 May. 2015]
18. CES-D Scale Available at: http://conservancy.umn.edu/bitstream/handle/11299/98561/v01n3p385.pdf?sequence=1 [Accessed 28 May. 2015]
19. Beck depression Inventory (BDI, BDI-1A, BDI-II)
20. PHQ-9 Questionnaire Available at: http://www.uspreventiveservicestaskforce.org/Home/GetFileByID/218 [Accessed 28 May. 2015]
21. Beck Questionnaire. Available at: http://www.juntadeandalucia.es/servicioandaluzdesalud/library/plantillas/externa.asp?pag=/contenidos/gestioncalidad/CuestEnf/PT10_Desesp_Beck.pdf [Accessed 28 May. 2015]
22. Goldberg Questionnaire. Available at: http://www.juntadeandalucia.es/servicioandaluzdesalud/library/plantillas/externa.asp?pag=/contenidos/gestioncalidad/CuestEnf/PT7_AnsDepGoldberg.pdf [Accessed 28 May. 2015]
23. Scherer, Klaus R, Angela Schorr, and Tom Johnstone (2001). Appraisal processes in emotion: Theory, methods, research. Oxford University Press

# Macroscopic Fluctuations in Results of Radioactivity Measurements Performed by Geiger-Müller Counters

V.A. Kolombet[1], V. Milián-Sánchez[2], G. Verdú-Martín[2], E.V. Kolombet[1], A. Mocholí-Salcedo[3]

[1] Institute of Theoretical and Experimental Biophysics of Russian Academy of Sciences, Laboratory of Physical Biochemistry, Pushchino, Russia; kolombet@iteb.ru.
[2] Chemical and Nuclear Engineering Department, Polytechnic University of Valencia, Spain; vicmisan@iqn.upv.es
[3] Grupo de Sistemas de Control de Tráfico, Instituto ITACA, Universitat Politécnica de Valencia, Camino de Vera, s/n, Valencia, Spain

**Abstract**. Fundamental physical nature of the so called macroscopic fluctuations (MF) of "instant" (v) and mean (V) velocities of a wide set of natural processes is clearly shown by discreteness of value of relative variance of measurement results $D=(\sigma/V)^2$; values D represent quantified spectrum $\boldsymbol{n}D_o = \boldsymbol{n}\alpha^{3/2}$, where $\alpha$ is the fine-structure constant of atomic spectra and $\boldsymbol{n}$ are small integer numbers; it was also shown that the (mean) values $\boldsymbol{n}$ close to squares of integers appear more often than others [1, 2-5]. The spectrum of mean values D appearing during the registration of radioactive decay was studied by means of Geiger-Müller counters. The phenomenon of quantification of D was observed in this investigation, means of quantum $D_o$ were experimentally obtained close to the same $\alpha^{3/2}$, and it was found that values $\boldsymbol{n}$ close to squares of integers are predominantly presented; in other words, the Geiger-Müller counters registered MF in these experiments. In this investigation, we also found numbers $\boldsymbol{n}$ shifted at 1/2 with respect to the integers.

## INTRODUCTION

The unity of natural phenomena was considered at the beginning of 20th century in form of universality of mathematical models; researchers noticed that sets of the most different phenomena are described by linear equations in partial derivatives of the second order. Now equations are found in most of the cases to be different but way of attractor complication, set of bifurcations or, as it is called, scenario of passage to chaos, appear to be the same. The unity appears to be connected to no analogous equations of systems under study but with universal qualitative behavior [6 - 10].

In some other investigations of chaotic processes, the mathematical apparatus is still not so clear and on the way to it, there is a hard task to search for key characteristics that could lead to the further theory with a steady mathematic framework. During the process of studying the intriguing "macroscopic fluctuations" (MF) the discreteness of relative variance D of measurement results could play the role of the key characteristic. MF is a designation for a set of unusual peculiarities found during the process of making long rows of measurements of "instant" (v) and mean characteristics (V) of many processes [11, 12, 13, 14]. In particular, v is the velocity of a biochemical reaction. As mentioned above, value D is defined as $(\sigma/V)^2$, and $\sigma$ is the standard deviation.

As a result of MF investigations, the experimentally-based reasons appear to indicate that set of experimental values D in case of biochemical reaction measurements could be fitted by the spectrum $\boldsymbol{n}\alpha^{3/2}$, where $\boldsymbol{n}$ are small integers [4, 5]. Here $\alpha$ is the fine-structure constant; it is a dimensionless combination of fundamental physical constants, a real number 1/137,0360 … , introduced in 1916 by A. Sommerfeld while he was working on the modeling of atomic spectra. Note that $\alpha^{-1}$ is almost integer number; this property is essentially used in the theory [9], which is the phenomenological version of the unified theory of matter and field.



C.Fernandez-Llatas and M.Guillen (Ed.):
Workshop on Innovation on
Information and Communication Technologies
(ITACA-WIICT 2015)

ISBN 978-84-608-4139-5

After additional analysis of various experimental data obtained in the analysis of some physical phenomena, another spectrum was phenomenologically added to the initial spectrum of $D = \boldsymbol{n}\alpha^{3/2}$; it is shifted on 1/3, that is, $(\boldsymbol{n}+1/3)\alpha^{3/2}$ [1].

Special measurements of mean values of D by Geiger-Müller counters in long series of stereotype measurements of radioactive decay rates of radium and cesium were performed in the UPV.

## EXPERIMENTAL INSTALLATON IN THE UPV

The purpose of the experiments was the search for MF in the results of radioactivity measurements of two standard preparations of Ra-226 and Cs-137; (preparation of Ra-226: 0.9 μCi, Amersham, model №184100; preparation of Cs-137: 5 μCi, Rs-214, model № A-0080). The experiments were performed using Geiger-Müller counters ZP-1430 manufactured by Philips. X-ray, γ- quanta, and β-particles were registered in the counter, as well as α-particles near the thin layer in the input part of the counter tube. The bombardment of gas by these particles and the subsequent development of avalanches of ionization, their quenching by reactions with participation of halogen, waves of heating and cooling, jumps of polarization, effects on walls and central string of the counter - all these circumstances lead to a picture that is obviously sufficient, regarding the level of complexity, for the occurrence of complex dynamic modes.

Two identical counters were used in the experiments. The counter tubes are filled with an inert gas in addition to halogen. The anode-cathode capacity is near 3.5 pF, the plateau slope is 0.04%, the plateau width is some hundred volts, dead time is near 0.2 ms. The particles counting lasted 6 seconds per measurement. The number of registered pulses does not exceed 3000 per 6 seconds, and in this way the mean time between pulses does not exceed 2 ms; actually, it was 10-100 times more than dead time. Results of long series of stereotype measurements were stored in a computer memory and after finishing the measurements they were treated with different programs, particularly with Excel of the Microsoft Office package.

Ra-226 and Cs-137 preparations were inserted on different distances from the tube in standard slots a 3 cm lead shield, Fig. 1. In these experiments of preliminary character it was not possible to vary continuously neither the intensity of the radioactive sources nor the distance to the counter tube.


**Fig. 1.** Lead shield and standard slots for radioactive sources positioning.

Each set of measurements had a rough duration of one day and near 14400 measurements were performed per day. The estimated error of value $(\sigma/V)^2$ was about 1% at such measurements.

## EXPERIMENTAL RESULTS

The experimental results corresponded considerably to the expectations formulated on the bases of previous results which were based, in particular, on biochemical reactions. Not continuous as usually considered but, to the contrary, discrete, quantified relative variance $(\sigma/V)^2$ of measurement results were again observed in these UPV experiments. The value of the "quantum" appears also to be practically equal to $\alpha^{3/2}$. As a result of the measurements performed in the UPV, the following discrete values $(\sigma/V)^2/\alpha^{3/2}$ were obtained in the measurements (Table 1):

Table 1. Discrete values of $(\sigma/V)^2/\alpha^{3/2}$

| | |
|---|---|
| **1.47** | |
| **2.32** | mean of two repetitions - 2.31 and 2.33 |
| **3.325** | mean of two repetitions - 3.29 and 3.36 |
| **4.50** | mean of four repetitions - 4.48, 4.52, 4.53 and 4.46 |
| **7.50** | mean of four repetitions - 7.55, 7.45, 7.45, 7.56 |
| **8.06** | |

Thus, value 8 from known spectrum $\boldsymbol{n}\alpha^{3/2}$ and two values 2+1/3 and 3+1/3 from known spectrum $(\mathbf{n}+1/3)\alpha^{3/2}$ were obtained in the experiments. In addition, three values 1+1/2, 4+1/2 and 7+1/2 were obtained, which could be considered as unambiguous evidence of earlier unknown spectrum $(\boldsymbol{n}+1/2)\alpha^{3/2}$ existence. Using analogy with atomic spectra, it could be supposed that the "additional quantum number" *l* exists in parallel with ***n***, "mean quantum number" of MF, and a generalized formula for MF spectrum could be represented as follows:

$$D = \left(n + \frac{1}{l}\right)\alpha^{\frac{3}{2}} \tag{1}$$

Deviations from ideal means described by phenomenological formula (1) are 2% for 1.47, 1% for 2.31, 0% for 2.33, 2% for 3.29, 1.5% for 3.36, 0.5% for 4.48, 0.5% for 4.52, 0.5% for 4.53, 1% for 4.46, 0.5% for 7.55, 0.5% for 7.45, 0.5% for 7.45, 1% for 7.56 and 1% for 8.06. The global mean of deviation of the measured values for the whole UPV-experiment is near to 1% , which corresponds to (the) estimations made during period of the experiment planning.

Repetitions of measurements essentially improve statistics; more precise meanings converge to meanings described by formula (1).

## DISCUSSION OF EXPERIMENTAL RESULTS

***1. On link of the discreteness of values V and $\sigma^2$***

It is known that variance $\boldsymbol{\sigma}^2$ of radioactive decay measurements numerically coincides in a range of statistically determined deviation with the mean value V of impulse counts, i.e. $\sigma^2/V \approx 1$. It means that $(\sigma/V)^2 \approx 1/V$. In this way, value $(\sigma/V)^2/\alpha^{3/2}$ transforms into $1/(V\alpha^{3/2})$, i.e. the experiment shows that the mean values of $1/(V\alpha^{3/2})$ belong to spectra ***n***, ***n***+1/3 and ***n***+1/2. One could reformulate this as,

$$\begin{aligned} V &= D_o/\boldsymbol{n} \\ V &= D_o/(\boldsymbol{n} + 1/3) \\ V &= D_o/(\boldsymbol{n} + 1/2) \end{aligned} \tag{2}$$

The last set of formulae testifies more evidently that the mean values V of counts have to endure high-amplitude discrete transitions in case of integer numbers **n** variations.

***2. On the discreteness of V-spectrum***

Naturally, those discrete changes of V were observed after each change of the setup configuration, such as change of the radioactive preparation and/or distance between (the) source and (the) counter. It did not lead to any astonishing discovery, but high-amplitude transitions between different mean values of V were sometimes observed during long series of stereotypical measurements without any influence of (the) experimenter. For example, a discrete transition of V from one level to another, in the same experimental configuration, took place in one experiment. It was a sharp jump (during a short time, compared to the time of one measurement) accompanied by mean value V lowering of approximately 2.5 times. High stabilization of V after the transition led to the possibility of calculating a stable mean value $(\sigma/V)^2/\alpha^{3/2}$. It was 1.47, which is practically 1+1/2; it looks like MF with $\boldsymbol{n}$ = 1 belonging to the spectrum D = $(\boldsymbol{n}+1/2)\alpha^{3/2}$.

In a subsequent experiment with the Ra-226 preparation, the jump of V of 2.6 times (from approximately 520 counts to 202 counts) led also to the stabilization of V, (Fig.2). Mean value for this stable stage of measurements is 8.01; (value $(\sigma/V)^2/\alpha^{3/2}$ is 8.06; value $1/(V\alpha^{3/2})$ is 7.94); this is a "spectral line" for case $\boldsymbol{n}$ = 8 in spectrum D = $\boldsymbol{n}\alpha^{3/2}$.

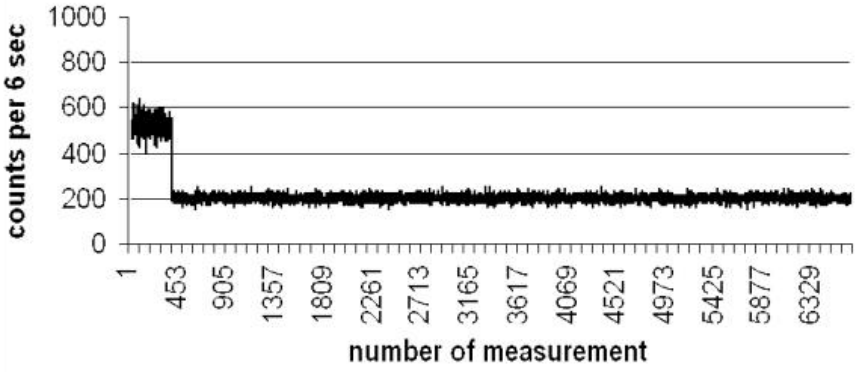


**Fig. 2.** Discrete transition from unstable results of counter to stable pulses registration caused by radioactive decay. Quantified macroscopic fluctuations with $\boldsymbol{n}$=8 in spectrum D = $\boldsymbol{n}\alpha^{3/2}$ correspond to the stable phase of the experiment.

What is the nature of this discreteness of value V?

In the case of this experiment, shown in Fig. 2, the calculations of $(\sigma/V)^2$ for no stationary stage (before the jump) leads practically to the same $\boldsymbol{n}$ = 8; note that this value has small statistical significance. In addition, the relationship $\sigma^2/V$ before the jump certainly differs from unit, i.e. results do not precisely agree with Poisson statistics during this stage of the experiment.

Practically the same was found in the jump described above, which was observed several days later. Measurements (after the jump) of V led to stable MF with $\boldsymbol{n}$ close to 1.5; analogous but not so statistically significant number $\boldsymbol{n}$ was found before the jump.

The discovery of such quantized levels and quantized jumps between them needs a specific way of thinking and proceeding. For example, (the) technical testing of the installation had led to the

discomfiture conclusion that the high voltage on the counter tube is not in strong correspondence with the observed counts. According to the usual thinking, the quantized phenomena can be considered as erroneous and turn to long process of the installation refinement. It should be noted, however, that in other systems there were similar discrete jumps of the mean of measured values in the course of MF experiments, and that these jumps were not caused by artifacts [1, 4]. In this way, we have to conclude that the small variations of the parameters that determine the pulses can sometimes be not accidental, but they are probably included in the process of the quantized fluctuations.

Changes on the counter tube voltage were applied during the course of good stages of measurements but the existence of the plateau lead to negligible influence of this drift in final measurement results and, importantly, it did not usually smooth the quantification of $(\sigma/V)^2$-s.

The analysis of the performed experiment errors shows that the quantification of relative variance is an easily recognizable effect and that the experimental revealing of MF does not require very expansive and excessively precise equipment. The main basis for the prolongation of this branch of investigations is the coincidence of experimental mean of $D_o^{-2/3}$ with fundamental physical constant $\alpha$ and the important role of value $\alpha^{-3/2}$ in the theory [9].

### *3. On the possible mechanism of the fluctuations macroscopization*

It is not a solved problem yet but it could be supposed that the fine-structure constant $\alpha$ that describes quantum electrodynamics phenomena in micro-world penetrates into macroscopic measurements through a mechanism of cancelling of the same factors that affect both $\sigma$ and V. The efficiency of counting the particles which penetrate into the Geiger-Müller counter depends on ensembles of parameters $k_1$, $k_2$, $k_3$, … influencing upon the probability of the appearance of an avalanche in the counter, but the width of distribution changes exactly in the same manner, therefore the relation $(\sigma * k_1 * k_2 * k_3 * \ldots)/(V * k_1 * k_2 * k_3 * \ldots) = \sigma/V$ does not change. This picture loses scale invariance, probably, only in quantum world at (the) moment of electromagnetic interaction whose probability is proportional to the mean of $\alpha$. If it is really so then experimentally determined meaning of $D_o$ have no additive inputs and its mean value equals precisely to $\alpha^{3/2}$.

Table 2 shows that the experimental mean of $D_o$ really equals to $\alpha^{3/2}$ within precision of the experiment: the mean of $\boldsymbol{n}_{exp}/\boldsymbol{n}_{hypot}$ is not shifted from 1: mean of the third column is 0,997.

Table 2. Calculation of ratio between experimental and rounded values of "unit of $\alpha^{3/2}$ ".

| No | $\boldsymbol{n}_{exp}$ - experimental mean of $\boldsymbol{n}$ | $\boldsymbol{n}_{hypot}$ - hypothetical mean of $\boldsymbol{n}$ | Mean of $(\boldsymbol{n}_{exp}/\boldsymbol{n}_{hypot})^*$ |
|---|---|---|---|
| 1 | 1,47 | 1.50 | 0.980 |
| 2 | 2,31 | 2.33 | 0.991 |
| 3 | 2,33 | 2.33 | 0.999 |
| 4 | 3,29 | 3.33 | 0.988 |
| 5 | 3,36 | 3.33 | 1.008 |
| 6 | 4,48 | 4.50 | 0.996 |
| 7 | 4,52 | 4.50 | 1.004 |
| 8 | 4,53 | 4.50 | 1.007 |
| 9 | 4,46 | 4.50 | 0.991 |
| 10 | 7,55 | 7.50 | 1.007 |
| 11 | 7,45 | 7.50 | 0.993 |
| 12 | 7,45 | 7.50 | 0.993 |
| 13 | 7,56 | | 1.008 |
| 14 | 8,06 | 7.50 | 0.993 |
| | | 8.00 | |
| (*) Mean of "unit of $\alpha^{3/2}$ " is $0.997 \approx 1.00$ | | | |

***4. On a probable way of a quick introduction of results of the MF studies***

One could try to perform a capital metrological work after avoiding the noted defects of experiment and after developing the new-found strategy of constant $D_o^{-2/3} \equiv \alpha$ measurement till sufficient degree of perfection. Revision of fundamental constant $\alpha$ value, that is the relation of square of elementary electrical charge to multiple of light velocity on "crossed" Plank constant, is one of serious tasks of modern fundamental physics.

The preliminary experiment made by means of Geiger-Muller counters still leads naturally to rough means of $\alpha$. Standard deviation in the experiment is 0.009; this means that experimental results of $\alpha^{3/2}$ scatter mainly between 0.988 and 1.006. The scatter of the mean is square root from 14 times less, i.e. approximately between 0.995 and 1.000.

Fine-structure constant $\alpha$ is $\alpha^{3/2}$ raised in the power 2/3. Because $(\alpha^{3/2})^{2/3}$ is located mainly inside interval $(0.995\times\alpha^{3/2})^{2/3}$ and $(1.000\times\alpha^{3/2})^{2/3}$ one could state that experimental means of $\alpha$ scatter between $(1-(2/3)\times0.005)\times\alpha$ and $(1+(2/3)\times0.000)\times\alpha$, i.e. approximately between 136.5 and 137.0. Really the interval is even slightly broader because here errors of rounding-up of the means, presented in the first column of the Table 2 were not taken into account.

The precision of the result obtained corresponds to the task of the described experiment that was of preliminary, prospecting aim. There are not any experimental limitations for much more precise experimentation in this direction. The more precise values 137.0, 137.04, 137.036, … of $\alpha$ are measured, the more promising will MF fundamental nature investigations become.

## FINAL REMARKS

Finding quantification in an experimentally registered chaotic process requires investigation of the already existing physical theory where chaotic disorder and quantified order are closely interconnected by respective manner. It seems promising within the framework of this problem that well-marked hints on existence of dynamic chaos with all its attributes like bifurcations, windows of orders embedded in chaos etc. have already appeared in the theory [9] where value $\alpha^{-3/2}$ plays essential role [6]. Moreover, because $\alpha$ is an electromagnetic constant, it is promising that dynamic chaos appears in electromagnetic sector of the unified theory [9].

The principal difference of the relative variance measurement methods of velocities of biochemical reactions [15-18] from the above described method of the relative variance measurement of the intensity of radioactivity counting rate, and at the same time the identity of both results could mean that the same physical phenomenon is registered in both investigations [2, 3, 19]; other possibility is that the same mathematics underlies essentially different systems [6-8].

In any case, the forthcoming joint development of theory [9, 10] and experiments [1, 4, 5, 8], will lead to the appearance of a new area of biophysics and fundamental physics, one of its innovative aspects being the possibility of measuring the fine structure constant simply by means of very long measurements of radioactivity.


### Acknowledgements

Authors are grateful to Prof. Simon Shnoll for his help in the UPV experiment preparation and for his participation in the discussion of the obtained results.

## REFERENCES


1. V.A. Kolombet. Macroscopic and fundamental fluctuations: similarity and difference. - Biophysics, 1995, vol. 40, No. 4, p. 875-882.
2. S.E. Shnoll, V.A. Kolombet, E.V. Pozharski, T.A. Zenchenko, I.M. Zvereva, A.A. Konradov. Realization of discrete states during fluctuations in macroscopic processes. - Uspekhi Fizicheskikh Nauk. 1998, vol. 41, iss. 10, 1025-1035
3. S.E Shnoll., Kolombet, V.A., Pozharski, E.V., Zenchenko, T.A., Zenchenko, K.I., and Konradov, A.A. Evidence for the influence of cosmophysical factors on the fine structure of experimental distributions - Uspekhi Fizicheskih Nauk, 2000, vol. 43, iss. 2, p. 214-218
4. V.A. Kolombet. On probability of representation of masses of elementary particles by system of integers. - Preprint, 1981, Pushchino, ONTI NCBI AN SSSR, 10 p.
5. V.A. Kolombet. Attempt of phenomenological synthesis of spectrum of masses with spectrum of dimentionless constants of interactions. High-ampli-tude discrete fluctuations of results of metrological and biochemical measurements. - VINITI, 03. 04. 1986, No. 2388-86 Dep., 135 p.
6. M.J. Feigenbaum. Quantitative universality for a class of nonlinear transformations. - J. Statist. Phys., 1978, vol. 19, No. 1, p. 25-56
7. M.J. Feigenbaum. The universal metric properties of nonlinear transforma-tions. - J. Statist. Phys., 1979, vol. 21, No. 6, p. 669-706
8. G.G. Malinetsky. Chaos. Structures. Calculative experiment: introduction into nonlinear dynamics. – Moscow: Science, 1997. p. 104-105
9. V.A. Kolombet. PhUT: Phenomenological Unified Theory. - In: Physical metrology. Eds: prof. A.E.Gorodetsky, V.G.Kurbanov. Saint Petersburg, Publ. House of SPbGTU, 2000, p. 9-13.
10. V.A. Kolombet. Clasification of low energy fundamental forces. - (In press)
11. V.A. Kolombet. Macroscopic fluctuations, masses of particles and discrete space-time. – Biophysics, 1991, vol. 37, iss. 3, p. 492-499.
12. V.A. Kolombet. Regular Measurement: A new method of biophysical experiment. Biophysics, 2006, Vol. 51, No. 3, pp. 504–509. Pleiades Publishing, Inc., 2006.
13. I.A. Rubinshtein, S. E. Shnoll, A.V. Kaminsky, V.A. Kolombet, M. E. Astashev, S.N. Shapovalov, B. I. Bokalenko, A.A. Andreeva, D. P. Kharakoz. Dependence of Changes of Histogram Shapes from Time and Space Direction is the Same when Fluctuation Intensities of Both Light-Diode Light Flow and 239Pu Alpha-Activity are Measured. Progress in Physics, Vol.3, July 2012.
14. A.V. Kaminsky, I. A. Rubinstein, S. N. Shapovalov, A. A. Tolokonnikova, V. A. Kolombet, S. E. Shnoll. "Macroscopic fluctuations" of light beams as a novel tool for astrophysical studies. Astrophysics and Space Science December 2014. DOI 10.1007/s10509-014-2143-0.
15. V.A. Kolombet, T.Ya. Britsina, N.P. Ivanova, S.E. Shnoll. Spectrum of macroscopic fluctuations of enzymatic activity of creatine kinase. - Biophysics, 1980, vol. 25, iss. 2, p. 213-217
16. S.E. Shnoll, N.P. Ivanova, T.Ya. Britsina, V.A. Kolombet. Dependence of spectra of macroscopic fluctuations of creatine kinase enzymatic activity from pH of protein solution. - Biophysics, 1980, vol. 25, iss. 2, p. 218
17. S.E. Shnoll, V.A. Kolombet. Macroscopic fluctuations and statistic spectral analysis of the states of aqueous protein solutions. - In: Soviet Scientific Reviews. Sect. D, Biol. Rev., Ed. OPA, N.Y., 1980, vol.1, p. 399 – 445
18. S.E. Shnoll, V.A. Kolombet, N.P. Ivanova, T.Ya. Britsina, Macroscopic fluctuations as common property of aqueous solutions of different enzymes and other substances. - Biophysics, 1980, vol. 25, iss. 3, p. 409 - 416
19. S. E. Shnoll. On spontaneous synchronous transitions of actomyosin molecules in solution from one state to another. - Questions of medical chemistry (Rus.) 1958, vol. 4, iss. 6, p. 443 – 454

# Identification of Atrial Sources by Causality Analysis during Atrial Fibrillation: a Computational Study

Miguel Rodrigo[1], Andreu M. Climent[2], Alejandro Liberos[1], Francisco Fernández-Avilés[2], Omer Berenfeld[3], Felipe Atienza[2], and María S. Guillem[1]

[1] BIO-ITACA, Universitat Politécnica de Valencia, Valencia, Spain.
Phone: +34-963-877-968; e-mail: mirodbor@teleco.upv.es
[2] Cardiology Department, Hospital General Universitario Gregorio Marañón, Madrid, Spain
[3] Center for Arrhythmia Research, University of Michigan, Ann Arbor, USA

**Abstract.** Ablation of electrical drivers during atrial fibrillation (AF) has been proved as an effective therapy to prevent recurrence of fibrillatory episodes. This study presents a new methodology based on causality analysis which is able to identify the hierarchical dominance of atrial areas driving AF. Realistic mathematical models of the atrial electrical activity during AF were analyzed using the causal method. Causal relationships between atrial electrograms were summarized into a recurrence map, highlighting the hierarchy and dominant areas and allowing the identification of sites responsible for maintenance of the arrhythmia. These maps located the position of the atrial driver in simulated fibrillatory processes with a single rotor, with 2 rotors or with several drivers. Additionally, the correspondence between the nodal values of the recurrence map and the distance to the rotor core has been established. Causal analysis consistently estimated propagation patterns and location of atrial drivers during AF.

## 1 Introduction

Atrial fibrillation (AF) can be driven by atrial areas responsible for the maintenance of the arrhythmia [1-3], and ablation of these dominant areas can prevent the arrhythmia recurrence [4]. Atrial drivers can be located everywhere in the atria [5], so their identification in each patient is a goal for the ablation therapy. Although there are some methods for locating these atrial sources [6-7], like the detection of the regions with highest dominant frequencies (DF), their efficiency remain elusive.

This work proposes a novel tool for dominant areas location based on the search for the strongest cause-effect relationships between multiple electrograms that allows locating the electrical sources driving AF. This analysis can be used to estimate the dominant propagation pattern and to locate the region that predominantly acts as a source of electrical activations. As a first approach and due to the difficulty in obtaining simultaneous recordings of the electrical activity across the whole atria, we have used here mathematical models of the atrial electrical activity during fibrillatory processes to assess the validity of our method.



C.Fernandez-Llatas and M.Guillen (Ed.):
Workshop on Innovation on
Information and Communication Technologies
(ITACA-WIICT 2015)

ISBN 978-84-608-4139-5

## 2 Methods

### 2.1 Mathematical models of the atrial electrical activity

A realistic 3D anatomical model of both atria was used to simulate the atrial electrical activity during fibrillatory processes (285,780 nodes and 566,549 triangular patches) [8]. A gradient of the electrophysiological properties (Ik,ACH) of the atrial myocardium was introduced into the mathematical model in order to obtain realistic propagation patterns with different activation rates. The reaction-diffusion system with the Courtemanche cell model kinetics [9-10] was solved by using the Runge-Kutta integration method with an adaptive temporal step on a graphic processors unit (NVIDIA Tesla C2075 6G) [11].

From each computational simulation, a uniform mesh of pseudo-unipolar electrograms was calculated under the assumption of a homogenous, unbounded and quasi-static medium by using the following expression:

$$V_{\vec{r}} = \sum_{\vec{r}} \left(\frac{\vec{r}}{r^3}\right) \cdot \vec{\nabla} V_m \quad \textbf{(1)}$$

where $r$ is the distance vector between the measuring point and a point in the tissue domain, $\nabla$ denotes the gradient operator and $Vm$ is the transmembrane potential distribution. Computed electrograms were stored for further processing at a sampling frequency of 1 kHz.

### 2.2 Causality Analysis Method

Causal relations were searched between $N$ simultaneous neighboring signals, which were divided into $K_n$ overlapping time segments of length equal to the inverse of the DF. Under the assumption that a given observation $x_i(t)$ can result from previous observations in neighboring nodes $x_j(t-\tau)$, their cause-effect relationship level can be assessed by a univariate autoregressive model (ARM):

$$x_i(t) = \sum_{\tau=t_{min}}^{t_{max}} a_\tau \cdot x_j(t-\tau) + \varepsilon_{ij}(t) \quad \textbf{(2)}$$

where $\alpha_\tau$ are the ARM coefficients and $\varepsilon_{ij}(t)$ is the error in the prediction of $x_i$ from $x_j$ by using the ARM, which can be assumed to be a white noise process characterized by its variance $\sigma^2_{\varepsilon ij}$. The order of the ARM model is given by $t_{max}$-$t_{min}$, where $t_{min}=d/v_{max}$, $t_{max}=d/v_{min}$, $d$ is the distance between electrodes, and $v_{max}$ and $v_{min}$ are the maximum and minimum conduction velocities respectively. ARM coefficients are estimated by using the least-squares method [12].

In order to compare the degree of causality between signals with inherent differences in their variance, we use a statistical approach based on influence measure. This measure compares the variance measured by applying the ARM model with source

and destiny signals $\sigma^2_{\varepsilon ij}$ with the variance value $\sigma^2_{\varepsilon ii}$ obtained by applying the model on the destiny signal itself. We defined the Influence Ratio matrix (IR, (3)), computed for a given pair of signals (i,j), as the ratio between variances of the error of ARM models for the source signal ($\sigma^2_{\varepsilon ij}$) and for itself ($\sigma^2_{\varepsilon ii}$):

$$IR_{ij} = \frac{\sigma^2_{\varepsilon_{ii}}}{\sigma^2_{\varepsilon_{ij}}} \quad (3)$$

$$IRN_{ij} = \frac{\frac{1}{K_n}\sum_{k=1}^{K_n} IR_{ij,k}}{\frac{1}{K_n}\sum_{k=1}^{K_n}\sum_{i=1}^{N} IR_{ij,k}} \quad (4)$$

The IR is measured for all the $K_n$ overlapping intervals ($IR_{ij,k}$) and the influence of a signal $x_j$ in a signal $x_i$ is summarized by normalizing the IR matrix (IRN, (4)), where $K_n$ is the number of signal segments under evaluation.

The Recurrence Map (RM) is then constructed by assigning a value between 0 and 1 to each node according to its probability of behaving as a signal source. These probability values (P) are computed by using the following expression:

$$P = M^{\infty} \times P^0 \; ; \; M^{\beta} = M^{\beta-1} \times M^{\beta-1} \; ; \; M^0 = IRN \quad (5)$$

where $M^{\infty}$ is the permanent regime value of IRN matrix and $P^0$ is the initial probability distribution where $P^0 = 1/N$. $M^{\infty}$ is reached when the value of $\xi = var(P^{\beta} - P^{\beta-1})$ reaches an upper threshold ($10^{-10}$).

## 3 Results

With the purpose of demonstrating that atrial drivers during AF can be identified by our causality method we used mathematical models of the atrial electrical activity with three different activation patterns; (i) a functional rotor at the left atrial roof and without a LA- to-RA DF gradient (Fig. 1); (ii) a functional double rotor in 8-figure at the free wall of the right atrium with RA-to-LA DF gradient (Fig. 2); and (iii) a complex pattern with several drivers: two functional reentries at the left atrial roof, two functional reentries at RA and an anatomical reentry around the RIPV (Fig. 3).

In the first mathematical simulation the fibrillatory process is maintained by a rotor placed on the left atrial roof (Fig. 1A), with a uniform activation frequency in both atria (12 Hz), and no DF gradient (Fig. 1B). The RM (Fig. 1C) depicts the results of the causal methodology on this model. It can be observed that the RM values reach 1 at the vicinity of the rotor, marking the position of the atrial driver. At the rest of the tissue the RM values remain close to 0 showing that there is no other atrial source different to the LA rotor.

In Fig. 2A the propagation pattern from a simulation in which the fibrillatory process is maintained by two counter-rotating rotors at the free wall of the RA is shown. In this case there is a RA-to-LA DF gradient (12 Hz RA, 6 Hz LA, Fig. 2B), and the RA, where the rotors are located, is the fastest. The RM (Fig. 2C) shows the highest

values at the free wall of the RA, where the rotors were located. Please note that in this case the area with highest RM values is wider than in the previous case, where there was only a single driver rotor.

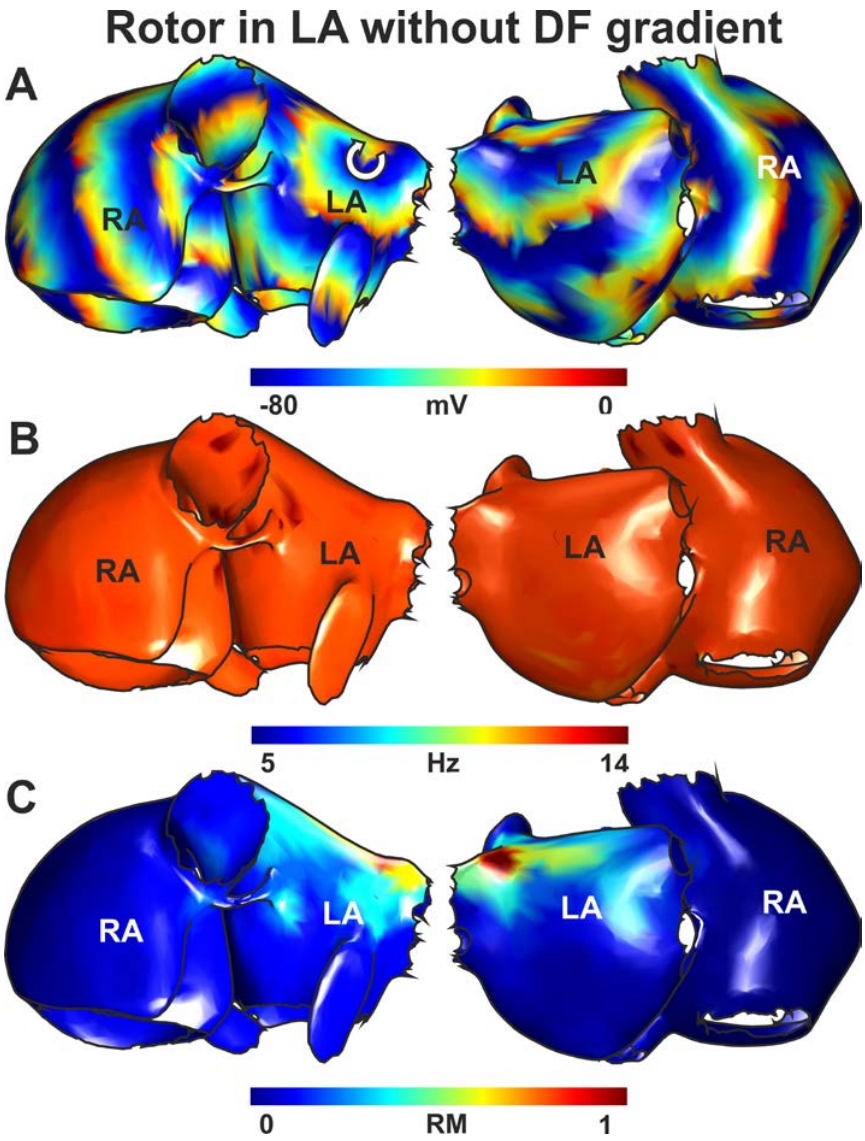


**Fig. 1.** Anterior and posterior views of atrial model with a rotor in LA without DF gradient. (A) Transmembrane potentials. (B) DF map. (C) Recurrence map.

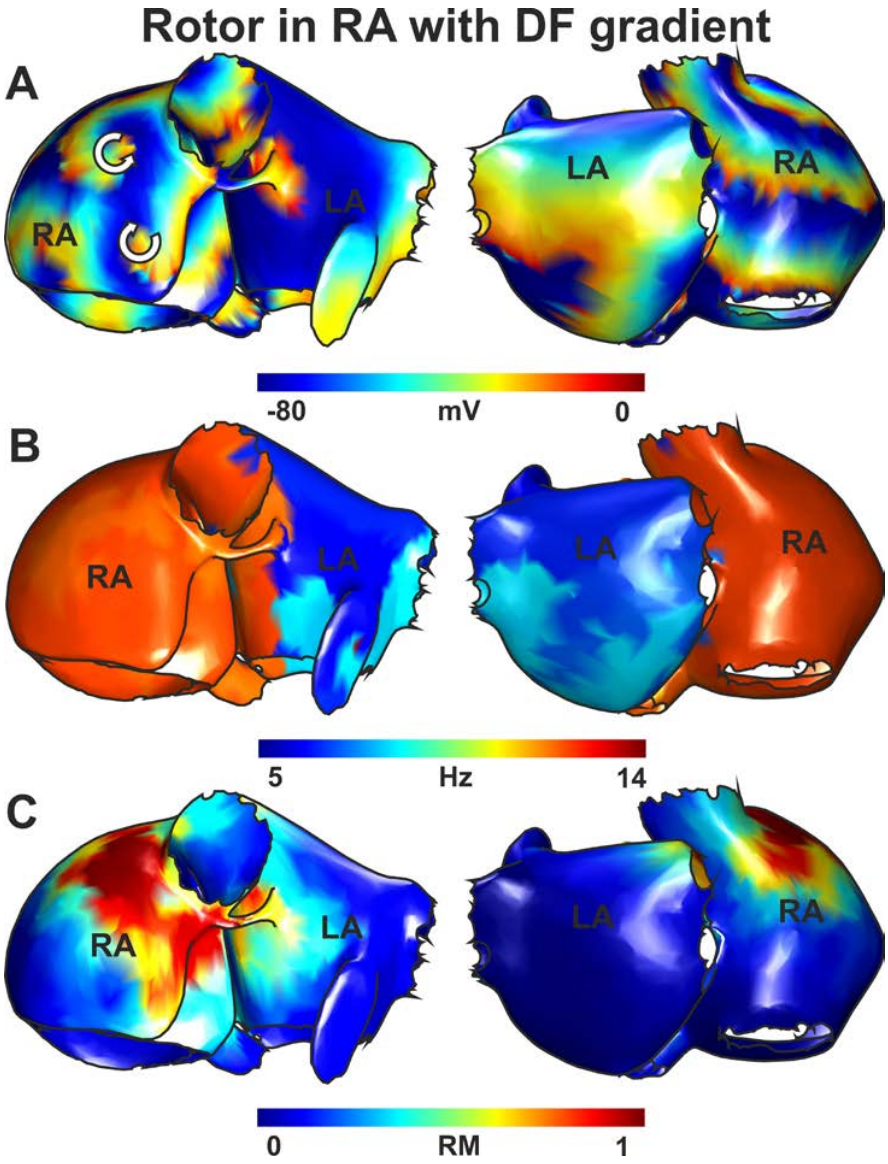


**Fig. 2.** Anterior and posterior views of atrial model with a rotor in RA with DF gradient. (A) Transmembrane potentials. (B) DF map. (C) Recurrence map.

Fig. 3A shows the transmembrane potential from a simulation with several drivers. In this case, the AF was maintained by 4 functional reentries (2 at the left atrial roof and 2 at the RA) and by an anatomical reentry around the RIPV. In this case there is no DF gradient: both atria were activated at the same frequency (12 Hz, Fig. 3B). The RM (Fig. 3C) exhibits several areas with values markedly larger than zero, all of them at positions of the atrial drivers: one at the RA and another at the left atrial roof that also extends around the RIPV. In this case, the RM values of the left atrial roof are higher (1) than the RM values at the RA (0.6).

In order to evaluate the spatial profile of AF sources, the RM nodal values obtained at the different atrial models where plotted against the distance to the source with the highest RM value. Fig. 4A shows the RM nodal values from the first model (maintained by a rotor in the LA roof) in comparison with the distance of those nodes to the rotor core. It can be shown as the closest nodes to the rotor core present higher values of the RM than those nodes placed away from the rotor. The RM values can be represented by an exponential decay function from the distance to the rotor core with relatively high accuracy ($R^2$=0.82). In Fig. 4B the same analysis for the model with two rotors in the RA can be shown. In this case the higher values of the RM are also in the vicinity of the rotors and present an exponential decay with the distance to the atrial driver. The decay curve presents a less steep decay and worse fitting ($R^2$=0.64), due to the presence of 2 rotors (the distance was obtained to the core of one of them) and the wider extension of the dominant area. Finally, Fig. 4C depicts the RM nodal values of the simulation maintained by multiple drivers. Here we can find 2 areas with high RM nodal values, corresponding to the 2 dominant regions in this model: the left atrial roof and the RA. Consequently, the fitted curve presents an adjusted coefficient ($R^2$=0.49) lower than the previous models.

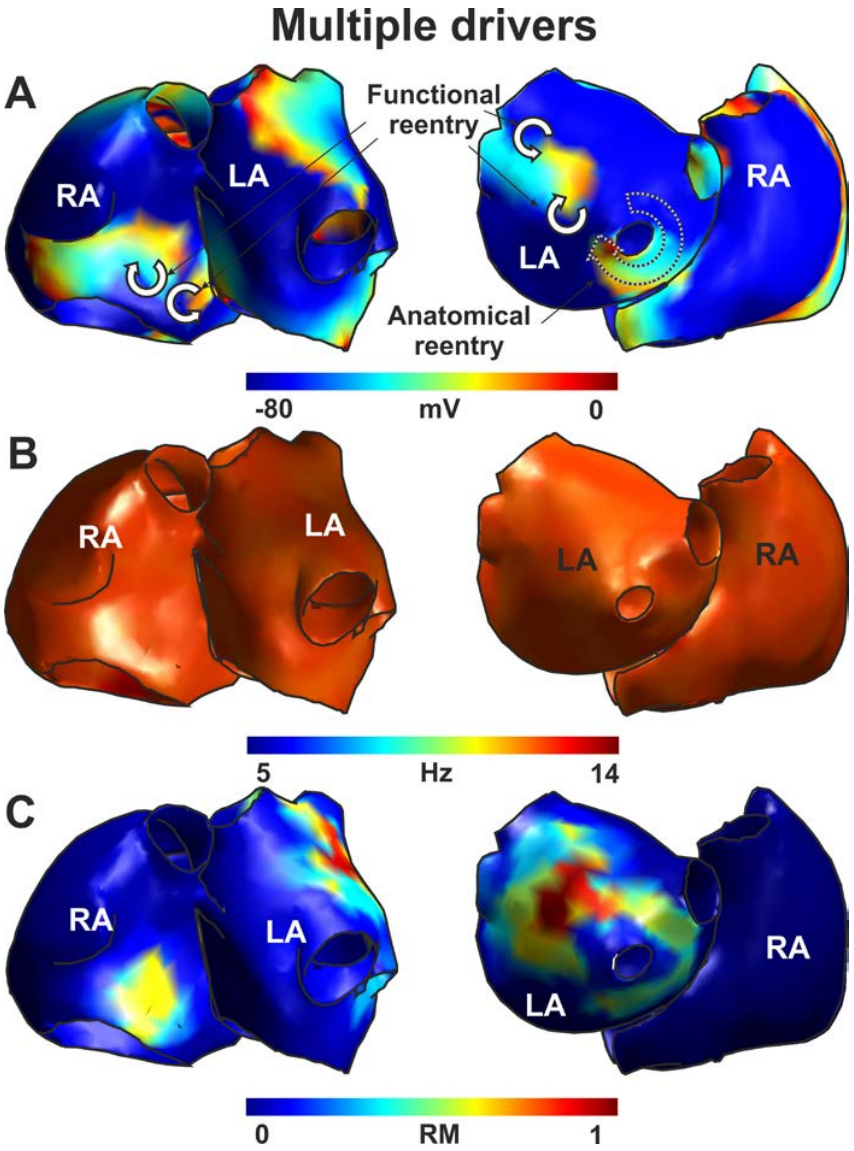


**Fig. 3.** Anterior and posterior views of atrial model with multiple drivers. (A) Transmembrane potentials. (B) DF map. (C) Recurrence map.

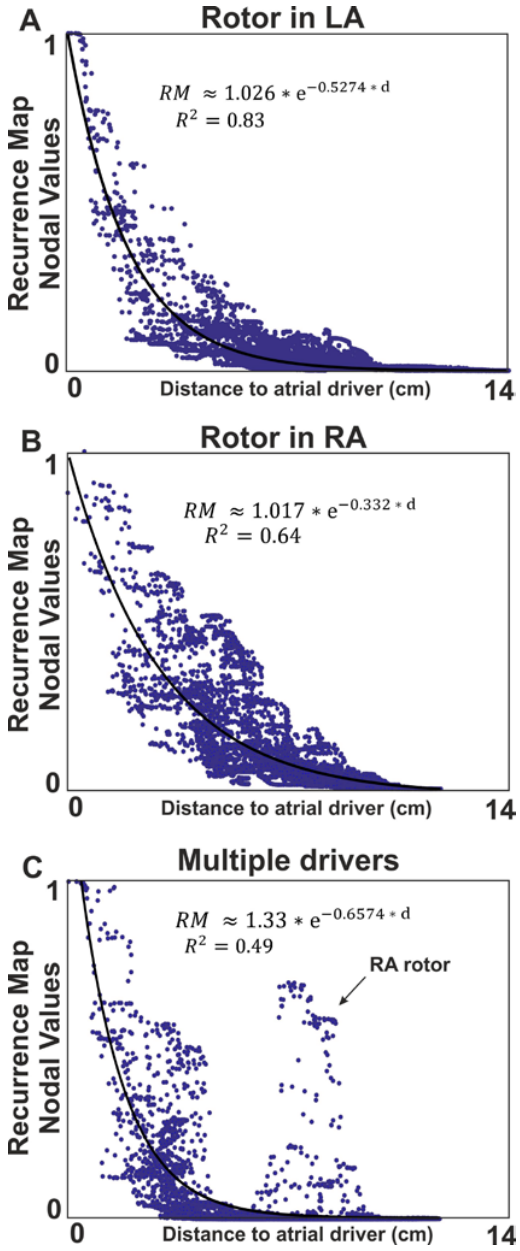


**Fig. 4.** Comparison between the RM values and the distance to the atrial driver for three simulations: (A) Rotor in LA without DF gradient; (B) double rotor in RA; and (C) multiple drivers. (*blue dots*) RM values obtained from the model. (*black line*) the best exponential decay model fitted for these points.

## 4 Discussion

Several clinical studies provide evidence supporting the existence of localized sources responsible for the maintenance of AF [1-5]. These atrial sources have been postulated to be a consequence of either ectopic activity [1-2], micro-reentries or rotors [3] and can be considered as the center of a hierarchical process in the fibrillatory activity. These hierarchical fibrillatory processes can be identified by their electrical activation pattern whereby the region activated at the highest rate and emitting outward waves is the dominant area. In this work we present a novel technique to analyze the electrical activation patterns to find such dominant regions.

The identification of fibrillatory drivers remains a challenging task due to the irregular wave electrical activity during AF. Isochronal and phase maps of cardiac activation are now quite commonly used to study arrhythmia mechanisms and to guide ablative therapies [3, 7]. However, the construction of isochronal and instantaneous phase maps consider of a short time interval for evaluation (i.e. a single activation cycle), which could be non-typical and could lead to maps that depend on the time interval analyzed and give information about the activity only in that time interval. The causal method reduces such limitation, since it summarizes the electrical activity during a longer time interval (i.e. cumulative activations) into a dominant propagation pattern that depicts the electrical activity in the analyzed interval [13].

The identification of the atrial drivers has also been extensively carried out by the dominant frequency (DF) analysis, since the regions higher activation rates are linked with the presence of atrial drivers [6]. However, in the absence of a left-to-right gradient the results of this approach were poor. Here, we demonstrate that in the presence of a DF gradient in the atria, both DF and causality analysis offer similar results. Nevertheless, the proposed method may allow detecting the origin of activations even in absence of DF gradients.

Identification of causal relationships during irregular activations requires a multipole catheter, with as many recording electrodes as possible. However, balloon (non-contact) or basket multi-electrodes are expensive, complex and not readily available. The presented analysis method could also be carried out by sequentially mapping the atria with a multipolar catheter, avoiding the need for the balloon or basket catheters. However, a study using real recordings of animal or human AF will be necessary to validate the usefulness of our methodology.

## 5 Conclusion

This work presented a novel methodology for the identification of the atrial sites which are responsible of AF maintenance. Recurrence maps highlight the top-hierarch of dominant regions in the atria and estimate the corresponding propagation pattern, independently of the spatial distribution of DF. The presented methodology is proposed to be useful for guiding ablation procedures in AF patients.

## References


1. Atienza F., Martins R.P., Jalife J.: Translational research in atrial fibrillation: a quest for mechanistically based diagnosis and therapy. Circ. Arrhythm. Electrophysiol. 5 (2012) 1207-1215
2. Atienza F., et al.: RADAR-AF investigators. Comparison of radiofrequency catheter ablation of drivers and circumferential pulmonary vein isolation in atrial fibrillation: a noninferiority randomized multicenter RADAR-AF trial. J. Am. Coll. Cardiol. 64 (2014) 2455-67
3. Narayan S.M., et al.: Direct or coincidental elimination of stable rotors or focal sources may explain successful atrial fibrillation ablation: on-treatment analysis of the CONFIRM (CONventional ablation for AF with or without focal impulse and rotor modulation) trial. J. Am. Coll. Cardiol. 62 (2013) 137-147
4. Di Biase L., et al.: Atrial fibrillation ablation strategies for paroxysmal patients: randomized comparison between different techniques. Circ. Arrhythm. Electrophysiol. 2 (2009) 113-119
5. Hsu L. F., et al.: Atrial fibrillation originating from persistent left superior vena cava. Circulation 109 (2004) 828–832
6. Atienza F., et al.: Real-time dominant frequency mapping and ablation of dominant frequency sites in atrial fibrillation with left-to-right frequency gradients predicts long-term maintenance of sinus rhythm. Heart Rhythm 6 (2009) 33-40
7. Ideker R.E., Rogers J.M.: Human ventricular fibrillation: wandering wavelets, mother rotors, or both? Circulation 114 (2006) 530-532
8. Harrild D., Henriquez C.A.: Computer model of normal conduction in the human atria. Circ. Res. 87 (2000) E25-36
9. Courtemanche M., Ramirez R.J., Nattel S.: Ionic mechanisms underlying human atrial action potential properties: insights from a mathematical model. Am. J. Physiol. 275 (1998) H301-321
10. Kneller J., Ramirez R.J., Chartier D., Courtemanche M., Nattel S., Time-dependent transients in an ionically based mathematical model of the canine atrial action potential. Am. J. Physiol. Heart Circ. Physiol. 282 (2002) H1437-1451
11. García V.M., et al.: Adaptive step ODE algorithms for the 3D simulation of electric heart activity with graphics processing units. Comput. Biol. Med. 44 (2014) 15-26
12. Richter U., et al.: A novel approach to propagation pattern analysis in intracardiac atrial fibrillation signals. Ann. Biomed. Eng. 39 (2011) 310-323
13. Berenfeld O., et al.: Frequency dependent breakdown of wave propagation into fibrillatory conduction across the pectinate muscle network in the isolated sheep right atrium. Circ. Res. 90 (2002) 1173-1180

# Performance Analysis of a Hybrid WSN Protocol with Congestion Control

Israel Leyva-Mayorga[1], Vicent Pla[1], and Mario E. Rivero-Angeles[2]

[1] ITACA, Universitat Politècnica de València, Valencia, Spain
isleyma@doctor.upv.es, vpla@upv.es
[2] Communication Networks Laboratory, CIC-IPN, Mexico City, Mexico
mriveroa@ipn.mx

**Abstract.** Wireless sensor networks (WSNs) are a cost-efficient solution for massive monitoring; hence they play a critical role in the development of smart environments. For this, a large number of nodes sense the environment and report the gathered data to entities with higher storage and processing capacity. For instance, LTE networks are usually used for relaying the gathered information. Since these networks may suffer from congestion in the physical random access channel (PRACH) due to the large number of connected devices, we propose a WSN protocol for reducing congestion in relaying networks. It focuses on reducing the loss of relevant information while performing continuous monitoring and event detection duties.

## 1 Introduction

The automation of environments and the development of Smart Cities [8] highly rely on wireless sensor networks (WSNs). These are formed by a large number of low cost nodes that auto-organize for data gathering and transmission. Since little to no further maintenance is needed after deployment, WSNs provide a cost-efficient solution to massive monitoring but, nodes being battery supplied, energy consumption was the major downside as replacing batteries may not be viable. However, as technology evolves, energy consumption issues are being mitigated by a longer battery life and the use of energy harvesting systems [7]. As such, the main focus of performance analysis is shifting towards other QoS parameters; i.e., report latency. The relevance of this parameter is application dependent [1]. As an example, agricultural applications may be delay tolerant since the user is interested in long-term evolution of physical parameters; on the other hand, disaster-management applications in industrial facilities require a swift response from the network to hazardous conditions such as chemical leaks, extreme pressure and temperature changes or a damaged component in the assembly line. These are known as critical-time applications. One of the major downsides of WSNs is the large number of nodes simultaneously transmitting data, which causes congestion in relaying networks such as LTE. Specifically, nodes must access the physical random access channel (PRACH) for synchronization or data transmission, but it is not designed to be used for machine to machine (M2M) communication.



C.Fernandez-Llatas and M.Guillen (Ed.):
Workshop on Innovation on
Information and Communication Technologies
(ITACA-WIICT 2015)

ISBN 978-84-608-4139-5

Cluster-based protocols have been widely used for reducing energy consumption [5, 11] and may serve as a simple solution for LTE network congestion. In these protocols, nodes are periodically organized in groups named clusters, each containing a cluster head (CH) and several cluster members (CMs). This organization is performed during a cluster formation (CF) phase. Then nodes proceed to perform environmental monitoring duties in the steady-state phase (SSP). Here, CHs serve as a relay node between the CMs and the sink or relaying network. As a result, fewer nodes must compete for the resources of the LTE network. Even though clustering methods may reduce medium congestion, it is also advisable to reduce the frequency of CH transmissions. In other words, cluster-based WSN protocols with infrequent medium access requests work best to mitigate congestion in relaying networks. Nevertheless, industrial applications may benefit from the inclusion of mobile nodes, which is oftentimes handled by including additional synchronization phases; thus increasing the traffic injected to the network. An interesting option for avoiding this issues are cognitive radio sensor networks (CRSN). In cognitive radio, devices with no frequency band concession sense the medium to identify access opportunities; hence transmitting its data without interfering with the primary users of the network. As such, mobile nodes may perform event reporting duties by means of CR. As a result, no further synchronization is required.

In this study we present WISPER (WIreless sensor network alternating cntm/cr Slots protocol for Preemptive Event Reporting), a cluster-based protocol that performs event reporting by means of a TDMA schedule. It uses a sleep-awake schedule [4] along with medium sensing in order to perform continuous monitoring (CntM) and event reporting simultaneously. Congestion control is also considered, along with cognitive radio, which enables this protocol to operate even when overlapping with other WSNs.

The rest of the paper is organized as follows: Section 2 summarizes previous studies on disaster management WSNs and cognitive radio sensor networks (CRSN), then, Section 3 describes WISPER, the proposed protocol for CntM and event reporting. We study the performance of this protocol and the article concludes with the conclusions and future work.

## 2 Related Work

Achieving continuous monitoring (CntM) and event reporting provides the sink with plenty of information to characterize the environment, along with a timely report of occurring events. This behavior may be achieved by either temporal or spatial segmentation of the network. In the former, nodes alternate between CntM and event detection (ED) duties [6] according to a predefined time schedule. In the latter, the network selects certain nodes to perform CntM while others perform [3]. Both approaches may enhance energy consumption and event report latency given the nodes rotate duties continuously. Otherwise the distribution of the consumed energy among nodes may not be uniform; hence certain nodes are prone to battery depletion. Additionally, industrial environments usually in-

clude mobile nodes for servicing purposes; hence the need for protocols that consider periodical synchronization phases between the CHs and mobile nodes [9]. These issues may be solved by CRSN, but first, some communication shortcomings must to be solved. First, adequate medium sensing must be conducted, which may be challenging for low cost devices. Some studies suggest the use of coordinators [10], which may be viable for industrial environments but not for some environmental applications where continuous energy supply is not possible. Also, CR is usually used in devices that are able to transmit data on several frequency bands. As stated earlier, nodes in WSNs are severely limited devices that may include a single antenna. Consequently, the use of CR over one frequency band has been studied [2]. We follow this approach for the transmission of event packets on WISPER.

## 3 WISPER

WISPER (WIreless sensor network alternating cntm/cr Slots protocol for Preemptive Event Reporting) is a cluster-based WSN protocol that relies on TDMA for CntM. On the other hand, event reporting is conducted by means of a single-frequency cognitive radio approach. The time schedule of WISPER (shown in Fig.1 is divided in rounds and each one starts with a cluster formation (CF) phase. During this phase CHs and CMs are selected randomly. Furthermore, CMs decide between performing CntM or ED for the present round. Once CF is over, nodes perform data transmission for a predefined number of time slots until the next scheduled CF phase. The TDMA schedule is comprised of $M$ time slots and the CH sequentially assigns one of these time slots to the CMs in charge of CntM. When $M$ time slots have elapsed, the CH sends the gathered data to the sink. We use a fixed value for $M$ to avoid frequent CH access to the medium in smaller clusters; i.e., in TDMA based protocols such as in [5], the length of TDMA schedules depends of the number of CMs.

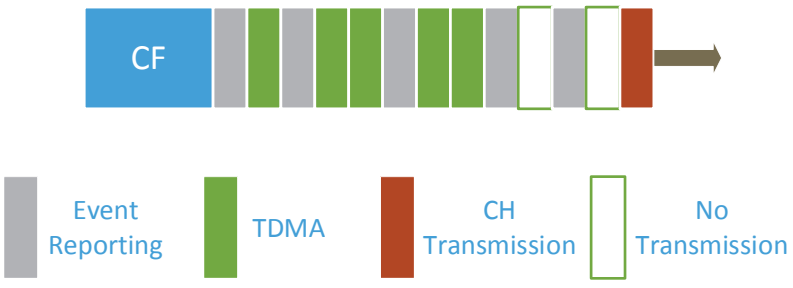


**Fig. 1.** Time schedule for WISPER.

In order to lower energy consumption, CntM CMs start the steady state phase (SSP) either awake, $A$ or asleep $B$, where $P(a) = 1 - P(b) = 0.5$ and alternate between sleep and awake states according to a random process with rates $\alpha$ and $\beta$. As such the probabilities of a node being on either state are given by

$$P(a) = \frac{1/\alpha}{1/\alpha + 1/\beta} \tag{1}$$

$$P(b) = \frac{1/\beta}{1/\alpha + 1/\beta} \tag{2}$$

Whenever a CntM is in sleep state it is unable to transmit data; therefore, the TDMA slot reserved for its transmission is not used. This liberates time slots that can be used for the ED CMs given an event is detected. For this, ED nodes use a single-band CR approach where they sense the medium to identify available time slots. Congestion control is performed by the CHs by counting the number of time slots that were not used during the last TDMA schedule and the number of transmitted event packets. For this, whenever transmission was not attempted for at least one time slot, no further action is needed. On the other hand, whenever transmission is attempted in every time slot and at least one event packet was received, the CH sends a congestion signal during its assigned time slot. When CntM nodes detect this signal, no TDMA transmissions are attempted for the next schedule. As a result, ED CMs are able to report the detected event.

## 4 Performance Analysis

Performance analysis of the proposed protocol is conducted by means of a discrete-time simulator we developed in $C++$. It has been validated in previous studies. Since event reporting is performed by means of CR on a TDMA-based schedule, report latency depends only on the size of $M$. Therefore, we focus our performance analysis in energy consumption and the number of packets discarded per TDMA schedule. As such, we first analyze the effect of $M$ on energy consumption. The main parameters used for the simulation are listed in Table 1.

As a result, the energy for transmitting a packet,

$$E_{tx}(l, d) = l \times E_{elec} + l \times \epsilon_{fs} \times d^2, \tag{3}$$

depends on the packet length, the transmission range, the energy required by the communication circuits, $E_{elec}$, and the energy consumed by the amplifier as in [5]. The energy for medium sensing depends on the number of sensed bits by

$$E_{rx}(l) = l \times E_{elec}. \tag{4}$$

For studying the viability CR for event reporting, we simulated time schedules where an event is detected by each CR node with probability $P(e)$ each $M$

**Table 1.** Simulation parameters.

| Parameter | Variable | Value |
|---|---|---|
| Network area | | $100 \times 100\ m$ |
| Deployed nodes | $N_t$ | 100 |
| Sink coordinates | | $(200\ m, 0)$ |
| Packet length | $l$ | $2\ kbits$ |
| Electronics energy | $E_{elec}$ | $50\ nJ/bit$ |
| Amplifier energy | $\epsilon_{fs}$ | $10\ pJ/bit/m^2$ |
| Transmission data rate | | $40\ kbps$ |
| CM transmission range | $d_{CM}$ | $35\ m$ |
| CH transmission range | $d_{CH}$ | $\sqrt{200^2 + 100^2}\ m$ |

time slots. The power consumption of WISPER is compared with the power consumption of a characteristic TDMA protocol; namely LEACH and shown in Fig. 2.

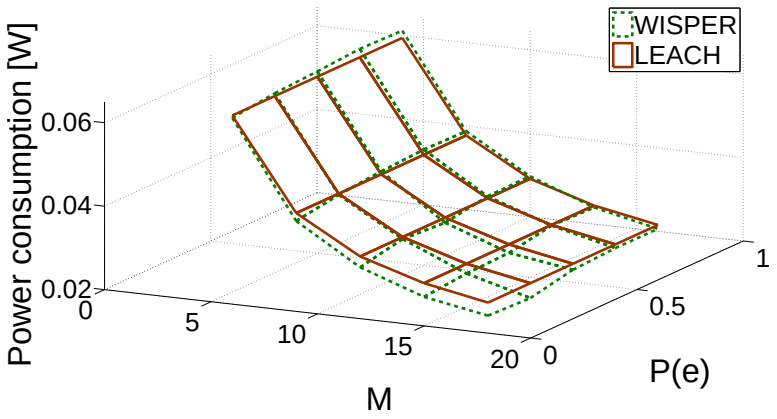


**Fig. 2.** Power consumption comparison between WISPER and LEACH.

Note that WISPER maintains adequate energy efficiency even when the medium is highly congested. This is an advantage of TDMA-based protocols when compared to RA, where a highly congested medium leads to collisions and energy wastage. Also, note the reduction in power consumption for larger values of $M$. This is due to the fact that the larger $M$, the higher probability that time slots are not assigned and CH transmissions (highly power consuming) are less frequent. As a result, the congestion of both, the WSN and relaying networks is reduced in exchange of a reduction in the volume of data sent to the sink. Consequently, the network administrator must select $M$ for obtaining the desired

volume of data while also maintaining energy efficiency and congestion levels in relaying networks.

In this same scenario we studied the number of discarded packets. It can be seen in Fig. 3 that the shorter the TDMA schedule, the larger the number of discarded event packets for higher $P(e)$. In addition, Fig. 3 illustrates the effect of the congestion control technique. Whenever the CH detects he medium as congested, sends a message for dropping CntM packets. As a result, the vast majority of time slots are used for event reporting. Despite this behavior, note that a large number of event packets are discarded when $M \leq 10$ because the number of time slots is insufficient for allocating the number of CR nodes with event packets. Also, observe that some event packets are discarded even when

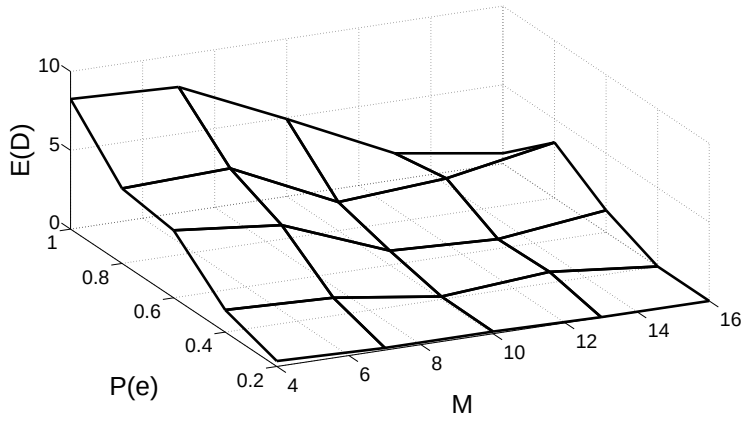


**Fig. 3.** Mean number of discarded packets.

$M = 16$. This is caused by sudden changes in the state of nodes; i.e., from asleep to awake. As a result, a time slot detected as available during on the past is now used and CR nodes are unable to transmit. Nevertheless, by using this protocol, the vast majority of event packets are transmitted successfully. Hence, it is a viable approach for the selected applications.

## 5 Conclusion

By identifying some issues in massive monitoring for smart environments, we were able to propose WISPER, a TDMA-based WSN protocol. The aim of WISPER is sending high volumes of CntM and ED data to the sink while maintaining energy efficiency and reducing the frequency of transmissions to relaying networks. By selecting longer TDMA schedules; i.e., larger values of $M$, the consumed energy per TDMA schedule rises, but the consumed power drops. Also,

the larger $M$, the lower the CH transmission frequency; hence reducing congestion in the uplink channel. This protocol also shows high immunity to medium congestion, which is a common problem in RA event reporting. As such, the number of discarded event packets is minimized. Furthermore, WISPER being a TDMA-based protocol, report latency remains adequate regardless of the event behavior.

During this study, we assume CR nodes are capable of detecting an available time slot and transmitting its event packet immediately; nevertheless, this may not be possible in real life applications. As such, medium sensing methods such as the use of coordinators decision factors can be proposed. Also, the inclusion of mobile CR nodes is not studied in this work, yet it seems like an efficient solution for synchronization issues in industrial environments with mobile servicing devices.

## 6 Acknowledgements

This work has been supported by the Ministry of Economy and Competitiveness of Spain through the project TIN2013-47272-C2-1-R.

## References

1. Akyildiz, I.F., Su, W., Sankarasubramaniam, Y., Cayirci, E.: Wireless sensor networks: A survey. Computer Networks 38(4), 393–422 (2002)
2. Bae, Y.H., Alfa, A.S., Choi, B.D.: Performance analysis of modified IEEE 802.11-based cognitive radio networks. IEEE Commun. Lett. 14(10), 975–977 (2010)
3. Bouabdallah, N., Rivero-Angeles, M.E., Sericola, B.: Continuous monitoring using event-driven reporting for cluster-based wireless sensor networks. IEEE Trans. Veh. Technol. 58(7), 3460–3479 (2009)
4. Guo, P., Jiang, T., Zhang, Q., Zhang, K.: Sleep scheduling for critical event monitoring in wireless sensor networks. IEEE Trans. Parallel Distrib. Syst. 23(2), 345–352 (2012)
5. Heinzelman, W.B., Chandrakasan, A.P., Balakrishnan, H.: An application-specific protocol architecture for wireless microsensor networks. IEEE Trans. Wireless Commun. 1(4), 660–670 (2002)
6. Leyva-Mayorga, I., Rivero-Angeles, M.E., Carreto-Arellano, C., Pla, V.: QoS analysis for a nonpreemptive continuous monitoring and event-driven WSN protocol in mobile environments. International Journal of Distributed Sensor Networks 2015 (2015)
7. Paradiso, J.A., Starner, T.: Energy scavenging for mobile and wireless electronics. IEEE Pervasive Comput. 4(1), 18–27 (2005)
8. Perera, C., Zaslavsky, A., Christen, P., Georgakopoulos, D.: Sensing as a service model for smart cities supported by internet of things. European Transactions on Telecommunications 25(1), 81–93 (2014)
9. Raja, A., Su, X.: A mobility adaptive hybrid protocol for wireless sensor networks. In: Proc. IEEE Consumer Communications and Networking Conference (CCNC). pp. 692–696 (2008)

10. Yau, K..A., Komisarczuk, P., Teal, P.D.: Cognitive radio-based wireless sensor networks: Conceptual design and open issues. In: Proc. Conference on Local Computer Networks (LCN). pp. 955–962 (2009)
11. Younis, O., Fahmy, S.: HEED: A hybrid, energy-efficient, distributed clustering approach for ad hoc sensor networks. IEEE Trans. Mobile Comput. 3(4), 366–379 (2004)

# Triggered TDMA approach for Energy Efficient Underwater Localization

Raúl Sáez-Cañete, Pedro Yuste, Angel Perles, Ricardo Mercado, and Juan Jose Serrano

Universitat Politècnica de València, Instituto ITACA,
Camí de Vera s/n, 46022 València, Spain.
rsaez@itaca.upv.es,pyuste@disca.upv.es,
aperles@disca.upv.es, rmercado@itaca.upv.es, jserrano@itaca.upv.es
Area of interest: Underwater Communications

**Abstract.** Energy efficiency is an important issue in underwater applications since underwater devices are energy-constrained and their recovery and replacement are expensive. Hence, underwater localization protocols must maintain the overhead of energy consumption as low as possible in order to achieve long term deployments.
This work examines the energy efficiency of a TDMA-based localization approach which uses underwater modems with wake-up systems in order to trigger the localization protocol. The trigger mechanism could allow devices to keep into low power mode as long as possible and avoid the additional synchronization mechanism needed in TDMA-based protocols. The proposal is evaluated by comparing it to an energy efficient TDMA approach through simulations. Results show that the proposal can achieve an energy efficiency close to efficient TDMA approach but without additional synchronization. A sea test performed at a harbor validates simulation results and confirms the feasibility of the proposal.

**Keywords:** underwater localization; energy efficiency; TDMA; wake-up; triggered wake-up; simulation; ns3

## 1 Introduction

The monitoring and exploration of Oceans are fundamental to increase the knowledge about biodiversity and the understanding on climate change. These important long term challenges are being faced with continuous research in mobile underwater sensor networks (UWSN). These networks are formed by a set of underwater sensors working together with one or several underwater vehicles forming a swarm. The localization information is a valuable resource for this type of networks. On the one hand, monitoring applications can use this information for locating events in an interest area. On the other hand, underwater vehicle navigation and underwater swarm formation can take advantage of this information to increase their precision and reliability.

The most common method for obtaining the localization information is ranging [1], a method based on the estimation of the underwater propagation time in



C.Fernandez-Llatas and M.Guillen (Ed.):
Workshop on Innovation on
Information and Communication Technologies
(ITACA-WIICT 2015)

ISBN 978-84-608-4139-5

order to calculate distances. This method has two different approaches, one-way travel time (OWTT) and two-way travel time (TWTT).

The OWTT approach obtains the ranging information from a single message sent by a node with known localization [2]. This approach requires strong synchronization between transmitter and receiver in order to estimate message propagation time from the transmission timestamp and the reception time. The TWTT approach is used for traditional localization systems such as long baseline (LBL) or ultra-short baseline (USBL). This approach obtains the ranging information for exchanging messages between the unlocalized node and one or several beacons with known location [3]. The message exchange mitigates the synchronization and avoids the need of additional synchronization mechanisms.

Regardless of the ranging method used, localization protocols must use a medium access control (MAC) protocol to ensure that all network devices have access to the underwater channel. Time division multiple access (TDMA) is used for underwater localization due to its simplicity and collision-free properties. Devices have a slot time assigned and messages can only be sent inside the slot. Thus, no retransmissions are needed for channel sharing and devices can save energy. However, TDMA suffers from clock drift hence synchronization mechanisms are required to compensate it periodically in long term applications.

This work proposes the use of underwater modems with an integrated wake-up system in a TDMA-based localization approach which uses a wake-up signal to trigger the localization protocol in a mobile UWSN with fixed beacons at known locations. The trigger mechanism is initiated by a vehicle only when it needs to know its localization. Hence, the beacons could remain into low power mode as long as possible. Besides, the trigger can be used to compensate for the clock drift suffered by TDMA and could allow obtaining TWTT ranging measures without previous synchronization.

To evaluate the proposal, ns3 models of the proposal were implemented and a comparison between the proposal and an energy efficient TDMA approach was performed through simulations. Results show that the proposal increases the energy efficiency of beacons thanks to the trigger mechanism and overcomes the efficient TDMA approach by achieving a lifetime of the overall system close to the TDMA approach but without the need of a periodic synchronization mechanism. These results were validated in a sea test performed at a harbor confirming the feasibility of the proposal.

The rest of the paper is organized as follows: section 2 presents the background of this work and describes related work in TDMA-based underwater localization. Section 3 describes the triggered TDMA approach. Section 4 presents simulations performed to compare the triggered TDMA approach to an energy efficient TDMA approach in terms of energy efficiency and discusses the obtained results. In section 5, a sea test performed at a harbor to validate simulation results is presented. Finally, in section 6, conclusions are drawn and the future work is presented.

## 2 Related Work

Underwater MAC protocols ensure that all devices of an underwater network have access to the underwater channel. Research in UWSN has resulted in many MAC protocols with different complexity and advantages. A complete review of underwater MAC protocols can be found in [4].

Underwater ranging-based localization protocols must consider the underlying MAC protocol used to access to the underwater channel due to the possible impact in the localization [5] and energy consumption. TDMA has been used both for the localization of vehicles in underwater mobile wireless networks [6] [7] as for the localization of underwater vehicle in swarms [8] due to its simplicity and collision-free properties. However, TDMA suffers from clock drift and collision-free property can not be maintained in long term applications. Consequently, periodical synchronization mechanisms are required to compensate the clock drift. This problem is solved in [9] by means of an on-demand approach in which the vehicle initiates TDMA broadcasting a message with a transmission timing delay sequence for anchor nodes.

Energy efficiency is a major requirement in underwater monitoring applications due to the needed of long term deployment. In [10], TDMA-W adapts the TDMA protocol to use an optimal sleep cycle in order to increase energy efficiency. In [11], a study of power management techniques shows that wake-up systems have a strong potential and perform almost as well as the ideal sleep cycle solution. In the last years, modems with integrated wake-up system such as the Wills modem [12] and the ITACA modem [13] have enabled the use of low power modes without previous synchronization by taking advantage of trigger wake-up signals. This has allowed the research of more energy efficient underwater protocols and the adaptation of existing protocols to increase the energy efficiency. In [14], a complete study of relevant underwater MAC protocols adapted to use wake-up systems can be found.

## 3 Triggered TDMA approach

The purpose of triggered TDMA approach is to support the localization of an underwater vehicle (AUV, glider, ROV, etc.) by means of a set of fixed beacons with known location maintaining the overhead in the energy consumption as low as possible. The beacons can be nodes of an underwater sensor network or beacons deployed specifically for that purpose.

In the triggered TDMA approach, the beacons are passive and remain into low power mode until the reception of a trigger sent by the vehicle when it needs to know its localization. The trigger consists in a wake-up signal followed by a data message. Both messages are separated by a time interval long enough to allow for receiver awakening.

When a beacon receives the first data bit, it schedules its TDMA slot and waits into low power mode after receiving the entire data message. In this way, the TDMA slot scheduling is independent of the wake up signal detection time

and the hardware wake-up time. Note that the beacon with the first slot starts its slot immediately hence the data reception is performed inside its slot, unlike other beacons.

Once the TDMA slot is reached, the beacon sends a data message inside the scheduled slot. When the vehicle receives this message, it can calculate the propagation time of the beacon using a two-way range estimation. After receiving the data of all beacons, the vehicle can enter low power mode. Figure 1 illustrates the described approach.

Two-way ranging does not need synchronization, hence the triggered TDMA approach can support the underwater localization without a previous synchronization protocol. However, the trigger mechanism has an overhead in the energy consumption both for the beacons and for the vehicle. The beacons increase their slot length due to the reception of vehicle data. Accordingly, the vehicle increases the overall reception time needed to receive the data from beacons.

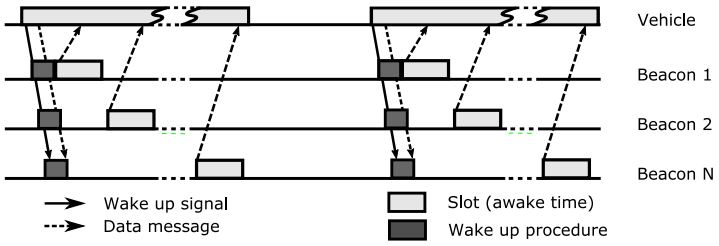


**Fig. 1.** Triggered TDMA.

In applications where the vehicle needs to know its localization frequently, the transmission of trigger messages together with high reception times can quickly exhaust its energy. To avoid this, the vehicle can use the low power mode intensively.

In the triggered TDMA with intensive low power, the vehicle enters low power mode after the reception or the transmission of any data message for saving energy. As a result, beacons must send a trigger to transmit data to the vehicle. Thus, the beacon slot is increased and the vehicle saves energy at the expense of increasing the energy consumption of all beacons. Note that the beacon data message is included into the trigger, this way no additional messages are needed. Figure 2 illustrates this approach.

It is noteworthy that the two triggered TDMA approaches can be used to perform bidirectional communications while the vehicle estimates its localization. This can be useful in several applications such as underwater monitoring and cooperative localization.

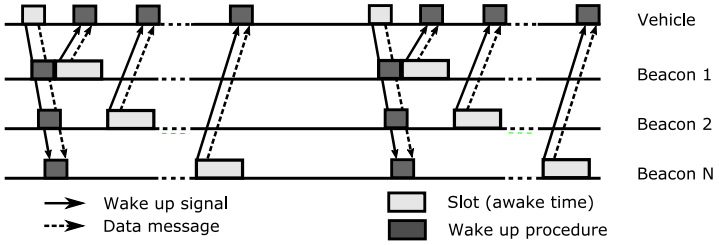


**Fig. 2.** Triggered TDMA with intensive low power.

## 4 Simulation

The aim of simulations is to assess the energy efficiency of two triggered TDMA approaches in order to ascertain its feasibility. For that, the two triggered TDMA approaches are compared to a TDMA approach in a simple scenario using the ns3 simulator. The TDMA approach consists of a set of beacons sending constantly a localization message following the TDMA-W protocol. Meanwhile, the vehicle listens to messages passively obtaining ranging information through OWTT.

### 4.1 Configuration

The simulation scenario consists in a square area of 4 x 4 meters with four beacons placed at the edges and a static vehicle placed at the center. All nodes are powered with a li-ion cell PowerStream Lir2032 [15] which is modeled by the ns3 LiIonEnergySource model with a total capacity of 466 Joules. The underwater channel characteristics are modeled by the ns3 thorp propagation model with a spreading coefficient of 1.5 and a sound speed of 1500 m/s, the default ns3 noise model described in [16] with a wind speed of 1 m/s without any boat traffic contribution to noise and the default ns3 error model which does not discard any packet in this scenario.

The vehicle is configured in a different way depending on the approach. In the two triggered TDMA approaches, the vehicle is configured for sending a trigger each 1320 milliseconds. In the TDMA approach, the vehicle is configured to remain in idle mode indefinitely. The beacons are configured to use a TDMA slot length of 390 milliseconds. This slot length is the biggest optimal slot of three approaches i.e. it is the optimal slot for triggered TDMA approach with intensive low power. The optimal slot for each approach can not be used because a smaller slot results in a higher number of sent messages during the same time interval, hence the obtained results of each approach will not be comparable. For this reason, the slot must be the same for all approaches. However, a slot longer than the optimal causes an overhead in the energy consumption produced by the idle state. For solving this problem, beacons switch to low power mode immediately upon sending their reply.

### 4.2 Results

Each approach is simulated until the vehicle is depleted or all beacons are depleted. Simulations are performed until getting a confidence interval of 1 Joule for energy with a confidence level of 95% for each approach. To assess independent replications, all simulations use the ns3 default seed for generating random numbers but advancing the substream [17] in each one. The obtained results are depicted in Fig. 4 and Fig. 3.

Figure 3 shows the vehicle remaining energy over time. As expected, the triggered TDMA approach has the highest energy consumption due to the overhead of trigger transmission. The triggered TDMA approach with intensive low power shows a power consumption close to TDMA approach. However, the intensive usage of low power mode can not compensate the overhead due to the trigger transmission and the constant passive idle mode of TDMA approach remains the best option.

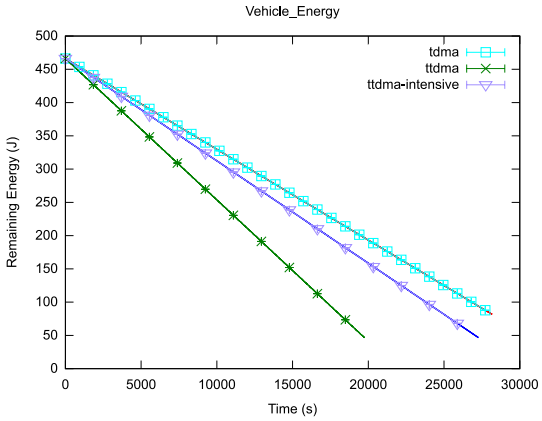


**Fig. 3.** Simulation results for the vehicle.

Figure 4 shows the remaining energy of beacons over time. All beacons show the same behavior except the beacon with the first slot. Its energy consumption is less than the other beacons since the reception of triggered data is performed inside its slot instead of inside the waiting time of the slot.

As expected, the TDMA approach has the highest energy consumption due to the transmission of useless messages when the vehicle is not interested. The triggered TDMA approach shows the lowest energy consumption but the vehicle is depleted rapidly and the lifetime of the overall system is the shortest. The triggered TDMA approach with intensive low power achieves an increase of the vehicle life time at the expense of the increase of the beacon energy consumption. Beacon triggered transmissions allow the vehicle to use the low power mode and

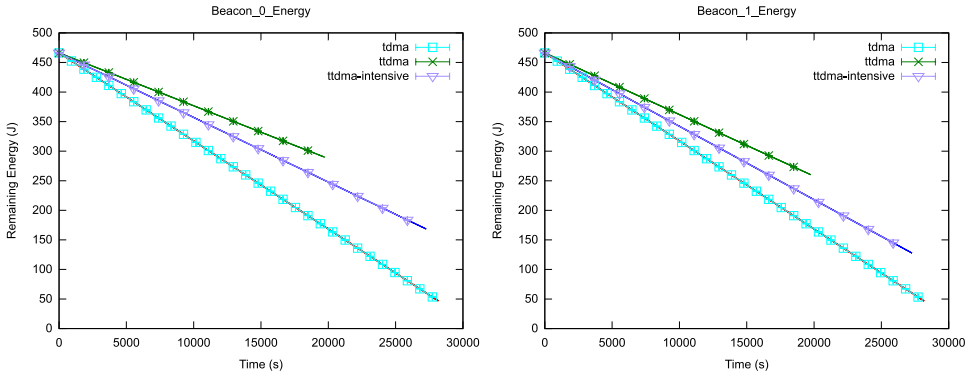


**Fig. 4.** Simulation results for beacons.

the lifetime of the overall system is increased until being close to the TDMA approach.

Note that the TDMA approach has the highest lifetime of the overall system but the beacons are depleted before the vehicle. In real applications, the vehicle is less energy constrained than beacons therefore the triggered TDMA approach with intensive low power should be most suitable in long term deployments.

## 5 Sea test

To validate simulation results, a sea test was performed at Pobla Marina (Valencia, Spain) harbor. The scenario modeled in simulations was built on a dock using telescopic poles and distances were maintained as similar as possible. The vehicle and the beacon side of protocols were implemented directly into ITACA modems and a hydrophone was used for recording transmissions. Nodes were powered with continuous 5v power supplies and the energy consumption in each node was derived from average current measured using a multimeter.

The TDMA slot used in simulations was expanded a 10% to deal with difficulties of a real sea test. The underwater environment is harsh, channel conditions change with the time (e.g: sound speed) and noise can take up the channel for some time. Besides, real clocks have limited precision and the drift can affect synchronization. Hence, the optimal TDMA slot can not be used safely in a real environment.

The sea test was conducted for 4 hours for each approach and the power consumption in each node was recorded manually each 5 minutes. For allowing the comparison with simulation results, the power consumption was converted in Joules and was subtracted to the total energy of battery used in simulations. The results are shown in Fig. 5 and Fig. 6.

Figure 5 shows the vehicle remaining energy over time. As in simulation results, the triggered TDMA approach has the highest energy consumption. How-

ever, the triggered TDMA with intensive low power approach presents a lower energy consumption than the TDMA approach.

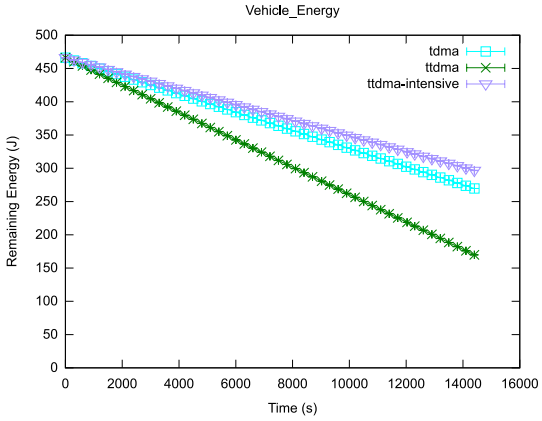


**Fig. 5.** Sea test results for the vehicle.

Figure 6 shows the remaining energy of beacons over time. As in simulation results, the beacon with the first slot has less energy consumption than others and the TDMA approach has the highest energy consumption. Nevertheless, the triggered TDMA approach presents less energy consumption than in simulations.

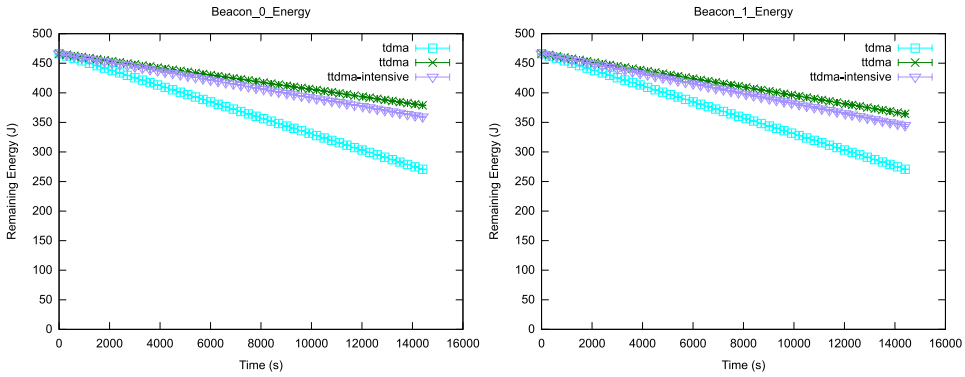


**Fig. 6.** Sea test results for beacons.

The lower energy consumption in triggered TDMA approaches does not mean that these approaches are better than expected in real environments. This be-

havior is due to trigger loss. When a vehicle trigger is lost, beacons do not wake up and do not send replies hence the beacon energy consumption does not increase. Similarly, in triggered TDMA with intensive low power approach, the vehicle is asleep waiting for beacon responses. If beacons do not send replies or the beacon trigger is lost, the vehicle does not wake up and consumes less energy.

## 6 Conclusions

This work has presented a triggered TDMA approach for underwater localization which takes advantage of triggered wake up systems in order to maintain nodes in low power mode as long as possible.

The approach has been tested and compared in terms of energy consumption with an energy efficient TDMA approach through simulations and a sea test. Simulation results show that this approach overcomes the TDMA approach in beacons and can achieve a lifetime of the overall system close to a TDMA approach but without the need for a periodic synchronization mechanism. Hence, this approach is a good starting point for further works. Sea test results validate this conclusion but expose a major limitation, the trigger loss.

Future work will include the evaluation of this approach using more realistic channel models, the evaluation in scenarios with mobility and, finally, the application in real vehicles. In addition, the trigger loss problem will be addressed through the research and evaluation of retransmission-based schemes which should maintain low power consumption limiting retransmissions, e.g. using adaptive timeouts.

## Acknowledgments

This work was supported by the Spanish government under projects CTM2011-29691-C02-01 and TIN2011-28435-C03-0.

## References

1. Erol-Kantarci, M., Mouftah, H., Oktug, S.: A survey of architectures and localization techniques for underwater acoustic sensor networks. Communications Surveys Tutorials, IEEE **13**(3) (Third 2011) 487–502
2. Eustice, R.M., Singh, H., Whitcomb, L.L.: Synchronous-clock, one-way-travel-time acoustic navigation for underwater vehicles. Journal of Field Robotics **28**(1) (2011) 121–136
3. Kussat, N., Chadwell, C., Zimmerman, R.: Absolute positioning of an autonomous underwater vehicle using gps and acoustic measurements. Oceanic Engineering, IEEE Journal of **30**(1) (Jan 2005) 153–164
4. Nguyen, H., Shin, S.Y., Park, S.H.: State-of-the-art in mac protocols for underwater acoustics sensor networks. In Denko, M., Shih, C.s., Li, K.C., Tsao, S.L., Zeng, Q.A., Park, S., Ko, Y.B., Hung, S.H., Park, J., eds.: Emerging Directions in Embedded and Ubiquitous Computing. Volume 4809 of Lecture Notes in Computer Science. Springer Berlin Heidelberg (2007) 482–493

5. Kim, J.P., Tan, H., Cho, H.S.: Impact of mac on localization in large-scale seabed sensor networks. In: Advanced Information Networking and Applications (AINA), 2011 IEEE International Conference on. (March 2011) 391–396
6. Corke, P., Detweiler, C., Dunbabin, M., Hamilton, M., Rus, D., Vasilescu, I.: Experiments with underwater robot localization and tracking. In: Robotics and Automation, 2007 IEEE International Conference on. (April 2007) 4556–4561
7. Munafo, A., Sliwka, J., Ferri, G., Vermeij, A., Goldhahn, R., Lepage, K., Alves, J., Potter, J.: Enhancing auv localization using underwater acoustic sensor networks: Results in long baseline navigation from the collab13 sea trial. In: Oceans - St. John's, 2014. (Sept 2014) 1–7
8. Caiti, A., Calabro, V., Fabbri, T., Fenucci, D., Munafo, A.: Underwater communication and distributed localization of auv teams. In: OCEANS - Bergen, 2013 MTS/IEEE. (June 2013) 1–8
9. Carroll, P., Mahmood, K., Zhou, S., Zhou, H., Xu, X., Cui, J.H.: On-demand asynchronous localization for underwater sensor networks. Signal Processing, IEEE Transactions on **62**(13) (July 2014) 3337–3348
10. Chen, Z., Khokhar, A.: Self organization and energy efficient tdma mac protocol by wake up for wireless sensor networks. In: Sensor and Ad Hoc Communications and Networks, 2004. IEEE SECON 2004. 2004 First Annual IEEE Communications Society Conference on. (Oct 2004) 335–341
11. Harris, III, A.F., Stojanovic, M., Zorzi, M.: Idle-time energy savings through wake-up modes in underwater acoustic networks. Ad Hoc Netw. **7**(4) (June 2009) 770–777
12. Wills, J., Ye, W., Heidemann, J.: Low-power acoustic modem for dense underwater sensor networks. In: Proceedings of the 1st ACM International Workshop on Underwater Networks. WUWNet '06, New York, NY, USA, ACM (2006) 79–85
13. Sánchez, A., Blanc, S., Yuste, P., Perles, A., Serrano, J.J.: An ultra-low power and flexible acoustic modem design to develop energy-efficient underwater sensor networks. Sensors **12**(6) (2012) 6837–6856
14. Climent, S., Capella, J.V., Blanc, S., Perles, A., Serrano, J.J.: A proposal for modeling real hardware, weather and marine conditions for underwater sensor networks. Sensors **13**(6) (2013) 7454–7471
15. PowerStream Li-ion Coin Cell Lir2032 Datasheet: http://www.powerstream.com/p/lir2032.pdf (last visited on june 2015)
16. Harris, III, A.F., Zorzi, M.: Modeling the underwater acoustic channel in ns2. In: Proceedings of the 2Nd International Conference on Performance Evaluation Methodologies and Tools. ValueTools '07, ICST, Brussels, Belgium, Belgium, ICST (Institute for Computer Sciences, Social-Informatics and Telecommunications Engineering) (2007) 18:1–18:8
17. Ns3 manual — random variables — seeding and independent replications: https://www.nsnam.org/docs/release/3.22/manual/html/random-variables.html (last visited on june 2015)

# Data transmission between magnetic loops

J. H. Arroyo-Núñez[1,2], A. Mocholí-Salcedo[1], I. Rivas-Cambero[2], C. Rueda Germán[2], A. Arroyo-Núñez[1].

[1] The Institute for the Applications of Advanced Information and Communication Technologies, Traffic Control Systems, Universidad Politécnica de Valencia,
Edificio 8G Camino de Vera s/n 46022 Valencia, Spain
http://www.itaca.upv.es/view.php/Investigacion/SCT

[2] Universidad Politécnica de Tulancingo, División de Ingenierías, Calle Ingenierías No. 100, Col. Huapalcalco, Tulancingo de Bravo 43629, Hidalgo, México.
http://www.upt.edu.mx

**Abstract.** This paper presents the results of the implementation of a system of short-range communication, using the magnetic induction as a means of communication. The ASK (Amplitude-shift keying) modulation was used to transmit digital information. These results will be used to design a short-range communication system for the exchange of information between road infrastructure and vehicles.

## 1 Introduction

The range is wide in communications technologies. Many of these technologies can be used in intelligent transportation systems (ITS), in order to solve traffic problem.

To achieve communication between vehicles and infrastructure, wireless communication is necessary. Incorporate mobile devices like media, involves a relatively high cost due to service charge. The other possibility is the use of dedicated short-range communication systems, which are exempt from payment of service, but this requires a high initial investment in installing the system.

The choice of the communication system depends on the specific application of ITS. The cost of communications is also based on the size of data required to transmit, as this involves increasing the bandwidth. The cost of communications is also based on the data size to transmit, as this involves increasing the bandwidth. The transmissions of data from conventional traffic sensors do not require a wide bandwidth, but if the data to be transmitted include images in real time, required bandwidth should be large [1].

The exchange of information between vehicle and infrastructure, is within DSRC (Dedicated Short Range Communications) systems for ITS [2] [3].

In late 2001 the ITS organizations noted the need to define standards for this type of communications, applied to transport. The difficulty presented in the development of standards, was the selection of a single radio frequency due to differences from one region to another. At that time, in Europe, it is considered to employ radio frequency of 5.8 GHz, with a wavelength of 850 nm for optical applications, while in Japan and North America was thought in a different frequency [4].



C.Fernandez-Llatas and M.Guillen (Ed.):
Workshop on Innovation on
Information and Communication Technologies
(ITACA-WIICT 2015)

ISBN 978-84-608-4139-5

The trend in the development of DSRC systems is the radio frequency use and therefore must meet specific standards to avoid interfering with other technologies. But it is possible to propose the development of a communication system that uses a magnetic coupling to avoid any interference.

For decades Magnetic loops devices have been used in vehicle detection [5]. Therefore is easy find this systems in many paths for this purpose, but the magnetic loops have a great potential to be used in other applications. For example, some loops have been utilized for obtain the magnetic profile of the vehicles [6]. In this case the loop works like a sensor that detect the amount of metal that passes over it, allowing to identify the type of vehicle.

The application of the magnetic loops as a means of communication, gives an additional feature to this type of device. This type of communication will be useful to exchange information between vehicles and infrastructure in the routes of terrestrial communication [7].

The results of the short-range communication system implementation that uses magnetic induction fields like transmission media are presented in this paper.

## 2 Theoretical analysis

The short range communication system uses magnetic coils as elements of emission and reception of the information. Based on the principle of magnetic induction is possible establish a communication between two loops. The emitted field depends on the electrical current, number of turns and loop dimension [8] [9]. The signal level detected by the receiving loop, similarly depends of the number of turns, the dimensions of the loop and the magnitude of the field generated by the transmitter [10] [11].

The ASK modulation has been used to transmit data between the loops for example in RFID systems, where this type of modulation is used for data transmission. In this type of modulation a modulating signal (binary information) is multiplied by a high frequency carrier signal [12]. "One logical" corresponds to the presence of signal and a "zero logical" corresponds to the absence of signal.

The block diagram of the stage of emission is shown in Fig 1. At this part, basically the digital information is modulated, amplified and issued through the loop.


Fig. 1 Emission stage.

The recovering information process, in the receiving stage where the signal is amplified, demodulated and conditioned. In the Fig 2 is shown the block diagram of this stage.


Fig. 2 Reception stage.

## 3 Experimentation

To establish the short-range communication, we designed two electronic devices. The first one corresponding to the stage of emission (see. Fig. 3) and the second to the stage of reception (see. Fig. 4).

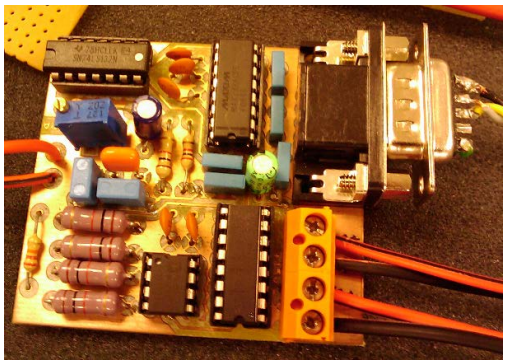

Fig. 3 Transmitter electronic device.

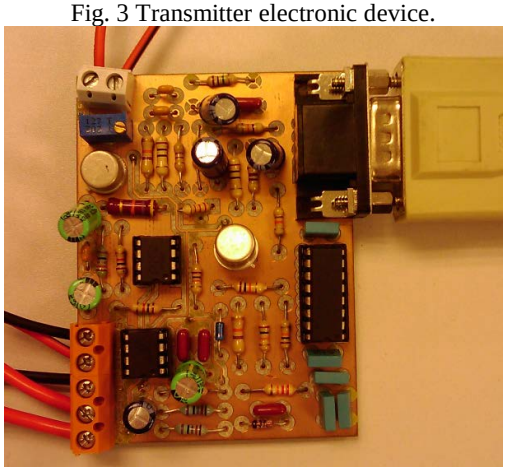

Fig 4 Receiver electronic device.

The following test was realized for verify if the system of emission and reception was functional. The receiver circuit will connect a coil loop with the following characteristics:

- Conductor type: tin copper wire coated with polyvinyl chloride, cross-section of 0,28 $mm^2$.
- Number of turns: 4
- Loop size: 1,20 x 0,46 m.

And the transmitter circuit will connect a coil loop with the following characteristics:

- Conductor type: tin copper wire coated with polyvinyl chloride, with a cross-section of 0,28 $mm^2$.
- Number of turns: 5
- The loop size: 0,30 x 0,20 m.

Computer serial port is used to send in hexadecimal format the following values: AA E3 AA, at 9600bit/sec baud rate. This values were chosen because in binary format, the bits are easily to identify. For example the AA value have the conversion to binary number “10101010” and E3 value is “11100011” in binary format.

The Fig 5 shows the signal emitted by the computer. A start bit "1" and one stop bit "0” are included in the hex values , the bits are transmitted in reverse form and reading is performed from right to left.

In the Fig 6 shows us the modulated signal to the output of the emitter circuit.

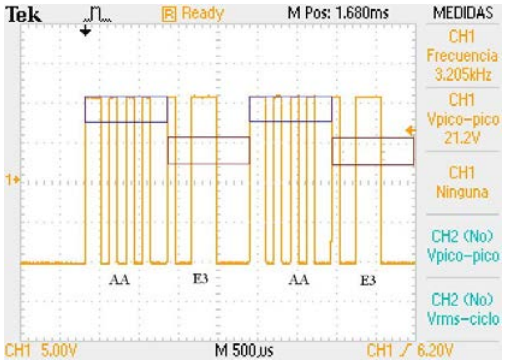


Fig. 5. Signal emitted by the computer serial port.

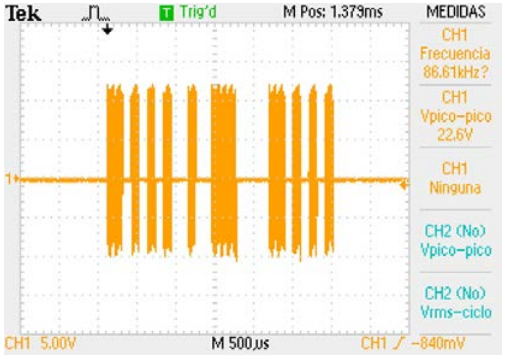


Fig. 6. Modulated signal transmitted by the emitter circuit.

To do the signal reading operation, the receiver loop was located at 0,4 m above the plane of the transmitter loop. The signal received and conditioned is shown in Fig. 7.

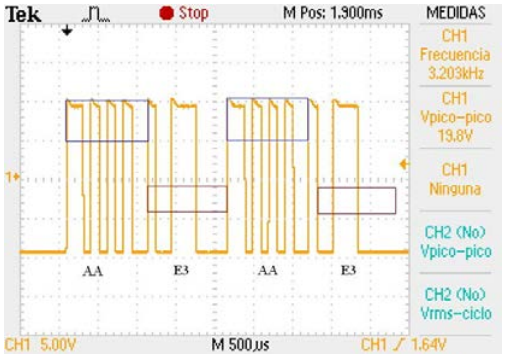

Fig. 7. Signal received and conditioned by the electronic device of reception.

Comparing signals Fig. 5 and Fig. 7, we can see differences in the top of the wave. These differences correspond to high frequency noise caused by the carrier signal. As the information being transmitted is a digital signal, these changes do not affect the information transmitted.

These results correspond to a connection between static magnetic loops. The next stage of research will correspond to test the data transmission, shifting the speed move of a coil. This research will determine the speed limit maximum possible, to transmit data between the two coils. The ultimate goal is to establish a system of short-range communication between vehicles and infrastructure without irradiate signal, because the information transfer will be performed by magnetic coupling.

## 4 Conclusions

Based on the results of the induction voltage between magnetic loops [3], it´s possible develop a short-range transmission device. The data transmission between the two magnetic loops, was conducted using ASK modulation and a baud rate of 9600 bit/s. It´s a sufficient rate to send information with the goal identify a vehicle through a code.

The reported results suggest that is possible the data transmission using magnetic loops, applying the principle of magnetic induction. This communication type is short-range, avoiding causing interference with other systems.

## References

1. «ITS Handbook, 2ª Edición, URL:http://road-network-operations.piarc.org/index.php?option=com_content&task=view&id=38&Itemid=71&lang=en

2. R. T. F. D. Subir Biswas, «Vehicle-to-Vehicle Wireless Communication Protocols for Enhancing Highway Traffic Safety,» IEEE Communications Magazine, pp. 74-82, January 2006.
3. J. S. F.-Y. W. W. N. N.-N. Z. Li Li, «New Developments and Research Trends for Intelligent Vehicles,» IEEE Intelligent Systems Magazine, pp. 10-14, 2005.
4. L. A. Klein, Sensor Technologies and Data Requirements for ITS, Artech House, 2001.
5. Traffic Detector Handbook, Third ed., U.S. Department of Transportation Federal Highway Administration, 2006.
6. A. Arroyo Núñez and A. Mocholí Salcedo, "Sistemas Sensores Empleados en ITS," in VII Congreso Español Sistemas Inteligentes de Transporte, Valencia, España, 2007.
7. I. H. M. H. MILAN VAJDÍK, «Data Transmission Using Inductive Method In Mobile Applications» 9th WSEAS International Conference on COMMUNICATIONS, Vouliagmeni, Athens, Greece, 2005.
8. J. H. Arroyo Núñez, A. Mocholí Salcedo and I. Rivas Cambero, Levels of induced voltage between rectangular magnetic loops, Valencia, España, 2014.
9. C. T. A. Johnk, Engineering Electromagnetic Fields and Waves, Second ed., John Wiley & Sons, 1988.
10. J. H. Arroyo Núñez and A. Mocholí Salcedo, "Communication Between Magnetic Loops," in 16th World Road Meeting, Lisbon, Portugal, 2010.
11. M. Misakian, "Equations for the Magnetic Field Produced by One or More Rectangular Loops of Wire in the Same Plane," Journal of Research of the National Institute of Stand-ards and Technology, vol. 105, no. 4, 2000.
12. K. Finkenzeller, RFID Handbook: Fundamentals and Applications in Contactless Smart Cards and Identifi-cation, John Wiley & Sons, 2003.

# Towards a control panel for assessing the temporal and multi-source variability of biomedical repositories

José Ramón Pardo Más[1-2], Carlos Sáez[2], Juan Miguel García-Gómez[2]

[1] Universitat Politècnica de València, Escòla Tècnica Superior en Enginyeria Informàtica, Camino de Vera, s/n, 46022 València, Valencia, Spain
joparma3@ei.upv.es
*https://www.**upv**.es/*
[2] ITACA, IBIME, Camino de Vera, s/n, 46022 València, Valencia, Spain
{ carsaesi, juanmig}@ibime.upv.es

**Abstract.** This work intends to create a panel for controlling the current state of clinical databases, comparing clinical databases among themselves. To facilitate the process, it was necessary to develop a web graphical user interface (GUI) based on D3.js and able to, working in soft real-time. This GUI is willing to be the panel for consulting the current stability state of clinical datasets from multiple sources. Internally the system is a distributed system, with a Storm central server, which task is to gather the data from the centers and make the necessary calculations to create the data file for the D3.js application.

## 1 Introduction

On-line datastream analysis can bring knowledge discovery on biomedical data, which can be generated from multiple sources. To compile this multi-source data may be a good sample from a wider and more representative population, this is the objective of the majority of these works. Nevertheless, the high possibility of contextual biases accidentally generated in the processes of data generation, can lead to undesired variability among the sources, which can give a contradictory result[1].

It is necessary to create new tools for Big Data management, and these tools must be visual and versatile, that and the commented before, is why we began this work, trying to create what really is necessary for being able to manage this amount of data.

This work proposes a distributed Storm system with a web graphical user interface (GUI) based on D3.js and able to work in soft real-time



C.Fernandez-Llatas and M.Guillen (Ed.):
Workshop on Innovation on
Information and Communication Technologies
(ITACA-WIICT 2015)

ISBN 978-84-608-4139-5

for the assessment of temporal changes in biomedical data, which can be used as a framework under a temporal stability data quality dimension. This is related to assessing the changes causing non-stationary behavior of data time series. Showing graphically the very differences among the centers and populations, in a visual way. One of the objectives of this work is, by using a web environment, and a dynamical interface, to use big data gathered from the centers to make this data variability comprehensible to unused people, or ones without a mathematical formation, so these can obtain an idea about what is happening among multiple databases, and notice about differences that could not be seen before, e.g. the difference of mortality among two centers in different seasons of the year, caused by different climatological behavior of the areas of the globe.

## 2 Materials and methods

The application distribution in the network proposed in this work is a centered Storm cluster that manages the information traveling between the nodes (e.g. hospitals) of the system. Hence it is a server-client configuration, executing on the client the GUI (Graphical User Interface), and receiving an up-to-date data file every time the server makes new calculations on the new data received from the centers nodes, that are “Spout” parts of the Storm server. Example in Figure 1.

### 2.1 Storm Server

A Storm cluster is superficially similar to a Hadoop cluster. Whereas Hadoop runs "MapReduce jobs", Storm runs "topologies". "Jobs" and "topologies" themselves are very different[2]. Specifically one key difference is that a MapReduce job eventually finishes, whereas a topology processes messages forever (or until it is killed).

#### 2.1.2 Workers and Structure

There are two kinds of nodes on a Storm cluster: the master node and the worker nodes. The master node runs a daemon called "Nimbus" that is similar to the Hadoop's "JobTracker". Nimbus is responsible for distributing code around the cluster, assigning tasks to machines, and

monitoring for failures.

Each worker node runs a daemon called the "Supervisor". A supervisor listens for work assigned to its machine and starts and stops worker processes as necessary based on what Nimbus has assigned to it. Each worker process executes a subset of a topology; a running topology consists of many worker processes spread across many machines. To do real-time computation on Storm, it's needed to create what are called "topologies"[3].

A topology is a graph of computation. Each node in a topology contains processing logic, and links between nodes indicate how data should be passed around between nodes. Networks of spouts and bolts are packaged into a "topology" which is the top-level abstraction that is submitted to Storm clusters for execution. A topology is a graph of stream transformations where each node is a spout or bolt. Edges in the graph indicate which bolts are subscribing to which streams. When a spout or bolt emits a tuple to a stream, it sends the tuple to every bolt that subscribed to that stream. We can see a reference to our work topology in Figure 1.

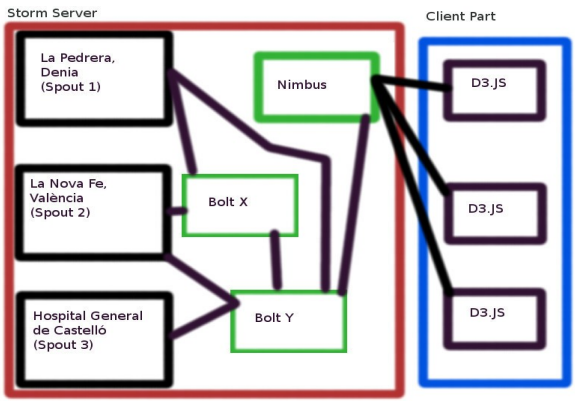


**Fig. 1:** Showing the work topology.

The core abstraction in Storm is the "stream". A stream is an unbounded sequence of tuples. Storm provides the primitives for transforming a stream into a new stream in a distributed and reliable way. For example, it is possible to transform a stream of tweets into a

stream of trending topics.

The basic primitives Storm provides for doing stream transformations are "spouts" and "bolts". Spouts and bolts have interfaces that can be implemented to run the application-specific logic.

### 2.2 D3.js

This graphical library for JavaScript provides the graphical web support of the application. Being library with capabilities to process a real-time data sets showing, and having a very elegant way to show the graphics, this one will be a very suitable solution to this part of the project.

The library basically runs a set of JavaScript functions that is called to represent different elements of the graphical interface. The tool is asynchronous, this means that the calls of the functions do not work in the sequential order of the code. Hence it is worth to be careful on when programming on D3. For an instance, in the project code, we call first the drawing functions, making a callback to retrieve the data, this happens because the JavaScript API executes the fast code first, so it makes the web application a fast one, so, if the data needs to be read before the drawing starts, it is necessary to call the data functions from the drawing ones, making sure the data sets needed are not empty.

## 3 Current results

Right now, the implementation carried out to demonstrate our idea has the graphical interface working, that reads in real-time, the files generated by the Strorm distributed system. Sending the data to the client part of the web environment ensures that the showed information will change as soon as it is read by the D3.js GUI .

### 3.1 Client-Server Model

As usual in web-distributed applications, and as said in the “Materials and methods” section of this application implements a client-server structure. The application has a parallel behavior, each possible bolt

runs the treatment of one or more center data. Therefore, it will receive the data from one or multiple spout parts of the Storm topology. The client is a passive member of the structure, with the unique task of reading the data file given by the server nodes of the structure, and convert it, using D3 library, to a graphical comprehensible display for the user of the application. Hence, the server part performs the necessary treatment and calculations on the information of the centers databases, to create the file needed, with readable series CSV format archive for the client.

### 3.2 Current Working Scheme

The graphical interface is now working, and the mathematical functions, provided by the methods in [4] and [5], are working, The GUI has diverse functionalities, it processes the data, and shows it, it is possible to select one of the series displayed, (Figure 3), to en light it, and on mouse-over functions, the name of the different centers is showed, to make it easy to differentiate one center of another, as we see in Figure 4.

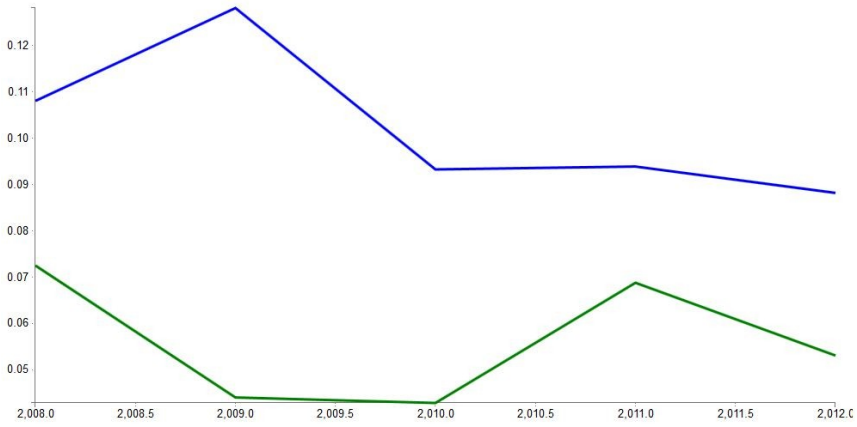


**Fig. 2:** Showing the standard behavior of the GUI.

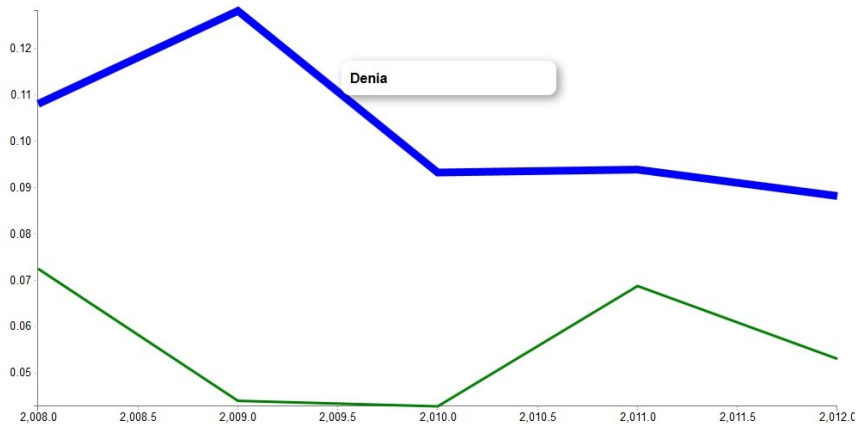


**Fig, 3:** Showing the behavior of the GUI when the mouse is over a series, it just changes the width of the series, and show the name of it.

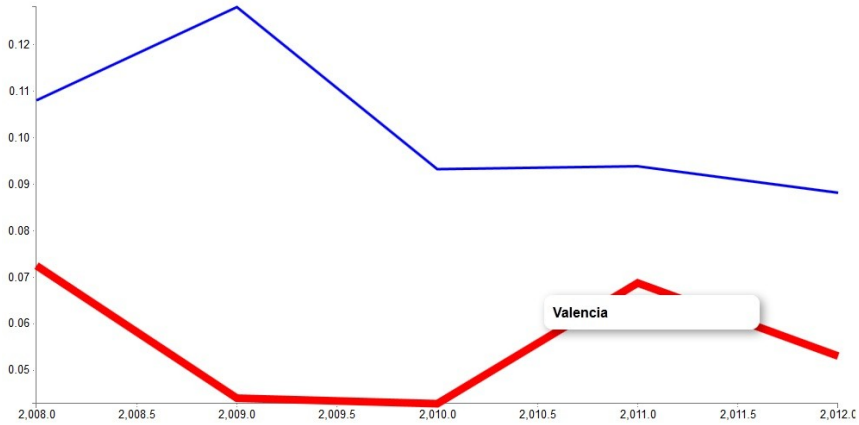


**Fig, 4:** Showing the behavior of the GUI when we click a series to select it, it gives different color to each selected item, to easily differentiate them.

## 4 Future Work

For the completion of the work, we will determinate the way of integrate the mathematical methods on the bolt parts of Storm, to properly process the data. Besides, it will be necessary to determinate a viable topology of the Storm cluster, and determinate the scheme of the client-server part to work along. In time, the service may acquire a preventive behavior, but this will be seen in future projects.

## 5 Conclusions

The data variability will always be a major problem in multi-modal, multi-center and multi-source data sets, but the very purpose of this work is to facilitate the detection and treatment of these problems. Thanks to this project, non-expert people will be able to detect the problems, and to call experts for solutions.

## References


1. Sáez C, Robles M and García-Gómez JM. Comparative study of probability distribution distances to define a metric for the stability of multi-source biomedical research data. In:Engineering in Medicine and Biology Society (EMBC),2013 35th annual international conference of the IEEE, Osaka, Japan: IEEE, 2013, pp. 3226–3229.

2. White Tom, Hadoop: The definitive guide, O'Rilley Inc

3. Vijay Srinivas Agneeswaran, Big Data Analytics Beyond Hadoop: Real-Time Applications with Storm, Spark, and More Hadoop Alternatives (FT Press Analytics)

4. Sáez C, Robles M, Garcia-Gomez JM. Stability metrics for multi-source biomedical data based on simplicial projections from probability distribution distances. Stat Methods Med Res [Internet]. 2014 Aug 4 [cited 2014 Nov 10]; Available from: http://smm.sagepub.com/cgi/doi/10.1177/0962280214545122

5. Sáez C, Rodrigues PP, Gama J, Robles M, García-Gómez JM. Probabilistic change detection and visualization methods for the assessment of temporal stability in biomedical data quality. Data Min Knowl Discov [Internet]. 2014 Sep 2 [cited 2014 Nov 10]; Available from: http://link.springer.com/10.1007/s10618-014-0378-6

# Comparing Benchmark Targets: Issues in the Analysis Model

Miquel Martínez, David de Andrés, and Juan-Carlos Ruiz

Instituto de Aplicaciones de las TIC Avanzadas (ITACA)
Universitat Politècnica de València, Campus de Vera s/n, 46022, Spain
Email: {mimarra2, ddandres, jcruizg}@disca.upv.es

**Abstract.** Benchmarks are tools applied to assess the behaviour of systems or components. When multiple targets are available, comparing their results with the aim of identifying the target that best suits the evaluators' requirements is not always an easy task. The way evaluators undertake this task of comparing targets is entirely related to how the results obtained from benchmarking them are analysed. The analysis of the results is driven according to the analysis model determined by the evaluator. This model, is conformed by various elements that might influence the final conclusions, leading to different classifications of the benchmarked targets. These elements encompass, among others, the normalization method applied to the results, the weights defining the importance of each measure for the analysis or the mathematical methodology used in the analysis. This work is aimed at making benchmark evaluators more conscious about the issues introduced by these elements in the analysis and their subsequent effects in the conclusions.

## 1 Introduction

The evaluation of the process of systems and components to perform their comparison has supposed a great challenge for researchers and people from the industry for many time. In fields like dependability benchmarking, reaching agreements among the community to determine *what* should be measured, and *how* those measurements should be taken, has not been an easy task. Here, works like [1] identify the aspects that measures should satisfy so they can be considered "quality measures" for a dependability benchmark. Also works like [2] established the main set of attributes that these benchmarks must fulfill to be considered valid to perform dependable evaluations of systems and components for a given domain. Thus, all these attributes have let evaluators to validate the process of a benchmark to be sure that its results will be consistent.

The quality of the results provided by benchmarks is of primary importance to achieve what is stated in [2] as the main goal of benchmarking, *allow the comparison of different systems or components to select the best choice*. It is true though, that the comparison of benchmark targets depends not only on the results obtained, but also in the process followed to compare them. But, an analysis of the literature in benchmarking reveals that little or no attention



C.Fernandez-Llatas and M.Guillen (Ed.):
Workshop on Innovation on
Information and Communication Technologies
(ITACA-WIICT 2015)

ISBN 978-84-608-4139-5

has been drawn to the part of the process devoted to compare benchmark results. This situation has lead to a point where there is no consensus on which methodology should be used to analyse the results. Works like [8] and [9] point out the fact that in some works results are analysed and conclusions are driven from the comparison of different targets, however, the process followed is not always made explicit, which makes difficult understanding how conclusions were obtained. Then, if the process can not be validated, its conclusions can hardly be trusted.

When various alternatives are benchmarked, it is should be possible to validate the process followed in the analysis of benchmark results to guarantee the quality of the conclusions. In that sense, the analysis process should be made explicit, so external evaluators could cross-compare their results applying the same methodology. Unclear analysis may rise questions like, *how can anyone be sure that those conclusions are not wrong?*. Explicit processes, in the other hand, make clear the origin of conclusions. Then, a good conclusions can be understood as those that have been obtained following the best possible procedure, and for that to happen, the procedure must be known.

In benchmarking, performing wrong decisions can derive into serious problems. For example, the failure of a product due to choosing the wrong component, can imply economical losses for a company, or even degrade its reputation. For these reasons, this work seeks to make evaluators aware of the need for explicit analysis processes. To do so, this works shows how common aspects to most analysis processes observed in the literature, like normalization of data, weighting of evaluation criteria or the mathematical methodology, can influence final conclusions. These aspects are part of what has been called in this work as the *analysis model*, and its influence in the conclusions are described and explained in this paper through a case study.

The aspects of the analysis model are first described in Section 2, and their influence on the conclusions is studied in Section 3 through a case study in the dependable evaluation of ad hoc routing protocols. Finally, the paper concludes in Section 4 describing the relevance that the findings of this work have for the benchmarking community, and introduce the ongoing work that is part of the current research.

## 2 Analysis Model in Benchmarking

The comparison of alternatives using benchmarks is not always straightforward and there are several things that must be considered when comparing alternatives. Results are usually provided in different types of unit or scales and to work with them, it is required to transform them into a common scale. This is done through normalization techniques [3]. But, this is not necessary when results are expressed in the same units, as it happens in well known benchmarks like EEMBC [4] or SPEC [11]. Another fact is the application context for which the alternatives are being evaluated. The results provided represent quantitatively the different attributes (or criteria) evaluated in the benchmark, thus, depend-

ing on the application context, evaluators can have different requirements to compare the alternatives. Weighting the criteria according to their relevance for the evaluator is used to mathematically represent those requirements. The mathematical method used to interoperate with the results is also a crucial fact, as it would determine how evaluators rank the alternatives and select the best possible one for their purpose.

In this work, the entity formed by the aggregation of these aspects is referred to as the *analysis model*. Their role in the analysis model are described next.

### 2.1 The normalization procedure

When results are expressed in different types of units, a first step to convert them into a normalized scale is required. This allows the evaluator to operate with the data from the criteria evaluated, and enables the comparison of alternatives.

In Table 1 it can be seen four of the most common normalization techniques used in the literature. The criteria considered in an analysis are depicted as $C = [C_1, C_2, \ldots, C_n]$, where for $n$ criteria, $C_i$ represents the $i^{th}$ criterion. The results from a benchmarked alternative are represented in an array form as $r = [r_1, r_2, \ldots, r_n]$, being $r_i$ the quantitative value of the $i^{th}$ criterion for an alternative. The normalized values obtained after the normalization are identified as $v = [v_1, v_2, \ldots, v_3]$.

**Table 1.** Common Normalization Techniques

| | **Technique 1** | **Technique 2** | **Technique 3** | **Technique 4** |
|---|---|---|---|---|
| *Formula* | $v_i = \frac{r_i}{max\ r_i}$ | $v_i = \frac{r_i - min\ r_i}{max\ r_i - min\ r_i}$ | $v_i = \frac{r_i}{\sum r_i}$ | $v_i = \frac{r_i}{\left(\sum (r_i)^2\right)^{1/2}}$ |
| *Scale* | $0 < v_i \leq 1$ | $0 \leq v_i \leq 1$ | $0 < v_i < 1$ | $0 < v_i < 1$ |

Techniques 1, 3 and 4 preserve the proportion among values after normalization, which means that $A(r_i)/B(r_i) = A(v_i)/B(v_i)$ for all alternatives. To be clear, if the result for the alternative A ($A(r_i)$) is the double of the result for the same criterion for the alternative B($B(r_i)$), after normalization, $A(v_i)$ will still be the double of $B(v_i)$. Technique number 2 does not keep proportion among normalized values, it distribute the values among the normalized scale [0,1] (both inclusive), while the other three tend to group them. Techniques 1 and 3 are frequently used, and its interpretation is quite intuitive, although number 3 tend to group normalized values in the lower part of the scale. The advantages of technique number 4 may not be intuitive for an evaluator with few mathematical skills, but it allows to entirely perform dimensionless comparisons of the criteria arrays of the problem.

### 2.2 Weighting the criteria

The application domain of a system or component needs to be considered when benchmark targets are compared. The results from a benchmark will characterise the behaviour of the benchmarked target according to the selected criteria, but the quality of such results will be conditioned by the evaluator's requirements. Those requirements determine the relative importance that evaluated criteria have among them for the evaluator. For instance, good values in a given criterion could be very important in a certain context while not being determinant in others.

These requirements can be expressed in terms of weights assigned to the criteria. Weights are used to quantify the relative importance that a criterion has for the evaluator's purpose. An array determined by $w = [w_1, w_2, \ldots, w_n]$, defines the set of weights assigned to the criteria, where out of $n$ criteria, $w_i$ is the weight assigned for the $i^{th}$ criterion.

Weights can be assigned by an evaluator, or by a group of experts in the field. For example, those involved in the definition of the requirements can quantify the importance of each criterion according to a given scale (0 to 1, 0 to 10, etc.). Then, the normalization of these values by the technique 3 shown in Table 1 assures that the sum of all calculated weights is 1.

### 2.3 Mathematical Method

The selection of the mathematical method used to perform the analysis is a decision that must be made explicit to understand the whole process of analysis. For example, well known benchmarks like those aforementioned, EEMBC and SPEC, make use of the *geometric mean*, considering all criteria equally important than the rest.

There is a wide variety of methods that could be used to perform the analysis, and deciding which one to use depends on the skills or preferences of the evaluator. Well known methods can be used in addition of weights, like the *weighted arithmetic mean* (Eq. 1), which is easy to be applied, or other of its variants like the *weighted geometric mean* (Eq. 2) or *weighted harmonic mean* (Eq. 3). There exist however, other kind of methods that are suitable to conduct this kind of analysis, the *multi-criteria decision making* (MCDM) methods [13][6]. Their application is out of the scope of this work, but studies about their suitability to compare and rank alternatives in benchmarking can be found in works like [10][8].

$$\sum_{i=1}^{n} v_i w_i \qquad (1) \qquad \left(\prod_{i=1}^{n} v_i^{w_i}\right)^{1/\sum_{i=1}^{n} w_i} \qquad (2) \qquad \frac{\sum_{i=1}^{n} w_i}{\sum_{i=1}^{n} \frac{w_i}{v_i}} \qquad (3)$$

The proper definition of the mathematical method used, together with the explicit declaration of the used weights and normalization techniques implies

**Table 2.** Average values and standard deviation of measures obtained during experimentation [5]

| **Protocol** | **RT** *(Kbps)* | **RD** *(ms)* | **EC** *(J)* | **RA** *(%)* | **RR** *(s)* |
|---|---|---|---|---|---|
| *v.0.4.10* | 145.7 ±8.9 | 48.2 ±4.7 | 8.2 ±0.6 | 73.6 ±6.0 | 27.2 ±1.6 |
| *v.0.5.6* | 145.6 ±2.0 | 55.6 ±6.2 | 8.2 ±0.9 | 73.4 ±7.2 | 45.2 ±4.8 |
| *v.0.6.0* | 145.3 ±9.4 | 52.3 ±6.4 | 8.1 ±0.7 | 72.9 ±3.7 | 44.9 ±1.6 |

that the *analysis model* is made explicit. This let evaluators revisit the process followed by others (or themselves) to provide the conclusions, and guarantee its correctness. Nevertheless, variations in these aspects may have an impact in the final conclusions. In next section a case study in ad hoc networks is used to support the description of these problems.

## 3 Issues in the Analysis: Dependability Benchmark of Ad Hoc Routing Protocols as a Case Study

In this section, the aforementioned problems in the conclusions are shown using data extracted from a real dependability benchmark performed in [5]. Here, three versions of the well known *Optimized Link State Routing* (OLSR) protocol [12] were evaluated in presence of perturbations.Table 2 lists the average values (AVG) and standard deviation (SD) for all reported measures when the protocols were evaluated in presence of *Ambient Noise*: *Route Throughput* (RT), *Route Delay* (RD), *Energy Consumption* (EC), *Route Availability* (RA), and *Route Restoration* (RR).

For this case study, analysis were performed using the *weighted arithmetic mean* (Eq. 1). Here, $n$ criteria are considered, $v_i$ represent the normalized value of the $i^{th}$ criterion, and $w_i$ its associated weight. The total score provided by this method represents the score for the given alternative.

Upcoming sections describe the impact that the normalization technique, the weighting of criteria and the mathematical methodology have in the conclusions drawn from the analysis.

### 3.1 Different normalizations may lead to different conclusions

To prove the impact that normalization has in the conclusions, the results of all the considered criteria were normalised to a common scale using the four procedures defined in Table 1. However, these procedures are used in benefit criteria, where values are considered the higher, the better. Then, cost criteria (the lower, the better) like Route Delay, Energy Consumption and Route Restoration, were first converted into benefit criteria by subtracting the average value of each alternative to the sum of average values obtained for all alternatives for such criteria.

To perceive that conclusions can differ depending on the normalization technique, a large number of comparisons was required. In that sense, as for each criteria and alternative results are compressed in the range $AVG \pm SD$, a large set of results was drawn by combining the values $AVG - SD$, $AVG$ and $AVG + SD$, from all the results, among them. Thus, as there are five criteria and three alternatives, the total number of combinations is $3^{3\times5} = 3^{15} = 14348907$. All criteria were considered equally important for the analysis.

The three protocols represent the benchmarked alternatives, so, if ties are not considered, there are only six possible ways to classify them. The percentage of times each classification was obtained from the analysis is shown in Figure 1 for each normalization technique.

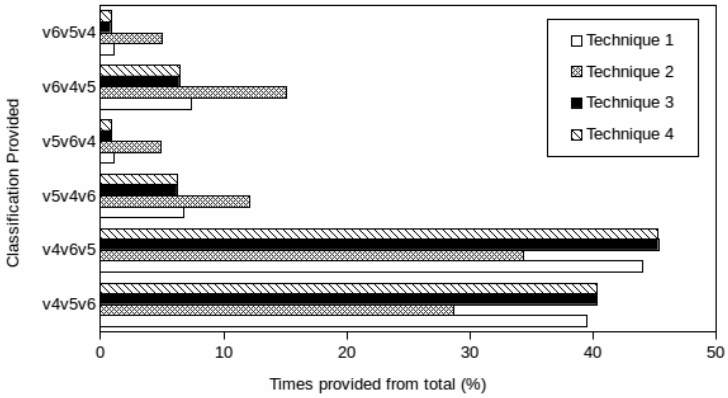


**Fig. 1.** Percentage of appearances of each ranking

It can be appreciated from the figure that techniques 3 and 4 provided identical classifications in almost the 14348907 analysis. However, when technique 1 is applied, even though the proportion of the values is kept (as it happens with technique 3 and 4), the number of occurrences for each classification slightly vary from those of technique 3 and 4. The differences between normalization techniques is more evident when technique 2 is compared with the rest. The main reason for this is that technique 2 does not keep proportion between values, as the values of each criteria are proportionally distributed according to the range determined by the minimum and the maximum values.

This example shows how different conclusions can be reached depending on which normalization technique is used. Nevertheless, it must be understood that this example does not reflect to what extent the classifications obtained from the analysis of the same values with different normalization techniques were the same.

### 3.2 Impact of weights in the conclusions

The various normalization procedures arrange values in the same scale ([0,1], for example) but the resultant values differ from one normalization to another, even when proportion between values is kept. Then, the weight assigned for each criterion has an influence in the final results of the analysis. To illustrate this, previous set of results are again analysed with the four normalization techniques, but this time each combination is analysed several times, considering different weights each time. One thousand combinations of weights is used, so $14348907 \times 1000$ analysis were performed using each normalization technique. The sum of weights for every analysis was: $\sum_{i=1}^{5} w_i = 1$.

To determine the impact that weights has in the conclusions, results were evaluated comparing the number of times classifications provided by the analysis of the same data matched for the normalization techniques from Table 1. Results were analysed in two ways: i) A first analysis was done to determine the coincidences in the classifications provided from normalizing the same data using the normalization techniques that keep the proportion (techniques 1, 3 and 4); and ii) a second analysis considering all normalization techniques. Figure 2 shows the results obtained for the thousand experiments.

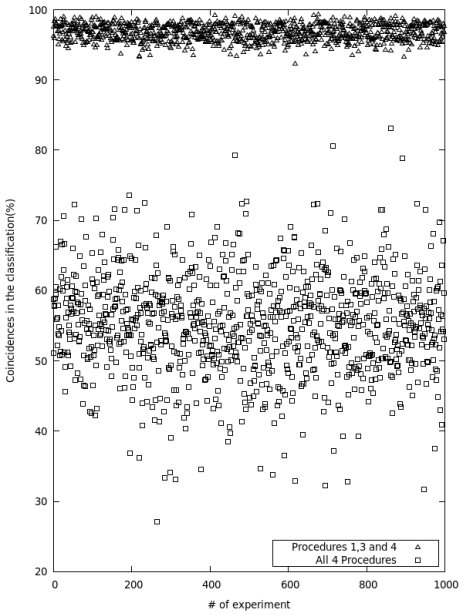


**Fig. 2.** Percentage of times the same classification is provided using different normalization techniques

The results of the first analysis show that in average, the three techniques (1, 3 and 4) agreed in their classifications the 96.79% of the times, which means that

in average, there was agreement in 13888307 out of 14348907 analysis. However, the highest amount of coincidences registered is 99.36%, and the lowest 92.28%, meaning that the differences in the weights of these experiments have supposed an increment of 1015902 mismatched conclusions from one experiment to the other.

In the other hand, results from the second analysis show clear evidences of the influence of weights in conclusions, where higher variations are found. When all four normalization techniques are considered, the difference between the highest amount of coincidences, 83.06%, and the lowest 27.13%, is of 8025343 mismatched conclusions. Meaning that variations in the weights can imply a disagreement in the conclusions between all four techniques in more of the half of the analysis.

### 3.3 The methodology matters

The selection of the mathematical methodology that is used to perform the analysis of the results is very sensitive to the evaluators preferences. Scoring different alternatives in order to compare them can be done through various methods. Each methods has its own particularities, thus its applications certainly have implications in the resultant conclusions. For example, the interpretation of the results from applying the geometric mean differ from how results should be understood if the analysis was performed using the arithmetic mean. Indeed, in other fields of research, exhaustive analysis have been done with these two methods to determine the benefits of applying one or the other [7]. Then, which method is used to perform the analysis is important to understand the origin of the conclusions.

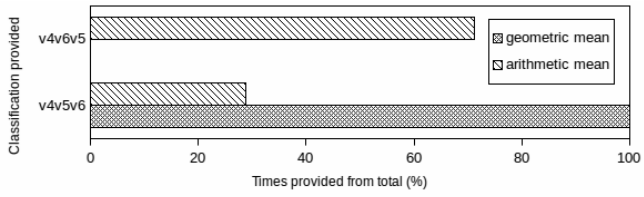


**Fig. 3.** Percentage of occurrences of each classification analysing the data with the geometric and arithmetic mean

With the aim of showing the impact that different mathematical methodologies may have in the conclusions derived from the analysis, the *geometric mean* and *arithmetic mean* were used to analyse a set of results. This results were obtained using $AVG-SD$ and $AVG+SD$ this time, so $2^{15} = 32768$ sets of possible data were normalized with normalization technique 1 (Table 1) and both methods. Figure 3 shows that both methods agree the 99.95% of the analysis that $v4$ in which is the best alternative (it is not shown in Figure 3, but the

geometric mean concluded in 0.05% of the analysis that the classification was *v6-v4-v5*). However, both methods only agree in 28.82% of the analysis in which alternative was the second best.

These results proved that even when applying variants of the mean, differences in the conclusions may occur. Thus, when it comes to performing the analysis of the results from a benchmark, the mathematical methodology used must be made explicit so the origin of the conclusions provided can be known.

## 4 Conclusions and Future Work

Many works can be found in the literature that propose improvements in the benchmarking process, thus assisting the development of better and more accurate benchmarks. However, there is a lack of works devoted to improve the process of analysis that let evaluators perform the comparison of alternatives to select the best choice for their purpose. This is quite surprising given the fact that as stated in [2], "*the main goal of benchmarking is to allow the comparison of systems and components*". Some works like [9], [8] and [10], have pointed out this fact and have suggested new approaches to deal with it.

This problems are more evident when in some works no signs that let the reader understand the process followed to obtain the presented conclusions can be found. It is in this cases when the confidence that can be placed in such conclusions can be questioned. Thus, making explicit how the analysis of results is conducted is of primary importance not only to increase the confidence that can be placed in conclusions, but also to improve cross-comparison of results among different works.

With this scope in mind, this work has described the main attributes that must be considered in the analysis, and their role in it. Their application for an analysis can be easily captured in any work so external evaluators can follow the analysis. Given the impact that variations in these attributes can have in the conclusions, it is essential that the process of analysis remains clear, so their influence in the conclusions can be detected by anyone.

The influence of these attributes have been shown in this work through the analysis of an extensive set of possible results. The results have shown how different normalization techniques, variations in weights and changing the mathematical method, may lead to completely different conclusions. With these results, this work seek to make evaluators realise of the importance that their decisions have for the analysis, and also to make them aware of the possible sources of discrepancies among conclusions from different works.

Following the line of thought of previous works ([9], [8] and [10]), the ongoing work is focused in the study of identifying how MCDM methods can be integrated in the benchmarking process in a way that the confidence placed in the conclusions can be increased. It is common to find data like the one presented in the case study, where results are expressed in terms of the mean and standard deviation of the results. Thus, the aim of our research is to reach mechanisms that let evaluators analyse the results and compare the alternatives considering

the range of possible values a criteria can have for an alternative, which is given in such cases by the mean and the standard deviation.

## Acknowledgment

Work partially supported by the Spanish project ARENES (TIN2012-38308-C02-01) and the "Programa de Ayudas de Investigación y Desarrollo" (PAID) from the Universitat Politècnica de València.

## References

1. Bondavalli, A., Ceccarelli, A., Falai, L., Vadursi, M.: Foundations of Measurement Theory Applied to the Evaluation of Dependability Attributes. In: 37th Annual IEEE/IFIP International Conference on Dependable Systems and Networks. pp. 522–533 (2007)
2. DBench: Dependability Benchmarking. IST Programme, European Commission, IST 2000-25425, [Online]. Available: http://www.laas.fr/DBench (2013)
3. Dutka, A.F., Hansen, H.H.: Fundamentals of Data Normalization. Addison-Wesley Longman Publishing Co., Inc., Boston, MA, USA (1989)
4. EEMBC's Benchmarks. Embedded Microprocessor Benchmark Consortium, [Online]. Available: http://www.eembc.org/benchmark/products.php (2014)
5. Friginal, J., de Andrés, D., Ruiz, J.C., Moraes, R.: Using Dependability Benchmarks to Support ISO/IEC SQuaRE. In: 2011 IEEE 17th Pacific Rim International Symposium on Dependable Computing. pp. 28–37 (2011)
6. Ishizaka, A., Nemery, P.: Multi-criteria Decision Analysis: Methods and Software. Wiley (2013)
7. Jacquier, E., Kane, A., Marcus, A.J.: Geometric or arithmetic mean: A reconsideration. Financial Analysts Journal 59(6), 46–53 (2003)
8. Martínez, M., de Andrés, D., Ruiz, J.C.: Gaining Confidence on Dependability Benchmarks' Conclusions through "Back-to-Back" Testing. In: 2014 Tenth European Dependable Computing Conference. pp. 130–137 (2014)
9. Martínez, M., de Andrés, D., Ruiz, J.C., Friginal, J.: Analysis of results in dependability benchmarking: Can we do better? M&N 2013, International Workshop on Measurements and Networking pp. 127–131 (2013)
10. Martínez, M., de Andrés, D., Ruiz, J.C., Friginal, J.: From Measures to Conclusions Using Analytic Hierarchy Process in Dependability Benchmarking. Instrumentation and Measurement, IEEE Transactions on 63(11), 2548–2556 (2014)
11. SPEC's Benchmarks. Standard Performance Evaluation Corporation, [Online]. Available: https://www.spec.org/benchmarks.html (2014)
12. T. Clausen and P. Jacquet: Optimized Link State Routing Protocol(OLSR). RFC 3626 (2003)
13. Zanakis, S.H., Solomon, A., Wishart, N., Dublish, S.: Multi-attribute decision making: A simulation comparison of select methods. European Journal of Operational Research 107(3), 507–529 (1998)

# Towards Studying the Representativeness of Simulation-Based Fault Injection on Different HDL-Description Levels

Ilya Tuzov, David de Andrés, and Juan-Carlos Ruiz

Fault-Tolerant Systems (STF), Instituto de Aplicaciones de las TIC Avanzadas (ITACA)
Universitat Politècnica de Vàlencia (UPV), Campus de Vera s/n, 46022, Valencia, Spain
Phone: +34 96 3877007 Ext {75774, 75752, 12017}, Fax: +34 96 3877579
{tuil, ddandres, jcruizg }@disca.upv.es
**Area: Fault Tolerant Systems**

**Abstract.** Fault injection is a privileged technique for VLSI verification and dependability assessment. The goal is to check the ability of a VLSI design to cope with its purpose in the presence of faults. The existence of Hardware Description Language (HDL) models enables the early verification of hardware designs through simulation-based fault injection (SBFI). The higher (and less accurate) is the level of description of the model, the earlier and faster it can be verified through SBFI and the lower will be the cost of fixing the detected problems. Although, at a first sight, early SBFI may seem the optimal choice for the verification of HDL designs, it is however not clear today to what extent the level of detail of such designs conditions the representativeness, and thus the usefulness, of SBFI results. This work defines a preliminary research towards studying the representativeness of SBFI on different HDL-description levels.

## 1 Introduction

As CMOS technologies achieve smaller transistors' size, the impact of hardware faults on VLSI circuits increases in number and importance. Wearout mechanisms become more intensive, provoking permanent faults and reducing the life cycle of circuits. Sensitivity to external effects (Single Event Effects – SEE) increases, leading to hard (burnout), potentially hard (latchup), or soft errors (Single Event Upsets – SEU) [1]. In addition, c ontinuous integration increases complexity and clock frequency of ASICs (Application Specific Integrated Circuits) and SOCs (Systems On Chip), requiring the implementation of advanced fault tolerance mechanisms and their resource-intensive verification.

Fault injection consists in the intentional introduction of faulty states into devices under test and is a well-known technique to solve numerous problems of design and verification in different contexts, such as fault tolerance techniques, recovery mechanisms, BIST (Built-In Self-Test), drivers, or security, among others [2]. Prototype-based techniques are divided according to fault targets into hardware implemented (HWIFI) and software implemented (SWIFI) fault injection [2]. Emulation-based techniques (e.g. FADES [3]) provide performance close to prototype-based, while


C.Fernandez-Llatas and M.Guillen (Ed.):
Workshop on Innovation on
Information and Communication Technologies
(ITACA-WIICT 2015)

ISBN 978-84-608-4139-5

they have shorter feedback loop and implementation cost is closer to simulation-based techniques. Simulation-based (SBFI) fault injection techniques (e.g. VERIFY [4], VFIT [5]) are much slower especially for complex models. However, they allow early detailed analysis and provide best observability and controllability of the entire experiment. According to the general Hardware Description Language (HDL)-design chain, fault simulation experiments can be performed at four distinct representation levels:

- Register Transfer Level (RTL) represents a circuit in terms of interconnected registers and the operations performed on signals between those registers.
- Logical level describes a circuit as a list of logic gates and list of connections between them (post-synthesis netlist). It can be either platform dependent or independent, and it can be used for approximated timing simulation.
- Post-map level describes a circuit as a list of library elements specific for a target device (post-map netlist), although the timing model is approximated.
- Post-Place & Route level adds information about routing, reflecting the actual timing behavior of the target device (post-implementation netlist).

HDL source codes are mainly developed on RT level and then are automatically translated into lower (logical, post-map, and post-place & route) levels by using synthesis, mapping, and routing tools, respectively. Careful verification of RTL model is an essential stage of the workflow, as it provides early detection of most functional errors. Thus, fault injection on RT level could be a suitable decision to verify devices' behavior in presence of faults with lowest cost of fixing design problems. However, SBFI at higher level might not represent the behavior of the real system in presence of faults, since the accuracy of the RTL model is low with respect to underlying levels: i) the logical level may widen the set of fault targets, ii) the post-map level describes properly the behavior of elements of target chip thus reflecting more accurately the propagation paths and recovery processes, and iii) the post-place & route level provides detailed delays which may affect results of SBFI. This brings us to the problem of exploring the representativeness of SBFI on different HDL description levels, i.e. finding out to what extent a similar faultload applied on different HDL description levels leads to similar results in terms of observed devices' behavior, detected errors/failures, propagation and recovery latencies, etc. Exploring the representativeness of faults at different description levels will enable us to understand when early and quick SBFI is accurate enough to make informed decisions about the fault tolerance needs of the system, and when lower level models (available late in the design cycle and slow to simulate) are required in order to obtain useful and precise results.

Some efforts in exploring representativeness of fault injection were undertaken in the past, although they focused on exploring fault models rather than studying such model from the perspective of HDL description levels. For instance, the report presented in [6] dealt with the problem of determining a representative faultload for benchmarking a VLSI system. It showed that i) most faults at logic level manifest at RT level as bit-flips, ii) the percentage of propagated transient faults and their multiplicity increases with fault duration, and iii) other fault models (delay, indetermination) are less representative, as their proportion in relation to bit-flips is much lower.

The rest of the paper discusses the differences between HDL levels affecting SBFI (Section 2), defines an experimental procedure for studying the representativeness of results when targeting equivalent elements on different HDL levels (Section 3), and provides the preliminary results of these experiments (Section 4).

## 2 HDL levels as targets for SBFI

There exist a number of factors that can affect the representativeness of SBFI between different HDL levels:

- Structural description: primitives, wires, and links between them.
- Behavioral description: trigger conditions, assignment semantics, etc.
- Timing description: delay values (estimated or actual) and delay models.

In order to identify structural differences between HDL levels we should examine the synthesized netlists and their relationship with the original RTL model. As a case study, we will consider a simple ALU (Aritmetic Logic Unit) having input registers for two operands and operation, and output registers for result and flags. The RTL model was described in SystemVerilog, verified and synthesized with Xilinx Vivado tool for Artix FPGA and with Altera Quartus for Cyclone FPGA. We implemented that design for two vendors in order to estimate the impact of different target libraries and synthesis tools on SBFI results. The diagram shown in Fig. 1 represents a brief matching of entities of RTL model and Xilinx post-map netlist.

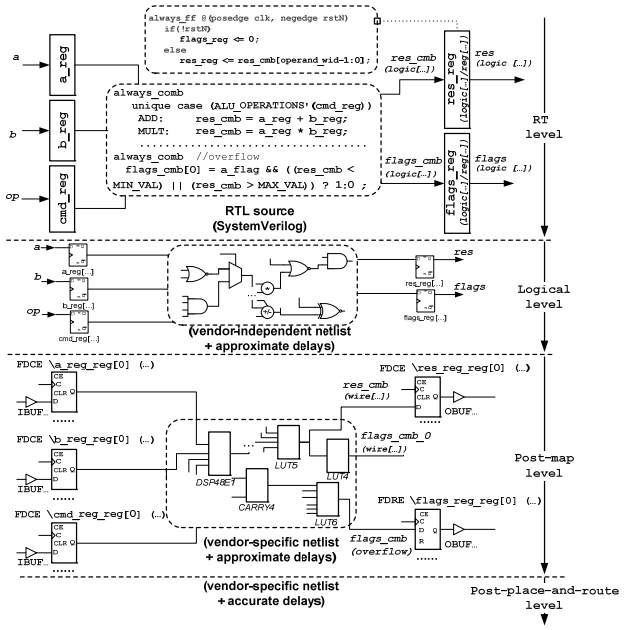


**Fig. 1.** Mapping entities from RTL model into Xilinx post-map netlist

We note that the general HDL design workflow defines four representation levels: RTL, logical, post-map, post-place & route. Real workflows, however, are vendor-specific and often provide a reduced set of representations available for simulation. Although some tools can synthesize vendor-independent netlist, in most cases the pure logical level can be eliminated, since it only reflects overall logic structure, but not properties of the target device. Xilinx Vivado refers to the post-map level as post-

synthesis netlist, and to the post-place & route level as post-implementation netlist, whereas Altera Quartus provides only just the post-place & route netlist.

Registers in RTL model are the entities, represented by packed arrays of basic type *reg* or *logic*, that receive their values by non-blocking assignments at sequential logic procedural blocks (*always_ff*) [7], as for instance *res_reg* (Fig. 1). At the RT level we can directly affect these variables with faults of selected fault models. In the gate-level netlist (both post-synthesis and post-implementation) these registers are represented by a set of flip-flops (FFs) as instances of corresponding modules of vendor-specific library: *FDCE* and *FDRE* for Xilinx, *dffeas* for Altera. Depending on synthesizer's options some FFs could be absent due to optimizations or duplicated due to fan-out. Since FFs on a netlist level are non-trivial entities, there are several things to consider when injecting faults. For instance, permanent faults (like stuck-at-1/0) applied to the *Q* output should reflect exactly the same behavior as for RTL. However, in order to properly simulate a bit-flip fault we should take into account behavioral aspects defined in the library code of the target FF – the target should be a variable, declared with basic type *reg*, that receives a value in a sequential procedural block (it is in charge of maintain the faulty state until the next write cycle).

Combinational logic represented at RTL level as *always_comb* procedural blocks and continuous assignments is implemented on the gate level as a set of Look-Up Tables (LUT), multiplexers, DSP (Digital Signal Processing) units etc. At the RT level we can identify some combinational targets for fault injection, consisting mainly of entities of type *wire* that receive their values on the left side of blocking assignment: *res_cmb* and *flags_cmb* in Fig.1. Depending on the selected synthesis tool and options, some of these wires can also be found in the gate level netlist but often with other semantics or word size. In our simple case study *res_cmb* has a double-word size at RTL level, where the high word is computes the overflow flag and the low word stores a result at *res_reg*. At the post-map netlist for Xilinx this wire is connected to the *d* input of the FFs containing the result. However, it implements only the low word, whereas the overflow flag now depends on a different logic. Thus the overflow flag cannot be affected anymore by faults injected at *res_cmb*. Wire *flags_cmb* is now divided into 2 entities (of 1 and 3 bits) and different wire name. The netlist obtained for Altera contains a set of single bit wires with different names instead. All other wires and variables at RTL level are untraceable at gate level.

The total number of high-level entities that can be targeted by fault injection are listed in Table 1. Most targets for fault injection are located in combinational logic on post-map level and, therefore, it is not clear whether they can be covered with fault injection experiments on RT level. Thus, we have defined two stages when studying the representativeness of fault injection results at different description levels. ***Stage 1***, addressed in this paper, just covers the injection of exactly the same faults at equivalent targets on different HDL levels – external interfaces and registers. As exactly the same targets are considered, the goal is to check whether results of SBFI experiments on RT level are consistent with those obtained at lower-level models (implementation level) in terms of detected errors and failures. As will be shown in section 4, behavioral aspects should always be considered as probable cause of differences between results obtained at different levels. It is also expected that timing aspects are important for detecting errors/failures when injecting transient faults.

***Stage 2,*** to be addressed in future work, covers the fault injection targets that are different between HDL levels (level-specific targets that cannot be precisely related to other elements in different models). The goal is to identify whether the consideration of all these elements really affects the results obtained at different description levels. In such a way, if those elements could be somehow traced among all the levels (maybe not individually but as a group of elements, like all the LUTs implementing an ALU), it could be possible to estimate the expected impact of a particular implementation from the original RTL description. Likewise, it might be possible to determine which part of the system should be simulated in a lower description (and thus more costly) level to obtain precise results that may influence decisions taken in the design, like deploying a particular fault tolerance mechanisms or another.

**Table 1.** Fault targets on different levels of Xilinx Vivado and Altera Quartus workflow

| *Simulation Level* / *Fault model* | *RTL* | *Post-synthesis (Xilinx)* | *Post-implementation (Xilinx)* | *Post-implementation (Altera)* |
|---|---|---|---|---|
| Input/output bits | 22/16 | 22/16 | 22/16 | 22/16 |
| Register bits/FFs | 36 | 33 | 33 | 35 |
| Wire bits | 25 | 445 | 444 | 372 |
| LUTs | - | 150 | 150 | 212 |
| DSP | - | 1 | 1 | 1 |
| Input/Output buffers | - | 22/16 | 22/16 | 22/16 |
| Other | - | 7 Carry cells | 7 Carry cells | - |
| Total (fault targets) | 99 | 712 | 711 | 696 |

## 3 Experimental procedure targeting equivalent fault targets

The first stage of the proposed study covers the same fault models injected at equivalent fault targets at different HDL levels. For a given set of HDL models (RTL, post-synthesis netlist, and post-implementation netlist) identical SBFI experiments should be executed to identify differences in system behavior and detected errors/failures. Simulations are executed by means of Mentor Graphic's Modelsim tool, along with some custom scripts that automate the definition of experiments, the fault injection process, and the analysis of results. Results from those experiments would be comparable under the following conditions:

- Correctness of golden run: each model is verified in absence of faults, using the same test environment and workload for each HDL level.
- Equivalence of fault targets: faults are injected into entities identified as equivalent at these HDL-levels by their behavior and semantics.
- Equality of faultload: for a given set of equivalent entities, the very same faults are injected (fault model, injection time, and duration).
- Equivalence of observation targets: value dumps (logs) used to observe the behavior of the target system should be captured for entities considered as equivalent at each HDL level.

The following experimental setup is considered for the previously described case study (one-cycle ALU at Fig. 1):

- Target HDL models: RTL, post-synthesis netlist for Xilinx with SFD (Standard Delay Format) file, post-implementation netlist for Xilinx with SDF file, and post-implementation netlist for Altera with SDF file.
- Workload: random sequence of independent operations run at 36 ns period ($T_{clk}$), close to the allowable minimum for the slowest model (Altera).
- Fault injection points (targets)**:**
  - Inputs: *a, b, op, clk, rstN*.
  - Registers: {*a, b, cmb, res, flags, error_code}_reg*.
- Fault types:
  - Permanent: stuck-at-1 and stuck-at-0 for registers and inputs, and indetermination just for registers.
  - Transient: bit-flip just for registers.
- Fault injection time: randomly generated along the workload time.
- Fault duration: randomly generated in the range of [$5*T_{clk}$ : $20*T_{clk}$].
- Number of experiments: as 5 faults were injected per each target, a total of 275 experiments were performed (165 for registers and 110 for inputs).

Thus, the experimental procedure consists in the following steps.

1. Create a list of fault targets specific for each model, taking care that the same targets are considered for each model.
2. Create a list of observation targets (registers and outputs) for each model.
3. Setup a configuration file with all the different parameters previously described (fault model, instant, duration, number of injections, etc.)
4. Execute the experiments: Golden Run (in absence of faults) and faulty (in presence of faults) experiments. Faults are injected by of simulator commands, like `[force signal_name value duration]` for stuck-at faults and `[force –deposit signal_name value]` for bit-flips. At the implementation-level, where bits of the same wire have different delays, it is very important to capture output signals only in stable states. To prevent capturing transients, the option `[add list clock –notrigger …]` instructs the simulator to capture values in the observation list only at clock edges, providing also a direct correspondence between recorded values by means of timestamps. Half of the period of this sampling clock defines the accuracy of errors/failures detection.
5. Analyze experimental results: identify differences in behavior from fault occurrence until failure detection or recovery instant. Custom scripts analyze dumps of internal states (registers) and output signals for Golden Run and faulty experiments. Mismatches in register values are reported as errors, whereas mismatches on the outputs are re-ported as failures.

## 4 Experimental Results

Results of SBFI at inputs and registers (equivalent targets) for each considered description level have been analyzed. Table 2 lists the mismatches detected for stuck-at-1 faults (in bold and red), when comparing error ($T_{err}$) and failure ($T_{fail}$) instants, and reference ($RES_{ref}$) and failure ($RES_{fail}$) values on outputs. RTL model propagates

errors from registers to failures on outputs immediately, preventing the detection of errors prior to failures. In order to fix this problem minimal delay (1 ns) has been added to continuous assignment operations (from registers to wires) and to non-blocking assignment (storing value at register). That minor modification improves representatives of fault injection at RT level. In all but 5 experiments the target ALU behaved exactly the same (number of errors and failures) in presence of stuck-at faults regardless the description level. However, fault and error propagation times varied depending on the considered delay model.

**Table 2.** Detected mismatches for stuck-at-1 faults at different description levels

| $N_{ex}$ | *Injection Time* | *Fault target* | *RTL + delay* | | *Synthesized XILINX (+SDF)* | | *Implemented XILINX (+SDF)* | | *Implemented ALTERA (+SDF)* | |
|---|---|---|---|---|---|---|---|---|---|---|
| | | | $T_{err}$<br>$T_{fail}$ | $RES_{ref}$<br>$RES_{fail}$ | $T_{err}$<br>$T_{fail}$ | $RES_{ref}$<br>$RES_{fail}$ | $T_{err}$<br>$T_{fail}$ | $RES_{ref}$<br>$RES_{fail}$ | $T_{err}$<br>$T_{fail}$ | $RES_{ref}$<br>$RES_{fail}$ |
| 2 | 569.70 | a_reg[2] | 570<br>595 | 10 8 0<br>18 0 0 | 570<br>600 | 10 8 0<br>18 0 0 | 570<br>603 | 10 8 0<br>18 0 0 | 572<br>788 | **60 5 0**<br>**64 d 0** |
| 4 | 718.88 | a_reg[4] | 719<br>740 | 3c 0 0<br>7c 8 0 | 719<br>744 | 3c 0 0<br>7c 8 0 | 720<br>747 | 3c 0 0<br>7c 8 0 | 720<br>896 | **00 2 0**<br>**10 8 0** |
| 5 | 1210.71 | a_reg[5] | 1315<br>1352 | 60 5 0<br>e0 d 0 | 1317<br>1356 | 60 5 0<br>e0 d 0 | 1320<br>1359 | 60 5 0<br>e0 d 0 | 1320<br>1436 | **4e 0 0**<br>**6e 8 0** |
| 11 | 678.45 | b_reg[3] | 703<br>740 | 3c 0 0<br>b4 1 0 | 705<br>744 | 3c 0 0<br>b4 1 0 | 708<br>747 | 3c 0 0<br>b4 1 0 | 708<br>932 | **81 1 0**<br>**89 9 0** |
| 28 | 901.95 | eror_code_reg[2] | 902<br>903 | 00 2 **0**<br>00 2 **4** | 902<br>905 | 00 2 **0**<br>00 2 **7** | 903<br>906 | 00 2 **0**<br>00 2 **7** | 904<br>912 | 0 2 **0**<br>0 2 **4** |

Mismatches detected for stuck-at faults originated from structural differences at gate-level. Injection at input registers (experiments number ($N_{ex}$) 2, 4, 5 and 11 in Table 2) causes mismatches between the Altera implementation and the rest of models when a multiplication operation is executed. The diagram for the case of *a_reg[2]* is presented at Fig 2, in which a stuck-at fault causes an error at *a_reg* for both Xilinx and Altera implementations. However this error is not propagated to a failure for the Altera netlist when a multiplication is executed (8h'0c*8h'02).

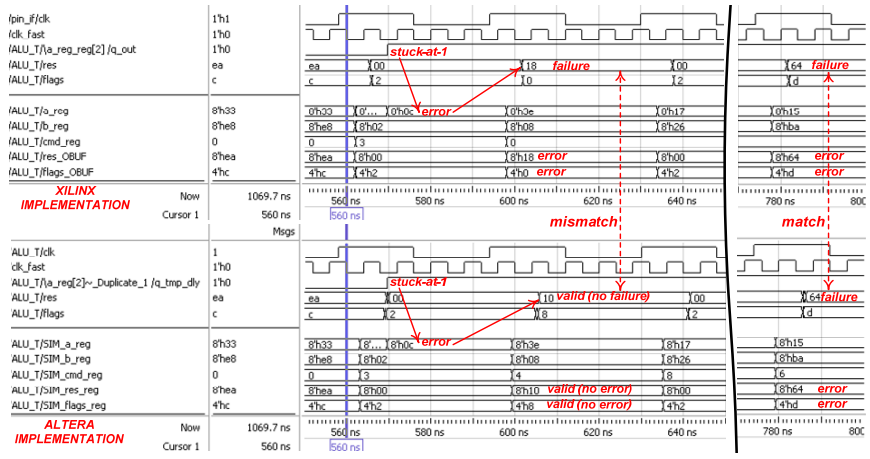


**Fig. 2.** Stuck-at-1 fault in *a_reg[2]* lead to different behavior between Altera and Xilinx implementations

Both Vivado and Quartus implemented multiplication with DSP units. Xilinx DSP units use system registers, whereas Altera *CycloneIEV_mac_mult* has its own registers and receives a value directly from the inputs, thus bypassing the system registers (c.f. Fig. 3). Consequently fault injection at *a_reg* or *b_reg* do not affect the result of multiplication, leading to mismatches with other models.

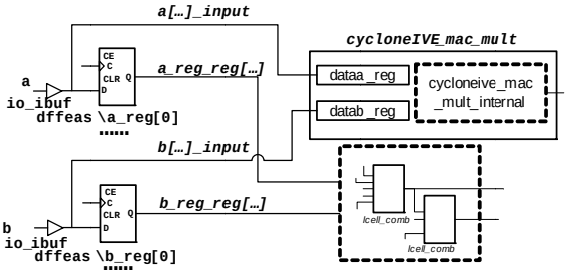


**Fig. 3.** Multiplication unit in Altera netlist receives inputs bypassing system registers

Injection of stuck-at in the *error_code* register causes a mismatch between gate-level for Xilinx and gate-level for Altera ($N_x$ 28 in Table 2). This particular situation is caused by structural differences in netlists synthesized by Vivado and Quartus (c.f. Fig. 4). The only value defined for error code at the RTL is 4'b0111 – 4 register bits. This was optimized by Quartus to 3 FFs that store exactly the same value. Vivado tool optimized this register to be just 1 FF driving the three lower bits of the output. Consequently injecting a stuck-at-1 fault at *error_code_reg[2]* for Altera leads to the failure 4'b0000 → 4'b0100 (4'h4), whereas for Xilinx is 4'b0000 → 4'b0111 (4'h7).

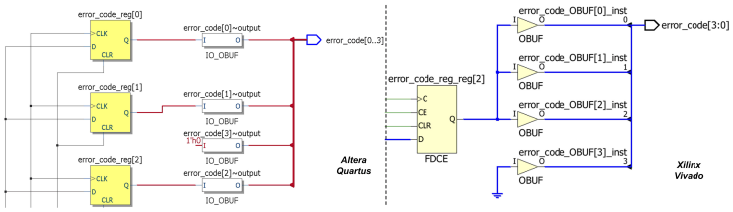


**Fig. 4.** Optimization differences at synthesis: Altera Quartus II (left), Xilinx Vivado (right)

The injection of bit-flip faults reveals differences in trigger behavior between RTL and gate-level descriptions. Faults targeting the low bit of the result register do not lead to errors/failures for RTL, whereas several are detected at gate-level for both Altera and Xilinx. The behavior of those models is compared in the timing diagram shown at Fig. 5, in which a bit-flip is injected at 881.56 ns just before the clock edge at 882 ns. At RTL code (without delays error) a failure appeared just for 0.44 ns and the normal behavior was restored immediately at the rising clock edge at 882 ns with only delta delay (case c in Fig. 5). Since samples are taken each 1 ns, the tool detected neither error nor failure because at 882 ns the correct behavior was already restored. For RTL code with delays (case b), error and failure were detected at 882 ns and 883 ns, respectively, due to non-zero propagation time. For both RTL models corrupted

trigger was restored on clock rising edge, while for gate-level netlist (case a) trigger *res_reg_reg[0]* was restored only one cycle later, not reacting on clock edge at 882 ns. It should also be noted that the results register stores the value computed by ALU (8h'00 on *res_cmb wire*) during two clock cycles (at 846 ns and at 882 ns).

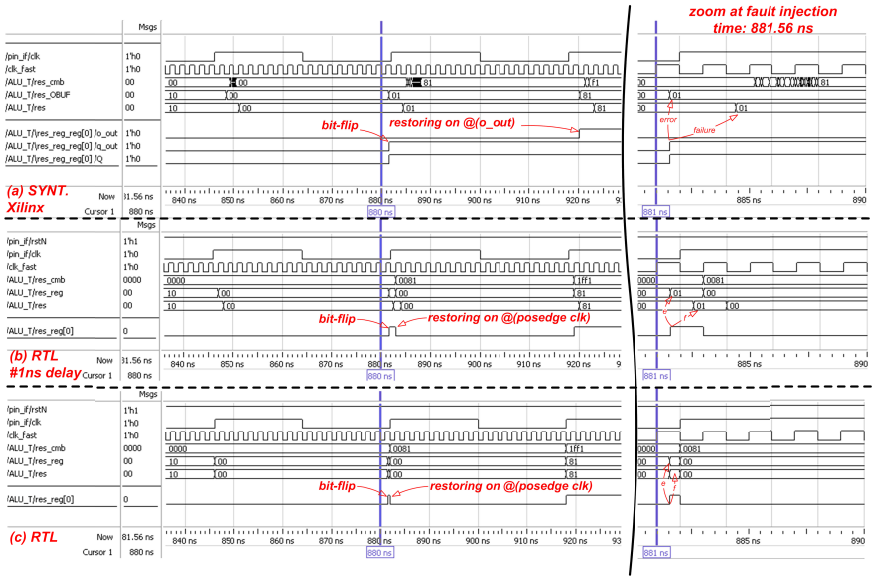


**Fig. 5.** Diagram illustrating differences between RTL and gate-level in fault propagation and restoration after injecting a bit-flip in the lowest bit of result register

In order to explain this behavior we refer to the assignment code for the register at RT level and *DFCE* (FF) code in Xilinx library (c.f. Table 3). At the RT level a new value to the *res_reg* is assigned at rising clock edges regardless of changes on *res_cmb* wire. On the gate-level *q_out* (that stores the value of the FF) updates its value only on *o_out* change, and *o_out* is connected to the output of the *ffsrce_fdce* primitive defined with a truth table. Therefore, the FF at gate-level only updates its value when input changes (8h'00 → 8'h81) on the next clock cycle (at 918 ns), maintaining its erroneous state unlike the RTL model. Altera's *dffeas* FF behaves similarly, retaining its erroneous value until the next clock cycle. Thereby timing aspects, like those related to the recovery of FFs, are not properly modeled at RTL level.

**Table 3.** Comparison of conditions for storing values at the registers for RT and gate levels

| | |
|---|---|
| *RTL* | `always_ff @(posedge clk, negedge rstN)`<br>`  if(!rstN) res_reg <= 0;`<br>`  else  res_reg <= res_cmb[operand_width-1:0];` |
| *Xilinx* | `module FDCE #( output Q, ...);`<br>`  reg q_out = INIT;`<br>`  assign Q = q_out;`<br>`  ...`<br>`  ffsrce_fdce (o_out,…);`<br>`  always @(o_out) q_out = o_out;` |

## 5 Conclusion and future work

The proposed roadmap to study the representativeness of fault injection at different description levels identifies two stages. The first one covers equivalent fault targets on each HDL level (interfaces and registers), and identifies scenarios where SBFI at higher level is not representative enough to make reasonable design decisions and therefore lower level models should be considered. Mismatches between levels detected in the simple case study presented are originated from structural and behavioral differences. Structural differences are mainly missing FFs and duplicated registers (case with DSP unit). Behavioral aspects concern elements of manufacturer's library and are important for estimating recovery latencies (case with bit-flip fault in result register). Delays from SDF files in our case study just increased fault/error propagation times and complicated matching with post-implementation level.

The second stage covers targets that are different among HDL levels and is a subject of ongoing work. The goal is to identify situations when, by taking into account combinational logic, DSP units and other untraceable elements at the higher level, additional results can be obtained to lead design decisions. In future work, the impact of synthesizers' options (optimization criteria, maintaining hierarchy, auto triplication, etc.), and of transport delay model [8] on representativeness will be explored.

## Acknowledgments

This work has been funded by the Spanish Ministry of Economy ARENES project (TIN2012-38308-C02-01).

## References

1. Nicolaidis, M.: Soft Errors in Modern Electronic Systems. Springer (2011)
2. Benso, A., Prinetto, P.: Fault Injection Techniques and Tools for Embedded Systems Reliability Evaluation. Springer (2003)
3. David de Andrés, D., Ruiz, J. C., Gil, D., Gil, P.: FADES: a Fault Emulation Tool for Fast Dependability Assessment. IEEE International Conference on Field Programmable Technology (2006) 221–228
4. Sieh, V., Tschäche, O., Balbach, F.: VERIFY: evaluation of reliability using VHDL-models with embedded fault descriptions. 27th International Symposium on Fault Tolerant Computing (1997) 32–36
5. Baraza, J. C., Gracia, J., Gil, D., Gil, P.: A prototype of a VHDL based fault injection tool: description and application. Journal of Systems Architecture, Vol. 47 (2002) 847– 867
6. Gil, P., Arlat, J., Madeira, H., Crouzet, Y., Jarboui, T., Kanoun, K., Marteau, T., Durães, J., Vieira, M., Gil, D., Baraza, J. C., Gracia, J.: Fault Representativeness. Technical report, IST-2000-25425 (2002)
7. IEEE Computer Society: IEEE Standard for SystemVerilog − Unified Hardware Design, Specification, and Verification Language. IEEE Std 1800™-2005 (2005)
8. Cummings, C.: Correct Methods For Adding Delays To Verilog Behavioral Models. International HDL Conference (1999)

# Inter-Subject variability in human atrial fibrillation. A computational population of models.

A Alejandro Liberos[1], Alfonso Bueno-Orivio[2], Miguel Rodrigo[1], Jose Millet[1] Ursula Ravens[3], Maria S. Guillem[1], Blanca Rodríguez[2]*, Andreu M. Climent[4]*

[1] BIO-ITACA, Universitat Politécnica de Valencia, Valencia, Spain.
Phone: +34-963-877-968; e-mail: allimas@upv.es
[2] Department of Computer Science, University of Oxford, Oxford, United Kingdom
[3] Department of Pharmacology and Toxicology, Dresden University of Technology, Dresden, Germany
[4] Cardiology Department, Hospital General Universitario Gregorio Marañón, Madrid, Spain
*Drs Rodríguez and Climent contributed equally as senior authors

**Abstract.** The lack of appropriated research models for persistent atrial fibrillation (AF) hampers the identification of appropriated antiarrhythmic targets. The aim of this study is to develop a realistic population of mathematical models of atrial cardiomyocytes that reproduce the large inter-subject variability of persistent AF patients.Biomarkers from patch clamp records on 149 patients diagnosed with AF were used to adjust a population of mathematical models of remodeled human atrial cardiomyocytes. The ranges of 6 biomarkers were measured from the patch-clamp studies. Only a subset of 173 mathematical models of the 16.384 simulated models fitted all biomarkers. The resulting population shows that multiple combinations of variations in the ionic conductances result in models that cover the range of biomarkers measured. Introducing restrictions associated with pacing rate limits the number of models, reduces the occurrence of anomalous calcium transients, and shows significant differences in the distribution of variation of parameters associated $I_{Na}$, $I_{Kr}$ and $I_{NAK}$ ion currents. Combinations of ionic currents with high variability resulted in realistic APs. Populations of models will improve antiarrhytmic studies based in mathematical modelling preventing undesired effects due to differences between individuals.

## 1 Introduction

Atrial fibrillation (AF) is the most common arrhythmia in the clinical practice [1, 2]. Antiarrhythmic drugs have a modest efficacy at the time of terminating the arrhythmia and sustaining sinus rhythm [3]. Those pharmacological treatment of the arrhythmia need from a deep research to understand the ionic mechanisms responsible of the maintenance of AF, mainly for long standing AF patients in which both electrical and structural atrial tissue remodeling promotes the maintenance of the arrhythmia [4, 5]. The lack of appropriated research models for persistent AF hampers the identification of appropriated antiarrhythmic targets. The aim of this study is to develop a realistic



C.Fernandez-Llatas and M.Guillen (Ed.):
Workshop on Innovation on
Information and Communication Technologies
(ITACA-WIICT 2015)

ISBN 978-84-608-4139-5

population of mathematical models of atrial cardiomyocytes that reproduce the large inter-subject variability of persistent AF patients.

## 2 Methods

### 2.1 Experimental Dataset and Biomarkers

Right atrial appendages of 149 patients diagnosed with chronic AF and who underwent cardiac surgery for myocardial or mitral/aortic valve replacement revascularization were obtained. Experimental data was recorded from human samples conforming the declaration of Helsinki, additionally the study was approved by the Ethics Committee of the Dresden University of Technology (Nº EK790799). All patients gave written, informed consent. Antiarrhythmic medication was interrupted before the study [6].

Standard intracellular microelectrodes were used to record action potentials (APs) in atrial trabeculae (n=215 of 149 patients) [7, 8]. Properties of bath solution (in mM): NaCl 127, KCl 4.5, MgCl2 1.5, CaCl2 1.8, glucose 10, NaHCO3 22, NaH2PO4 0.42, equilibrated with O2-CO2 [95:5] at 36.5±0.58 ° C, pH 7.4. The preparations were stimulated at 1 Hz no less than 1 h before data acquisition [7, 8].

Variability in the population related to APs in human atria was described with the measure of the biomarkers listed: APD (AP duration) at 20, 50, and 90% of repolarization (APD20, APD50, APD90 respectively), AP amplitude (APA), resting membrane potential (RMP), AP plateau was characterized by measuring the potential at 20% of APD90 (V20). See Figure 1.

A subset of this database n = 9 cells was also recorded at different pacing frequencies f = 1, 2, 3 and 4 Hz.

### 2.2 Electrophysiological Cellular Model

As a basis of the study, the atrial myocyte mathematical model of Koivumaki et al [9] has been used. Some modifications have been applied to implement remodeling of chronic AF: $I_{CaL}$ (-59%), $I_{to}$ (-62%), $I_{Kur}$ (-38%), $I_{K1}$ (+ 62%), $I_{NCX}$ (+ 50%), expression of SERCA (-16%) and PLB to SERCA (+ 18%) and SLN to SERCA (-40%). These variations are based on a literature study of different works facing atrial remodeling from different perspectives and with different databases, which are compiled in the work of Koivumaki et al. [10]. We will refer to this model as 'baseline AF model', we will refer to the model with no modifications as 'Koivumaki original model'.

### 2.3 Population of Models

In order to model variability between subjects, a population of models was generated from the electrophysiological model described above by varying a set of parameters from its original value: $g_{Na}$, maximum $I_{NaK}$, $g_{K1}$, $g_{CaL}$, $k_{NaCa}$, $g_{to}$, $g_{Kur}$, $g_{Kr}$, $g_{Ks}$ and ex-

pression of cpumps in SERCA and Jrel in RyR. Latin Hypercube Sampling Method [11, 12] was used to generate 16.384 combinations of the currents listed sampled from -100% to + 200% of the original values.

The resulting 16,384 unicellular models were stimulated at different frequencies: 1, 2, 3 and 4 Hz with square stimulus with duration 2 ms and amplitude 1250 pA, followed by negative amplitude in the remainder of the period to maintain current conservation in the model. All models were analyzed from period 91 to 100 in the different frequencies to extract biomarkers APD90, APD50, APD20, APA, RMP and V20 also dV / dt max and the time from stimulus onset to the peak of the AP voltage were measured.

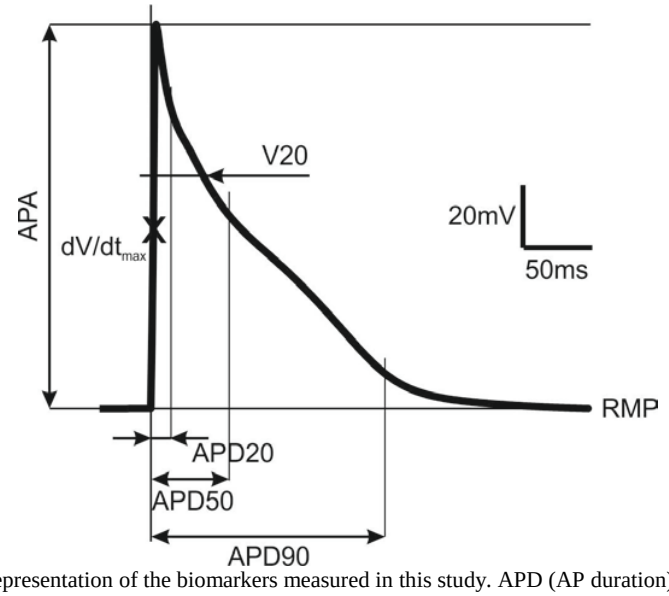


**Fig. 1.** Representation of the biomarkers measured in this study. APD (AP duration) at 20, 50, and 90% of repolarization (APD20, APD50, APD90 respectively), AP amplitude (APA), resting membrane potential (RMP), and V20 the potential at 20% of APD90 (V20). dV/dtmax is calculated as the maximum gradient of membrane voltage against time before the peak of the membrane voltage.

### 2.4 Population Calibration

The initial population consisting on 16.384 models was calibrated based on the biomarkers measured in experimental data. That is, the biomarkers obtained in the simulations were subjected to satisfy some of the conditions that describe experimental models. To do this, two different filters were used.

In the first filter, Filter 1, we ensure that biomarkers APD90, APD50, APD20, APA, RMP and V20 at 1 Hz remain restricted to the maximum and minimum values measured experimentally. To ensure biological depolarization transient, two extra constraints in biomarkers were introduced, the time from stimulus onset to the peak of the AP voltage must be lower than 20 ms and dVdtmax higher than 20 V/s.

In the case of Filter 2, the aim was that the resulting population show properties similar to that present in experimental data in terms of activation rate dependence. Specifically, we focus on establishing conditions with respect to the two biomarkers that are more sensitive to activation rate modifications (i.e. APD90 and APD50). For the evaluation of shortening or lengthening of the APs at a frequency f, APDratio(f) was defined as APD (f) divided by APD at 1 Hz for APD90 and APD50. It was observed in experimental data that the higher the APD at 1 Hz, the lower the APDratio (f). This reflects a greater shortening of APD with pacing frequency in the case of long APDs at 1Hz.

To define the constraints for the calibration of the resulting population, linear regression of APDratio vs APD 1 Hz was computed. Filter 2 consisted in accepting models that presented APDratios, for APD90 and APD50, with an error to the estimated line lower than the observed in experimental data.

### 2.5 Statistical analysis

The effects introduced by rate dependent biomarkers in the distribution of parameter variations will be evaluated. Mann-Whitney U-test was used to evaluate statistical significance between variables, statistical significance was considered for $p<.01$.

## 3 Results

### 3.1 Experimental Dataset and Biomarkers

Minimum and maximum values of the biomarkers measured with pacing frequency 1Hz are filed in Table 1.

**Table 1.**

| | Minimum Value | Maximum Value |
|---|---|---|
| APD90 (ms) | 140 | 330 |
| APD50 (ms) | 30 | 180 |
| APD20 (ms) | 1 | 75 |
| APA (mV) | 80 | 130 |
| RMP (mV) | -85 | -65 |
| V20 (mV) | -30 | 20 |

Minimum and maximum values of APD90 and APD50 in the subset recorded at different frequencies were: 167-236, 148-220, 134-199 and 121-176 ms in case of APD90 for 1, 2, 3 and 4 Hz respectively; and 59-121, 65-118, 62-108, 56-96 ms in case of ADP50.

### 3.2 Resulting Population

Filter 1 has limited the number of valid models to 1.118 from the original 16.384, by discarding those models that do not fit in the range of biomarkers presented in Table 1. Adding the filter 2 this number is reduced to 173 different models, obtaining APs with a response to pacing frequency similar to that observed experimentally.

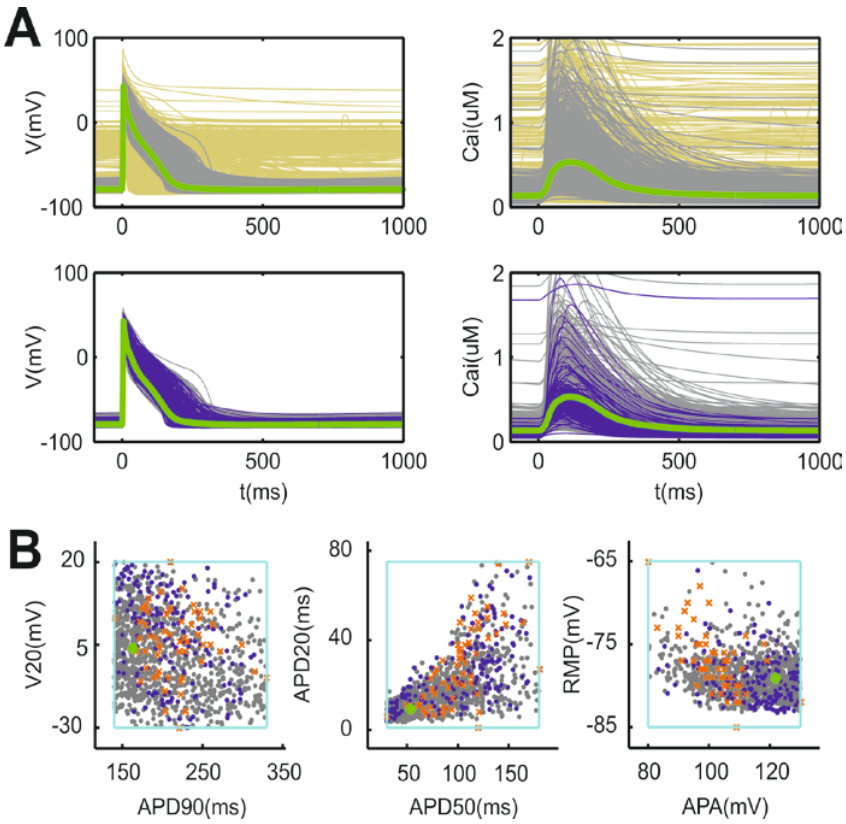


**Fig. 2.** Population of models calibration and biomarkers at 1Hz. Panel A depicts AP and intracellular calcium tracing. Green lines represent the signals corresponding to the baseline AF model; yellow, gray and blue lines correspond to all the models simulated (N=16384), those that fitted the conditions of filter 1 (N=1118) and those that satisfied the constraints of both filters respectively. Panel B shows the values of the biomarkers –V20, APD20, APD50, APD90, RMP and APA- in the populations, the subgroups of the populations correspond again with the colors previously described. Orange crosses correspond with a random sort of values measured in experimental preparations, experimental biomarker limits are depicted in turquoise.

In Figure 2, the effect of the filters used on the population at 1Hz is described. APs and Calcium tracings presented in Panel A, exhibit how filter 1 dramatically reduces the variability in RMP and in APD, it also eliminates those models which APA was

out of the established ranges. In case of intracellular calcium, it is observed that diastolic Ca2+ is reduced to values values than 0.5 uM in most cases. The second row in panel A, evince how the filter 2 has no significant effect in reducing the variability in biomarkers of voltage, however it can be observed how the number of cases outside of the outlying areas was reduced in diastolic Ca2+ and Ca2+ amplitude.

Panel B shows how models achieve the coverage of six biomarkers at 1Hz, the experimental range of values is reasonably covered having all the experimental values nearby points.

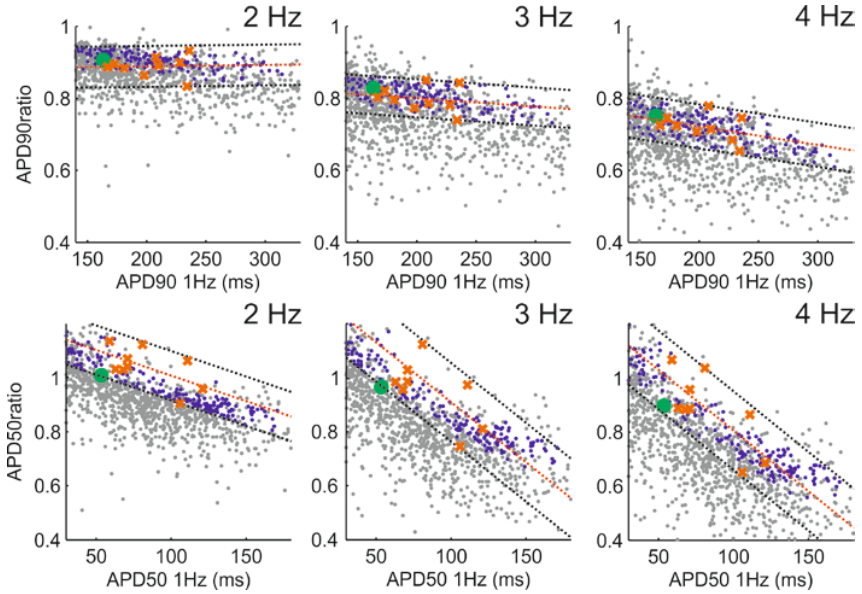


**Fig. 3.** Population of models calibration and pacing frequency dependence. Only the models with a deviation from regression lines –depicted in red- lower than those observed in experimental measurements were accepted. APD ratios are plotted versus APDs at pacing frequencies 2, 3 and 4 Hz, orange crosses correspond with experimental values while green, gray and blue dots correspond with the baseline model, the models accepted by filter 1 and the final population respectively. Note that the gray dots can be present between both error lines –depicted in black- as the condition needs to be satisfied in the six cases, leading to the final population depicted in blue.

Figure 3 shows the coverage of APD50 and 90 ratios for the resulting population of 173 models. It is observed that the most of the models that achieve constraints of Filter 1, voltage biomarkers at 1Hz, present lower values in APDratio than the observed in experimental measurements. It is also observed that the most of the models that satisfied the conditions of biomarkers at 1Hz do not accomplish the pacing frequency constraints in the six scenarios, only the resulting population depicted in blue covered all the conditions.

Figure 4 present the distribution parameter variations for different ionic currents. It can be observed a high variability as the most of the parameters as they cover the whole range of variations from -100% to +200%, $g_{Na}$ is an exception as it was the most constrained current with limits in overexpression and blockade of +65% and -90% respectively. $g_{Na}$ was one of the parameters that presented significant alterations at the time of accomplish the rate dependence constraints, $g_{Na}$ was more constrained in the resulting population and showed a lower median than in the case of the models that only covered the conditions of biomarkers at 1Hz.

Regarding $I_{NaK,max}$, the sodium potassium pump needed a significant overexpression to cover rate dependence requirements, in this case the median value differs a lot from both the original and baseline AF models, this is due to the need of restoring ionic concentrations from beat to beat.

The other current that showed significant differences due to the need of covering rate dependence conditions was $g_{Kr}$, it presented a higher overexpression when rate dependence conditions were imposed. The median value was also higher than the baseline AF model.

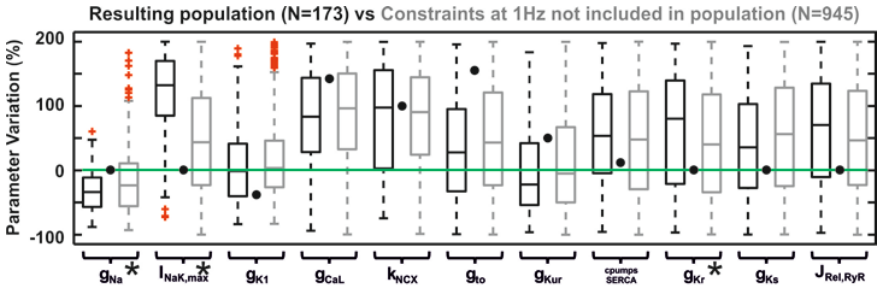


**Figure 4.** Box plot of the ionic current parameter variations in the population of models. The boxplots in black correspond to the final population, it means the models that fitted the constraints of biomarkers at 1Hz and the conditions of rate dependence. In gray the models that fitted the constraints of biomarkers at 1Hz but cannot accomplish the conditions of rate dependence. The green line depicts the baseline values –i.e. the Koivumaki AF model or baseline AF model- while black dots represent the original Koivumaki model. A high variability in conductances covering the whole range of values (from -100% to 200%) can be observed. It is also observed how the most constrained current is INa with limits in overexpression and blockade of +65% and -90% respectively in the resulting population.

The rest of parameters didn't present significant difference because of rate dependence conditions, note that the median value in the case of $g_{K1}$ were in the baseline level in both groups. Regarding $g_{CaL}$, the median is situated between the baseline AF model and the original Koivumaki model. It means that to cover the range of biomarkers it was not necessary an strong blockade of this current. Something similar happens in relation with $k_{NCX}$, that presented a median closer to the original Koivumaki model than to the baseline AF model.

$g_{to}$ and $g_{Kur}$ present medians close to the baseline AF model , while in the case of cpumps SERCA, $g_{Ks}$, JRel,RyR presented a high variability in the variations and me-

dians close to 50% of variation showing that this parameters are not determinant at the time of covering the range of biomarkers.

## 4 Discussion

In this work, a population of models of atrial cells suffering of AF has been implemented. Experimental data of cells paced at different frequencies were used in order to achieve a population with a realistic response in episodes of atrial fibrillation. For this purpose and because the number of cells recorded at various frequencies was lower and presented less variability in biomarkers, APDratio ratio was introduced to extend this data to the original dataset with 149 patients. It was observed that models with longer APDs at 1Hz presented more important shorten –showing lower APDratios-that models with models with lower APDs. It was also observed how atrial cells with short APD50s presented a lengthen with the increase of pacing frequency, this behavior was emulated in the resulting population of models.

The resulting population shows that even with a limited variability in biomarkers, it is possible to fulfill these conditions with multiple combinations of variations in the ionic conductances. Thus, very high variability occurs in the parameters associated with the ionic currents having acceptable variations in most parameters in the range -100, + 200%. It has also shown how the resulting population covers a reasonably variability of biomarkers at 1Hz and conforms to the limitations associated with rate dependence. The models that covered the conditions of rate dependence presented significant differences in $g_{Na}$, $I_{NaK,max}$ and $g_{Kr}$. It was also observed that the resulting population presented a distribution of parameter variations showing that $g_{K1}$ was centered around the baseline model presented by Koivumaki while $I_{CaL}$ and $I_{NCX}$ didn't show the need of a blockade as strong as presented in a sort of previous works [13-16].

Latin Hypercube Sampling Method allows sampling a high dimensional space efficiently, in this case 11 dimensions corresponding with each paramenter. Sampling every possible combination of dimensions with an adequate resolution should be computationally unfeasible. The method used allowed the sampling in the space and without bias. In order to differentiate those parameters with a median value model with those having a modest effect on biomarkers and therefore with a median close to the midpoint of the variation ranges, an asymmetric variation of the parameters was implemented. It highlighted the strength of a sort of currents $g_{Na}$, $I_{NaK,max}$, $I_{K1}$, $k_{NCX}$ or $I_{Kur}$.

In-silico studies have evaluated the effect of blocking different currents both in isolated cells [10, 17] and tissue models [18] to evaluate the effects in APs or in the dynamics of functional reentries or rotors. However, models developed to study atrial electrophysiology, are the synthesis from many experiments and cells, even from cells of different species. Variability is present in the most of biological structures in nature. It makes healthy individuals of the same species exhibit such differences in some biomarkers which often hinder the definition of pathological behaviors, and its thera-

pies. Scientific experiments are generally performed in highly controlled environments and models, plus the results obtained are usually averaged to reduce errors.

AP is not an exception and presents important differences in morphology to the same species and area. However, electrophysiological models are obtained from an average of many experimental results with the aim of performing a typical behavior. This methodology easies understanding of electrophysiological mechanisms, but sometimes hinders the extrapolation to clinical practice.

In conclusion, this study shows the ability of a different of combinations of ionic currents in reflecting realistic AP. Intersubject variability should be taken into account when proposing pharmacological treatments on individuals. Populations of models will improve viability studies of these treatments based in mathematical modelling and will avoid undesired effects.

## References


1. Baldonado, M., Chang, C.-C.K., Gravano, L., Paepcke, A.: The Stanford Digital Library Metadata Architecture. Int. J. Digit. Libr. 1 (1997) 108–121
2. Bruce, K.B., Cardelli, L., Pierce, B.C.: Comparing Object Encodings. In: Abadi, M., Ito, T. (eds.): Theoretical Aspects of Computer Software. Lecture Notes in Computer Science, Vol. 1281. Springer-Verlag, Berlin Heidelberg New York (1997) 415–438
3. van Leeuwen, J. (ed.): Computer Science Today. Recent Trends and Developments. Lecture Notes in Computer Science, Vol. 1000. Springer-Verlag, Berlin Heidelberg New York (1995)
4. Michalewicz, Z.: Genetic Algorithms + Data Structures = Evolution Programs. 3rd edn. Springer-Verlag, Berlin Heidelberg New York (1996)

1. Haissaguerre, M. et al. Catheter ablation of chronic atrial fibrillation targeting the reinitiating triggers. J. Cardiovasc. Electrophysiol. 11 (2000), 2-10
2. Pedersen, O. D. et al. Atrial fibrillation, ischaemic heart disease, and the risk of death in patients with heart failure. Eur. Heart J. 27 (2006) 2866-2870
3. Nattel, S. New ideas about atrial fibrillation 50 years on. Nature 415 (2002) 219-226
4. Jalife, J., Berenfeld, O. & Mansour, M. Mother rotors and fibrillatory conduction: a mechanism of atrial fibrillation. Cardiovasc. Res. 54 (2002) 204-216
5. Pandit, S. V. & Jalife, J. Rotors and the Dynamics of Cardiac Fibrillation. Circ. Res. 112 (2013) 849-862
6. Sanchez, C. et al. Inter-Subject Variability in Human Atrial Action Potential in Sinus Rhythm versus Chronic Atrial Fibrillation. PLoS One 9 (2014) e105897
7. Wettwer, E. et al. Role of I-Kur in controlling action potential shape and contractility in the human atrium - Influence of chronic atrial fibrillation. Circulation 110 (2004) 2299-2306
8. Wettwer, E. et al. The new antiarrhythmic drug vernakalant: ex vivo study of human atrial tissue from sinus rhythm and chronic atrial fibrillation. Cardiovasc. Res. 98 (2013) 145-154
9. Koivumaki, J. T., Korhonen, T. & Tavi, P. Impact of Sarcoplasmic Reticulum Calcium Release on Calcium Dynamics and Action Potential Morphology in Human Atrial Myocytes: A Computational Study. PLoS Comput. Biol. 7 (2011) e1001067
10. Koivumaki, J. T., Seemann, G., Maleckar, M. M. & Tavi, P. In Silico Screening of the Key Cellular Remodeling Targets in Chronic Atrial Fibrillation. PLoS Comput. Biol. 10 (2014) e1003620

11. Mckay, M., Beckman, R. & Conover, W. A comparison of three methods for selecting values of input variables in the analysis of output from a computer code. Technometrics 42 (2000) 55-61
12. Britton, O. J. et al. Experimentally calibrated population of models predicts and explains intersubject variability in cardiac cellular electrophysiology. Proc. Natl. Acad. Sci. U. S. A. 110 (2013) E2098-E2105
13. Bosch, R. F. et al. Ionic mechanisms of electrical remodeling in human atrial fibrillation. Cardiovasc. Res. 44 (1999) 121-131
14. Van Wagoner, D. R. et al. Atrial L-type Ca2+ currents and human atrial fibrillation. Circ. Res. 85 (1999) 428-436
15. Workman, A. J., Kane, A. K. & Rankin, A. C. The contribution of ionic currents to changes in refractoriness of human atrial myocytes associated with chronic atrial fibrillation. Cardiovasc. Res. 52 (2001) 226-235
16. Gaborit, N. et al. Human atrial ion channel and transporter subunit gene-expression remodeling associated with valvular heart disease and atrial fibrillation. Circulation 112 (2005) 471-481
17. Courtemanche, M., Ramirez, R. & Nattel, S. Ionic targets for drug therapy and atrial fibrillation-induced electrical remodeling: insights from a mathematical model. Cardiovasc. Res. 42 (1999) 477-489
18. Pandit, S. et al. Ionic determinants of functional reentry in a 2-D model of human atrial cells during simulated chronic atrial fibrillation. Biophys. J. 88 (2005) 3806-3821

# Analysis of LTE-A Random Access Procedure: A Foundation to Propose Mechanisms for Managing the M2M Massive Access in Wireless Cellular Networks *

Luis Tello-Oquendo, Israel Leyva-Mayorga, Vicent Pla, Jorge Martinez-Bauset and Vicente Casares-Giner

ITACA Research Institute
Universitat Politècnica de València, Spain

**Abstract.** Machine-to-machine (M2M) communication or machine-type communication (MTC) is considered an integral part of the so-called Internet of Things. M2M provides ubiquitous connectivity among devices without human intervention. Using cellular networks to provide M2M connectivity presents numerous advantages (coverage, roaming support, interoperability, well developed charging, quality of service, and security solutions among others). However, a large number of devices, that may need to communicate over a short period of time, can cause problematic situations which hugely impacts the radio access and core networks of the cellular system. In this paper, we provide a comprehensive survey on random access procedure in the context of 3GPP Long-Term Evolution (LTE) and LTE-Advanced (LTE-A). Specifically, we give a complete description of the parameters and the information necessary to evaluate the random access procedure when the cellular network is subjected to M2M traffic. It will be useful for designing mechanisms and algorithms to efficiently manage the massive accesses on the air interface.

## 1 Introduction

The world is moving beyond standalone devices into a new technological age in which everything is connected. Machine-to-Machine (M2M) communication stands for the ubiquitous automated exchange of information between devices on the edge of networks (computers, sensors, actuators, cars or mobile devices) inside a common network, the so-called Internet of Things (IoT).

M2M is what provides the IoT with the connectivity that enables capabilities, which would not be possible without it. A wide area of applications have already started to emerge in several fields, such as health-care, smart robots, smart grids, smart home technologies, intelligent transportation systems and smart cities [16]. One of the major motivating factors of MTC, besides the total automation of devices without involving human effort, is that MTC devices get smaller and more power efficient, while gaining more computing power.

* This work has been supported by the Ministry of Economy and Competitiveness of Spain through the project TIN2013-47272-C2-1-R.



C.Fernandez-Llatas and M.Guillen (Ed.):
Workshop on Innovation on
Information and Communication Technologies
(ITACA-WIICT 2015)

ISBN 978-84-608-4139-5

All of these properties would be of no use without a network to link those devices together. Two main approaches have emerged for this purpose. One the one hand are short or medium range wireless networks (IEEE 802.15.4 (ZigBee) and IEEE 802.11 (WiFi) [10, 13]) that can be used in a given area. On the other hand are cellular networks that offer many benefits, such as ubiquitous coverage by widely deployed infrastructure, global connectivity with a number of providers, and well developed charging and security solutions. Therefore, the cellular networks may be the solution for linking MTC devices by providing a solid infrastructure, high mobility, easy deployment and most importantly, wide area of coverage [19, 21].

In recent years, most research focuses on Long Term Evolution Advanced (LTE-A) as the technology enabling M2M communications. LTE-A is the most recent standard of wireless communication proposed by the 3rd Generation Partnership Project (3GPP) to serve its cellular mobile users by providing high data bandwidth. LTE-A cellular networks were not designed for M2M traffic. Instead, they were mainly designed to support human-to-human (H2H) services such as voice and web browsing, and bandwidth demanding services such as video streaming.

The nature of M2M communication is different from that of regular H2H communication and it is mainly characterized by a high device density in a cell, small amounts of payload, low traffic volumes per device, predominance of up-link traffic, low device mobility, low device processing capacity and battery operated devices [3]. Although MTC devices generate small amount of data traffic, the massive amount of MTC devices could create an overload problem which hugely impacts the radio access and core networks of the system, reducing the overall performance of LTE-A [20]. To mitigate this problem, besides to improve the system [4,5], it is important to provide an efficient way for managing the massive access in the radio access network and to minimize the network overload.

In this paper, we study the random access (RA) procedure of LTE-A networks. MTC devices must perform it for initial and periodic RA, in order to request resources to the network before they transmit data. The aim is to provide a complete description of the parameters and the information necessary to evaluate the RA procedure of LTE-A. We consider this work as the first step to propose efficient mechanisms and algorithms to mitigate the overload in the radio access network.

The remainder of the paper is organized as follows. Section 2 describes the LTE-A radio interface. Section 3 presents the RA procedure, key in mobile networks, which enables user equipment (UE) to initiate communications to a base station. Section 4 details the considerations to evaluate the RA performance when the cellular network is subjected to M2M traffic. Section 5 provides numeric results of access success probability. Finally, the conclusions are presented in Section 6.

## 2 Brief Overview of LTE-A Radio Interface

The LTE-A radio access network consists of the base stations, denoted as enhanced NodeB (eNB), that are connected to each other through the X2

interface and to the evolved packet core (EPC) through the S1 interface. The mobile terminal or MTC device is denoted as user equipment (UE). In this section, we describe briefly the LTE-A radio interface. We focus in the physical layer characteristics which provide the resources for the RA procedure. A more detailed description can be found in [2, 9, 11, 14, 15].

In LTE-A, orthogonal frequency-division multiplexing (OFDM) is the down-link (DL) multiple access scheme, while single-carrier frequency-division multiple access (SC-FDMA) is the up-link (UL) multiple access scheme. LTE-A also supports scalable bandwidth up to 20 MHz per component carrier (a maximum of 100 MHz with carrier aggregation); it uses DL/UL frequency selective and DL frequency diverse scheduling. In the UL, like the DL, frequency domain orthogonality is maintained among intra-cell users, which allows the eNB the ability to efficiently manage the amount of interference seen at the base station.

The UL and DL sub-frame structure is common to both time-division duplex (TDD) and frequency-division duplex (FDD). Each sub-frame consists of two slots of length 0.5 ms (7 OFDM symbols for normal cyclic prefix) with reference symbols located within each slot. UL control signaling such as channel quality indication (CQI) and acknowledgment/negative acknowledgment (ACK/NACK) is located in the system band-edge.

Each portion in the time and frequency resource grid is called a resource element (RE). Users are assigned data allocation in amounts of resource blocks (RBs), where a RB is defined as 12 REs by one slot. Each DL sub-frame contains reference signals, control information, and data transmission. The following physical channels provide DL control signaling: physical control format indicator channel (PCFICH), physical hybrid automatic repeat request (HARQ) indicator channel (PHICH), and physical DL control channel (PDCCH). The DL and UL scheduling assignment transmitted on the PDCCH is addressed to a specific user, and contains control information needed for data reception and demodulation. Table 1 summarizes the available DL and UL physical channels and their purpose.

**Table 1.** Physical Channels in LTE

| Channel | | Purpose |
|---|---|---|
| **DL** | PDSCH | Carry user data (DL) |
| | Physical broadcast channel (PBCH) | Carry broadcast information |
| | Physical multi-cast channel (PMCH) | Carry multi-cast services |
| | PCFICH | Indicate the size of the control region in number of OFDM symbols |
| | PHICH | Carry ACK/NACK associated with UL transmission |
| | PHICH | Carry DL scheduling assignments and UL scheduling grants |
| **UL** | PUSCH | Carry user data (UL) |
| | PUCCH | Carry ACK/NACK associated with DL transmission, scheduling request, and feedback of DL channel quality and precoding vector |
| | Physical random access channel (PRACH) | Initiate random access procedure |

### 2.1 LTE-A Physical Random Access Channel

The Physical Random Access Channel (PRACH) is used to signal a connection request when a UE desires to access the cellular network (call origination or paging response). The PRACH carries the preamble (explained below) for initial access to the network. It uses small preamble to lower overhead and it is orthogonal to PUSCH/PUCCH.

Random access attempts are done in predefined time/frequency resources called RA slots herein. In the time domain, the duration of each RA slot depends on the format of the access requests (as shown in Fig. 1). In the frequency domain, each RA slot occupies 1.08 MHz, which corresponds to the bandwidth of 6 RBs. These RA slots are reserved in the UL channel of the network for the transmission of access requests. The eNB broadcasts the periodicity of the RA slot by means of a variable referred to as the PRACH Configuration Index. The periodicity varies between a minimum of 1 RA slot every 2 frames, i.e., every 20 ms, and a maximum of 1 RA slot per 1 sub-frame, i.e., every 1 ms [6, 17].

**Random Access Preamble** If a UE tries to access to a RA slot, it must select randomly a preamble (signature) for the very first message of RA procedure. There are up to 64 orthogonal preambles available to the UEs per cell. These preambles are generated by Zadoff-Chu (ZC) sequences due to their good correlation properties [6, 22].

There are altogether 5 formats of RA preambles, format 0 to format 4. From Fig. 1, we can see the format 0 to 3 have different lengths. These should be chosen specifically according to different cell size. In cells with larger size, longer preamble must be used since the UL timing difference between the farthest and nearest UE is larger. On the other hand, shorter preamble should be used in small cells to avoid unnecessary wastage of the resources. The format 4 is not shown in Fig. 1; it is available only for the TDD system.

Preambles are split into two sets:

- Contention-free: it is used for critical situations such as handover, DL data arrival or positioning, where there is a coordinated assignment of preambles so collision is avoided. eNB can only assign these preambles for specific slots to specific UEs. UEs can only use these, if assigned by the eNB, and for the specific slots assigned.
- Contention-based: it is the standard mode for network access (there are more preambles in this set). Preambles are selected in a random fashion, so there is risk of collision, i.e., there is a probability that multiple UEs in the cell could pick the same preamble signature and the eNB would assign the same RB to both UEs; therefore contention resolution is needed.

## 3 Random Access Procedure

This section provides a general overview of the RACH operation of LTE-A. We focus on contention-based RA mechanism. A UE can only be selected for UL transmission if it is time-synchronized. The main role of the RA procedure is to request for UL resources, for that it is necessary to assure such time synchronization for a UE which either has not yet acquired, or has lost its UL synchronization [22].

### 3.1 Contention-Based Random Access Procedure

In order to explain the RA procedure, we use the message exchange represented in Fig. 2. The eNB broadcasts information (through System Information Blocks)

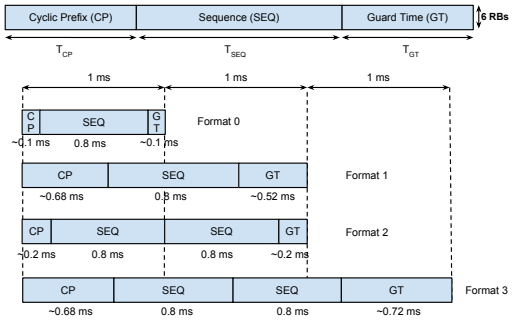


**Fig. 1.** Structure and Preamble Formats

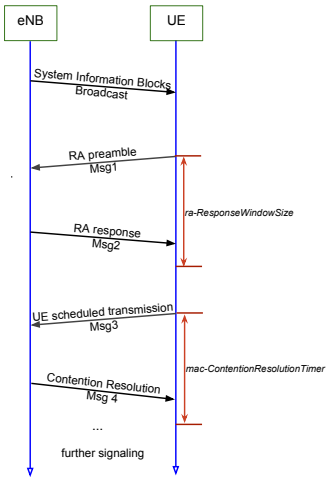


**Fig. 2.** Contention-based RA Procedure

about which RA slot the preamble transmission is allowed; in each RA slot, the eNB reserves a number of preambles for UEs to perform RA. A UE sends a randomly chosen preamble in a RA slot (Msg1) and waits for a time window to receive a response from the eNB. Then, the eNB sends the RA response (Msg2); it includes information about identification of detected preamble, time alignment instructions, UL grant for Msg3 transmission, a Temporary Cell Radio Network Temporary Identifier (T_C-RNTI) and Back-off Indicator. If more than two UEs choose the same preamble in the RA slot, a collision will occur in the transmission of Msg3. The eNB can detect non-collided UEs with a probability which mainly depend on the transmission power of the UE. The UEs which are collided or not detected by the eNB are referred as failed UEs. The failed UEs should ramp up its power, and retransmit a new randomly chosen preamble in a new RA slot based on a uniform back-off algorithm; they repeat this process until a transmission limit is reached. The UEs which not collided will exchange Msg3 with eNB through dedicated channels and hybrid automatic repeat request (HARQ) is used to protect the message transmission. The eNB transmits a Contention Resolution message (Msg4) as an answer to Msg3. A UE which does not receive Msg4 declares a failure in the contention resolution and schedules a new access attempt, i.e., a new preamble transmission, starting the process over again. Each UE keeps a preamble transmission counter that is increased after each unsuccessful attempt. When the counter reaches the maximum allowed value (informed as system information by the eNB), the network is declared unavailable by the UE and a RA problem is indicated to upper layers [2, 7, 8, 12, 17].

Algorithm 1 presents the procedure used by the UE to perform the RA as defined by [2, 7]. For message definitions and field description of information elements please refer to Sections 6.2.2, 6.3.1 and 6.3.2 in [8]. The MAC layer parameters are borrowed from [2] and for the most part detail of Algorithm 1.

**Algorithm 1** LTE-A Random Access Procedure

1: UE gets System Information Blocks from eNB. UE needs to access eNB.
2: (a) Flush the Msg3 buffer; set the $Preamble\_Transmission\_Counter$ to 1; set the $backoffParameterValue$ to 0 ms;
3: Is $Preamble\_Transmission\_Counter = preambleTransMax + 1$?:
   – If yes: ACCESS FAILURE; indicate a RA problem to upper layers.
   – Otherwise: go to step 4.
4: Select a random back-off time according to $unif\{0, backoffParameterValue\}$ and delay the subsequent RA transmission by the back-off time;
5: Select randomly a preamble sequence; determine the next available sub-frame containing PRACH and proceed to the transmission of the preamble.
6: Monitor the PDCCH for Msg2, identified by the $RA\text{-}RNTI$, within the $ra\text{-}ResponseWindowSize$.
7: Did UE receive Msg2 within $ra\text{-}ResponseWindowSize$ and $RAPID$ matches $RA\text{-}RNTI$ on PDCCH?
   – If yes:
     (a) set the $backoffParameterValue$ as indicated by the Back-off Indicator; set the $T\_C\text{-}RNTI$ to the value received in Msg2; process the received TAC; process the received UL grant value and indicate it to the lower layers;
     (b) indicate to lower layers the $preambleInitialReceivedTargetPower$ and the amount of power ramping $((Preamble\_Transmission\_Counter - 1) * powerRampingStep)$ applied to the latest preamble transmission;
     (c) transmit the initial Msg3 four sub-frames later in PUSCH location assigned in the UL grant. If $C\text{-}RNTI$ is not yet assigned, UE uses the $T\_C\text{-}RNTI$ and CCCH SDU is included in Msg3. Otherwise, UE sends message in PDCCH;
     (d) start $mac\text{-}ContentionResolutionTimer$ and restart it at each HARQ retransmission; go to step 9.
   – Otherwise: go to step 8.
8: Did the UE receive a notification of power ramping suspension?
   – If yes: increment $Preamble\_Transmission\_Counter$ by 1 and suspend power ramping; go to step 3.
   – Otherwise: increment $Preamble\_Transmission\_Counter$ by 1 and boost power by $powerRampingStep$ factor in dB; go to step 3.
9: Did $mac\text{-}ContentionResolutionTimer$ expire?
   – If yes: discard the $T\_C\text{-}RNTI$; flush the HARQ buffer; go to step 8.
   – Otherwise: go to step 10.
10: Did UE receive notification of a reception of a PDCCH transmission from lower layers?
   – If yes: Is the PDCCH transmission addressed to the $C\text{-}RNTI$?
     • If yes: Contention Resolution successful; stop $mac\text{-}ContentionResolutionTimer$; discard the $Temporary\_C\text{-}RNTI$; RA procedure successfully completed.
     • Otherwise: Does the decoded MAC PDU contain a UE Contention Resolution Identity MAC control element and it matches the CCCH SDU transmitted in Msg3?
       * If yes: Contention Resolution successful; stop $mac\text{-}ContentionResolutionTimer$; set the $C\text{-}RNTI$ to the value of the $T\_C\text{-}RNTI$ and discard it; RA procedure successfully completed.
       * Otherwise: discard the successfully decoded MAC PDU; go to step 9.
   – Otherwise: go to step 9.

C-RNTI, Cell Radio Network Temporary Identifier; RA-RNTI, Random Access Radio Network Temporary Identifier; RAPID, Random Access Preamble ID; MAC, Medium Access Control; SDU, Segment Data Unit; PDU, Packet Data Unit; TAC, Timing Advance Command.

## 4 Evaluation of LTE-A FDD RACH for M2M communication

In order to evaluate the network performance under M2M traffic, a single cell environment is assumed. The network is subjected to different access intensities; for that, 3GPP TR 37.868 [1] defined two different traffic models for the evaluation of network performance, these are listed in Table 2. Traffic model 1 can be considered as a realistic scenario in which MTC devices access the network uniformly over a period of time, i.e. in a non-synchronized manner. Traffic model 2 can be considered as an extreme scenario in which a large amount of MTC devices access the network in a highly synchronized manner, e.g. after a power outage.

**Table 2.** Traffic Model for RACH Evaluation [1]

| **Characteristics** | **Traffic Model 1** | **Traffic Model 2** |
|---|---|---|
| Number of MTC devices (N) | 1000, 3000, 5000, 10000, 30000 | 1000, 3000, 5000, 10000, 30000 |
| Arrival distribution | Uniform distribution over T | Beta distribution over T |
| Distribution period (T) | 60 seconds | 10 seconds |

**Table 3.** Basic Simulation Parameters for LTE FDD RACH Capacity Evaluation

| **Parameter** | **Setting** |
|---|---|
| Cell bandwidth | 5 MHz |
| PRACH Configuration Index | 6 |
| Total number of preambles (M) | 54 |
| $preambleTransMax$ | 10 |
| Number of UL grants per RAR | 3 |
| Number of CCEs allocated for PDCCH | 16 |
| Number of CCEs per PDCCH | 4 |
| $ra\text{-}ResponseWindowSize$ | 5 sub-frames |
| $mac\text{-}ContentionResolutionTimer$ | 48 sub-frames |
| Backoff Indicator (BI) | 20 ms |
| HARQ retransmission probability for Msg3 andMsg4 (non-adaptive HARQ) | 10% |
| Maximum number of HARQ TX for Msg3 andMsg4 (non-adaptive HARQ) | 5 |
| Periodicity of PRACH opportunities | 5 ms |
| Preamble transmission time | 1 ms |

If two (or more) MTC devices select the same preamble at the same time, it is assumed that the eNB will not be able to decode any of the preambles; hence, the eNB will not send the Random Access Response (Msg2). MTC devices will only detect a collision if Msg2 is not received in the $ra\text{-}ResponseWindowSize$. In case of no collision, $1-(1/e^i)$ preamble detection probability is assumed, where $i$ indicates the $i-th$ preamble transmission to take into account the effects of radio channels, for example path-loss, fading, inter-cell interference, etc [1].

The following measures could be taken into account for the purpose of RACH capacity evaluation [1]:

1. Access success probability, defined as the probability to successfully complete the RA procedure within the maximum number of preamble transmissions.
2. Statistics of number of preamble transmissions, defined as the cumulative distribution function (CDF) of the number of preamble transmissions to perform a RA procedure, for the successfully accessed MTC devices.

3. Statistics of access delay, defined as the CDF of the delay for each RA procedure between the first RA attempt and the completion of the RA procedure, for the successfully accessed MTC devices.

## 5 Numerical Results

In this section we show some results according the methodology proposed in [1] and detailed in Section 4. In order to understand the limits of the LTE-A RACH, we analyze the overloaded scenario, i.e., more than 1.000 devices that need to access the network simultaneously.

The system setup and simulation parameters follow Tables 2 and 3. There is a RA slot every 5 ms and 54 out of the 64 available preambles are used for contention-based access, while the remaining 10 preambles are reserved for contention-free access. Under these conditions, the system offers 200 RA slots per second; the maximum number of preamble transmission is set to 10 [17, 18, 23].

Figure 3 illustrates the total, failed, re-transmitted and successful average number of RA attempts per slot. The reason for access failure is because the difficulty of selecting a unique preamble when a large number of access request happen simultaneously. Note that the contention-based operation of the RACH is based on ALOHA-type access, i.e., transmit the request in the first available opportunity [17]. In case of collision, UE tries again after the back-off time.

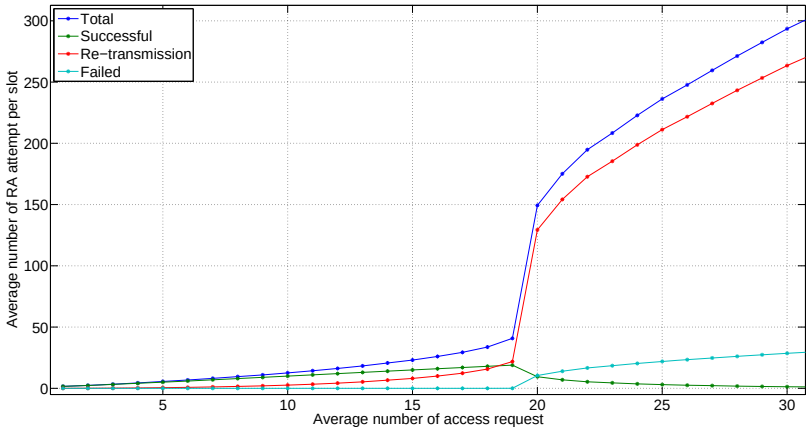


**Fig. 3.** Random Access Attempts per Slot. N=30000; M=54.

According to [18], the expected number of successful RA requests per PRACH slot is $N(1-1/M)^{N-1}$ for $N$ RA requests and $M$ preambles; Fig. 4(a) illustrates this computation for different values of $M$.

Let $P_s$ be the access success probability per device (including the back-off mechanism), it can be computed as $P_s = (N_r \cdot P_r)/N_a$, where $P_r$ is the success probability per slot, $N_a$ is the average number of new accesses per slot, and $N_r$ the average number of total accesses (news+retx) per slot. If we define the

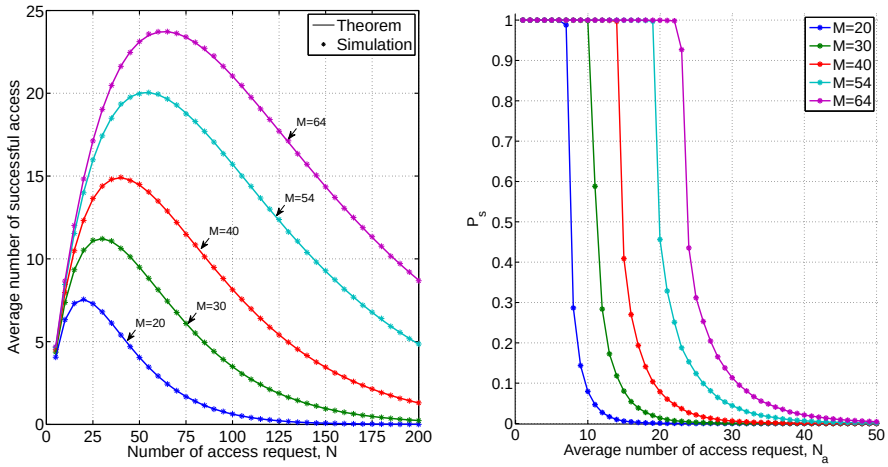


(a) Average Number of Successful Access (b) Access Success Probability

**Fig. 4.** System Capacity

mean number of trials as $N_i = N_r/N_a$ then $P_s = N_i \cdot P_r$. The system capacity per PRACH slot is computed as $c = \left\lfloor log(\frac{M}{M-1}) \right\rfloor^{-1} (1 - \frac{1}{M})^{\left\lfloor log(\frac{M}{M-1}) \right\rfloor^{-1}}$ [18]. From Figs. 4(a) and 4(b) we observe that $c$ can be approximated as $max\{N_a : P_s(N_a) \geq (1-\epsilon)\}$, $0.6 \leq \epsilon < 1$. Finally, Fig. 4(b) shows that, in the current random access mechanism, the maximum capacity increases slightly as the number of preambles available for the UEs increases. Note that, an access attempt can be successful when the total number of access requests is lower than the system capacity.

## 6 Conclusions

The random access procedure is key in mobile networks since it enables the user equipment to initiate communications and time synchronization with a base station. We show that the current mechanism to request access to the cellular network system suffer from congestion and overloading in the presence of a huge number of devices. Therefore, more efficient methods for managing the access to these networks in such circumstances are necessary. Finally, further work on LTE-A and next generations of cellular networks in order to make them capable and efficient to provide M2M services is still ongoing, and a follow-up to this paper will be published at a later date.

## References

1. 3GPP: Study on RAN Improvements for Machine Type Communications. TR 37.868, 3rd Generation Partnership Project (3GPP) (Sep 2011)
2. 3GPP: Medium access control (MAC) protocol specification. TS 36.321, 3rd Generation Partnership Project (3GPP) (Sep 2012)

3. 3GPP: Service requirements for Machine-Type Communication. TS 22.368, 3rd Generation Partnership Project (3GPP) (Sep 2012)
4. 3GPP: System improvement for Machine-Type Communications. TR 23.888, 3rd Generation Partnership Project (3GPP) (Sep 2012)
5. 3GPP: Study on enhancements for Machine-Type Communications. TR 22.888, 3rd Generation Partnership Project (3GPP) (Mar 2013)
6. 3GPP: Physical channels and modulation. TS 36.211, 3rd Generation Partnership Project (3GPP) (Dec 2014)
7. 3GPP: Physical layer procedures. TS 36.213, 3rd Generation Partnership Project (3GPP) (Dec 2014)
8. 3GPP: Radio Resource Control (RRC), Protocol specification. TS 36.331, 3rd Generation Partnership Project (3GPP) (Dec 2014)
9. 3GPP: Evolved Universal Terrestrial Radio Access (E-UTRA) and Evolved Universal Terrestrial Radio Access Network (E-UTRAN), Overall Description, Stage 2. TS 36.300, 3rd Generation Partnership Project (3GPP) (Dec 2014)
10. Ahmad, F., M.S.Z.Y., Görg, C.: Tailoring LTE-Advanced for M2M communication using wireless inband relay node. In: World Telecommunications Congress (WTC) (2014)
11. Akyildiz, I.F., Gutierrez-Estevez, D.M., Reyes, E.C.: The evolution to 4G cellular systems: LTE-Advanced. Phys. Commun. 3(4), 217–244 (Dec 2010)
12. Cheng, R., Chen, J., Chen, D., Wei, C.: Modeling and analysis of an extended access barring scheme for machine-type communications in LTE networks. Wireless Communications, IEEE Transactions on PP(99), 1–1 (2015)
13. Ghavimi, F., Chen, H.: M2M communications in 3GPP LTE/LTE-A networks: Architectures, service requirements, challenges, and applications. Communications Surveys Tutorials, IEEE 17(2), 525–549 (Secondquarter 2015)
14. Ghosh, A., Ratasuk, R., Mondal, B., Mangalvedhe, N., Thomas, T.: LTE-Advanced: next-generation wireless broadband technology [invited paper]. Wireless Communications, IEEE 17(3), 10–22 (June 2010)
15. Larmo, A., Lindstrom, M., Meyer, M., Pelletier, G., Torsner, J., Wiemann, H.: The lte link-layer design. Communications Magazine, IEEE 47(4), 52–59 (April 2009)
16. Lawton, G.: Machine-to-machine technology gears up for growth. Computer 37(9), 12–15 (Sept 2004)
17. Laya, A., Alonso, L., Alonso-Zarate, J.: Is the random access channel of LTE and LTE-A suitable for M2M communications? a survey of alternatives. Communications Surveys Tutorials, IEEE 16(1), 4–16 (First 2014)
18. Lin, T.M., Lee, C.H., Cheng, J.P., Chen, W.T.: PRADA: Prioritized random access with dynamic access barring for MTC in 3GPP LTE-A networks. Vehicular Technology, IEEE Transactions on 63(5), 2467–2472 (Jun 2014)
19. Lo, A., Law, Y., Jacobsson, M.: A cellular-centric service architecture for machine-to-machine (M2M) communications. Wireless Communications, IEEE 20(5), 143–151 (October 2013)
20. Pötsch, T., Khan Marwat, S., Zaki, Y., Görg, C.: Influence of future M2M communication on the LTE system. In: Wireless and Mobile Networking Conference (WMNC), 2013 6th Joint IFIP. pp. 1–4 (April 2013)
21. Russler, N.: Networks of the future: Ideas and concepts (August 2014), http://www.whitebyte.info/wp-content/uploads/2014/08/
22. Ubeda, C., Pedraza, S., Regueira, M., Romero, J.: LTE FDD physical random access channel dimensioning and planning. In: Vehicular Technology Conference (VTC Fall), 2012 IEEE. pp. 1–5. IEEE (2012)
23. WG2, G.T.R.: RACH overload solutions. TR N. 70bis R2-103742, 3rd Generation Partnership Project (3GPP) (june 2010)

# *In silico* experimentation: study of PDGF and EGF signal transduction pathways affected by oncology drugs

Miquel Oltra[1], Jaime Font de Mora[2]and Juan Miguel García-Gómez[1]

[1]Grupo de Informática Biomédica (IBIME), Instituto de Aplicaciones de las Tecnologías de la Información y de las Comunicaciones Avanzadas (ITACA), Universitat Politècnica de València (Spain)
[2]Head ofLaboratory of Cellular and Molecular Biology, Center of Translational Medicine, La Fe Hospital Research Institute, Valencia (Spain)

***Abstract*** - How can a drug modify the normal behavior of a biological pathway? Is an oncology drug causing side effects? Nowadays the scientific community is reviewing cancer treatments because the pharmacology industry is focusing to a more personalized way to heal cancer patients. Here we present an *in silico* methodology that can be applied in any targeted pathway by a drug or a combination of them, in order to determine the treatment effect. The implemented method describes the steps needed to carry out this analysis: select targeted biological pathways, convert them to networks where data mining can be applied and finally, apply a new graphical style in order to facilitate the understanding of the generated network. At the end, this method offers a novel approach to merge multiple pathways saving time with technical issues and provide investigators a new tool to test *in silico* targeting molecules in the fight against cancer.

***Key words****: computational molecular biology, high-throughput screenings, signal transduction pathway (STP), oncology drugs, PDGF, EGF, in silico networks, Cytoscape*

## I. Introduction

Signal transduction is a process in which extracellular signals elicit changes in cell state and activity. Transmembrane receptors sense changes in the cellular environment by binding ligands, such as hormones and growth factors. Stimulation of transmembrane receptors leads to their conformational change which propagates the signal to the cytoplasm by activating downstream signaling cascades. Depending on the cellular context, this may impact cellular proliferation, differentiation, metabolism and survival. On the organism level, signal transduction pathways (STP) regulates overall growth and behavior [1].

Plateled-derived Growth Factor (PDGF) signaling pathway has been related with many cancer types and it it has become a major target for cancer treatment. In addition to its role in autocrine growth stimulation of tumor cells, PDGF has also been suggested to regulate tumor stroma fibroblasts and tumor angiogenesis. The occurrence of clinically useful PDGF receptor antagonists,like imatinib, now allows for an evaluation of the importance of PDGF receptor signaling in malignancies (Buchdunger *et al*., 1996andCapdeville *et al*., 2002) [2].

Another important pathway associated with many tumors is the Epidermal Growth Factor (EGF); human carcinomas frequently express high levels of members of the EGF receptor family and/or their ligands.Overexpression of two of these receptors, the EGF receptor (EGFR) and



C.Fernandez-Llatas and M.Guillen (Ed.):
Workshop on Innovation on
Information and Communication Technologies
(ITACA-WIICT 2015)

ISBN 978-84-608-4139-5

EGFR2, also known as ErbB2, have been associated with a more aggressive clinical behavior [3]. Furthermore, transfection or overactivation of either of these two receptors in nonmalignant cell lines can lead to a transformed phenotype. For these reasons, therapies directed at preventing the function of these receptors have been the focus of anti-cancer treatments in many clinical trials.

Predicting the response of a specific cancer to a therapy is a major goal in modern oncology that should ultimately lead to a personalised treatment [4]. High-throughput screenings of potentially active compounds against a panel of genomically heterogeneous cancer cell lines have unveiled multiple relationships between genomic alterations and drug responses. The behaviour of drugs within our body and the way they interact with our cells and other components of our body has been studied in many *in silico* models, with the main purpose of clarifying the final effect produced [5] [6] [7]. Notably, the effect of a combination of drugs in order to fight against the cancer cells has been studied for many drugs and targets, as described in Tonissi et al. [8]. Therefore, it is also very important (Scior et al. [9]) the implementation of methods on *in silico* models because the correct results interpretation will let to guide the following tests either *in vitro* as at the end *in vivo*. The great advantage of these methodologies is that they can be applied for various purposes in different scenarios. For instance, they can predict the final outcome produced by a combination of drugs targeting some signaling pathways that are altered in human cancer cells.

From a molecular point of view there are many experimental approaches used to monitorwhat happens inside the cell. Computational modeling of biochemical systems based on top-down and bottom-up approaches has been well studied over the last decade. Some experimental results indicate that this kind of model can help us understand the relationships among biochemical reactants [10]. In addition, hidden reactants of the target biochemical system can be obtained by generating complex reactants in corresponding composed models [11]. Moreover, qualitatively learned models with inferred reactants and alternative topologies can be used for further web-lab experimental investigations by biologists, which may result in a better understanding of the system.

## II. Materials and information sources

Our methodology is based on public and curated databases for biological reactions and drugs. We have used a consolidated platform for bioinformatics network analysis as Cytoscape, and also we need to take advantage of interoperability standard models like BioPAX (**Bio**logical **Pa**thway E**x**change) and XGMML (e**X**tensible **G**raph **M**arkup and **M**odeling **L**anguage).

a) Public databases:

·*Reactome*: is a free, open-source, curated and peer reviewed pathway database. Its goal is to provide intuitive bioinformatics tools for the visualization, interpretation and analysis of pathways' knowledge to support basic research, genome analysis, modeling, systems biology and education.

·*DrugBank*: the DrugBank database is a unique bioinformatics and cheminformatics resource that combines detailed drug data with comprehensive drug target information. Each DrugCard entry contains more than 200 data fields.

· *UniProt*: is a comprehensive resource for protein sequence and annotation data. The name comes from Universal Protein Resource. The UniProt databases are the UniProt Knowledgebase (UniProtKB), the UniProt Reference Clusters (UniRef), and the UniProt Archive (UniParc).

b) Framework for modeling biological networks (graphs): Cytoscape and some specific apps (plugins) designed for accomplish specific functions, like Pesca.

c) Specific language to export and import networks:

· *BioPAX (version 3)*: is a standard language that aims to enable integration, exchange and analysis of biological pathway data. It is expressed in OWL. The last specification is BioPAX Level 3. BioPAX is supported by many pathway database or processing tools (http://www.biopax.org).

·*XGMML*: is an XML application based on GML which is used for graph description. XGMML uses
tags to describe nodes and edges of a graph. The purpose of XGMML is to make possible the exchange of graphs between different authoring and browsing tools for graphs.

# III. Methods

In order to predict the outcome of a drug in a STPwe have studyed the signaling pathway by using a graph approach. For this purpose we have transformed the signaling pathway into a directed graph so that functions and algorithms can be apply into it. A graph is a set of nodes and edges that allows the representation of the relations among the elements of the set. Applying it to our context, the set would be one or more STPs, where nodes representing the different elements that participate in the pathway (e.g. a protein or a biological reaction) and the edges represent any type of relation between two nodes (e.g. left or member).

The first encountered problem is the lack of directionality in the relation between complexes and their components. This problem results from the lack of direction for chemical compounds in Biopax standard. Nevertheless, in order to solve the set of edges affected by a therapy we aimed to work with directed graphs. Hence the directionality concept is very important to get reliable results and thus, we have implemented a script to add double directionality between nodes that require it. In this sense, we have considered necessary the implementation of a methodology to visualize everything underlying the target of a specific drug

*A. Procedure*

**Step 1**: search STPs in public databases.
The first task was searching the required information needed to retrieve data from available public databases. We chose Reactome Because it has an interactive pathway browser that allows understanding the relationship between the elements of many signal transduction pathways, it provides the connection to the literature describing these procesess and it also

gives the chance to export any pathway in various formats: Biopax, SBML, PDF, Protege, Molecules and Word. We decided to use the standard Biopax because it encapsulates all the information required for our work, and also because Cytoscape supports this format (only needs a reader to be installed, and it is embedded in some apps).

Taking a look at the “Signaling by PDGF” pathway, we noted all the reactions occurring in it as well as all the involved components for each reaction: inputs, outputs, catalyst activity and location (cellular compartment). Each reaction and its participants are translated into nodes in Cytoscape, and based on the Biopax standard the edges indicate the type of relation between them.

**Step 2**: once the selected STP is exported to a file, it can be imported to Cytoscape to automatically generate a new network. Thereafter the file is renamed for readability.

Now it is necessary to reproduce the double directionality noted in some cases in Reactome. In particular, all the edges whose interaction type has the value “member”or “contains”must be directed in both ways: from source to target and vice versa. This is a technical problem produced randomly when the network has been generated and has to be solved.

**Step 3**: export the network to a XGMML format for preserving all node and edge attributes. At this point, an AWK script has been developed in order to add all the edges needed to a file that has been previously formatted in a compatible way to support the script. Below is the AWK code block used:

```
awk '{if($12 ~ /"contains"/) {sub("source","target",$4);
sub("target","source",$5); print $0;}  }' OriginalFile.xml >
OriginalFile_EdgesContains.xml

awk '{if($12 ~ /"member"/) {sub("source","target",$4);
sub("target","source",$5); print $0;}  }' OriginalFile.xml >
OriginalFile_EdgesMember.xml
```

*Figure. Example of the AWK code for complete the directionality of the graph.*

All edge blocks are thereafter replaced in the original XML file before importing it into Cytoscape to generate a new network with the same number of nodes but with all the edges required to be a directed graph.

**Step 4**: targets of selected drugs to study are searched in the *DrugBank* database, aiming to select those nodes on our network. Only the targets of the STP network used are considered. Then the *UniProt* idenfier associated with the target is used in Cytoscape for select the right “start node”.

**Step 5**: the main functionality of our methodology is to obtain the reachable nodes from the drug targets. This can be implemented by applying to each drug target the multi-shortest path tree algorithm. As a result, a list of subnetworks of nodes and the edges to reach the nodes connected from the targets represents the possible paths to achievable reactions and components.

**Step 6**: once all the networks for every target are created, it is needed to merge them into a single network. Cytoscape can automatically merge many networks at once,. It is important to remark that the merged network should contain  all the information avoiding duplicate nodes or edges.For that purpose we made the union operation of all the networks.

**Step 7**: apply our personal style created according to the Biopax standard from the “Style”tab, as it is seen in Table 1.

*B. Graphical representation*

We have created our own graphical style based on both Biopax standard and the representation used in Reactome.

The new style is called “Biopax_Propio”and we use it at the end of our process, in order to make easier the interpretability of the different elements in the network. Below is a table listing the edges and their characteristics.

*Table 1. Possible interaction values of the edges with their graphical representation.*

| Interaction value | Target arrow shape | Line type | Color |
|---|---|---|---|
| Member | Circle | Parallel lines | - |
| Contains | Circle | Parallel lines | - |
| Left | Delta | Solid | - |
| Right | Delta | Solid | - |
| Activation | Arrow | Contiguous arrow | Green |
| Inhibition | T | Dash dot | Red |
| Controller | None | Separate arrow | - |

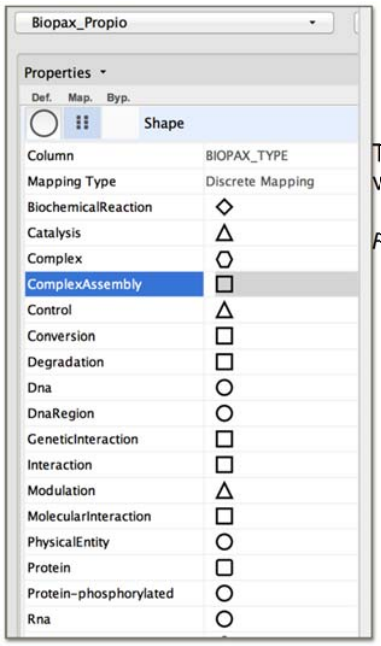


The shapes of nodes are drawn based on the “Biopax_type”column value. In Figure 1 all the possible mappings are defined.

*Figure 1. Symbols used to represent every different biopax_type value.*

# IV. Use-case: imatinib, dasatinib and dacomitinib effects on PDGF/Src and EGF signaling pathways

In this practical case, we are willing to analyze the scope of the oncology drugs imatinib, dasatinib and dacomitinib on the STPs selected for the study: PDGF/Src and EGF. Our goal is to determine the impact of the combination of three drugs inside the cell, in the meaning of the selected STPs.

As we mentioned in the introduction, both signaling pathways are related with many cancers so they are interesting targets for cancer treatment. We have chosen them because they are two principal pathways related with the hallmarks detected on tumor cells [12], such as increased cell growth and resistance to programmed cell death (also known as *apoptosis*).

For the selection of, We have chosen the oncology drugs imatinib, dasatinib and dacomitinib based on their proven effect in brain tumors. Moreover, all of them are tyrosine kinase inhibitors and are strongly related with cancer.

We used the DrugBank database to retrieve the known targets for these drugs and to establish the “starting points”on the network:.

- Targets of imatinib contained in “Signaling by PDGF” STP

    1) PDGFRA (platelet-derived growth factor receptor alpha)
    2) PDGFRB (platelet-derived growth factor receptor beta)
    3) KIT (mast/stem cell growth factor receptor Kit)

- Targets of dasatinib containedin “Signaling by PDGF” STP

    1) SRC (proto-oncogene tyrosine-protein kinase Src
    2) LCK (tyrosine-protein kinase Lck
    3) KIT (mast/stem cell growth factor receptor Kit
    4) PDGFRB (platelet-derived growth factor receptor beta
    5) STAT5B (signal transducer and activator of transcription 5B
    6) FYN (tyrosine-protein kinase Fyn

- Targets of dacomitinib contained in “Signaling by EGF” STP

    1) EGFR (epidermal growth factor receptor)
    2) ErbB2 (receptor tyrosine-protein kinase erbB-2)
    3) ErbB4 (receptor tyrosine-protein kinase erbB-4)

After picking the molecular targets of the selected drugs, we identified all connected nodes with them followed by step 5 in the “Procedure”section and all paths related. We finally generated a new network that includes the selected edges.

Once the required networks are generated, we then merged them in a final network. with a new style defined by us. Our aim was to provide a better graphical representation allowing investigators a global overview and quick access to data and features on the network. This can be achieved through the style functionality that offers Cytoscape.

## .V. Results

The first step has been the selection of curated biological networks as our primary source. In this study, we have chosen the signal transduction pathways “Signaling by PDGF”and “Signaling by EGF”, located under the signal transduction section of the Reactome tree of pathways. We can see an example of the graphical representation in the *Figure 2*.

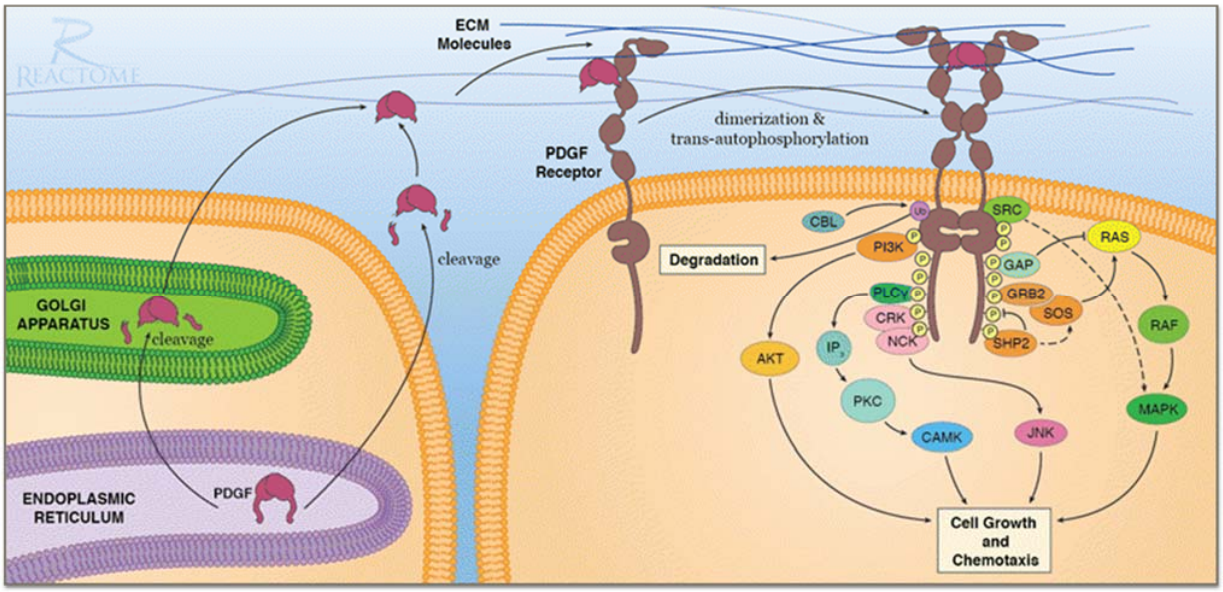


*Figure 2. Original Reactome representation of “Signaling by PDGF”pathway.*

After importing the Reactome network to Cytoscape, using the Biopax3 format, the necessary edges for reproduce the right direction in complexes need to be addedto the original imported network. Once this problem is solved, the first targeted network is generated following the methodology explained before (in methods section). After the execution of these steps, we get the network “PDGF_Pathway_AllPaths_PDGFRB” as the result for the target PDGFRB. At this point, the cytoscape control panel looks like the Figure 3 image.

*Figure 3. Cytoscape control panel with the original network with bidirectional edges and the first target*

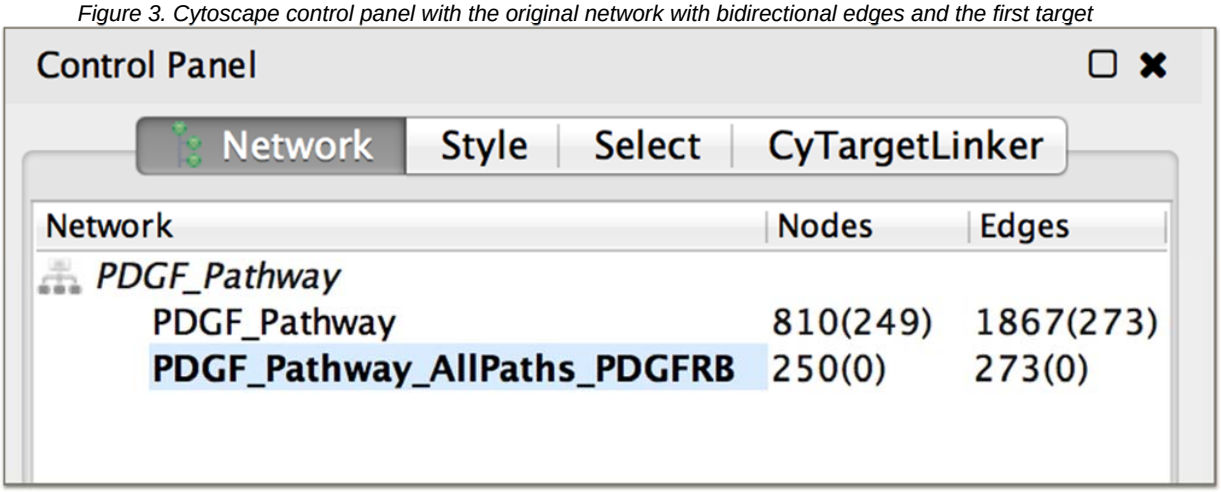

*affected network*.

These steps were repeated for every target of each drug being studied. At the end of the process, we generated 15 networks, each one with its own features. Further statistical network attributes were included by executing the network analyzer Cytoscape built-in function in order to analyze the network topology.

A brief summary on the comparison of number of nodes, edges and reactions of every network generated is shown on Table 2.

| Network name | Number of nodes | Number of edges | Number of reactions |
|---|---|---|---|
| PDGF_Pathway (Original) | 810 | 1867 | 86 |
| PDGF_Pathway_AllPaths_PDGFRB | 250 | 273 | 28 |
| PDGF_Pathway_AllPaths_PDGFRA | 113 | 121 | 11 |
| PDGF_Pathway_AllPaths_KIT | 176 | 211 | 22 |
| PDGF_Pathway_AllPaths_SRC | 78 | 84 | 16 |
| PDGF_Pathway_AllPaths_LCK | 142 | 152 | 14 |
| PDGF_Pathway_AllPaths_STAT5B | 63 | 67 | 6 |
| PDGF_Pathway_AllPaths_FYN | 190 | 206 | 24 |
| PDGF_Imatinib_Affected | 331 | 395 | 45 |
| PDGF_Dasatinib_Affected | 410 | 492 | 60 |
| PDGF_Imatinib+Dasatinib_Affected | 416 | 499 | 61 |
| EGF_Pathway (Original) | 779 | 1918 | 108 |
| EGF_Dacomitinib_Affected | 87 | 100 | 14 |
| EGF_PDGF_Affected_By_3_drugs | 450 | 554 | 66 |

*Table 2. Comparison of the different networks generated*

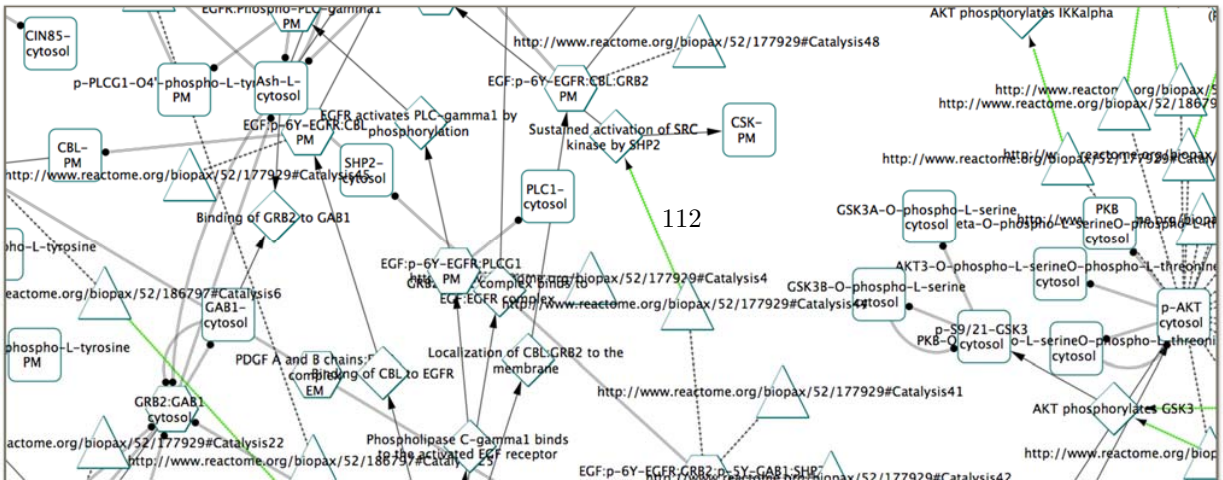

*Figure 4. Partial overview of the new generated network that combines the effect of the 3 selected oncology drugs on the STPs studied.*

Single networks affected by each drug were merged in order to generate the final network of interest. At the end of the applied process, theaffected network bythe oncology drugs administrated hasbeen achieved, in an in silico model context; this is represented in the network called “EGF_PDGF_Affected_By_3_drugs”(last row in Table 2).

Finally, the cytoscape option “force-directed”was used for the layoutand our definedgraphical style was appliedfor the visualization of the network (see Figure 4).

## VI. Discussion

One major reasons for using the Reactome database is its frequent update. Reactome’s latest version is 52 and it was released on March 23rd, 2015. Therefore, our analysis is based on refreshed data since the building of any model starts from the existing curated pathways on this database.

On the other hand, the main limitation of the approach presented in this work is that *in vivo* conditions always change from the ones *in silico*. As a consequence, in our model we do not have unexpected *stimuli* that can modify some already known behaviors. In other words, we have always the same conditions. In this regard, we are planning to incorporate the dissociation constant ($K_d$) of the biochemical reactions to quantify the final output of our model.

The resulting number of nodes presented on Table 2show that the merged network affected by targeting PDGF with imatinib have 331 nodes instead of 539 nodes that results from adding the nodes of the three individual networks. Hence, we have gained more readability, clarity and easiness representation of the biological STP, selecting only the involved nodes in the therapy. Noteworthy, this network may also be used to implement any test that we need to perform in it.

A similar analysis can be made comparing the results of the dasatinib effect on the PDGF pathway. After getting the six individual networks, one for each target, and merge them using the union operation, we generated a unified network with 410 nodes rather than 899. Moreover, when we finally join both networks together, the number of nodes is almost reduced by half: 416 vs. 810. Interestingly, only 6 nodes are affected by imatinib and not by dasatinib. On the other hand, 85 nodes are only present when dasatinib is administrated. All the other nodes (325) are shared by both networks. In other words, dasatinib administration can have repercussions on 79 more nodes in the PDGF pathway. In addition, out of the original 779 network nodes in the EGF pathway, only 87 are affected by dacomitinib drug. This means that the affected part of the pathway represents only the 12%. Edges are also reduced to from 1918 existing in the pathway to 100.

Comparison of both networks independently by terms of number of nodes and edges (network dimension), vs. our merged network, the reduction in complexity is highly impressive: 72% reduction in nodes (450 vs. 1589 ) and 85% reduction in edges (554 vs. 3785). These results show a relevant improvement for the analysis of big and complex pathwaysandalso for study the features of the affected nodes (it is important to remark that a node can be a protein, dna, rna, etc.), helping scientists to focus on the altered or affected molecules in a specific cancer.

## VII. Conclusion

In this work we propose a methodology for allowing *in silico* experimentation of combined treatments. For this purpose, we have transformed biological networks into graphs for a further analysis and we resolved the technical problems in the generation of models that attempt to simulate the real biological conditions.

Our goal is to provide a clear methodology to integrate multiple pathways targeted by different drugs in one single network. This novel approach to merge multiple pathways will save a lot of time with technical issues, and offer investigators a new tool to test *in silico* targeting molecules in the fight against cancer. The aim is to abstract the investigators as much as possible about specific and technical problems that are not related with the real problem being studied; for instance, automatizing the import or export process of the different networks that are going to be analyzed.

### Acknowledges

Juan M. Garcia-Gomez acknowledges Project TIN2013-43457-R: Caracterización de firmas biológicas de glioblastomas mediante modelos no-supervisados de prediccióon estructurada basados en biomarcadores de imagen, co-funded by the Ministerio de Economía y Competitividad of Spain.

### REFERENCES

[1] Signal Transduction (REACTOME)
Bevan, AP, Charalambous, M, Gopinathrao, G, Joshi-Tope, G, Rothfels, Karen, Orlic-Milacic, Marija, 2005-05-06.

[2] PDGF receptors as cancer drug targets.
Kristian Pietras, Tobias Sjöblom, Kristofer Rubin, Carl-Henrik Heldin, Arne Östman.
URL: http://www.sciencedirect.com/science/article/pii/S1535610803000898

[3] The EGF receptor family as targets for cancer therapy.
Mendelsohn J., Baselga J.
Department of Medicine, The University of Texas, MD Anderson Cancer Center, Houston, 77030-4009, USA.
Oncogene [2000, 19(56):6550-6565]
URL: http://europepmc.org/abstract/med/11426640

[4] Machine learning prediction of cancer cell sensitivity to drugs based on genomic and chemical properties.

Menden MP1, Iorio F, Garnett M, McDermott U, Benes CH, Ballester PJ, Saez-Rodriguez J.
PLoS One. 2013 Apr 30

[5] Honokiol inhibits the growth of head and neck squamous cell carcinoma by targeting epidermal growth factor receptor.
Singh T, Gupta NA, Xu S, Prasad R, Velu SE, Katiyar SK
Oncotarget. 2015 May 19.
URL: http://www.ncbi.nlm.nih.gov/pubmed/26020804

[6] A high-throughput in vitro drug screen in a genetically engineered mouse model of diffuse intrinsic pontine glioma identifies BMS-754807 as a promising therapeutic agent.
Halvorson KG, Barton KL, Schroeder K, Misuraca KL, Hoeman C, Chung A, Crabtree DM, Cordero FJ, Singh R, Spasojevic I, Berlow N, Pal R, Becher OJ.
PLoS One. 2015 Mar 6
URL: http://www.ncbi.nlm.nih.gov/pubmed/25748921

[7] Anti-HER3 monoclonal antibody patritumab sensitizes refractory non-small cell lung cancer to the epidermal growth factor receptor inhibitor erlotinib.
Yonesaka K, Hirotani K, Kawakami H, Takeda M, Kaneda H, Sakai K, Okamoto I, Nishio K, Jänne PA, Nakagawa K.
Oncogene. 2015 May 11
URL: http://www.ncbi.nlm.nih.gov/pubmed/25961915

[8] The effect of paclitaxel and nab-paclitaxel in combination with anti-angiogenic therapy in breast cancer cell lines.
Tonissi F1, Lattanzio L, Merlano MC, Infante L, Lo Nigro C, Garrone O.
Invest New Drugs. 2015 May 7
URL: http://www.ncbi.nlm.nih.gov/pubmed/25947567

[9] Los modelos in silico, una herramienta para el conocimiento farmacológico.
Scior, T., Martínez, M.E., y Salinas, S.E.
Elementos. 68:25-28 (2007).

[10] MRI biomarkers identify the differential response of glioblastoma multiforme to anti-angiogenic therapy.
Jalali S1, Chung C1, Foltz W1, Burrell K1, Singh S1, Hill R1, Zadeh G1.
Neuro Oncol. 2014 Jun;16(6):868-79. doi: 10.1093/neuonc/nou040. Epub 2014 Apr 23.
URL: http://www.ncbi.nlm.nih.gov/pubmed/24759636

[11] An integrative top-down and bottom-up qualitative model construction framework for exploration of biochemical systems.
Wu Z, Pang W, Coghill GM.
Soft comput. 2015
URL: http://www.ncbi.nlm.nih.gov/pubmed/25999782

[12] Hallmarks of Cancer: The Next Generation.
Hanahan D, Weinberg RA.
Cell. 2011;144(5):646-674. doi:10.1016/j.cell.2011.02.013

# A Web Application for Professional Monitoring of Behavioural Intervention for Prevention of Obesity and Eating Disorders

Isabel Martí[1], Juan-Bautista Mocholí[1], Juan-Pablo Lázaro[1]

[1] Soluciones Tecnológicas para la Salud y el Bienestar S.L. Ronda Auguste y Louis Lumiere 23, Nave 13. Paterna (Valencia) SPAIN
{imarti,jbmocholi,jplazaro}@tsbtecnologias.es
http://tsbtecnologias.es

**Abstract.** According to WHO, obesity has more than doubled since 1980. Worldwide, there are more than 1.9 billion overweight adults, 600 million obese. On the other side of the spectrum, up to 24 million people of all ages and genders suffer from an eating disorder. Both extremes in eating behaviour can cause severe health problems, leading persons who suffer them to a need for treatment. SPLENDID program aims at recognizing persons at risk of obesity or eating disorders and re-educate them to follow an adequate eating behaviour. This paper presents a web-based tool for professionals in nutrition to manage all stages of the SPLENDID Program: preliminary screening, assessment of current behaviour and finally treatment definition and guidance for behavioural change. The tool has been co-designed with the health professionals in order to offer them a useful and usable application to review nutritional data.

## 1 Introduction

According to WHO, overweigh and obesity are defined as excess as abnormal or excessive fat accumulation that may impair health [1] and it has more doubled since 1980. In 2014 more than 1.9 billion adults worldwide were overweight, with 600 million of obese persons. That means that, a year ago, 13% of world adult population was classified as obese.

The epidemic proportions of obesity are one of the major health concerns. Being overweight or obese increases the risk for diet-related diseases, such as type 2 diabetes, cardiovascular disease, hypertension and stroke, and certain forms of cancer. The consequences of suffering these diseases can vary from a reduced quality of life to premature death.

It is even more concerning that obesity is also increasing in children and young adults. In 2013, 42 million children under the age of 5 were overweight or obese. Not only the prevalence of overweight and obesity has increased to 23.8% in boys and 22.6% in girls in developed countries, but also is increasing to alarming 12.9% in boys and 13.4% in girls in developing countries [2].



C.Fernandez-Llatas and M.Guillen (Ed.):
Workshop on Innovation on
Information and Communication Technologies
(ITACA-WIICT 2015)

ISBN 978-84-608-4139-5

The Global Strategy on Diet, Physical Activity and Health (DPAS) developed by WHO in 2004 aims at improving global diet and physical activity patterns, in order to reduce problems associated with obesity. The DPAS framework proposes national governments to implement policies and programs to promote supportive environments for health. Figure 1 shows the schematic model on how to implement DPAS at national level.

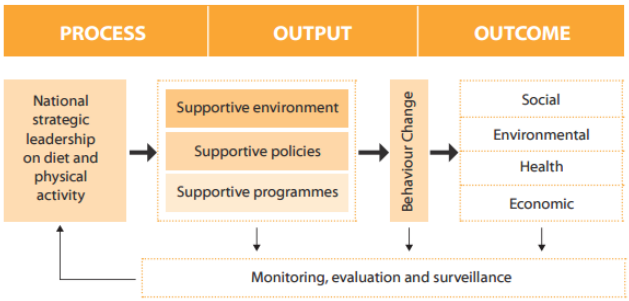


**Figure 1 Schematic model to apply DPAS at national level**

As can be extracted from the schema in Figure 1, the main objective is to implement policies based on supportive environment and programs in order to produce a behavioural change that will avoid the incidence of overweight and obesity in the individuals.

On the opposite extreme of abnormal eating behaviour are eating disorders. According to WHO, anorexia nervosa occurs in 0.5–1% and bulimia nervosa in 0.9–4.1% of the female adolescent and young adult population, while an additional 5–13% suffer from partial syndrome eating disorders[3]. These disorders are associated with long term physical consequences like osteoporosis, infertility, gastrointestinal dysfunction due to excessive laxative usage, and heart attack. In addition to physical consequences, eating disorders negatively influence the patient's academic, occupational, and interpersonal function [4], and, although mortality rates are considerably lower than the obesity related deaths, anorexia nervosa has the highest standardized mortality ratio of any psychiatric illness, with 15 to 19% of sufferers succumbing to starvation or suicide [5].

Traditional treatments for eating disorders have had poor success rates [6] [7] and high levels of relapse [8] [9]. A possible reason for this is that these treatments have traditionally concentrate on symptoms that might not be casually related to the problem [10]. Recently, there are several works that have proved that, as in the case of obesity, a modification on eating behaviour might be important in the field of eating disorders [11][12].

Given that obesity and eating disorders are at the opposite extremes of the normal eating behaviour [13], and that in both scenarios, training patients to exercise and eat in non-pathological ways has been demonstrated effective[14][15], it is possible to design a tool to administer a behavioural intervention for both eating disorder and obese patients.

The main goal of the SPLENDID platform is to develop a system that can efficiently detect and normalize eating behaviours that put individuals at risk of developing obesity or eating disorders in a non-invasive, unobtrusive, personalized and cost-efficient way.

## 2 The SPLENDID Program

Based on the proved benefits of behavioural modification intervention in patients with obesity and eating disorders, the next step is to apply similar methodologies to the general population to detect eating behaviours that put individuals at risk of developing obesity or eating disorders and normalize them, so they don't develop the problem.

In that line of work, the aim of the SPLENDID program is to provide personalized guidance to young individuals to adopt healthy eating and physical activity patterns that will prevent the onset of obesity and eating disorders by the means of:

- Measuring eating and physical activity behaviour in real life conditions through different types of sensors.
- Executing a novel set of algorithms over the data extracted from the sensors, in order to assess the risk for obesity or eating disorders of the individual.
- Empower and guide the young individuals at risk to modify their eating and activity behaviour through a set of goals, in order to achieve normal behaviour.

### 2. 1 Target users through the program

The solution developed by the SPLENDID system has two different settings:

- Screening and prevention at schools with the aim of identifying adolescents at risk in early stages. First, a Primary Screening will be performed over the school population to identify eating behaviours pointing at future risk. The subjects identified will perform a personalized Behavioural Assessment, based on eating and activity patterns, to determine their actual risk. Finally, subjects definitely identified as at risk will have a Personalize Guidance developed by a clinical expert, to achieve a normal behaviour.
- Consumer lifestyle management, targeting young overweight adults to prevent the risk to progressing to obesity. In this scenario, a Behavioural Assessment will be performed to identify which are the abnormal behaviours and stablish a Personalized Guidance to correct them.

Figure 2 summarizes the target users and how they go through the program.

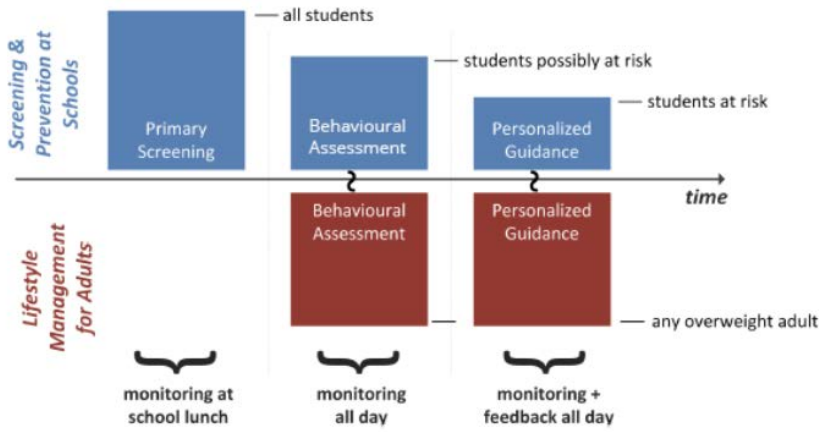


**Figure 2 Outline of the target users of SPLENDID**

### 2.2 System Architecture

The architecture of the SPLENDID platform has 5 different interconnected parts:

- A set of sensors gathering the information related to eating and activity behaviour. The sensors include a Mandometer®, which is a scale that analyses how a person eats; a chewing sensor to detect snaking events and an accelerometer for activity detection, both last ones integrated in a device named DataLogger.
- A mobile app collecting the information of the sensors and offering the information to the subject.
- A web application for professionals to monitor the behaviour of the subjects.
- A decision support system (DSS) analysing the collected data to detect risky behaviours and compliance with the Personalized Guidance goals.
- A backend which interconnects all different elements of the system.

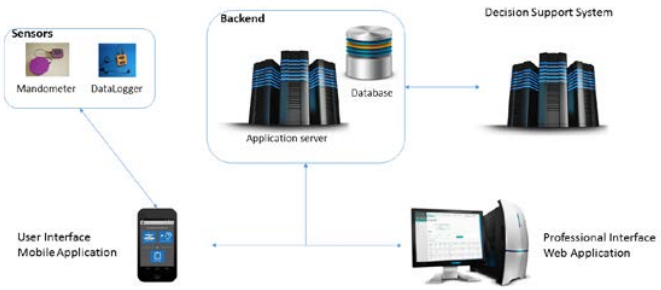


**Figure 3 SPLENDID Platform Architecture**

In this paper we will focus on the description of the professional web application and how the professionals interact with the system in order to analyse users' behaviour patterns and goal accomplishment.

## 3 Professional Web Tool

The main goal of the Professional Web Tool (PWT) is to allow the health professionals to analyse the behavioural eating and activity data of each individual in order to decide whether they are at risk of obesity or eating disorders. For an individual at risk, the professional will create a personalized set of goals the individual should follow during the Personalized Guidance Stage in order to modify the detected abnormal behaviour.

In order to develop a tool which will be useful and easy to use for the professionals, the methodology used was based on a co-design of the application between the technical team and the professionals in different stages.

Figure 4 shows the co-creation process for the PWT. First step was gather functional requirements for the different stages (Primary Screening, Behavioural Assessment and Personalized Guidance) and elaborate a series of use cases that were transformed in mock-ups of what would be the applications.

Those first mock-ups where presented to a group of health professionals, who express their thoughts, doubts and needs, in a Customer Acceptance Test (CAT)

Based on the professionals' feedback from that first CAT, a first functional prototype was developed.

As can be seen in Figure 4, the after each functional prototype, another CAT is performed until professionals approve a prototype that will become the final version of the app. This way we ensure that the developed application is what the professionals need and desire. Currently, we have an approved version for the Primary Screening, while we are still developing and testing different prototypes for the other stages of the program. Thus, in this paper we focus on the results obtained for the Primary Screening.

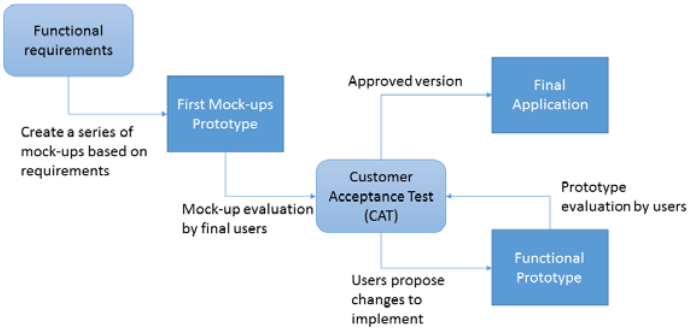


**Figure 4 Co-creation process of the PWT**

### 3.2 Primary Screening Professional Application

The Primary Screening is the first step of the SPLENDID Program for schools. This stage is a one day event were the students have lunch using the Mandometer®, then, based on the data obtained from that meal, the DSS assesses the risk of each individual of suffering from obesity or eating disorders. This risk is based in several factors such as speed of eating, bite size variance, bite frequency, etc [18].

There are several studies that relate the way we eat with the possibility of suffering from obesity or eating disorders. After studies that identify two ways of eating: linear, with a constant eating speed from the beginning to the end of the meal; and decelerated, were the speed of eating decreases during meal[16], there have been multiple studies linking high linear or decelerated behaviours with over- and underweight individuals in comparison with normal weight individuals[17].Based on these studies, a trained health professional can predict the risk of obesity or eating disorder based on the eating curve obtained from the Mandometer® data.

A health professional examines the information obtained from the meal with the risk assessed by the DSS and decides if it's possible that the individual is at risk and it's necessary to make a longer Behavioural Assessment.

The professionals had two basic needs to execute this stage:

1. Being able to create the event for a school.
2. Being able to review the information obtained for each individual.

These needs imply that there are very different actions a professional has to do, some of them that require a big amount of information shown at the screen at the same time.

The basic schema for the web application was defined as Figure 5. The result is a screen where the professional always has visible the main menu as a tab bar on top, to change between the different actions. The rest of the screens is split in two parts, the right part containing the main information of the page the professional is looking at and the left part, that contains additional information and actions that support the work in the main screen.

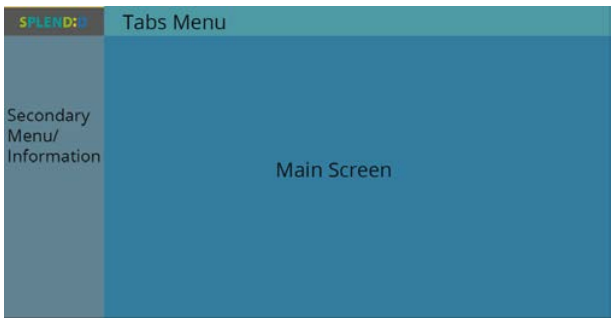


**Figure 5 Basic schema of the PWT**

The main actions the professional can do are:

- Create a new Primary Screening for a school.
- Manage how other professionals relate with the group he's managing.
- Check the list of user's in a group and in which stage they are.
- Check the data and risk assessment of an individual.

The screens for the first two actions are basically forms that allow the professional to introduce the necessary information, so they have no scientific value to be presented in this article.

However, it was necessary to design an easy way for the professional to see all the individuals he's managing and a new way to show all the information gathered from a meal at the same time together with the DSS risk assessment in the same screen, in a comfortable way, so the professional has all information at hand to compare and make his final risk assessment.

Figure 6 shows the main screen the professional sees when entering in the application. The left menu of this screen allows professionals to select between the different groups he manages.

The right part contains the basic information about the group and the list of users with some filters defined by the professionals, so it's easier for them to find individuals in a large group. The list of user's gives information to the professional about in which stages of the program the user has data and allows them to navigate to that data.

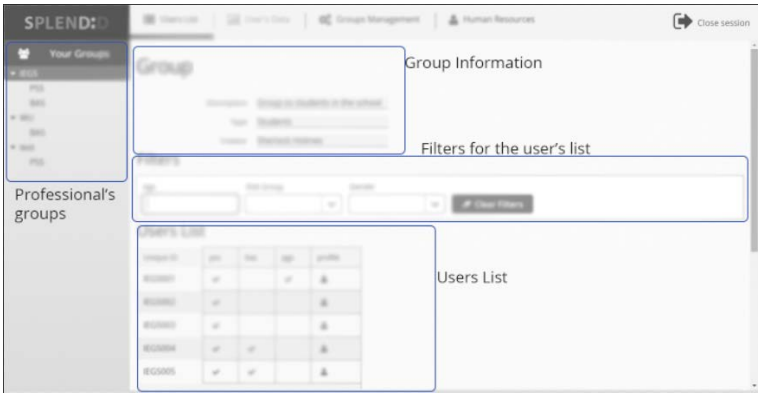


**Figure 6 Application's main screen. Professional's groups and users list**

Figure 7 shows the most important screen in the Primary Screening. This screen shows all data collected for an individual during the meal at school and the result of the risk assessment by the DSS.

The left part of the screen shows the personal information of the individual who is being reviewed. There's physiological information, but also self-reported information about dieting habits.

The main screen shows the meal data collected and the risk assessment in three differentiated parts.

One part shows a chart with the Mandometer® extracted curves. This chart shows the raw curve obtained from the Mandometer® and curve processed by the DSS where the noise produce by the fork in the plate is cleaned up and food additions are considered.

Another part shows the values for the different indicators the DSS extracted from the Mandometer® raw information and used to calculate the risk assessment. These indicators have been developed by a team of the SPLENDID project composed by signal experts and health professionals and are described in [18].

Finally, the third part of this screen shows the risk assessment made by the DSS, with the probability of obesity or eating disorder risk and the justification of this assessment. In this part the health professional can introduce a final risk and decide if the individual should continue with a Behavioural Assessment.

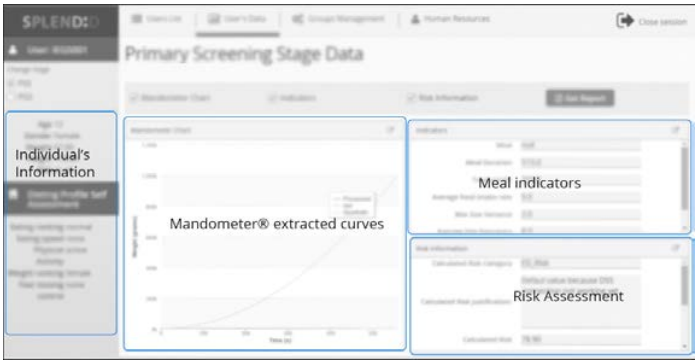


**Figure 7 Primary Screening Data Information**

In order to make easier to the professional to view all information at the same time, all three parts of the main menu containing the meal related information can be extracted as resizable, movable pop-up windows, so the professional can make them bigger than they are and arrange them in the screen as he wishes.

## 4 Conclusions and Future Work

Nowadays, there's a global public health issue related to levels of obesity and eating disorders. The SPLENDID program is an ongoing investigation aimed at preventing the development of these problems in adolescent and your adults at risk, by guiding them to ha behavioural change.

In this paper, we have introduced the Professional Web Tool (PWT), a web application whose objective it to help the health professionals manage the programme. This tool allows them to create new screening events, follow up the results of the screening, helps them decide which individuals are at risk and analyse their eating and activity behaviour in order to decide which goals the individual needs to achieve healthy eating and activity patterns.

The presented set of screens for the Primary Screening is the result of a co-design of the application between the designers and the health professionals, which guarantees that the application offers them all they need to accomplish their goal.

As a future work, we will continue the process of co-design for the other stages of the SPLENDID program, in order to achieve a full web application easy to use and meaningful for the professionals.

## Acknowledgment

The work leading to these results has received funding from the European Community's ICT Programme under Grant Agreement No. 610746, 01/10/2013 - 30/09/2016.

## References


1. WHO – Fact Sheet – Obesity and overweight. http://www.who.int/mediacentre/factsheets/fs311/en/ Last access:15/06/2015
2. Ng, Marie; Fleming, Tom, et al. : Global, regional, and national prevalence of overweight and obesity in children and adults during 1980–2013: a systematic analysis for the Global Burden of Disease Study 2013. The Lancet. Volume 384, Issue 9945, 30 August–5 September 2014, Pages 766–781
3. World Health Organization (2004). Prevention of mental disorders: Effective interventions and policy options http://www.who.int/mental_health/evidence/en/prevention_of_mental_disorders_sr.pdf Last access:15/06/2015
4. Crow, S.J. & Peterson, C.B. (2003). The economic and social burden of eating disorders: A review. Eating Disorders.
5. Zhu, A.J., & Walsh, T. (2002). Pharmacologic treatment of eating disorders. The Canadian Journal of Psychiatry, 47, 227-234.
6. Striegel-Moore RH, Bulik CM. Risk factors for eating disorders. Am Psychol. 2007;62(3):181–98.
7. Treasure J, Claudino AM, Zucker N. Eating disorders. Lancet. 2010;375(9714):583–93.
8. Steinhausen H-C. The outcome of anorexia nervosa in the 20th century. Am J Psychiatry. 2002;159(8):1284–93.
9. Berkman ND, Lohr KN, Bulik CM. Outcomes of eating disorders: a systematic review of the literature. Int J Eat Disord. 2007;40(4):293–309.
10. Ioakimidis I, Zandian M, Ulbl F, Bergh C, Leon M, Södersten P. How eating affects mood. Physiol Behav. 2011;103(3-4):290–4.
11. Walsh BT. The importance of eating behavior in eating disorders. Physiol. Behav. 2011 Sep 26;104(4):525–9.
12. Treasure J, Cardi V, Kan C. Eating in eating disorders. Eur Eat Disord Rev. 2012 Jan;20(1):e42–49.
13. Bergh C, Sabin M, Shield J, Hellers G, Zandian M, Palmberg K, et al. A framework for the treatment of obesity. In: Blass EM, editor. Obesity: Causes, mechanisms, and prevention. Sunderland: Sinauer Assoc, Inc; 2008:399-425.
14. Bergh C, Brodin U, Lindberg G, Södersten P. Randomized controlled trial of a treatment for anorexia and bulimia nervosa. Proc. Natl. Acad. Sci. U.S.A. 2002;99(14):9486–91.
15. Ford AL, Bergh C, Södersten P, Sabin MA, Hollinghurst S, Hunt LP, et al. Treatment of childhood obesity by retraining eating behaviour: randomised controlled trial. BMJ. 2010;340:b5388
16. M. Westerterp-Plantenga et al., The shape of the cumulative food intake curve in humans, during basic and manipulated meals. Physiol. Behav, vol. 47, no. 3, pp. 569–76, Mar 1990.
17. I. Ioakimidis et al., A method for the control of eating rate: a potential intervention in eating disorders. Behav Res Methods, vol. 41, no. 3, pp. 755–60, 2009.
18. Ioannis Sarafis, Christos Diou, Anastasios Delopoulos. D3.2 Formal ontology for the eating and activity behaviour domain. SPLENDID Public Deliverable

# Service-Oriented Architecture for the Integration of Heterogeneous Sources for Physical Exercise Data: the HeartWays Case

A. Martinez-Romero[1], R. Serafin[2], J.P. Lázaro Ramos[2], V. Traver[1]

[1] SABIEN, ITACA, Universitat Politècnica de Valéncia s/n,
46022 Valencia, Spain
{almarro1, vtraver}@itaca.upv.es
[2] Soluciones Tecnológicas para la Salud y el Bienestar, Ronda Auguste y Louis Lumiere 23, 46980 Valencia, Spain
{rserafin, jplazaro}@tsbtecnologias.es

**Abstract.** On the edge of telemedicine and hospital information systems, the following manuscript presents a platform which integrates already existing products in the field of nursing (eNursing) and chronic patients management (Nomhad Chronic), which also includes innovative algorithms in cardiovascular risk prediction. The middleware solution implemented has been developed on top of a cross-platform communication library providing secure data exchange capabilities, defining a virtual network in which each product is mapped as an independent 'node' and registered using a unique address. The analysis of integration needs between the different commercial products led to the definition of four basic services, which were implemented by the middleware. In order to verify that the logic of such services was working as defined, a simulation of the entire network was done using mocking technologies and a complete battery of interaction scenarios was prepared using unit and behaviour driven test frameworks. The simulation proved that 100% of service interactions were working as expected and helped profiling and increasing the middleware performance.

## 1 Introduction

Chronic diseases are diseases of long duration and generally slow progression, which are by far the leading cause of mortality in the world. Among all chronic illnesses, cardiovascular diseases (CVDs) are the number one cause of global deaths (more people die annually from CVDs than from any other cause).[1,2] Furthermore, studies related to economic burden of cardiovascular diseases reveal that CVDs costs to the Health Care Systems of the EU just under 110 billion € in 2006, representing around 10% of the total EU Health Care expenditure.[3] Recent research is supportive of the beneficial effects of exercise based cardiac rehabilitation in patients with heart failure as well as in older patients.[4]–[6] Unfortunately, exercise based cardiac rehabilitation continues to be considerably underutilized with poor referral and enrolment rates, especially in phase III of the rehabilitation model.[7] Implementing quality performance measures, automated referral systems, and the option of home-based cardiac rehabilitation for some patients may all help to increase participation.[8] In addition, innovative exercise training regimens may help enhancing the beneficial effects of cardiac rehabilitation.[9]–[11]

During the last decade, the European Commission has made a priority the fight against cardiovascular diseases through a closer follow-up and prevention programs.[12] Since the 6th Framework Program, different topics in this area have funded several research projects targeting specific chronic conditions and spanning from individual hardware sensors to complete closed-loop management systems.[13] These solutions normally use proprietary data models and protocols and are tailored to specific deployment site's requirements, a fact that makes them little interoperable.

The application of SoA principles can help in simplifying the exchange of data across heterogeneous products[14], making it possible to reuse features and share data through the definition of a common interface.[15] This way, a product can benefit from the capabilities another product is providing or expose data from sensors using legacy protocols to third party products by just using the own product as gateway without the need of upgrading the firmware to support new protocols.[16], [17] This means that existing system capabilities increase in value as they are packaged and exposed as services.



C.Fernandez-Llatas and M.Guillen (Ed.):
Workshop on Innovation on
Information and Communication Technologies
(ITACA-WIICT 2015)

ISBN 978-84-608-4139-5

SOA defines a service as an independent unit of work that is self contained and has well-defined, understood capabilities. A unit of work may be an entire process, a function supporting a process, or a step of a business process.
The current work presents the strategy used to integrate four commercial products into a wider platform, which has been specialized for the prescription, monitoring and follow-up of cardiac rehabilitation routines based on physical exercise. The SoA strategy adopted follows an 'event-driven messaging' pattern[18], in which services automatically issue notifications on relevant events to interested subscribers, being these last ones responsible of initiating the communication. The use of this pattern allows a minimal modification of the original product, as the interaction logic can be decoupled and managed by an external entity: the middleware.

## 2 Materials and Methods

### 2.1 Integrated solution

HeartWays[19] system is composed by the integration of currently existing products and platforms with the aim of creating a new product offering cardiac rehabilitation therapies based on physical exercise, using features that each individual system provides. The resulting solution is divided into three subsystems, each one addressed to specific role in the cardiac rehabilitation process:

a) Doctors and medical professionals use an application based on the integration of NomhadChonic and Fortel. NohmadChronic is a management platform designed to empower the deployment of services for chronic patients based in ICT. The system is based on the coordinated work of several components: *NomhadCore* (core services such as security, storage, advanced data processing, etc.), *Professional Station* (clinical interface for in-house professional which allows the definition of care plans and the follow-up of therapies), and the *Patient Station* (device operated by the patient himself and used to retrieve information about the specific care plan for the patient). Fortel is a professional and high quality remote ECG monitoring providing continuous 3-lead ECG records and real-time arrhythmia detection.
b) Nurses use an application based on eNursing[20], which is a management system that allows grouping all the nursing interventions into nursing sheets and implement nursing care plans.
c) Patients make use of a system integrating 3 different exercise guidance and monitoring capabilities: *GOW Mobile*, which is a phone app that records activity using a wireless heart rate monitor attached to a textile sensor on a t-shirt and tracks distance using the built-in GPS chip. This app also offers a web portal where users can obtain training plans and track their evolution; *OZIMS[21]*, is a body sensor network capable of acquiring and processing kinesiologic data in real-time. It offers a PC application that models extremity movements and uses that network to guide the user on how to correctly perform them; and finally, *NomhadMobile*, which is a mobile application focused on the management of specific pathologies. This application is aimed at patients with more self-management abilities, usually in earlier stages of their pathologies, with less risk of decompensating and with mobility needs and is able to synchronize the care plans with NomhadChronic.

The integrated solution makes use of flexyNET[22], a cross-platform light-weight library providing data transfer capabilities with support for both the exchange of small data tokens (packet transmission similar to UDP) and streamed data (similar to TCP).
Additionally, the HeartWays solution adds external risk tools and algorithms[23]–[25] that are executed autonomously and can be used by any of other solutions.

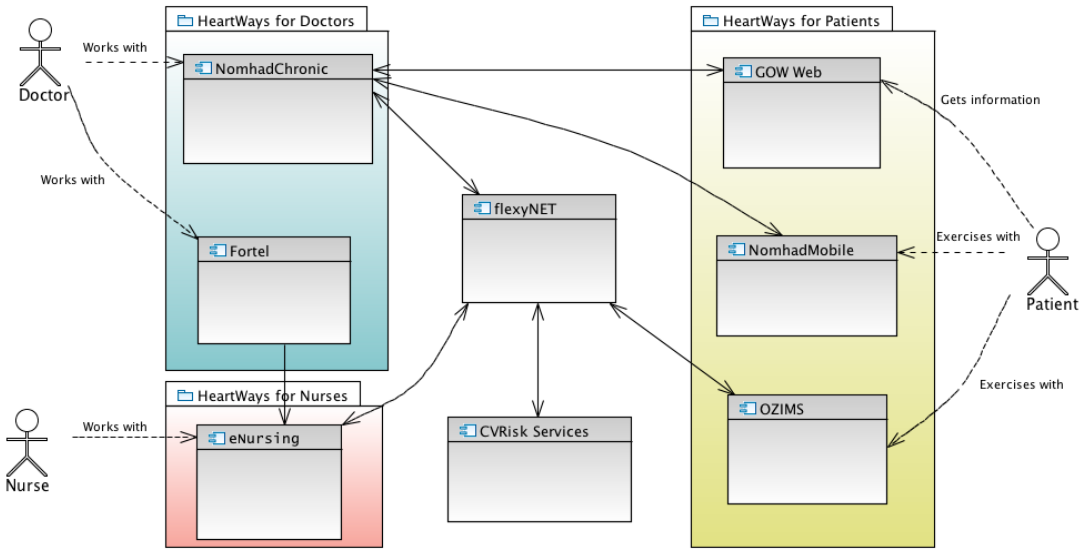


**Fig. 1**. Integrated HeartWays solution, showing the different commercial products that have been integrated to generate three specific user-based sub-systems: HeartWays for doctors, for nurses and for patients. Solid arrows in the diagram depict the integration strategy used to communicate different parts of the system (how data really flows within the HeartWays system).

***HeartWays for Doctors.***

This sub-system is the core of the HeartWays solution.[26] It coordinates the general administration routines such as creating user profiles, create care teams, prescribe treatments and process data recordings, etc.

On admission to the cardiac rehabilitation service, the system provides some profiling questionnaires, which allow the identification of risk factors and a proper calibration of the exercise plan through the realization of a stress test using an ergometer.

A patient care plan is dived into two main parts, a configuration part and an activity part, where the former is used to provide configuration parameters, like the reference ranges for the collected indicators or the parameters to be used for alarm generation, while the latter part contains the scheduling of the activities that the patient (or the other actors supported by the system) will be performing.

The exercise plan can is divided into phases, where every phase lasts from one to several weeks. Each phase is used to mark a progression in the exercise plan and with each new phase the intensity of the prescribed exercise is increased, either by augmenting the duration of each exercise, the number of times per week the patient should be exercising, the hearth rate level at which he should exercise (for endurance session), or the number of sets or repetitions per set (for strength session). The system already offers some templates, which implement cardiac rehabilitation therapies as recommended by international guidelines. The professional just has to personalize the configurable values using results from a recent stress test and specify the number of times per week the exercise should be performed, the duration of each exercise session and, finally, the heart rate objective for the patient during the session, expressed as a percentage with respect to the heart rate derived from the stress test.

HeartWays for Doctors is structured in several modules that allow a seamless patient monitoring and treatment. These modules are:

*Patient monitoring*

Allows browsing all historical data related with vital sign monitoring, symptoms (through questionnaires), medication and physical exercise session, either collected by the patient or introduced by professionals themselves. The data is presented following the dashboard design patter and can be viewed in various formats,

either as graphs or tables. The available information is divided into tabs, with the first screen presented to the user being a summary of the most important indicators and then one tab for each of the dimensions of the patient being monitored.

*Endurance session result*

It provides a list of all exercise sessions the patient performed during the last month. When a session is selected, summary information is presented, along with the details of the data collected during the session. Apart from the details of each session, the professional can also see the evolution in time of the most relevant indicators, like the maximum heart rate or the calories burned.

*Strength session result*

Strength session results in the professional application only provide computed parameters related tothe overall quality and performance of the session, since the details of the exercise recordings are presented in the application for nurses.

*Monitoring alarms and intervention*

Received monitoring data is analysed it and generates alarms for the professional according to the algorithms defined in the care plan. Alarms and interventions are grouped into incidents: a new incident is open when the first alarm is generated and it keeps accumulating alarms and intervention until a professional marks the incident as completed. Access to previous incidents is provided along with the details of all the alarms and interventions performed.
For each intervention the professional can record the evolution of the patient and select the action that he will perform from a list presented by the system. The list is divided into two parts: one part contains generic actions that can be performed in any circumstance, like calling the patient or adjusting the care plan; the other part contains the actions that should be performed to manage any of the detected alerts, organized by alert.

*Risk assessment*

This module of the professional application allows the professional to invoke the risk assessment and trend prediction algorithms provided by an external service. The algorithms receive as input the data collected by the patient during normal monitoring, lab test results, as well as well information about the patient condition collected by the doctor (mostly the presence of certain diagnostics and procedures in the patient clinical history). These algorithms provide three outcomes: the assessment of long term cardiovascular risk, the short term prediction of relevant vital signs, and the evaluation of alarms related with the evolution of the patient clinical history.

a) Cardiovascular risk assessment: With this functionality the professional can request the execution of the cardiovascular risk assessment algorithm and receive the risk evaluation.
b) Vital signs evolution prediction and related alarms: vital signs prediction works by comparing the patient data from the last fifteen days with a database of vital signs samples and looking for matching trends. The received data is then displayed to the professional and analyzed using the same reference ranges and alerts defined for the actual vital signs.
c) Cardiovascular condition evolution alarms: it checks for variation in a set of data related with the cardiovascular condition of the patient and generates new alerts if a worsening of the condition is detected.

***HeartWays for Nurses.*** This is the main interface for nurses, which manages those patients that are included in the nursing routines. From this list, nurses can open the patient profile and access the rehabilitation plan prescribed by the doctor and, specially, they can personalize the different strength exercises in a way that they are fit to the patient's physical condition in order to maximize the benefits of the physical activity. Each exercise

can be parameterized and fine-tuned independently from the rest of routines in the plan. New exercises can be added at any moment from a predefined list.

Once the patient completes the exercise routine, the results are stored in the system and the nurse can access to them and check a summary of the exercises and repetitions performed. It is also added the results from the Exercise Completeness Index algorithm (ECI), which gives an overview of the percentage of the routine effectively done by patients.

***HeartWays for Patients.*** This is the subsystem that patients use to perform the physical activity exercises prescribed by the medical team. Depending on the type of activity (strength or endurance), patients use a different set of devices and sensors to monitor the exercise and record the required data. Patients also have available a web portal where they can information about their rehabilitation plan, personalize some of its aspects, and see results from done exercises.

*Endurance Session*

Prescribed endurance exercises information is automatically downloaded to an application running on android mobile devices. This application informs the user about his/her activity and guides him/her throughout all the session to perform it in a correct and healthy way in order to achieve the expected goals.
The endurance session execution is composed of several steps: preparation phase, execution phase and finalization.
During the initialization, the application configures the internal parameters that guidance algorithms will use, connects to the heart rate sensor using a Bluetooth interface, and initializes other subsystems such as the GPS if the patient has enabled location services on the mobile.
During the execution, the application guides the patient through audio messages on how to reach and maintain the beneficial heart rate during the exercise. The patient can also check on the screen different information such as current heart rate compared to the prescribed value, exertion time and time left, respiration rate, distance covered (only if GPS is enabled) and an estimation of calories burned.
While the session is performed, data received from the sensors are checked to know if the exercise is being done correctly and report to the user when these data are out of the thresholds defined. Two different ways are used to guide during the session:

- Playing audio messages about the current status and the planned (i.e. “Your heart rate is 100 beats per minute, increase the intensity to 120 beats per minute for 2 minutes 40 seconds).
- Using visual resources that are easily understandable:
    - Changing the color of the heart rate value to know whether it should be higher (blue color), lower (red color), or it is correct (green).
    - Showing an icon to indicate whether the intensity must be increased (dart to up), decreased (dart to down), or kept (ok icon) to indicate the current heart rate is between the thresholds planned in that moment. These icons also are in the same color that the current heart rate.

To ensure that the session is performed without risks for the user, the application also performs several safe-checks in real-time:

1. Health problem detection: The application checks if the heart rate recorded is higher than a maximum threshold or it is lower than a minimum threshold defined for the user. When some of these situations occur, an audio message is played to suggest the user to stop the exercise. (i.e. “Your heart rate is too high. Stop right now”).
2. User reports health problem: In the application screens there is a button that can be pressed by the user when he/she feels health problem during the session. Then an audio message is played to report the user that must stop the exercise. (i.e. “You have notified a health problem. Stop right now”). Both safety risk detections, by the user or by the application, are reported to the HeartWays system, so the professional staff will have the information about these events to analyze them.

3. Unbalanced workload intensity information: It is possible that heart rate monitored is correct but the exercise intensity is out of normal values, so it is also checked if the heart rate data is not related to the pace data. If the heart rate is high and the pace is low it could be symptom of a health problem (i.e., the heart rate is 160 bpm and the pace is 10:30 per km). When it occurs, an audio message is played to ask a question about the user health status (i.e. "Your pace is low compared with your heart rate, are you exhausted? Do you feel fine?").

During the finalization phase, recorded data is compressed and transferred to the HeartWays system.

*Strength Session*

Prescribed strength exercises are executed using a resident PC application, which aids the patient throughout all the session providing visual guidance on how to perform movements correctly.
Before each exercise, the application shows instructions on how to perform the movements.
During the execution of exercises, the application processes in real time the information coming from the movement sensors to extract information about the performed number of cycles and repetitions for each exercise, along with an evaluation of the correctness of each repetition. A virtual trainer shows guidance on the movement and tempo that the patient should match with its own movements. Every repetition cycle is evaluated and the result displayed on the screen using a colored code: green for repetitions performed correctly and red for invalid ones.
After completion, all the data recorded is compressed and transferred to the HeartWays system.

## 2.2 Architecture

The strategy used to integrate the different components follows the principles of a service-oriented architecture. The implementing middleware is built on top of the flexyNet library, which creates a virtual network of nodes serving and consuming services provided by end-systems, and acts as a central router for all the communications.

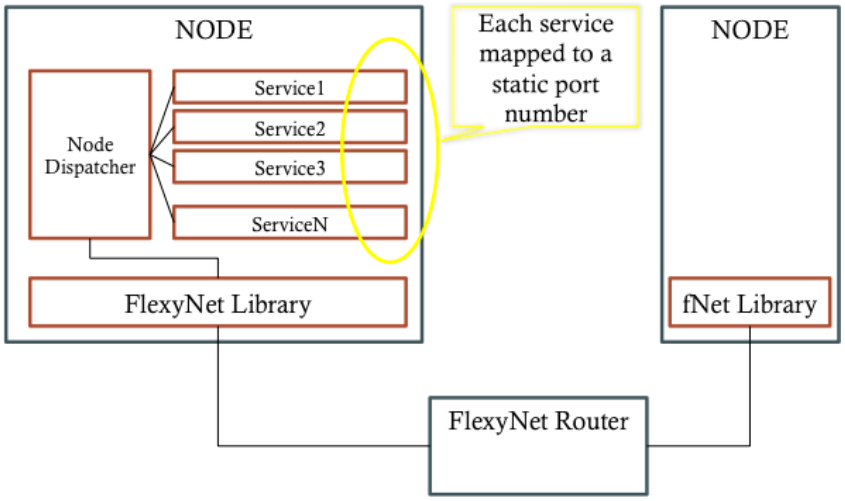


**Fig. 2**. Integration middleware architecture. Nodes are the base element of the network, hosting services and consuming services from remote nodes. Communication and routing is done using a messaging library (flexyNet), which is a multi-platform lightweight framework for streamed and packet-based end-to-end communications. Communication between nodes is done at a service level using a pull paradigm: when a node has information of interest available, it alerts the entire network and those nodes interested pull the information.

The HeartWays middleware defines the concept of *node* as the main deployable unit in the virtual network that has a unique address and that is able to serve and/or consume services. The concept of *service* in this context is

the same as in any other SOA architecture: a logical representation of repeatable business activity that has a specified outcome, is self-contained, may be composed of other services and it is a 'black box' to consumers.[1] HeartWays defines two types of services depending on the way they are activated: *on demand*, which are services waiting to be activated by other services requiring its functionality, and random broadcast, which are services that are self-activated from the node they are contained. The first type is normally used for node-to-node communications and the second one for distribution of information to all the nodes connected to the network.

### 2.3 Service design

The methodology used to create the services deployed onto the HeartWays middleware is based on the UML design principles and divided into XX steps:

1) Decide which feature from one of the end-systems needs to be exposed to the rest of the network.
2) Analyse the data requirements to execute the feature and provide a valid result. This step produces a '.proto' file that defines which is the mandatory information to execute the service, and which data can be considered as optional. Optional data can potentially be used to increase the precision of the service outcomes if provided.
3) Define which are the roles of the systems involved in the service execution. In the context of this middleware, we consider that a node can play the role of server or the role of client.
4) Specify the interactions between these actors, understanding interactions as units of communication between with the aim of exchanging data. These are modelled as Interaction Diagrams using UML.
5) Specify the interfaces to that will enable these interactions. Each interaction is assigned a unique identifier and a specific data signature.

### 2.4 Data Encapsulation

FlexyNet library can be efficiently used to transfer live data from sensors and data profiled as primitive data types. However, it has a limitation on the ability to transfer composite or non-primitive objects, as serialization is dependent on the technology (e.g., a JAVA object is serialized into bytecodes which cannot be decoded from .NET).

To solve this limitation it is necessary to provide the data encapsulated in a byte array that can be correctly de-serialized by a remote system, independently of the technology used.

This is a typical problem in system interoperability that is usually solved by using technologies such as XML and JSON as data encapsulation standards. These 2 technologies rely on creating a self-describing text document representing the information, but at the cost of increasing the size of the data significantly. As the data volume increases the use of plain-text standards becomes inefficient and, the use of binary interoperability technologies is recommended instead.

The HeartWays middleware makes use of "Protocol Buffers[2]", which has support for both Java (native support) and .NET (through third-part add-ons[3]).

Protocol buffers require that the data to be transferred (called *message*) be defined in a proto definition file, which describes the message structure and data types to be used. That proto file can then be compiled with specific tools for each technology, which generates the code that can be invoked by sender and receiver parties to serialize and de-serialize the information.

Canonically, Protocol Buffers are serialized into a binary wire format, which is compact, forwards compatible, backwards-compatible, but not self-describing (that is, there is no way to tell the names, meaning, or full data types of fields, without having an external specification).

The model that HeartWays uses for data encapsulation and transfer over the network is presented in Fig. 3.

---

[1] Service-Oriented Architecture: What is SOA? – The Open Group - http://www.opengroup.org/soa/source-book/soa/soa.htm

[2] https://developers.google.com/protocol-buffers/

[3] http://code.google.com/p/protobuf-net/

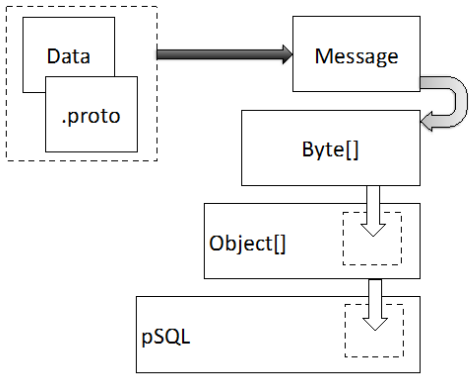


**Fig. 3**. The combination of data and a template '.proto' file produces a message instance. This message is serialized into a byte array which is embedded into a pSQL structure that flexyNET uses for transmission. The wired byte array can be used on destination to reconstruct the original message and, with the help of the proper '.proto' file, extract the data.

For any data exchange need, there is a prototype (.proto file) modelling the data that allows converting that data into a platform independent message. That message is serialized to a byte array using ASCII encoding. That array is the data that will be transferred to a remote system using flexyNet, so it needs to be encapsulated inside the pSQL object that flexyNet is able to serialize.

### 2.5 Integration Testing Methodology

The standard IEC 62304 (Medical device software – software lifecycle processes) defines integrates the software verification and integration into the whole development lifecycle. The way the standard "verification" is: confirmation through provision of evidence that specified requirements has been fulfilled.
According to the standard, the software under development must be split into different software units, which have to be treated as independent elements, which should undergo the application of the whole standard.
The most relevant activities described in the standards that concern HeartWays middleware are:

- Establish tests for software requirements: establish and perform a set of tests, expressed as input stimuli, expected outcomes, pass/fail criteria and procedures for conducting the testing, so all the requirements are covered.
- Use software problem resolution process: define a software resolution process and apply it to the anomalies detected during testing.
- Retest after changes: when changes are done during the software testing:
    - Repeat tests, perform modified tests or perform additional tests, as appropriate, to verify the effectiveness of the change in correcting the problem.
    - Conduct testing appropriate to demonstrate that unintended side effects have not been introduced
    - Perform relevant risk management activities.

The specific procedure adopted for the validation of HeartWays Middleware is the following:

- Define a set of tests implementing scenarios classified as 'unitary tests' or 'integration tests'. The first group checks features that are independent from other subsystems in the HeartWays network and therefore can be checked in standalone mode. The second group relates to those features that need communication to a different element in the network, and therefore require a more complex infrastructure.
- Define a minimum percentage of code that needs to be targeted during tests. This way we will ensure that the most relevant features implemented are successfully tested. To measure code coverage, we will use "cobertura"[4] which is a free tool that calculates the percentage of code accessed by tests.

[4] http://cobertura.github.io/cobertura/

- Analyse the code for potential errors using external tools such as “FindBugs”[5] / “CodeRush”[6] (static source code analysers to detect bug patterns and violation of coding best practices) and “PMD”[7] (a source code analyser that finds common programming flaws like unused variables, empty catch blocks, unnecessary object creation, and so forth).

Since integration tests are covering the communication between middleware instances running in different ecosystems, and potentially using different implementing technologies (e.g., JAVA, .NET, Matlab), part of this process needs to be done manually, since the automation of this process is a challenge by itself. In order to automate the testing as much as possible, integration testing was divided into two separate activities:

a) Manual testing: tests in which a person was directly checking on a screen the outcome from test cases. These cases were reduced to the verification of serialization and deserialization of Protobuf messages and the integrity of the data at both ends.

b) Automatic testing: test cases in which remote nodes are simulated using local instances implemented on the same technology as the node under test. This testing was used in combination with mocking technologies (such as Mockito[8] and Moq[9]) to verify that interactions at a node level were triggered successfully and that the complete service logic was executed as designed. This automatic testing was replicated for each implementing technology to ensure the services have a homogeneous behaviour.

# 3 Results

Middeware was produced for two implemented technologies: Java and .NET. Analysis of integration requirements came up with the definition of four core services.

## 3.1 Services

### *Notification Service*

This is an internal service to the HeartWays node structure that is in charge of receiving notifications from remote services and alerts the corresponding service at the hosting node.

The reason why this service was added is because of the nature on the communications through the flexyNET network: a service port is configured to work as packet-oriented or stream-oriented, but cannot support both. If each service had to support both modalities, then 2 ports would be needed for each service: the packet port and the stream port. To avoid this problem, the notification service gets all the notifications and relays them to the correct service.

To do so, the structure of notifications has to be changed to add the target service within the packet, as depicted in Fig. 4.

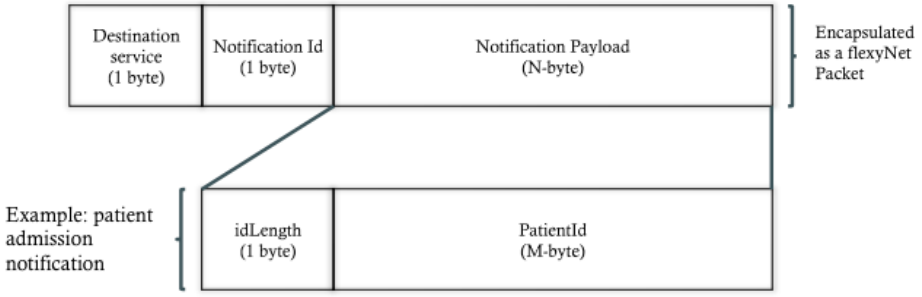


[5] http://findbugs.sourceforge.net/
[6] https://www.devexpress.com/Products/CodeRush/
[7] http://pmd.sourceforge.net/
[8] https://code.google.com/p/mockito/
[9] https://github.com/Moq/moq

**Fig. 4**. Notification's frame. Destination service indicates which service should read and interpret this notification. Notification id should be unique at service level and provides information on how to read the payload field.

***Patient Management***

The patient management service controls the creation of patient profiles and how the system handles a patient at each time.

Like in a real hospital, HeartWays system uses the concept of admission when a patient needs treatment and discharge when the treatment is finished. During that period, the patient can be in a series of states that will determine how the system is handling the data. Fig. 5 shows in detail the state-diagram used.

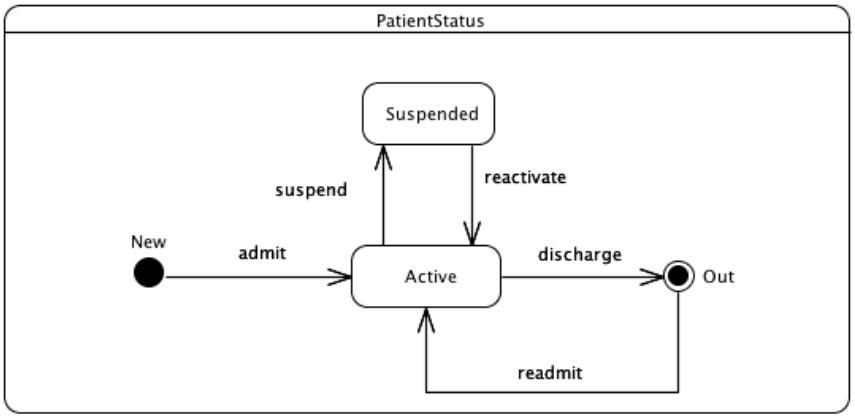


**Fig. 5**. Each node in the HeartWays network synchronizes the patient status with the rest of the nodes using this state diagram. Patients under treatment are in 'active' state. 'suspended' patients are still admitted but treatments and follow-up are not executed (useful, e.g., when patient has a medical emergency that is incompatible with the current treatment). On admission, the status will be 'new' if the node didn't have information about the patient, requiring a local profile creation. On discharge, the status changes to 'out'. Nodes can decide whether to hold the patient profile or delete it.

*Roles.* The service implements two roles, based on which node has information (server - represents the node where changes to the patient profile occur and where the notifications to the HeartWays network are originated.) and which node is requesting that information (client -represents the node plugged to the HeartWays network receiving a notification and requesting the patient profile to the 'server' if necessary.). The following diagram shows the methods and events each role is implementing.

*Notifications*

a) Patient Admission: when a patient is admitted to a server node, it broadcast *PatientAdmissionNotification* to the network. Client nodes will receive the notification and decide if further actions are required.
b) Patient Status Changed: server nodes broadcast a *PatientStatusChangedNotification* when the patient status is changed.
c) Patient Discharged: similar to the admission case, but the *PatientDischargedNotification* is broadcast when the patient is discharged at the server node.

*Interactions*

a) GET_PATIEN_PROFILE: client nodes initiate this interaction upon the reception of any of the three notifications. The client requests the patient profile data and the server returns it using the *PatientProfile* message.

***Exercise Plan Management***

The Exercise Plan Management service handles all the interactions related to the creation and modification of exercise routines prescribed as rehabilitation plans as well as the exchange of data recorded during the execution of such routines.

*Roles.*

The service implements two roles.

a) Server: represents the node where the creation/edition of rehabilitation plans take place. It is also where exercise results are stored after they are received from the patient's application, and it is where notifications are created and broadcast to the network.
b) Client: represents the node plugged to the HeartWays network receiving a notification and requesting the exercise plan/exercise results to the 'server' if necessary.

*Notifications*

a) NewExercisePlan: when the server node detects the creation of a new plan, a *NewExerciplanNotification* is broadcast to the network. This notification contains as payload the patient identifier and the plan identifier.
b) NewExerciseResults: when a server node receives data recordings from an exercise session, it locally stores them and triggers either the *ResistanceExerciResulstNotification* or the *StrengthExerciResulstNotification*, which broadcast the identifiers for the patient, plan and exercise session.
c) ExercisePlanPersonalized: when a server node receives personalization information for a specific exercise plan, it stores that information locally and broadcast a *ExercisePlanPersonalizedNotification* to the network to indicate the rest of the nodes the availability of such information. This notification contains as payload the patient identifier and the plan identifier.

*Interactions*

a) GET_EXERCISE_PLAN: client nodes begin this interaction is started after the reception of either a *NewExerciplanNotification* or an *ExercisePlanPersonalizationNotification*. The server node responds with an *ExercisePlan* message.
b) GET_STRENGTH_EXERCISE: client nodes initiate this interaction upon the reception of the *StrengthExerciResulstNotification* notification. The server will respond with a *StrengthExerciseResults* message.
c) GET_RESISTANCE_EXERCISE: client nodes initiate this interaction upon the reception of the *ResistanceExerciResulstNotification* notification. The server will respond with a *ResistanceExerciseResults* message.

*Data mappings*

The model used to represent an exercise plan, as well as the different elements involved, is represented in figure Fig. 6.

a) ExercisePlan

The *ExercisePlan* message is a container for the different elements modelled in the rehabilitation plan. It can contain a set of exercise prescriptions categorized in either strength exercises (*StrengthExerciseSession*) or resistance exercises (*ResistanceExerciseSession*).

b) ResistanceExerciseSession

This object represents a cardiovascular activity within the training plan. It contains the following information:

- Identification: fields 'fullName' and 'description', giving the display name and specific execution instructions.

- Session global values, such as heart rate thresholds (maximimSafeHR, minimumSafeHR and totalDuration)
- Repeatability: weekly frequency (timesPerWeek) and scheduling (repetitions and designatedTime)
- Session structure: parts and duration.

c) ExerciseRepetition

The object *ExerciseRepetition* is used to represent scheduling information for a specific exercise. The field 'date' contains the date a patient will do time an exercise. This scheduling info should be interpreted as 'day of week', not as a specific point in time.

d) SessionPart

A session part determines the different components each exercise session will be composed of. Each part defines specific values for parameters that are used to monitor and control resistance exercises, such as the target heart rate and the heart rate safety interval.

The enumeration *ExercisePartType* determines the behaviour of the system when the patient performs the exercise. It can take any of the following values:

- WARM_UP: period before the exercise to help the patient achieve an optimal heart rate before starting the cardio activity.
- CORE: period during which the patient is doing a cardio activity.
- COOL_DOWN: period after one or more cardio activities to help the patient decrease the working heart rate towards basal levels.
- STRETCHING: a period of time at which the patient is not doing a cardio activity but doing some stretching exercises.

e) StrenghtExerciseSession

This object represents a strength training activity within the training plan. It contains the following information:

- Repeatability: weekly frequency (timesPerWeek) and scheduling (repetitions and designatedTime)
- Exercise structure: exercises.

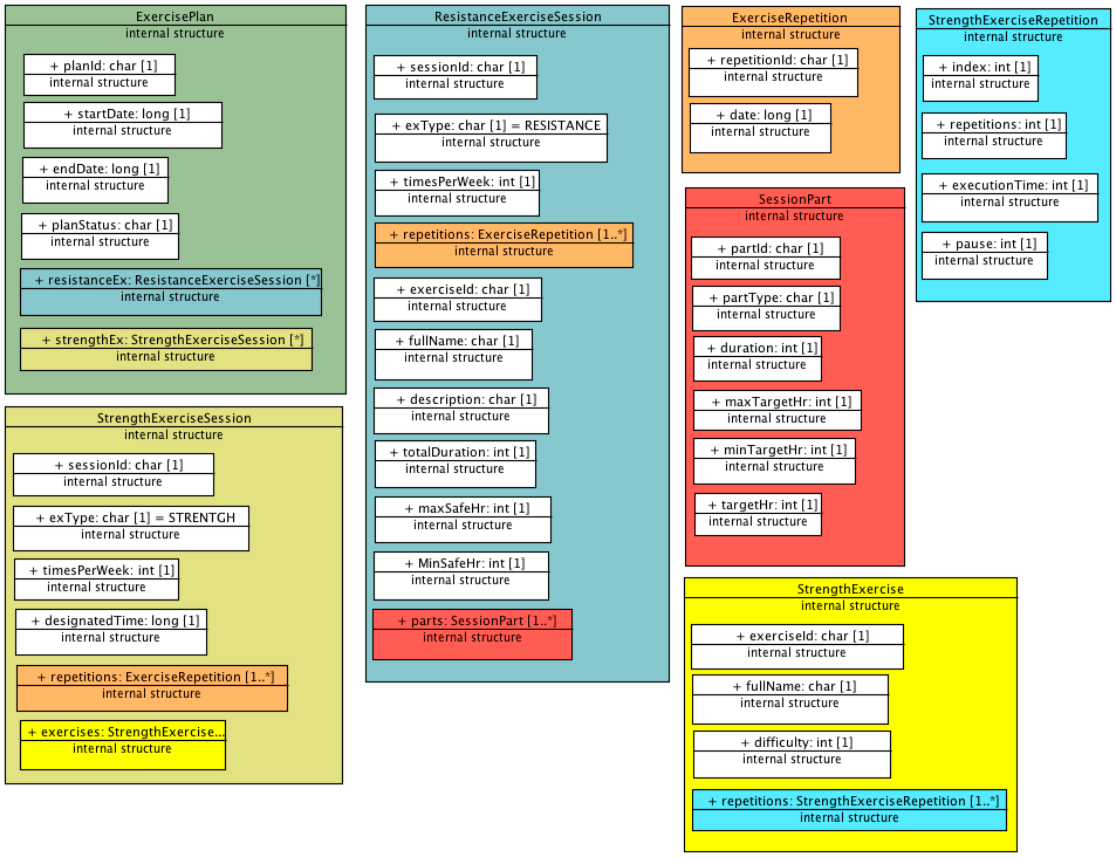


**Fig. 6**. Data mappings for exercise plans and exercise sessions. Background colour provides indication on the level of nesting of the different structures. Plans have sessions (strength and/or resistance). Resistance sessions have parts, each one defining a different cardiovascular activity with specific configuration parameters (e.g., warm-up, stretching, main exercise, etc.); strength sessions define a set of exercises, each one with a number of repetitions and specific configuration parameters (e.g., 15 pull-ups with 3kg).

f) StrengthExercise

This object contains the information about each strength exercise included in the training plan.

The fields 'fullName' and 'description' contain the display name and specific guidance on how to perform the exercise. The field 'difficulty' can take the values 'EASY', 'MEDIUM', 'HARD' and 'PROFESSIONAL' and it indicates how much weight or resistance should be used to do this exercise.

The field 'repetitions' contains the number of movements and the tempo the patient should use.

g) StrengthExerciseRepetition

This object contains information on how the patient has to execute the movements within each strength exercise. The field 'repetitions' indicate how many times the movement has to be repeated. 'executionTime' indicates how long the movement should last and 'pause' indicates how much time the patient has to rest within repetitions.

h) ResistanceExerciseResults

The *ResistanceExerciseResults* message is a wrapper to embed and transfer all the vital signals and information recorded during a resistance exercise session. The object hierarchy can be seen at Fig. 7.

The data is grouped using the concept of *source device*, meaning the physical (hardware) or logical device used to record that information. In this model we have three main source devices:

- BloodPressureMonitoringDevice: used to hold the data coming from an external BP monitor.
- ExerciseMonitoringDevice: used to gather and hold sampled signals such as ECG, HR, BreathRate, accelerometer axis, etc.
- QuestionnaireFillingDevice: used to hold the different questionnaires that the patient is prompted with during the session.

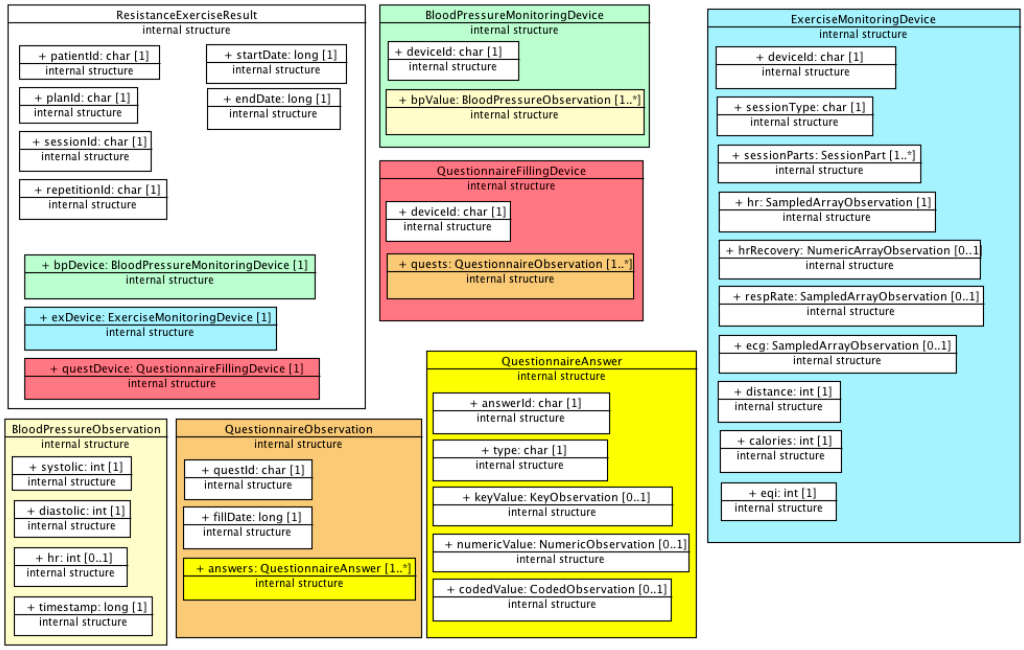


**Fig. 7**. Resistance exercises results data mapping. Each exercise has a set of vital signs, which may have acquired with different sensors. The information about the source device is maintained as it abstracts the underlying hardware and allows changing the sensor while keeping the information intact. Each device attaches metadata to the recordings that might be required when feed to processing algorithms (e.g., sampling freq., gain, bit resolutions, etc.).

i) StrengthExerciseResults

The data model for strength exercises is simpler than for resistance ones. As raw signals are not transferred, the *StrengthExerciseResults* message only contains processing results such as the repetition status (classified as GRAY, GREEN, YELLOW, RED to indicate if the repetition was not done, it was done correctly, it was done more or less correctly or the repetition was not done properly), the exercise quality index and the exercise completeness index, and an estimation of the calories used during the exercise.

***CVRisk***

The CVRisk service is a wrapper library connecting the 'Personalized CV Risk Prediction' service, implementing the interactions to invoke the patient stratification and the CV alerts computation.
Roles. The service implements two roles, based on which node performs all the computations (server) and which node is invoking such computation (client).

*Notifications.*

a) AlarmsReadyNotification: indicates that the results from a CV alarms computation is ready and can be retrieved using the GET_CV_ALARMS interaction. The notification defines as payload the patient identifier for which the computation has been done.

b) CVRiskReadyNotification: indicates that the results from a CV Risk computation is ready and can be retrieved using the GET_CV_RISK interaction. The notification defines as payload the patient identifier for which the computation has been done.

*Interactions.*

a) INVOKE_CV_ALARM

This interaction is started by a client node and requests the server node to compute a set of CV alarms. The client node is sending together with the request a dataset of vital measurements that is required to run the calculation. This dataset is defined by the message *AlertRequest*.

The server node is not responding the requester node directly. Instead, it is generating a broadcast notification of type *AlarmsReadyNotification* through the router, which will notify all the nodes in the network.

It is the responsibility of each client willing to receive the results from the CV Alarms computation to initiate a GET_CV_ALARM interaction to retrieve them

b) GET_CV_ALARM

The client node initiates this interaction when it wants to retrieve the results from a CV Alarms computation. The interaction is prepared to work both in synchronous and asynchronous communications. The alarms processing results are returned using an *AlertResponse* message.

c) INVOKE_CV_RISK

This interaction is similar to the previous one but the data set provided to the server when the service is invoked contains the data defined at *RiskRequest* message.

The server will broadcast a *CVRiskReadyNotification* when the result is ready. Any client node receiving the notification can then use the GET_CV_RISK interaction to request the outcome from the patient stratification.

d) GET_CV_RISK

The client node starts this interaction after the *CVRiskReadyNotification* is received. The server node will answer with a *RiskResponse*.

### 3.2 System Testing

The resulting set of services developed as middleware were tested using a set of 86 test cases, which covered 92% of the developed code, with a 77% of branch coverage. The analysis of the 8% code proved to be exception-handling code unlikely to be executed, while the 23% left in branch coverage was due to safe 'if' conditions that would never require an 'else' action (e.g., checking non-null instances before using them in asynchronous operations).

The code analysis in search for bugs detected 0 violations in 262 classes, while it detected 9 possible code duplicities in 7 classes. A deeper analysis of the duplicity report showed that these were false positives due to similarity in methods signature and variable names, but all these cases were related to independent pieces of code which could not be refactored, as they were specific callbacks for asynchronous processing.

Table 1 shows a summary of tests and coverage for each middleware service.

**Table 1.** Summary of test coverage using JUNIT/NUNIT. Test cases were replicated for Java and .NET code and same results were obtained for both technologies. Using 'Cobertura', we obtained the percentage of the code and branches covered by test cases. Cobertura reports were analysed to check the non-covered areas of code and it proved to be exception-handling code unlikely to execute in a real scenario.

| Middleware part | # classes | # test cases | Lines coverage | Branch coverage |
|---|---|---|---|---|
| Core | 5 | 15 | 91% | 87% |
| CVRisk service | 12 | 12 | 89% | 71% |
| Exercise Plan management | 14 | 39 | 93% | 79% |
| Patient management | 9 | 17 | 90% | 73% |
| Notifications service | 2 | 3 | 90% | N/A |

## 4 Discussion

We have described in this article how to develop a Service Oriented Architecture to integrate already existing products into a fully configurable software solution, externalizing most of the integration logic into a middleware handling communication and business intelligence. As a result, we have obtained product in which some individual product features are made available to the rest of the products without the need of replication and minimizing the impact of plugging/unplugging new features, since each product is still handling the data processing tasks and informing the rest of products when outcomes are available.

The resulting middleware has been tested using continuous automatic integration techniques and has been proved reliable and robust for production environments.

However, some limitations apply to integration solution, since there were constrains in the modification of based products. The integration middleware was designed keeping the simplicity as a key factor, and assuming most of the implementation complexity. That makes integration of third party systems easy and fast, as no modifications to the product itself are required, but that limits the integration to the set of services pre-defined. The definition of new services requires that nodes are updated to be able to serve/consume them.

Finally, the fact that the middleware is not implementing any service discovery service mechanism, simplifies the interaction mechanism, as service contracts are static and the middleware only needs to take care of the data exchange itself. However, in a wider scenario, this approach is not optimal as it makes the middleware harder to maintain and upgrade as additional nodes are added to the network.

## References


[1] P. D. Thompson, D. Buchner, I. L. Piña, G. J. Balady, M. A. Williams, B. H. Marcus, K. Berra, S. N. Blair, F. Costa, B. Franklin, G. F. Fletcher, N. F. Gordon, R. R. Pate, B. L. Rodriguez, A. K. Yancey, y N. K. Wenger, «Exercise and Physical Activity in the Prevention and Treatment of Atherosclerotic Cardiovascular Disease A Statement From the Council on Clinical Cardiology (Subcommittee on Exercise, Rehabilitation, and Prevention) and the Council on Nutrition, Physical Activity, and Metabolism (Subcommittee on Physical Activity)», *Circulation*, vol. 107, n.º 24, pp. 3109-3116, jun. 2003.

[2] M. Nocon, T. Hiemann, F. Müller-Riemenschneider, F. Thalau, S. Roll, y S. N. Willich, «Association of physical activity with all-cause and cardiovascular mortality: a systematic review and meta-analysis», *Eur. J. Cardiovasc. Prev. Rehabil. Off. J. Eur. Soc. Cardiol. Work. Groups Epidemiol. Prev. Card. Rehabil. Exerc. Physiol.*, vol. 15, n.º 3, pp. 239-246, jun. 2008.

[3] European Heart Network and European Society of Cardiology, «European Cardiovascular Disease Statistics», sep. 2012.

[4] J. A. Jolliffe, K. Rees, R. S. Taylor, D. Thompson, N. Oldridge, y S. Ebrahim, «Exercise-based rehabilitation for coronary heart disease», *Cochrane Database Syst. Rev.*, n.º 1, p. CD001800, 2001.

[5] R. S. Taylor, A. Brown, S. Ebrahim, J. Jolliffe, H. Noorani, K. Rees, B. Skidmore, J. A. Stone, D. R. Thompson, y N. Oldridge, «Exercise-based rehabilitation for patients with coronary heart disease: systematic review and meta-analysis of randomized controlled trials», *Am. J. Med.*, vol. 116, n.º 10, pp. 682-692, may 2004.

[6] M. Tanasescu, M. F. Leitzmann, E. B. Rimm, y F. B. Hu, «Physical activity in relation to cardiovascular disease and total mortality among men with type 2 diabetes», *Circulation*, vol. 107, n.º 19, pp. 2435-2439, may 2003.

[7] R. Arena, M. Williams, D. E. Forman, L. P. Cahalin, L. Coke, J. Myers, L. Hamm, P. Kris-Etherton, R. Humphrey, V. Bittner, C. J. Lavie, on behalf of the A. H. A. Exercise, C. R. and P. C. of the C. on C. Cardiology, C. on E. and Prevention, and C. on Nutrition, y P. A. and Metabolism, «Increasing Referral and Participation Rates to Outpatient Cardiac Rehabilitation: The Valuable Role of Healthcare Professionals in the Inpatient and Home Health Settings A Science Advisory From the American Heart Association», *Circulation*, vol. 125, n.º 10, pp. 1321-1329, mar. 2012.

[8] A. M.-R. Erik Skobel, «Evaluation of a newly designed shirt-based ECG and breathing sensor for home-based training as part of cardiac rehabilitation for coronary artery disease», *Eur. J. Prev. Cardiol.*, vol. 21, n.º 11, 2013.

[9] A. Radzewitz, E. Miche, G. Herrmann, M. Nowak, U. Montanus, U. Adam, Y. Stockmann, y M. Barth, «Exercise and muscle strength training and their effect on quality of life in patients with chronic heart failure», *Eur. J. Heart Fail.*, vol. 4, n.º 5, pp. 627-634, oct. 2002.

[10] L. L. Andersen, S. P. Magnusson, M. Nielsen, J. Haleem, K. Poulsen, y P. Aagaard, «Neuromuscular activation in conventional therapeutic exercises and heavy resistance exercises: implications for rehabilitation», *Phys. Ther.*, vol. 86, n.º 5, pp. 683-697, may 2006.
[11] M. E. Nelson, W. J. Rejeski, S. N. Blair, P. W. Duncan, J. O. Judge, A. C. King, C. A. Macera, y C. Castaneda-Sceppa, «Physical activity and public health in older adults: recommendation from the American College of Sports Medicine and the American Heart Association», *Med. Sci. Sports Exerc.*, vol. 39, n.º 8, pp. 1435-1445, ago. 2007.
[12] COUNCIL OF THE EUROPEAN UNION, «2586th Council Meeting Employment, Social Policy, Health and Consumer Affairs». 01-jun-2004.
[13] A. T. Harald Reiter, «HeartCycle: From insights to clinically evaluated ICT solutions for Telehealth.», *Conf. Proc. Annu. Int. Conf. IEEE Eng. Med. Biol. Soc. IEEE Eng. Med. Biol. Soc. Conf.*, vol. 2013, pp. 6992-6995, 2013.
[14] A. Grzech, K. Juszczyszyn, G. Kołaczek, J. Kwiatkowski, J. Sobecki, P. Świątek, y A. Wasilewski, «Specifications and Deployment of SOA Business Applications Within a Configurable Framework Provided as a Service», en *Advanced SOA Tools and Applications*, S. Ambroszkiewicz, J. Brzeziński, W. Cellary, A. Grzech, y K. Zieliński, Eds. Springer Berlin Heidelberg, 2014, pp. 7-71.
[15] A. Dan, R. D. Johnson, y T. Carrato, «SOA Service Reuse by Design», en *Proceedings of the 2Nd International Workshop on Systems Development in SOA Environments*, New York, NY, USA, 2008, pp. 25–28.
[16] R. Kyusakov, J. Eliasson, J. Delsing, J. van Deventer, y J. Gustafsson, «Integration of Wireless Sensor and Actuator Nodes With IT Infrastructure Using Service-Oriented Architecture», *IEEE Trans. Ind. Inform.*, vol. 9, n.º 1, pp. 43-51, feb. 2013.
[17] F. Jammes y H. Smit, «Service-oriented paradigms in industrial automation», *IEEE Trans. Ind. Inform.*, vol. 1, n.º 1, pp. 62-70, feb. 2005.
[18] T. Erl, *SOA Design Patterns*. Pearson Education, 2008.
[19] J. P. Lázaro, S. Guillén, T. Meneu, y A. Martínez, «HeartWays Solution for Exercise Based Cardiac Rehabilitation», en *The International Conference on Health Informatics*, Y.-T. Zhang, Ed. Springer International Publishing, 2014, pp. 343-346.
[20] S. Drobnjak, «Expanding the Scope of Electronic Nursing Documentation», en *The International Conference on Health Informatics*, Y.-T. Zhang, Ed. Springer International Publishing, 2014, pp. 351-354.
[21] L. Celić, M. Varga, T. Pozaić, S. Žulj, D. Džaja, y R. Magjarević, «WBAN for Physical Activity Monitoring in Health Care and Wellness», en *World Congress on Medical Physics and Biomedical Engineering May 26-31, 2012, Beijing, China*, M. Long, Ed. Springer Berlin Heidelberg, 2013, pp. 2228-2231.
[22] L. Celić, «Energy efficiency in wireless sensor networks for healthcare».
[23] T. Marques, J. Henriques, S. Paredes, y P. Carvalho, «Personalization Based on Grouping Strategies for Short-Term Cardiovascular Event Risk Assessment», en *The International Conference on Health Informatics*, Y.-T. Zhang, Ed. Springer International Publishing, 2014, pp. 171-174.
[24] D. Mendes, S. Paredes, T. Rocha, P. Carvalho, T. Marques, J. Henriques, y J. Morais, «Short-Term Cardiovascular Disease Risk Assessment: Comparison of Two Combination Approaches», en *6th European Conference of the International Federation for Medical and Biological Engineering*, I. Lacković y D. Vasic, Eds. Springer International Publishing, 2015, pp. 670-673.
[25] P. Carvalho, J. Henriques, S. Paredes, T. Rocha, y J. Ramos, «Cardiovascular Risk Prediction during Cardiac Rehabilitation», en *The International Conference on Health Informatics*, Y.-T. Zhang, Ed. Springer International Publishing, 2014, pp. 205-209.
[26] A. Martinez-Romero, S. Drobnjak, R. Serafin, y T. Meneu, «Management Tools for Medical Professionals for Prescription and Follow-Up of Cardiac Rehabilitation Based on Physical Exercise Therapies», en *The International Conference on Health Informatics*, Y.-T. Zhang, Ed. Springer International Publishing, 2014, pp. 347-350.

# Project BREATHE, Breathing Life into Informal Caregivers

Juan-Bautista Mocholí[1], Ángel Martínez[1], Juan-Pablo Lázaro[1]

[1] Soluciones Tecnológicas para la Salud y el Bienestar, Ronda Auguste y Louis Lumiere 23, Nave 13, Parque Tecnológico de Valencia, 46980 Paterna, Spain
{jbmocholi, amartinez, jplazaro}@tsbtecnologias.es
http://tsbtecnologias.es/

**Abstract.** This paper presents the BREATHE project and the solution developed by the project to help informal carers to take care for the cared person, but also to take care for themselves. There are a number of problems that informal carers have to face: lack of experience and formal education in care, limited societal support, and lack of specific tools to manage the whole care cycle, problems with coordinating care and other employment for carers (mostly women), stress and depression. The problem is highly topical and pertinent since family carers provide 80% of long-term care to dependent elder people in Europe, and family care breakdown leads to expensive and hospitalization and/or institutionalization.

## 1 Introduction

BREATHE[1] is an Ambient Assisted Living (AAL) project that aims to provide a *platform for self-assessment and efficient management for informal caregivers*, which is in fact the project's actual full title. This title is significant because most of services and applications currently available focus on the specific needs of the person cared for and few support the needs of the carer, which are mainly informal caregivers (family carers, unpaid carers) that are in charge of caring long-term condition people.

Nowadays informal caregivers deal with several difficulties, especially the ones related to care because of their poor experience in caring, lack of understanding of the local health and social care system, etc.; but also psychological issues such as stress, anxiety or depression [2]. At the end, these difficulties turn into poor quality of care and emotional dissonance, which throws the person to the 'caregiver syndrome', characterized by:

- Social isolation.
- Psychological distress.
- Anxiety.

[1] BREATHE Project has been co-funded by the Ambient Assisted Living Joint Programme (Call 5, 2012) and some National Authorities and local Research Programmes in Spain, United Kingdom, Ireland and Italy.



C.Fernandez-Llatas and M.Guillen (Ed.):
Workshop on Innovation on
Information and Communication Technologies
(ITACA-WIICT 2015)

ISBN 978-84-608-4139-5

- Depression.
- Loss of self-esteem.
- Guilty feelings.
- Fear of becoming a patient.

### 1.1 Context

As it was once said by former USA First Lady Rosalynn Carter, *"There are only four kinds of people in the world – those who have been caregivers, those who currently are caregivers, those who will be caregivers and those who need caregivers"*.

Informal caregivers are generally relatives to the cared person. In fact, family carers provide 80% of long-term care to dependent elder people in Europe. Population is now ageing world-wide, and it is also valid for Europe's population [4]. As a result of prolonged life expectancies, around 7% of total population are expected to be aged 80 and over in 2030, and 12,3% in 2080. **Table 1** shows the population structure based on population projection data calculated on 2013.

**Table 1.** Population structure by major age groups, EU-28, 2013–80[2], % of total population

| | 2013 | 2020 | 2030 | 2040 | 2050 | 2060 | 2070 | 2080 |
|---|---|---|---|---|---|---|---|---|
| 0–14 years | 15,6 | 15,6 | 14,9 | 14,6 | 15,0 | 15,0 | 15,0 | 15,1 |
| 15–64 years | 66,2 | 64,1 | 61,2 | 58,5 | 56,9 | 56,6 | 56,9 | 56,2 |
| 65–79 years | 13,1 | 14,6 | 16,8 | 17,9 | 17,2 | 16,6 | 15,9 | 16,4 |
| 80+ years | 5,1 | 5,8 | 7,1 | 9,0 | 10,9 | 11,8 | 12,2 | 12,3 |

There is also known that the number of elder people who want to live independently at their own home is increasing, nevertheless, ageing at home may need some support and/or assistance. Based on the literature revised at the beginning of the project (2013), the context of care was defined by:

- Assisted persons in EU27 prefer be cared for at home by a relative.
- In USA, 21% of population is considered to be unpaid caregivers.
- Presently public support to long-term care is extremely limited.

At the initial phase, the project collected its own data by means of conducting both face-to-face and focus groups interviews in three countries (Ireland, Spain and United Kingdom). The conclusions [1] were close to the obtained by the literature. Moreover, after analysing the collected data, some new points relevant to Breathe were identified. The **Table 2** shows the informal care profile identified by the literature and the BREATHE project.

**Table 2.** Informal caregiver profile (literature vs BREATHE analysis of data)

| Literature | BREATHE analysis |
|---|---|
| - Female (76%). | - Female (73 %) |

[2] 2020-80 projections from EUROPOP2013.

| | |
|---|---|
| - Mean age: 55 years old.<br>- 46 hours/week dedication.<br>- Total caring process 60 month.<br>- Less than half are employed.<br>- Limited computer skills. | - Mean age (in years) around 54.8<br>- 52 hours/week dedication<br>- Unknown data<br>- 64 % are unemployed and/or housewife<br>- Limited computer skills BUT:<br>o 97 % used the Internet (daily-weekly frequency of use)<br>o Owned devices like desktops, laptops, tabletsPC and smartphones<br>o Users of social media and instant messaging mobile applications<br>- 56 % live with the cared for person<br>- Cameras accepted as assisted technology in emergency situations (100 %)<br>- The majority of ICs accepted cameras as assisted technology in non-emergency situations |

## 2 The Breathe Solution

BREATHE's main assumption is based on the premise that the process of caring for people with long-term conditions by informal carers is an extremely difficult and complex process due to the specific needs of the carers. This situation could be improved by the introduction of technologies that support the carers in their job and, by following this way, may also reflect in the quality and duration of the assisted person's care in their own home.

The solution offered by BREATHE (depicted by Fig. 1) consists in a platform that comprises two modules, the AAL home system and the informal caregiver tool, and a common back-end shared by both on the server side.

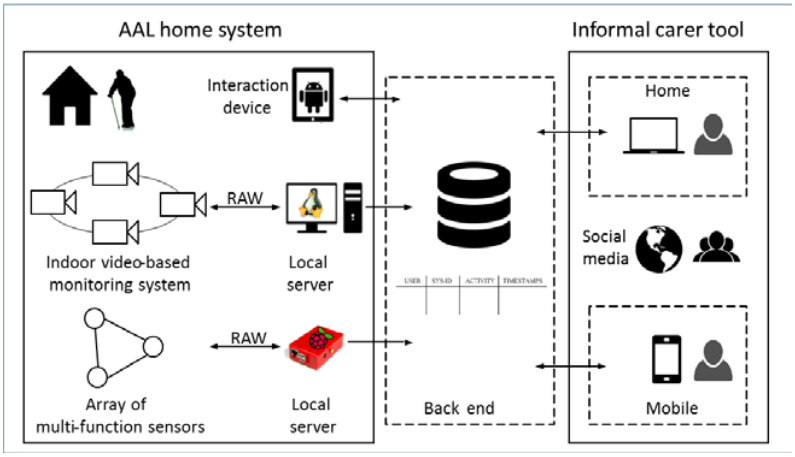


**Fig. 1.** The BREATHE solution.

**AAL Home System.** The first module is composed by a server side solution, the back-end, and an at home solution. The at home solution is installed at the home of the person cared. It is composed by cameras and an array of multi-function sensors, with their associated software and controllers to upload de collected data to the server. The cared person uses an interaction device to set up the application and access to some data. The function of this first module is to collect information periodically, upload to the server, process it and extract information about the cared person's daily routine, behaviours and activities.

The array of multi-function sensors is composed by Z-Wave sensors and a Raspberry Pi with a Z-Wave card to communicate with the sensors, collect the data from them, and upload the data processed to the back-end. The final installation at home may differ depending on the needs of each person, but basically the sensors to be installed consist on motion sensors to determine when and where a person is moving around the home; plug-in power monitors to check when home appliances like a microwave, an electric kettle or a television are being used; door sensors placed on each exit door used by the person, or on the fridge, etc.

The indoor video-based monitoring system consist of wide-angle fisheye cameras placed in the centre of the ceiling of the room to be monitored. These kind of cameras offers a top-down view point of an entire room, and can be accessed in real-time. The systems is completed by a processing machine to run the algorithms that analyse the video captured by the cameras, and acts as an entry point to the online streaming.

The interaction device acts as the cared person interface to manage the configuration of the system. It is a touchscreen tablet running the BREATHE application that allows the cared person to turn on/off the video systems, and also manages the access to the real-time streaming after a request from its informal caregiver.

**Informal Carer Tool.** The second module, is a server side solution that offers two interfaces, a web-based tool and a mobile application. This module provides the carer with the guidance and support required to improve their quality of life as well as their working conditions, with the aim of producing as a result, a greater efficiency of their care.

The web-based tool offers to the informal caregiver a dashboard with an overview of the main features and two main views: features related to the cared person, and features related to itself.

The features related to the cared person provide access to all the data collected from the AAL home system, but processed in a way that the informal caregiver can check the statistics of each kind of event or activity collected, check also for tendencies and behaviours, and compare them with the ones collected a month before, a week before, or 48 hours before. The tool also presents a day calendar view where the different activities are placed as events as them occur and are received and processed by the back-end. It also allows the informal caregiver to configure the notifications from the AAL home system it wants to receive on the mobile application. Finally, there is also the live view option that access to the real-time streaming video from the cameras available at the cared person's home. Note that a message is sent to the cared person's interaction device to inform it that is being monitored in real-time by the carer, then the cared person can turn off the vision system and deny the access to the real-time streaming video.

The features related to the informal caregiver are the access to its profile settings, a self-assessment questionnaire that is presented periodically, a module in charge of the analysis of sentences introduced by itself, and a module with the summary of the informal caregiver's personal status and the information, action and advices based on the current status. These features will be further explained in the chapter 3 of this article.

The mobile application tool shows the notifications for activities or actions performed by the cared person at home, allows also the informal caregiver to set which activities and action will be notified, as well as obtain the activities performed by the cared person last 24 hours.

**The Back-End.** The server side solution of both modules, the back-end, resides on the same server and shares the same database. This back-end is fed by three independent information sources:

- Ambient Assisted Living (AAL) system that gathers information about daily life activities of the elderly at home.
- Structured information that both caregiver and assisted person provide (e.g. through questionnaires).
- Non-structured sources of information such as a diary, notes and posts on social networks.

## 3 Helping Informal Carers

The common informal carer is so occupied in their role of caregiver that usually forgets its own care. The BREATHE solution offers strategic support and customized guidance for the informal caregiver in all the stages of the long-term care process, and also for improving the quality of life of informal caregivers at all levels.

Currently, there are a number of assessment tools available to determine carer satisfaction, burden and/or management e.g. The Barthel Index (Mahoney and Barthel, 1965), Caregiver Burden Scale (Zarit et al. 1980), but not infrequently the outcomes of these assessments fall short of any substantial meaningful interventions to support care giving; they remain only an assessment of burden.

Specifically, the aim of the informal caregiver tool is to get a better understanding about the real conditions of the cared person, to improve the skills of the informal carer through an education and training programme and to avoid the social isolation of the informal carer by increasing the communication channels with professionals (formal carers), other informal carers and other relatives of the assisted person.

**Self-Assessment Questionnaire.** [8] [9] after accessing the appropriate section in the informal career tool, the IC will be invited to fill-in a self-assessment questionnaire in order to measure its level of burden in a concise and validated way.

The questions presented are related to the feelings preforming the care activities during the previous week. The tool also offers the opportunity of fill-in the questionnaire for the feelings related to activities performed two weeks ago in case it remains unfilled, but if it is not filled within two weeks, it will not be presented to be filled-in in future.

In more detail, these questions collects data about five different features:

- Overload.
- Emotional competences, and emotional intelligence (positive attitude, self-knowledge, empathy, self-esteem).
- Temporal dedication (hours per week). Social activities/individual activities, activities with exercise/sedentary activities, indoors activities/outdoors activities.
- Sociability, leisure (time the informal care spent):
- Physical status: Number of medical visits last 12 or 6 months, chronic ailments or diseases, dizziness, headache, backaches, tiredness, etc.

The temporal dedication to care is a fundamental dimension, because as caring gets longer the probability of overload increases too. A longer temporal dedication may also be translated to a poor management of emotional competences.

**Sentiment Analysis.** The informal carer tool also provides an interface to the informal carer with the aim of writing periodically its feelings as a career with sentences less than 140 characters long, like a tweet in Twitter. From time to time the tool will encourage the informal carer to write about how it feels as a career. This interface is connected to a module in charge of the analysis of the sentences introduced, producing at the end a kind of sentimental analysis.

Project BREATHE assumes the premise that regular writing can have a positive impact in the life of the informal carer. Specially, the following aspects about regular writing are relevant:

- Regular writing about stressful events helps the IC re-live the events experienced in a safe environment without fear or stress (i.e. to deal with them [5]).
- Regular writing can serve as a track record of mistakes and successes the IC wants to remember in the future (significant lessons/important learnings).
- Regular writing is a good tool for clarifying the thoughts and goals of the IC as well as to put things in perspective (writing in general helps people to disentangle their thoughts).
- Regular writing lets the informal carer to put the focus on as well as to really understand its context of life.
- Regular writing naturally forces people in general to plan next steps so the informal carer can take advantage of the diary functionality as a good tool of decision making.

The objective followed by BREATHE is to be able to distinguish whether a piece of text written by the informal carer is positive, negative or neutral.

**Composing a personalized recommendation**. Based on answers to the questionnaires, the output from the sentiment analysis, and the current knowledge of the activities of the cared person, BREATHE characterizes the current status for an informal carer. Breathe has established four different states, these states are set from less to more necessities:

- *S0*: The informal carer feels good and does not requires for specific support or guidance.
- *S1*: The informal carer basically needs information, by means of information resources or tools.
- *S2*: The informal carer needs help and guidance, basically recommendations and concrete actions to perform.
- *S3*: The informal carer does not support its current condition, needs professional therapeutic support and guidance.

The **Table 3** shows the classification that models the state of the informal carer based on computing all data collected. Based on the state showed in the table the informal carer will receive a different output: proposing the informal care read a book about something specific, go to hairdressing, go to the cinema, etc.; showing reinforcement messages or documents;

**Table 3.** Classification of the informal carer's state based on the Burden scale and the total temporal dedication per week in hours

| Burden | 0-6 | 7-12 | 13-18 | 19-24 |
|---|---|---|---|---|
| 0-4 | *S0* | *S0* | *S1* | *S1* |
| 5-8 | *S1* | *S1* | *S2* | *S2* |
| 9-12 | *S2* | *S2* | *S3* | *S3* |
| 13-16 | *S3* | *S3* | *S3* | *S3* |

## 4 Conclusions

This paper has introduced the aims and goals of project BREATHE. The paper previous chapters have presented the problems that informal carers have to face, and also the solutions that the project provides to solve them, solutions that also help the informal carer to improve its quality of life.

Long-term Care is not only related to the person to take care for, but also the people that have to take care of them. In Europe, Informal caregivers are providing 80% of long-term care to dependent elder people. By monitoring their work and their own situation will help to detect problems of the cared person, or problems of the carer itself, and also to reduce the final amount spent regarding health factors.

The goal of the validation phase is to demonstrate the hypothesis in which the project is based. These hypothesis were defined as a consequence of an intensive process of interviews with informal carers and cared persons where BREATHE identified and filtered proposals. At this point the consortium have developed the current solution and now is going to check how well the system adapts to their real situation.

In the following months the project will conduct the trials of the whole solution in Ireland (16 participants), Spain (10) and United Kingdom (10), which will consist on the installation of the AAL home system at the home of the person cared, and teaching both the person cared and the informal cared about how to use the system and the specific applications developed for each of them.

## References


1. Deliverable D1.1 – Needs and requirements of AAL and ICT solutions for the informal. Public document available on: http://www.breathe-project.eu/en/publications/. (Last access June 2015).
2. Long-term care challenges in an ageing society: the role of ICT and migrants. Results from a study on England, Germany, Italy and Spain. JRC scientific and technical reports. European Commission (EUR 24382 EN). 2010. Public document available on: http://ftp.jrc.es/EURdoc/JRC58533.pdf.
3. Negative caregiving effects among caregivers of Veterans with dementia. Bass D, Judge K, Snow A, et al. American Journal of Geriatric Psychiatry 20(3):239-247. 2012.

4. Population structure and ageing. Statistics Explained, EuroStat. Online article available on http://ec.europa.eu/eurostat/statistics-explained/index.php/Population_structure_and_ageing. (Last access June 2015).
5. Journaling about stressful events: effects of cognitive processing and emotional expression. Philip M. Ullrich and Susan K. Lutgendorf. University of Iowa. 2002.
6. Sentiment Analysis and Opinion Mining. Bing Liu. Morgan & Claypool publishers. 2012.
7. DepecheMood: a lexicon for emotion analysis from crowd-annotated news. Jacopo Staiano. University of Trento. 2014.
8. Validación de escalas abreviadas de zarit para la medición de síndrome del cuidador primario del adulto mayor en Medellín. Johana María Vélez Lopera, Dedsy Berbesí Fernández, et al. Revista Atención Primaria, Vol. 44. Núm 07. Julio 2012.
9. Competencias emocionales de los cuidadores de personas mayores. Begoña Ibarrola. La inteligencia emocional y su aplicación en la atención de las personas mayores, Servicios Centrales del Imserso, Madrid 17-18 junio de 2014. Public document available on http://www.imserso.es/InterPresent1/groups/imserso/documents/binario/ciemo_ibarrola.pdf. (Last access June 2015).

# Support to the optimization of medical processes by semantic annotation of locations

Aroa Lizondo José Luis Bayo Vicente Traver
Carlos Fernandez-Llatas

June 16, 2015

**Abstract**

Currently, companies tends to standardize their processes in order to optimize them. This practice could be applied in the medical scope too, where provide patients the best care is essential. The necessary information for the optimization is obtained detecting the activities that are occurring at each moment and their duration. Nowadays, these information is provided manually by the processes actors, noting it down on paper or digitally. Taking advantage of that hospitals are recently equipping their buildings with Real-Time Location Systems to monitor their actives and to provide people locations, the authors propose that, is possible to know the activity of the process that the patient is doing due to a semantic associated with the locations. This paper describes a methodology to perform the semantic mapping and the data collection.

## 1 Introduction

In the current industrialized society is increasingly finding common techniques to make the business processes the most efficient possible, obtaining the same production and quality results with the least possible resources. According to this idea, to improve processes is necessary to make the rules that are going to regulate them. This is called processes standardization, which allows to apply processes in an optimal way [1].

Medicine is one of the fields in which the processes standardization is at its peak. Traditionally, medicine was a field where professionals created the processes individual and unilaterally and that's why the clinical environment is defined by procedures written in natural language, away from this standardization [2].

Within medicine area and focusing in the hospital scope, the surgical block constitutes an essential element due to the broad scale of resources that mobilizes and its significance in costs (until the 14 % of the hospital). Therefore an improvement in the efficiency of the surgical block management is the key to increase the hospitals efficacy[3]. Here is where the processes work is going to be dealt with.

Once the processes are standardized, in order to achieve an optimization of them is necessary to know for each process: when an activity has been realized and how long has it taken. As is indicated in [4] to allow the surgical block



C.Fernandez-Llatas and M.Guillen (Ed.):
Workshop on Innovation on
Information and Communication Technologies
(ITACA-WIICT 2015)

ISBN 978-84-608-4139-5

optimization is necessary to measure running indicators related to operations times (start of the first activity, time between activities, etc.) on operations rooms and to the process (cancellations).

The main disadvantage in the surgical blocks is that the patient monitoring is often made manually by nurses and that constitutes a bottleneck in the system [5]. These manual notes also can cause program mistakes: unnecessary delays, under-use of the operation rooms, unnecessary transfers, etc. In addition it could cause the increase of the adverse effects in the surgical process probability and, according to [6] they represent the 40% of all the adverse effects in hospitals. To collect these times, in [7] a pragmatic stance is advised, being the optimal, to have limited but relevant data collected automatically.

Nowadays, hospitals are equipping them with Real-Time Location System (RTLS) to manage the location of patients and actives. Based on the premise that hospitals have this technology available, the authors working hypothesis is that assigning semantic to the areas locations and to the process activities is possible to know,for each process, what activity is doing the patient and its duration. The purpose of this article is to present a methodology that allow us to start the study and to validate the hypothesis.

## 2 Matherials and Methods

The main idea of our hypothesis is based on the requirement that we have a precise log of the locations of a person in the study area. As a result we need to review if there are at the market commercial products that can cover our necessities.

To analyze the different products have been defined some parameters on which we have to focus:

- The system needs to work inside buildings and in complicated places like surgical areas.
- The product must be well-tried for medical use:
  - Not cause interferences on medical devices.
  - Sterilizable.
- The locations provided for the system must be reliable and the minimum resolution must be per room.
- The changes on the locations have to be detected with the minimum delay.
- The system has to be as least intrusive as possible:
  - Lightweight.
  - Small size.
  - No battery recharge needed during long term hospitalizations.
  - Shockproof.
  - Waterproof.
- Data logged and associated to the patients must be stored and a method to consult or export this data has to be provided.

At the literature many different RTLS to track location of people can be found. Mainly this systems can be classified as either outdoor or indoor location systems, based on the context where they are used.

The most known RTLS is the Global Positioning System (GPS). Nowadays this system is one of the most used outdoor system, widely used on devices like mobile phones. This kind of system is not suitable for our goal, due to we need a reliable indoor positioning and GPS is not designed for this purpose.

For the indoor use there are different kinds of technologies that can be applied. Each of them provide different grade of resolution that usually determines where to use it [8, Figure 1].

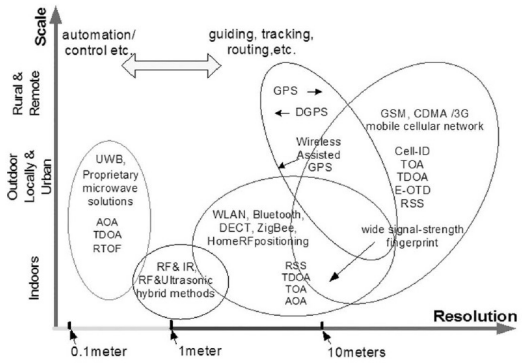


Figure 1: Outline of wireless-based positioning systems.

The most used technologies are Radio-frequency identification (RFID), Ultra-wideband (UWB), Wireless Local Area Network (WLAN), Bluetooth, Infrared IR. Each of them has advantages and disadvantages and it is responsibility of the vendor of each product, to solve its weaknesses and take benefit from its strengths[8, 9].

There are two main design approaches on which we can catalogue the different location systems. The first of them creates its own network infrastructure and the second one reuses pre existing wireless infrastructure. The main advantage to use its own infrastructure is that specifications are more controlled and is easier to assurance quality. The main advantage of reuse infrastructure is to reduce costs of implantation[8].

Several commercial products that apply RTL to the healthcare environments, have been reviewed to analyze whether it meets with the requirements defined in this section. Below we detail a short summary of some of them:

**Ekahau RTLS**

This product provides a healthcare solution based on RFID-over-WIFI, uses an active smart tag like a watch to localize the user and a combination of the wifi infrastructure of the hospital and extra IR beacons when it is needed. Provides room level location accuracy (1-3 meters). The location tag blinks every 15 seconds and his battery remains up to 500 hours without recharge, its dimensions are 51,5 x 50 x 17,5 mm, has a weight of 31 g and it is waterproof. The system provides an Application Programming Interface (API) to access the data collected[10].

**VERSUS**

System to supply location in healthcare contexts, based on the use of IR-RFID badges combined width IR and Low-power RFID sensors. It provides location accuracy at room, bed or chair level, depending on type and quantity of sensors used. The badges can be configured in a flash rate between 3 and 15 seconds, providing a range of 8 to 13 months of battery duration. This product is designed to be easy to clean, scratch resistant and with protection against water. The product offers a integration framework to access the data registered[11].

**MYSPHERA**

This solution is especially designed for hospital environments, uses RFID technology to communicate bracelet tags with fixed beacons to provide room level location. The bracelets refresh its location each 2,5 to 10 seconds, providing between 1 to 4 years of battery life. This tags are waterproof for an easy sterilization. The system provides integration of data and exchange mechanisms with third party systems[12].

**Sonitor Sense TM**

Sonitor is a RTLS to supply location services in health environment, based on three combined technologies Ultrasound, Wifi and Low Frequency (LF). At this system the location áreas are delimited by ultrasound transmitters that act like a virtual walls, it is the tag given to the patient who collects data and transmits it each 1 to 3 seconds using wifi signal to be used into the Software Location Engine. The tags are waterproof and designed with long battery life[13].

The RTL systems analyzed by the authors fit on the requirements needed to validate the proposed hypothesis. The MYSPHERA RTLS has been selected to the next phases of the study, because as well as be suitable to the requirements it implies practical connotation, as it is installed in the reference hospitals at geographical area of the authors.

# 3 Results

In this section the aim is present a methodology 2 able to validate the working hypothesis proposed by the authors in the introduction.

As we see in the flow chart 2(a), the first step is to define the activities followed by patients in a surgical block, what will constitute the different processes. To do that, a distinction among subjects access is needed. For example, we can differentiate between patients with or without hospitalization.

Once these activities had been differentiated, illustrative flows of the path that patients will follow must to be elaborated. Figure 3 illustrate an example: the patients without hospitalization's flow. This patients, after being registered in the system, sequentially pass through three activities: a preoperative process, the operation and a postoperative process. Sometimes these patients will require a change of clothes in a locker room or an environment adaptation process.

The next step would be to identify the patient's crossing points2(b). To do this, the hospital have to be divided into logical areas like the waiting room, the reception room, the pre and post surgical areas, the operating room or the locker rooms. The localization beacons are collocated into this areas.

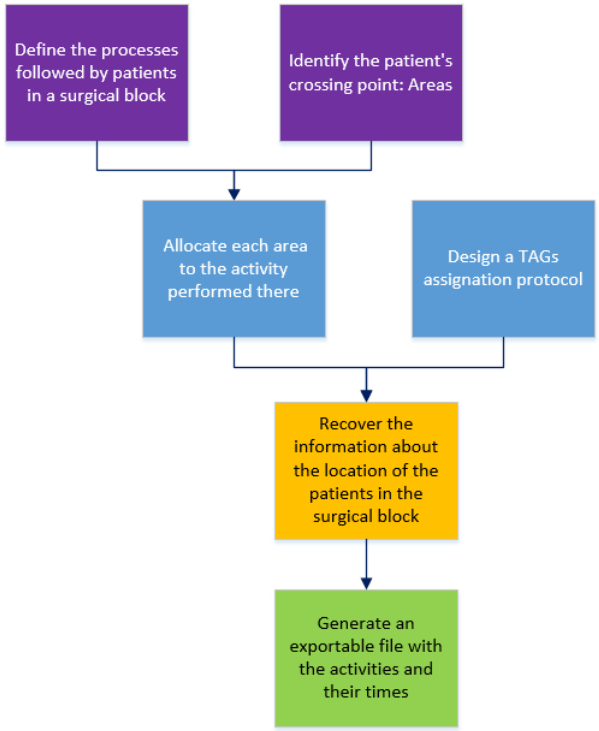


Figure 2: Flow chart of the methodology.


Figure 3: Flow of the path follow by a patient without hospitalization.

One the processes and the zones already defined, in order to provide the system with semantic, each area needs to be allocated to the activity that will be follow there 2(c). For example, the operations would be allocated into the operating rooms. There are some hospital areas in which distinct activities could be carried out. For example, if the postoperative rooms are saturated, patients can stay in the preoperative rooms during their recuperation after the operation. At these cases, the system must infer in which stage of the process are the patients at the room, taking care of the previous activities. At the example of the preoperative room, the system must to detect that the patient has already passed the intervention activity and it must to detect that this patient is in the recovery time even when he is in the preoperative room.

Although it is necessary to design a protocol in order to deliver, to assign, to pick up and to deallocate the TAGs 2(d). With this protocol, we will be able to have times of every activity followed by patients available, since they arrive to the surgical block until they receive the discharge. To register all the process, the TAGs must to be placed and assigned with the patient's arrival to the reception and it must to be removed and deallocated when the patient is recovered and he has received the discharge. To control the process of the patients who are hospitalized, the TAGs must to be assigned the day before and they will be placed by orderlies when they pick up the patient in their rooms.

Getting all the information collected by TAGs, the system will generate a file 2(f), which needs to be exportable, like a CSV file. This file will contain each process followed by patients, with an anonymous identifier. The patients process will be made up by different activities, being each activity the distinct locations with the exact time of arrival and finish.

# 4 Conclusions

This paper has presented a methodology able to know the process flow that patients follow in the hospital, having information of which activity is carrying on at specific time and their duration. This methodology is based on patients location in the hospital, that is provided by a RTLS technology installed there. The gather information could be used by hospitals to improve their efficiency and their safety in the operation rooms trough the optimization of their processes. Future work claims to check this methodology in a hospital and to develop a tool for analyzing the data.

# References


[1] Thomas H Davenport and James E Short. Information technology and business process redesign. *Operations management: critical perspectives on business and management*, 1:97, 2003.

[2] Carlos Fernández Llatas. *Representación, interpretación y aprendizaje de flujos de trabajo basado en actividades para la estandarización de vías clínicas.* PhD thesis, 2009.

[3] OMS. Safe Surgery Saves Lives. `http:\\www.mdpi.com/1424-8220/13/11/15434`. [Online; accessed 16-June-2015].

[4] Misterio de Sanidad y Política Social. Bloque quirúrgico. estándares y recomendaciones. informes, estudios e investigación 2009.

[5] Alessandro Redondi, Marco Chirico, Luca Borsani, Matteo Cesana, and Marco Tagliasacchi. An integrated system based on wireless sensor networks for patient monitoring, localization and tracking. *Ad Hoc Networks*, 11(1):39–53, 2013.

[6] Eefje N de Vries, Maya A Ramrattan, Susanne M Smorenburg, Dirk J Gouma, and Marja A Boermeester. The incidence and nature of in-hospital adverse events: a systematic review. *Quality and Safety in Health Care*, 17(3):216–223, 2008.

[7] García del Valle S. González Arévalo A., Gómez Arnau J. *Coordinación y gestión de las áreas quirúrgicas.*, chapter Tratado de Anestesia y Reanimación, pages 221–238. En Torres LM, Madrid: Arán Ediciones S.A., 2001.

[8] Hui Liu, H. Darabi, P. Banerjee, and Jing Liu. Survey of Wireless Indoor Positioning Techniques and Systems. *IEEE Transactions on Systems, Man, and Cybernetics, Part C: Applications and Reviews*, 37(6):1067–1080, November 2007.

[9] D. Dardari, P. Closas, and P.M. Djuric. Indoor Tracking: Theory, Methods, and Technologies. *IEEE Transactions on Vehicular Technology*, 64(4):1263–1278, April 2015.

[10] ekahau Real-Time Location System.

[11] VERSUS Locating Advantages for HealthCare.

[12] MYSPHERA-RTLS technology for hospital solutions.

[13] Sonitor RTLS technologies.

# Towards a new WSN/VANET development ecosystem focused on reliability and intelligent techniques based on simulation and real HW implementation

José Navarro, Pablo Cardós, Juan V. Capella, Alberto Bonastre, Rafael Ors

Institute ITACA, Universitat Politècnica de València,
46022 Valencia, Spain
{jonaal1, pabcarma, jcapella, bonastre,
rors}@upv.es

**Abstract.** In this paper an ecosystem for wireless sensor networks and vehicular networks simulation and development is proposed. This ecosystem consists on a pair of simulators, the ns-3 (Network Simulator) and SUMO (Simulation of Urban MObility), and a set of WSN/VANET protocols that have been developed recently and others considered as reference. To mobility simulation the SUMO protocol is used. SUMO is appropriately interconnected with ns-3, to perform the network simulations. Finally, is possible to implement on real systems in a systematic manner the proposals developed with this ecosystem, using the Robot Operating System (ROS). As a result, with the proposed WSN/VANET ecosystem will possible to develop, compare, adjust and validate new proposals that can be implemented from the developed models in a natural and systematic manner.

## 1 Introduction

In the last years the sensor networks based on wireless technologies are having greater relevance in mobile scenarios, (unmanned vehicles, autonomous robots, etc.), hence the increasing need to carry out research and to develop new communication protocols that offer reliability and take advantage of geolocation devices in these scenarios among other characteristics. Furthermore, these protocols have been to take certain decisions on the fly, being necessary to apply intelligent techniques. To simulate the network operation a simulator such as the ns-3 [1] is used. On the other hand, a mobility simulator such as SUMO [2] is necessary to provide all the traffic generation and simulation. In this manner, it is necessary to dispose of a complete ecosystem, that assemble the appropriate simulators as well as different protocol models and load/traffic generators, allowing developing, adjusting and validating new protocols and that allows the comparison with other recent protocols or standards. The next step, consists on implement successful developments and protocols over real devices. Low cost and low consumption commercial devices will be proposed for this phase, p.e BeagleBone Black or another devices with similar features.



C.Fernandez-Llatas and M.Guillen (Ed.):
Workshop on Innovation on
Information and Communication Technologies
(ITACA-WIICT 2015)

ISBN 978-84-608-4139-5

## 2 Related work

The protocols considered to be implemented and incorporated in the proposed simulation ecosystem are related in the following paragraphs.
ERBA protocol [4] using the vehicle movement trend it is capable to distinguish between vehicles. In this approach every vehicle is equipped with GPS and several sensors.
In [5] the authors present an parallel evolutionary algorithm that applied to configure the OLRS protocol. These configurations are obtains with the methodologies that employ techniques of Evolutionary Computation.
In paper [6] presented problem to scalability in the VANET protocol and offer a solution, HLAR, protocol based on AODV and combine greedy-forwarding geographic routing protocol for to obtain the best route.
SRR protocol [8] is based on fuzzy-logic. This protocol uses a GPS in order to know the closest vehicle and take decisions with this information to send the packages to destination.
Finally, in [7] the devices that incorporate the vehicles for intelligent transport systems are presented.

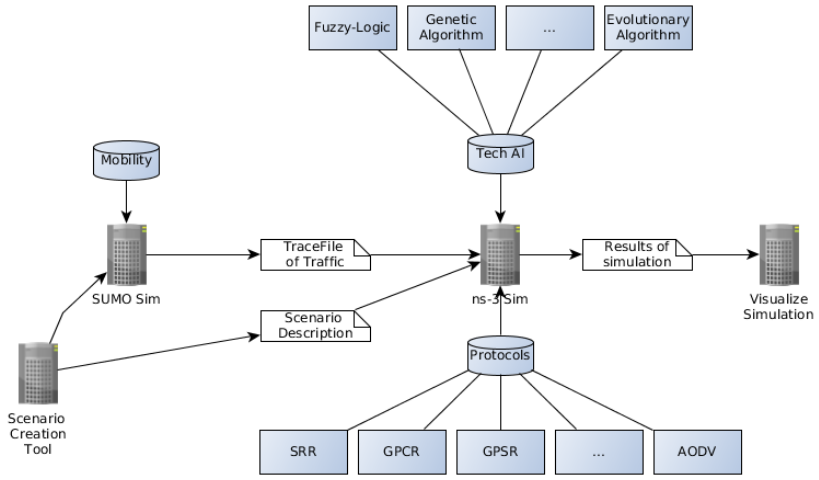


**Fig. 1.** Block diagram of the proposed simulation ecosystem

## 3 Proposed simulation ecosystem

The proposed ecosystem will be constituted by several simulators, as shown in Fig. 1, in order to perform complete simulations of wireless sensor network and mobility. On one hand, the network simulator (ns-3), that will be used in order to compare, adjust and validate all develops, allowing proposing and evaluating new improvements and protocols [9,10].
To complete this ecosystem, is necessary to provide mobility pattern generator and analyzer, being selected for this task the SUMO simulator.
Furthermore, in recent years has appeared the necessity to perform simulations that involve intelligent techniques. For this reason evolutionary algorithms and fuzzy logic rules, among others have been introduced in the ecosystem.
As a result, a complete ecosystem that addresses all these needs, based on ns-3 simulator and SUMO traffic generator have been proposed, where among others the SRR, GPCR, GPSR, OLSR protocols [11,12,12,13] have been implemented and incorporated (see table 1), in order to simulate with different approaches the network issues and mobility patterns. In this manner, it is possible to develop efficiently new proposals, compare with the existents, improve and validate. More and more with a systematic methodology, the models that define in C/C++ language the new proposals can be implemented over real systems in a natural and efficient manner.

**Table 1.** Implemented protocols in the simulation ecosystem

| Acronym | Protocol name |
|---|---|
| SRR | **Stability and Reliability aware Routing** |
| GPCR | **Greedy Perimeter Coordinator Routing** |
| GPSR | **Greedy Perimeter Stateless Routing** |
| OLSR | **Optimized Link State Routing** |
| AODV | **Ad hoc On demand Distance Vector** |

## 4 A HW implementation approach

Finally, when the experimentation based on simulation have been concluded, and the proposal is tuned and validated, it can be implemented in real system in an efficient manner in order to apply and validate over real hardware the proposal.

Therefore, have been proposed the implementation using an embedded system of last generation, as BeagleBone Black, where several peripherals (an IMU, altimeters, GPS and long range wireless devices, among others) were added (Fig. 2).

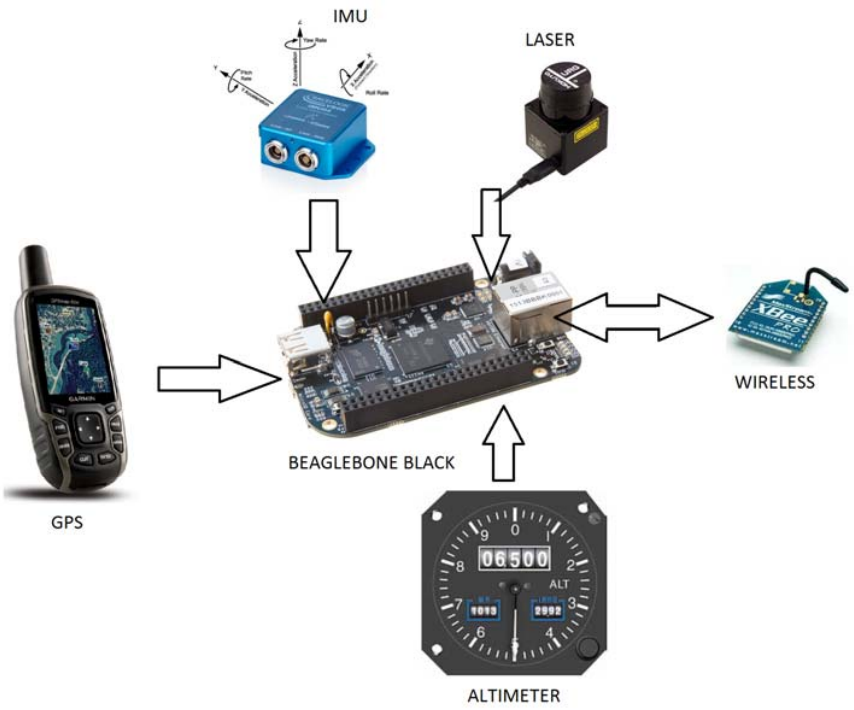


**Fig. 2.** Platform and proposed components for the HW implementations

This target is governed for a Linux Ubuntu OS, where the Robot Operating System (ROS) was installed. With this proposed system relevant control actions for vehicles, robots, etc. can be applied with the network capabilities developed and tested with the simulator ecosystem. Fig.3 shows an example of mobile robots real application where has been applied this approach.

For integrate the protocols and implementations [14,15] in ROS it is not immediate but possible, because ROS it is written in C/C++ language. It is necessary to configure several files that call libraries included in ROS or third parties, and know how to publish and subscribe for obtain values an how to realize the control action over vehicles, as well as the dependencies with the Operating system and the compiler.

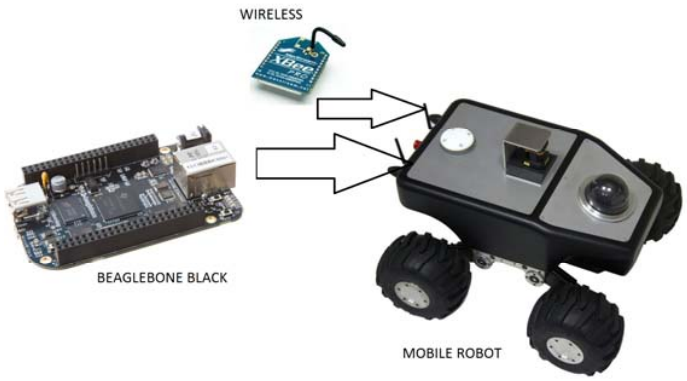


**Fig. 3.** Example of application

## 5 Conclusions

A new complete ecosystem for WSN/VANET development has been proposed. Special emphasis on reliability and introduction of intelligent techniques have been realized, in order to facilitate the development and validation of new robust WSN/VANET protocols that incorporates AI techniques to improve the energy efficiency, reliability and mobility.
Also, an example to implement in real systems is provided, allowing developing a methodology to implement the new proposals evaluated in the simulation ecosystem over real hardware.
As future work, it will be necessary to incorporate more WSN/VANET protocols in the simulation ecosystem. As well as new mechanisms to facilitate the inclusion of AI and reliable techniques, and the more automated methodology to implement in the proposed real systems new developments.

## Acknowledgements

The authors gratefully acknowledge the financial support from the Valencian Regional Government under Research Project GV/2014/012, and Universitat Politècnica de València (Research Project UPV PAID-06-12 SP20120889).

## References


1. http://nsnam.isi.edu ns-3 simulator (accessed on June 2015)
2. http://sumo.dlr.de SUMO simulator (accessed on June 2015)
3. http://www.ros.org .ROS (accessed on June 2015)
4. Zhang D, Yang Z, Raychoudhury V, Chen Z, Lloret J: An Energy-Efficient Routing Protocol Using Movement Trends in VehicularAd hoc Networks. The Computer Jour-nal (2013) 56(8): 938-946.
5. Toutouh J, Nesmachnow S, Alba E: Fast energy-aware OLSR routing in VANETs by means of a parallel evolutionary algorithm. Cluster Comput (2013) 16(3):435–450
6. Al-Rabayah M, Malaney R: A new Scalable Hybrid Routing Protocol for VANETs. Vehicular Technology, IEEE Transactions on(2012) 61(6): 2625 - 2635
7. Banda L, Mzyece M, Noel G: IP Mobility Support: Solutions for Vehicular Networks. Vehicular Technology Magazine, IEEE (2012) 7(4): 77 – 87
8. Zrar Ghafoor K, Aziz Mohammed M, Lloret J, Abu Bakar K, M. Zainuddin Z: Routing Protocols in Vehicular Ad hoc Networks: Survey and Research Challenges. Network Protocols and Algorithms (2013) 5(4): 39 – 83
9. Climent, S., Sánchez, A., Blanc, S., Capella, J.V., Ors, R. Wireless sensor networks with energy harvesting: Modeling and simulation based on a practical architecture using real radiation levels. Concurrency and Computation: Practice and Experience. Vol. 26, 2013.
10. Capella, J.V, Campelo, J.C., Bonastre, A., Ors. R. Improving reliability in wireless sensor networks: towards intelligent monitoring platforms. Workshop on Innovation on Information and Communication Technologies, Valencia, 2014, pp. 173-178.
11. Zrar Ghafoor K, Aziz Mohammed M, Lloret J, Abu Bakar K, M. Zainuddin Z: Adaptive Reactive Routing for VANET in City Environments. Pervasive Systems, Algorithms, and Networks (ISPAN), 2009 10th International Symposium on (2009) : 610 – 614
12. Zeinab Rezaeifar, Faramarz Hendessi, Behrouz Shahgholi Ghahfarokhi, T. Aaron Gulliver: A Reliable Geocast Routing Protocol for Vehicular Ad Hoc Networks. Wireless Pers Commun (2015) 83(1): 281 – 295
13. David Chunhu Li, Li-Der Chou, Li-Ming Tseng, Yi-Ming Chen, and Kai-Wei Kuo: A Bipolar Traffic Density Awareness Routing Protocol for Vehicular Ad Hoc Networks. Mo-bile Information Systems, vol. 2015, Article ID 401518, 12 pages
14. Li-Der Chou, Jyun-Yan Yang, Ying-Cheng Hsieh, Chi-Feng Tung: Intersection-Based Routing Protocol for VANETs. Ubiquitous and Future Networks (ICUFN), 2010 Second International Conference on(2010) pages 268 - 272
15. Zrar Ghafoor K, Kamalrulnizam Abu Bakar, Shaharuddin Salleh, Kevin C. Lee, Mohd Murtadha Mohamad, Maznah Kamat, Marina Md Arshad: Fuzzy logic-assisted geographical routing over vehicular ad hoc networks. International Journal Computing, Information and Control (2012) 8(7): 5095 – 5120.

## Appendix: Springer-Author Discount

The appendix should appear directly after the references, and not on a new page

*All authors or editors of Springer books*, in particular authors contributing to any LNCS or LNAI proceedings volume, are entitled to buy any book published by Springer-Verlag for personal use at the "Springer-author" discount of one third off the list price. Such preferential orders can only be processed through Springer directly (and not through bookstores); reference to a Springer publication has to be given with such orders. Any Springer office may be contacted, particularly those in Heidelberg and New York:

Springer Auslieferungsgesellschaft
Haberstrasse 7
69126 Heidelberg
Germany
Fax: +49 6221 345-229
Phone: +49 6221 345-0

Springer-Verlag New York Inc.
P.O. Box 2485
Secaucus, NJ 07096-2485
USA
Fax: +1 201 348 4505
Phone: +1-800-SPRINGER
(+1 800 777 4643), toll-free in USA

Preferential orders can also be placed by sending an email to
orders@springer.de or orders@springer-ny.com.
For information about shipping, please contact one of the above mentioned orders departments. Sales tax is required for residents of: CA, IL, MA, MO, NJ, NY, PA, TX, VA, and VT. Canadian residents please add 7% GST. Payment for the book(s) plus shipping charges can be made by giving a credit card number together with the expiration date (American Express, Eurocard/Mastercard, Discover, and Visa are accepted) or by enclosing a check (mail orders only).

# Patient empowerment through wearable and mobile technologies

Alvaro Martinez-Romero[1,3], Manuel Traver[1,3], Antonio Martínez-Millana[2,3], Carlos Fernández-Llatas[1,3], and Vicente Traver [1,3]

[1] SABIEN-ITACA Institute Universitat Politècnica de València, València 46021 Spain
{almarro, mtraver, cfllatas, vtraver } @itaca.upv.es
[2] Tecnologias para la Salud y el Bienestar S.A. Ronda Auguste y Louis Lumiere 23, Paterna, Valencia 46980, Spain
{amartinez}@tsbtecnologias.es
[3] Unidad Mixta de Reingeniería de Procesos Sociosanitarios (eRPSS), Instituto de Investigación Sanitaria del Hospital Universitario y Politécnico La Fe, Bulevar Sur S/N, Valencia 46026, Spain

**Abstract.** Wearable and mobile technologies are playing a major role in our daily life. This position paper aims at setting the scene about the crucial role of such technologies for the patient empowerment, identifying some lessons learnt and raising some questions worth to be addressed. Patient empowerment will happen through these technologies but that is not enough and other factors from different fields need to be considered in order to guarantee patient acceptance, use, and impact from the health and social perspective. Therefore, some future trends are identified where researchers in this field need to devote new resources and focus their efforts.

## 1 Introduction

There is a global consensus about the fact that current health systems are not any longer sustainable in Western or Eastern countries, just being able to break the bank as Dr. Margarite Chan, WHO General Director stated [1]. There is a need to change the system as a whole, involving all the health cocreators stakeholders and not only the traditional health regulated market stakeholders [2]. This task is not easy because even agreement about simple issues, as the definition of what does Active and Healthy Ageing mean is not easy; everybody agrees about the importance of Active and Healthy Ageing but there are more than 25 different definitions about the same topic even though some advances are happening towards a common understanding of some hot topics [3].

Currently, around the central concept of patient empowerment, different concepts, ideas and products are emerging but always with the same objective, moving from a regulated health service provider centered approach towards an open citizen centered approach. This change is powered by what Dr. Eric Topol has labeled as “medicine's



C.Fernandez-Llatas and M.Guillen (Ed.):
Workshop on Innovation on
Information and Communication Technologies
(ITACA-WIICT 2015)

ISBN 978-84-608-4139-5

Gutenberg moment". Much as the printing press irruption took learning out of the hands of a reduced breed, wearable and mobile technologies are doing the same for health, giving patients the chance to have an unprecedented control over their healthcare. With these technologies in our hand, we are no longer reduced to a paternalistic system in which "doctor knows best" [4].

Beside this, being aware of important related concepts (sometimes, even cooler than the patient empowerment term), as crowdsourcing [5], open data [6], or behavior change [7][8], it is key to distinguish between the final goal and the tools, to keep the focus on the important issue, the patient empowerment as tools are in a perpetual beta and the current wearable and mobile gadgets will be obsolete in a short period of time.

To deal with this challenge and bring some ideas and evidences for discussion to the arena, this position paper is structured as follows. Section II will introduce the concept of patient empowerment, which roles an empowered patient can play, the benefits and the main features of a successful empowerment intervention. Wearable and mobile technologies will be introduced in Section III, presenting different classifications and concepts as nowadays, that covers a broader spectrum than even the most advanced smartphone. Section IV will introduce a key driver for patient empowerment when talking about wearable and mobile technologies: the apps whereas Section V will show the current use of technologies to foster the patient empowerment though a set of not systematic but specific use cases, extracting a set of lessons learnt. To end up, in Section VI; Discussion and Conclusions, some not yet answered questions will be drawn to stimulate the debate and raise the future trends where researchers in this field need to focus their efforts. The preparation of manuscripts which are to be reproduced by photo-offset requires special care. Papers submitted in a technically unsuitable form will be returned for retyping, or canceled if the volume cannot otherwise be finished on time.

## 2 Patient empowerment

No definition of patient empowerment has been widely accepted. Having analyzed different sources [9][10], it seems quite acceptable the one developed by the EMPATHiE consortium [11]: "An empowered patient was defined as having control over the management of their condition in daily life, with the capacity to participate in decisions related to their condition to the extent that they wish to do so; to become "co-managers" of their condition in partnership with health professionals; and to develop the self-confidence, self-esteem and coping skills to manage the impacts of their illness on everyday living"

An empowered patient is able to play more than one role, as it was stated by Traver during a conference about personalized health [12]. Content provider, broker for the exchange of good practices, advisor to peers, contents curator, promoter of healthy lifestyles, manager of the personal health folder, and creator of patient communities are some of such roles.

Benefits of patient empowerment have been properly and continuously described in the literature and even though evidence has shown that activated patients have signifi-

cantly better health, and lower rates of doctor office visits, emergency room visits, and hospital admissions [13] [14] there are also studies from the other side, stating that informed or empowered patient demand more health services or are not healthier than the rest [15].
Based on our own work [12] [16] [17] and existing reviews in the field [10] [11][18] [19], authors raise that key features of a successful empowerment intervention are:
• self quantifying; it is important the patient involvement in the process. To evaluate an intervention impact, quantified measurements are the most proper tool.
• feedback; as this is a bidirectional communication, not the traditional and paternalistic single direction communication between doctor and patient.
• ease of use; not additional technological or medical knowledge needs to be required and when possible, it should happen in an unobtrusive way with a reduced or null learning curve.
• availability; citizen needs to have the freedom to get or provide data from everywhere at any time from any device.
Being aware about these facts since long time ago, it is now when thanks to the use of wearable and mobile technologies, these previously mentioned features are almost guaranteed and the patient empowerment process is becoming a reality.

## 3 Wearable and mobile technologies

Not so long ago, wearable and mobile technologies were synonymous of a small sensor in a garment and a mobile phone respectively [20]. Nowadays, such concepts are more complex and new devices are included under these categories as glasses, smartphones, smart watches, wrist bands, shoes, and caps and the frontier between wearable and mobile technologies is more diffuse and even some authors consider wearable just as the most modern evolution of mobile technologies [21]. Nevertheless, independently from the wide range of devices available, it seems clear that the smartphone has assumed the role of hub/brain of each personal ecosystem.

Wearable and mobile devices for patient empowerment can be classified according different perspectives [20]. According to role (They can be used for sensing, storing, data exchange, processing, and/or displaying), to device (They can be inside or outside the smartphone), to clustering (All available functionalities are in a unique device, as Swiss army knife or each specific feature is in a different device, acting the smartphone as hub) or to diseases (As the device can be useful for one or for a set of specific diseases)

## 4 Apps

Apps have revolutionized the way users take care of their own health, even considering barriers as privacy concerns, regulatory control and certification [22]. Nowadays, half of smartphone owners use their devices to get health information whereas one-fifth of smartphone users have health apps on their devices [23].

Typical features of health apps related to patient empowerment are: self-monitoring, integration of social media functions, education, disease-related alarms and reminders, disease-related data export and communication, and synchronization with Personal Health Record (PHR) systems or patient portals.

Are apps medical devices? If they are just bringing personalized information to the patient or just calculating Body Mass Index (BMI) based on patient data, this is not needed to be considered medical device. However, a dosage calculator that recommends a dose based on individual patient information should be considered as medical device according to the EU Medical Device Directive MDD 93/42/EEC.

According to reports [23] [24], there are more than 40.000 apps related to health and wellbeing in the iTunes and Play Google market. Therefore, finding the proper trustworthy app among the apps jungle is not an easy task and quality stamps, specific rankings [25], and crowdsourcing (through peers, patients associations and medical staff) help considerably the patient empowerment processes.

## 5 Some lessons learnt about the use of wearables and mobile technologies for patient empowerments

Next, we present a not exhaustive list of patient empowerment examples from where authors extract a set of lessons learnt and challenges for future work:

- Active and performance fitness managers: MyFitnesPal or Fitbit [26] are good examples of an ecosystem that integrates multiple devices (smartphone, tablet or PC) and sensors (weight, activity, sleep) with an Application Program Interface (API) for third party developers. Patient empowerment works through self quantifying a non-obtrusive way, making use of gamification techniques, including feedback and a social dimension.
- Physical activity managers: Endomondo, Runtastic and Strava are the top apps for physical activity management using only the smartphone [27]. Up to now, most of them do not offer API for third party developers but they connect with similar applications for data exchange. Gamification techniques are applied, providing feedback and social challenges for different physical activities as jogging, cycling, basket, football, or dancing.
- Garment for rehabilitation: These systems, as Nuubo [28], include an smartphone plus a set of wearable sensors [29], [30]. Through self quantifying and a proper feedback, patients feel more secure and know more about his diseases, taking a major control of their own health.
- Smart watches: Being a cool concept, it moved fast towards the market [31] without clear evidence that it would improve our health. Used to be part of a bigger ecosystem with additional sensors, some companies have decided to appoint the watch as the hub device where others still consider the smart watch an add-on for the smartphone [32]. Self quantifying happens through sensors for disease management and/or prevention, offering in most of the cases an API for third party developers to extend functionalities and create communities.

- Smart glasses: One of the first suggested uses for Google Glasses was the ehealth field as doctors are early adopters of such technologies[33] but nowadays, they seem quite far from a massive use in any sector. Being quite obtrusive, smartphone dependant and far from the typical patient empowerment apps characteristics, they can be adopted for some specific niche markets.
- Educational content providers: Being trustworthy and personalized information a need for the empowered patient, the use of mobile technologies guarantees the access to valuable information from everywhere, promoting the health literacy skills [34], [35]. Medline Plus [36] is a good proof of that, offering such information adapted to different mobile user interfaces.

TABLE I. FEATURES FOR A SUCCESSFUL PATIENT EMPOWERMENT INTERVENTION THROUGH USE OF WEARABLE AND MOBILE TECHNOLOGIES

| **Case** | ***Self quantifying*** | ***App*** | ***Personalized feedback*** | ***Social media*** | ***Ease of use and availability*** | ***API for 3rd parties*** |
|---|---|---|---|---|---|---|
| Active and performance fitness managers | X | X | X | X | X | X |
| Physical activity managers | X | X | X | X | X | |
| Garment for rehabilitation | X | X | X | | | X |
| Smartwatches | X | X | X | X | X | |
| Smartglasses | | X | | | | X |
| Content providers | | X | X | X | X | X |

Table 1 shows the main features that guarantee a successful patient empowerment intervention making use of wearable and mobile technologies for the different analyzed use cases. Therefore, it is easy to observe that few more X have a use case is closer to the market, showing the right path to other not still mature technologies as the Google Glasses or some wearables to the mass market.

There are other lessons learnt extracted from the performed analysis, that are aligned with conclusions extracted from other patient empowerment reviews [37]. There are lot of easy to use apps and devices addressed for patient empowerment; most of them provide self quantifying, feedback, sharing capabilities with your social network. However, there is very little educational content in most of the cases and especially for the apps that offer diseases management, there are very few options for the patient to establish contact with peers suffering the same diseases.

## 6. Discussion and conclusions

From a holistic approach, this position paper aims at drawing the fast moving picture about the crucial role of wearable and mobile technologies for patient empowerment, identifying some lessons learnt and raising some questions worth to be addressed

Therefore, for existing and future wearable and mobile technologies, there are some facts that can make the difference towards success and massive use when dealing about patient empowerment: the chance to self quantify to be aware about his health status, the easiness of use and availability, the existence of an API for external partners, the provision of personalized feedback, the opportunity to share and interact through your social media are key success factors.

But that is not all. There are more pending issues to be addressed from a holistic perspective that need to be solved by large and multidisciplinary teams. Authors raise some questions about these possible future challenges in order stimulate the debate concerning where researchers in this field need to focus further efforts.

- There is a need to improve the access to educational material making use of mobile technologies and enhancing the social dimension, as nowadays they can share information in a very easy way, as tweeting but it is not so easy to establish contact with peers through apps, wearable and mobile technologies. Are the MOOCs a possible solution for this? Do we envisage new solutions? Do we need a course curator that provides personalized hints from our smartphone?
- Patients want to share this information with their doctor. Additionally, new stakeholders (e.g. gyms, supermarkets, and restaurants) in the patient empowerment ecosystem need to get access to such data and provide new services. Again, use of wearable and mobile technologies is needed to deal with but new rules of the game have to be defined [2]. Who will take over the definition of such new rules?
- How wearable and mobile technologies can help to the citizens still reluctant to be empowered? Is it still a technological issue? Behavior change and gamification theories need to have a greater consideration of which they have achieved so far.
- Even personalized feedback is happening, that is usually done with the dataset collected by the service provider. How can this personalization be improved? Could the citizen collect all his diffused information around Internet (health care providers, Google, Amazon information) creating a better accurate profile stored in the smartphone? And by the way, how do we will convince citizens to be aware about the importance of personal data and keep them safe?
- And around ease of use and availability, is the battery life of our wearable and mobile devices no longer a problem?

## References


[1] Margaret Chan, "Noncommunicable diseases damage health, including economic health. presented at the 2011 United Nations General Assembly". April 2015; Available: http://www.who.int/dg/speeches/2011/medicines_access_20110218/en/

[2] A. Honka, K. Kaipainen, H. Hietala, and N. Saranummi, "Rethinking Health: ICT-Enabled Services to Empower People to Manage Their Health", *IEEE Rev. Biomed. Eng.*, vol. 4, pp. 119-139, 2011.

[3] J. Bousquet, D. Kuh, M. Bewick, T. Strandberg, et al, "Operative definition of active and healthy ageing (AHA): Meeting report. Montpellier October 20–21, 2014", *Eur. Geriatr. Med.*, vol. 6, n.º 2, pp. 196-200, abr. 2015.

[4] E. J. Topol, *The patient will see you now: the future of medicine is in your hands*. New York: Basic Books, 2015.
[5] M. Swan, "Health 2050: The Realization of Personalized Medicine through Crowdsourcing, the Quantified Self, and the Participatory Biocitizen", *J. Pers. Med.*, vol. 2, n.º 4, pp. 93-118, sep. 2012.
[6] R. Sandoval-Almazan, J. R. Gil-Garcia, L. F. Luna-Reyes, D. E. Luna, and Y. Rojas-Romero, "Open government 2.0: citizen empowerment through open data, web and mobile apps", 2012, p. 30.
[7] S. M. Noar, C. N. Benac, and M. S. Harris, "Does tailoring matter? Meta-analytic review of tailored print health behavior change interventions.", *Psychol. Bull.*, vol. 133, n.º 4, pp. 673-693, 2007.
[8] R. Schwarzer, "Modeling Health Behavior Change: How to Predict and Modify the Adoption and Maintenance of Health Behaviors", *Appl. Psychol.*, vol. 57, n.º 1, pp. 1-29, ene. 2008.
[9] M. McAllister, G. Dunn, K. Payne, L. Davies, and C. Todd, "Patient empowerment: The need to consider it as a measurable patient-reported outcome for chronic conditions", *BMC Health Serv. Res.*, vol. 12, n.º 1, p. 157, 2012.
[10] C. Luttrell, S. Quiroz, and E. Overseas Development Institute (London, *Understanding and operationalising empowerment*. London: Overseas Development Institute, 2009.
[11] EMPATHIE consortium "EMPATHiE Empowering patients in the management of chronic diseases".
[12] V. Traver, L. Fernandez-Luque, F. J. Grajales III, and R. Karlsen, "The paradigm shift: the roles of patient 2.0 in today's healthcare systems", en *6th edition of the International Workshop on Wearable Micro and Nano Technologies for Personalised Health - pHealth 2009 Proceedings*, Oslo, 2009, p. 53.
[13] S. E. Mitchell, P. M. Gardiner, E. Sadikova, J. M. Martin, B. W. Jack, J. H. Hibbard, and M. K. Paasche-Orlow, "Patient Activation and 30-Day Post-Discharge Hospital Utilization", *J. Gen. Intern. Med.*, vol. 29, n.º 2, pp. 349-355, feb. 2014.
[14] A. Tzeng, T. H. Tzeng, S. Vasdev, A. Grindy, J. K. Saleh, and K. J. Saleh, "The Role of Patient Activation in Achieving Better Outcomes and Cost-Effectiveness in Patient Care", *JBJS Rev.*, vol. 3, n.º 1, pp. e4-e4, ene. 2015.
[15] The Look AHEAD Research Group, "Cardiovascular Effects of Intensive Lifestyle Intervention in Type 2 Diabetes", *N. Engl. J. Med.*, vol. 369, n.º 2, pp. 145-154, jul. 2013.
[16] V. Traver and R. Faubel, "Personal Health: The New Paradigm to Make Sustainable the Health Care System", Springer, 2011.
[17] V. Traver and L. Fernández-Luque, *El ePaciente y las redes sociales* Valencia: Publidisa, 2011.
[18] The Lancet, "Patient empowerment—who empowers whom?", *The Lancet*, vol. 379, n.º 9827, p. 1677, may 2012.
[19] W. Kuijpers, W. G. Groen, N. K. Aaronson, and W. H. van Harten, "A Systematic Review of Web-Based Interventions for Patient Empowerment and Physical Activity in Chronic Diseases: Relevance for Cancer Survivors", *J. Med. Internet Res.*, vol. 15, n.º 2, p. e37, feb. 2013.
[20] H. F. Rashvand, V. Traver Salcedo, E. Montón Sánchez, and D. Iliescu, "Ubiquitous wireless telemedicine", *IET Commun.*, vol. 2, n.º 2, p. 237, 2008.
[21] Sungmee Park and S. Jayaraman, "Enhancing the quality of life through wearable technology", *IEEE Eng. Med. Biol. Mag.*, vol. 22, n.º 3, pp. 41-48, may 2003.
[22] M. N. Kamel Boulos, A. C. Brewer, C. Karimkhani, D. B. Buller, and R. P. Dellavalle, "Mobile medical and health apps: state of the art, concerns, regulatory control and certification", *Online J. Public Health Inform.*, vol. 5, n.º 3, feb. 2014.
[23] S. Fox and M. Duggan, *Mobile Health 2012*. Washington DC: Pew Research Center's Internet & American Life Project 2012.
[24] IMS Institute for Healthcare Informatics, *Patient Apps for Improved Healthcare: From noveltry to mainstream*. 2013.
[25] M. I. Grau, "Exploring the Quality of Health Apps: The ISYS Ranking System", en *Medicine 2.0 Conference*, 2014.
[26] "Fitbit". April 2015; Available: https://www.fitbit.com/.
[27] F. Mulas, P. Pilloni, M. Manca, L. Boratto, and S. Carta, "Linking Human-Computer Interaction with the Social Web: A web application to improve motivation in the exercising activity of users", 2013, pp. 351-356.
[28] "nECG Platform | Nuubo". April 2015; Available: https://www.nuubo.com/index.php?q=es/node/163.
[29] J. P. Lázaro, S. Guillén, T. Meneu, and A. Martínez, "HeartWays Solution for Exercise Based Cardiac Rehabilitation", en *The International Conference on Health Informatics*, vol. 42, Y.-T. Zhang, Ed. Cham: Springer International Publishing, 2014, pp. 343-346.

[30] S. Patel, H. Park, P. Bonato, L. Chan, and M. Rodgers, “A review of wearable sensors and systems with application in rehabilitation”, *J. NeuroEngineering Rehabil.*, vol. 9, n.º 1, p. 21, 2012.
[31] M. Swan, “Sensor Mania! The Internet of Things, Wearable Computing, Objective Metrics, and the Quantified Self 2.0”, *J. Sens. Actuator Netw.*, vol. 1, n.º 3, pp. 217-253, nov. 2012.
[32] Ki Eun Seong, Kyung Chun Lee, and S. J. Kang, “Self M2M based wearable watch platform for collecting personal activity in real-time”, 2014, pp. 286-290.
[33] W. Glauser, “Doctors among early adopters of Google Glass”, *Can. Med. Assoc. J.*, vol. 185, n.º 16, pp. 1385-1385, nov. 2013.
[34] F. Lupiáñez-Villanueva, “Health and the Internet: Beyond the Quality of Information”, *Rev. Esp. Cardiol. Engl. Ed.*, vol. 64, n.º 10, pp. 849-850, oct. 2011.
[35] R. Cullen, “Empowering patients through health information literacy training”, *Libr. Rev.*, vol. 54, n.º 4, pp. 231-244, may 2005.
[36] “MedlinePlus - Health Information from the National Library of Medicine”. April 2015; Available: www.nlm.nih.gov/medlineplus/.
[37] T. Chomutare, L. Fernandez-Luque, E. Årsand, and G. Hartvigsen, “Features of Mobile Diabetes Applications: Review of the Literature and Analysis of Current Applications Compared Against Evidence-Based Guidelines”, *J. Med. Internet Res.*, vol. 13, n.º 3, p. e65, sep. 2011.

# Protection of Processor Registers by using Very Fast Single Error Correction Codes

Joaquín Gracia-Morán, Luis-J. Saiz-Adalid, Pedro-J. Gil-Vicente,
Daniel Gil-Tomás, and J.-Carlos Baraza

Instituto ITACA, Universitat Politècnica de Valencia,
Camino de Vera s/n, 46022 Valencia, Spain
{jgracia, ljsaiz, pgil, dgil, jcbaraza}@itaca.upv.es

**Area of Interest**: Fault Tolerant Systems

**Abstract.** Error correction codes (ECCs) are a common fault-tolerant technique used to protect information in computer systems. Due to continuous technology scaling, soft errors on registers have become a major concern. ECCs are one of the most typical mechanism used to protect them. However, using an ECC increases delay, area and power consumption, so ECCs design focuses on minimizing the number of redundant bits added. This is important in memories, as these bits are added to each word in the whole memory, but not so significant in registers, whose size is much smaller. In this case, minimizing the encoding and decoding delay may be more interesting. This paper summarizes a method to develop codes with 1-gate delay encoders and 4-gate delay decoders, independently of the word length.

## 1 Introduction

Information can be altered when it is transmitted via noisy channels, so some protection against this undesired effect must be included. Due to different physical mechanisms that may alter the information stored or transmitted, storage elements, such as registers and memories, as well as interconnection lines, can be considered as noisy channels [1], [2].

Error correction codes (ECCs) have been traditionally employed to protect information against errors in computer systems. In fault-tolerant computer systems, many types of ECCs have been applied to memory subsystems and processors, in order to achieve efficient and reliable data processing and storage [3], [4].

However, when using an ECC, the circuit's delay, area and power consumption are increased. As data have to be encoded when stored/sent and decoded when loaded/received, the delay increases. Area and power overhead is caused by the redundant bits added by the ECC, as well as the encoding and decoding circuits. So, efficient designing of ECCs is needed to decrease the included overhead.

Traditionally, the main concern was to reduce the redundancy, i.e. to minimize the number of bits added by the code [5], [6]. For example, when ECCs are applied to



C.Fernandez-Llatas and M.Guillen (Ed.):
Workshop on Innovation on
Information and Communication Technologies
(ITACA-WIICT 2015)

ISBN 978-84-608-4139-5

memories, these redundant bits are added to each word stored in the memory, so a bigger memory implies a bigger redundancy.

Nevertheless, in some system areas, minimizing the delay introduced by the ECC can be more important than reducing the spatial overhead. For example, register files are one of the most frequently accessed parts of the microprocessor, although the overall area of this element is small. When protecting microprocessor registers using an ECC, encoding and decoding operations should be as fast as possible. An excessive delay introduced by these operations might increase the duration of the clock cycle and hence decrement the microprocessor working frequency.

Most of faults that affect the architectural state of a processor come from the register file [7]. Corrupted data in the register file can spread quickly to other parts of the system. Due to technology scaling, registers are operated at low supply voltage levels. Thus, they are vulnerable to external disturbances that can induce transient faults and soft errors [8]. Aircraft and space electronics intensify this problem because high-energy neutrons at higher altitudes, as well as heavy ions in space, are more abundant. In this way, register files have to be protected to tolerate soft errors as its fault rate will increase exponentially.

Single error correction (SEC) codes are frequently included in memory designs to enhance their reliability. For example, Hamming codes [5] allow single error correction with low redundancy and simple and fast encoding and decoding operations. Nevertheless, a reduction in the delays introduced by the encoding and decoding circuits is needed due to the working frequency increase of VLSI systems. For instance, ECCs proposed in [9] achieve lower delay than Hamming codes, at the cost of a higher redundancy. On the other hand, these codes do not correct errors in the redundant bits, thus reducing the decoding latency.

The work presented in this paper introduces a new method to build SEC codes with still lower delays than previous approaches. Only data bits are corrected, like the codes presented in [9], but the encoder has only 1-gate delay, and the decoder has 4-gate delay. Also, the delays are independent of the data word length, whereas in the former codes the delays depend on the word size. As far as we know, there is no known code with similar features. Existing codes present either longer delays or the delay scales with the data word length.

The main problem of the codes proposed in this work is their very high redundancy. Nevertheless, some system components, such as the register file, would require fast encoders and decoders, while the redundancy would be a minor issue, as the area used by the registers is small. Also, the error correction in parity bits of registers has little interest, because the registers' contents are usually updated frequently, and the input data come from other circuit elements [9].

This paper is organized as follows. Section II introduces the temporal faults and soft errors in storage elements, while Section III presents the basics of single error correction codes. The methodology to build the proposed codes is described in Section IV. Finally, Section V presents some conclusions and ideas for future work.

## 2 Temporal Faults and Soft Errors in Storage Elements

Temporal faults manifest as soft errors, and they can be transient or intermittent [3]. Transient faults are characterized by their short duration and they do not introduce physical defects in the circuitry. On the other hand, intermittent faults appear repetitively and non-deterministically in the same place due to a combination of defective hardware and environmental conditions.

Traditionally, the main causes of transient faults were α and cosmic radiation [2], [10]. Nowadays, and due to the high working frequencies, some other causes provoke transient faults. For instance, the skin effect [11] or the Miller effect [12] can provoke temporal violations that can modify the delay of the logic circuit. In addition, electromagnetic interferences can produce crosstalk.

Fig. 1 shows the causes and mechanisms that provoke the apparition of transient faults. In this figure, those that provoke the apparition of transient faults in storage elements are highlighted.

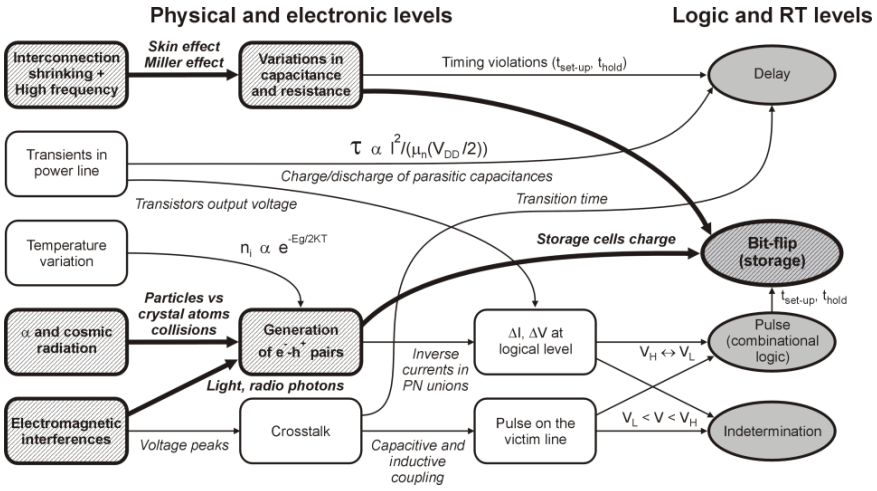


**Fig. 1.** Transient fault mechanisms and their equivalent fault models [10].

On the other hand, the complexity of the manufacturing process (which produces residues and process variations), together with special aging mechanisms, may increase the presence of intermittent faults [13]. These faults appear in a defective hardware, which is not permanently damaged. Also, intermittent faults can be activated or deactivated under certain environmental conditions (e.g. changes in temperature, voltage or frequency).

Some of the physical mechanisms that lead to intermittent faults in storage elements are presented in Table I. A more detailed explanation can be found in [14].

**Table 1.** Some intermittent faults mechanisms and models in storage elements [14].

| Causes | Targets | Fault mechanisms | Type of fault | Fault models |
|---|---|---|---|---|
| Residues in cells | Memory and registers | Intermittent contacts | Manufacturing defect | *Intermittent stuck-at* |
| Gate oxide soft breakdown | NMOS transistors in SRAM cells | Leakage current fluctuation | Wearout-Timing | *Intermittent delay*<br>*Intermittent Indetermination* |
| Negative bias-temperature instability (NBTI) | PMOS transistors in SRAM cells | Local mismatches among cell transistors, decrease of static noise margin | Wearout | *Intermittent bit-flip* |
| Doping profile and gate length deviations | MOS transistors in combinational logic and memory | Deviations in $V_{TH}$<br>Deviations in operation speed | Manufacturing variations | *Intermittent delay* |

## 3 Correcting Single Errors: Hamming Codes

Hamming codes [5] are able to correct single errors with the lowest redundancy. These codes take $k$ data bits and produce an $n$-bit block, being the $n–k$ bits added the parity bits. Hamming codes can be described by its parity check matrix **H**. For example, the matrix for the Hamming (7, 4), i.e. $n = 7$ and $k = 4$ is shown in Equation (1). This matrix describes the encoding and decoding operations.

$$\mathbf{H} = \begin{bmatrix} 1010101 \\ 0110011 \\ 0001111 \end{bmatrix} \quad (1)$$

Let $\mathbf{u} = (u_0, u_1, \ldots, u_{k-1})$ be the original data word, and $\mathbf{b} = (b_0, b_1, \ldots, b_{n-1})$ the encoded word. Using the parity check matrix (1), the encoding formulas are obtained:

| $b_0$ | $b_1$ | $b_2$ | $b_3$ | $b_4$ | $b_5$ | $b_6$ | ***Encoding formulas*** |
|---|---|---|---|---|---|---|---|
| | | $u_0$ | | $u_1$ | $u_2$ | $u_3$ | |
| 1 | 0 | 1 | 0 | 1 | 0 | 1 | $b_0 = u_0 \oplus u_1 \oplus u_3$ |
| 0 | 1 | 1 | 0 | 0 | 1 | 1 | $b_1 = u_0 \oplus u_2 \oplus u_3$ |
| 0 | 0 | 0 | 1 | 1 | 1 | 1 | $b_3 = u_1 \oplus u_2 \oplus u_3$ |

The decoding formulas are also obtained from (1). Being $\mathbf{r} = (r_0, r_1, \ldots, r_{n-1})$ the received word (i.e. the word to be decoded), the syndrome bits are calculated as:

| $r_0$ | $r_1$ | $r_2$ | $r_3$ | $r_4$ | $r_5$ | $r_6$ | ***Syndrome bits*** |
|---|---|---|---|---|---|---|---|
| | | $u_0$ | | $u_1$ | $u_2$ | $u_3$ | |
| 1 | 0 | 1 | 0 | 1 | 0 | 1 | $s_0 = r_0 \oplus r_2 \oplus r_4 \oplus r_6$ |
| 0 | 1 | 1 | 0 | 0 | 1 | 1 | $s_1 = r_1 \oplus r_2 \oplus r_5 \oplus r_6$ |
| 0 | 0 | 0 | 1 | 1 | 1 | 1 | $s_2 = r_3 \oplus r_4 \oplus r_5 \oplus r_6$ |

The syndrome bits will point the position of the erroneous bit if they are distinct to zero. Otherwise, the received word is correct. Fig. 2 shows the encoder and decoder circuits for this example. We have assumed a hardware implementation using 2 input XOR gates for the "exclusive or" operations. There exist also (12, 8), (21, 16), (38, 32) and (71, 64) SEC Hamming codes for other word sizes. It is remarkable that the logic depth of these circuits scales with the word length, provoking an increment in the latency introduced by the encoding and decoding circuits.

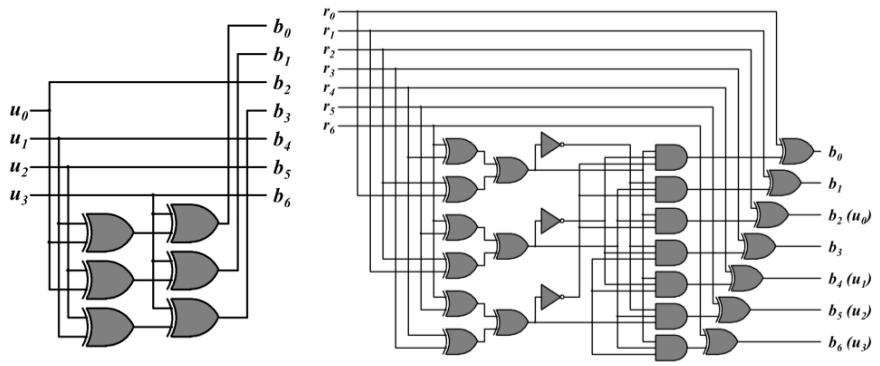


a) b)

**Fig. 2.** a) Hamming (7, 4) encoder circuit. b) Hamming (7, 4) decoder circuit.

## 4 Very Fast Single Error Correction Codes

### A. Fundamentals

The main objective of our proposal is to reduce the latency introduced in the system by the encoder and decoder circuits. This is a similar approach to [9], but including additional restrictions to obtain faster circuits.

By reducing the number of 1s (i.e. the Hamming weight $w$) in each row and in each column of the **H** matrix, the delay provoked by computing the parity bits in the encoder and the syndrome bits in the decoder is also decreased.

In order to maintain the redundancy as low as possible, it is necessary to find the smallest value of $n–k$ (the number of parity bits) for which Equation (2) is true. In a second step, an $((n–k) \times n)$ parity check matrix **H** is generated. The $n–k$ columns for parity bits form an identity matrix. The remaining $k$ columns are different, and all of them have Hamming weight $w$. Equation (2) guarantees that there are enough different combinations.

Nevertheless, the reduction of the Hamming weight in the rows implies a higher value of $n–k$, that is, the redundancy increases. The question is if it is possible to find

codes whose parity check matrices have Hamming weight 3 in all their rows. If so, this would minimize the logic operations required to calculate the parity bits during the encoding, and the syndrome bits during the decoding.

$$\binom{n-k}{w} \geq k \tag{2}$$

In this way, the requirements to construct the SEC codes presented in this paper are:

- To correct single errors, each column has to be different and nonzero.
- Each column assigned to parity bits must have Hamming weight $w = 1$ (minimum Hamming weight). This permits a code be separable (i.e. parity and data bits can be distinguished in an encoded word).
- Each column assigned to data bits must have Hamming weight $w = 2$. If only data bits correction is required, this value of $w$ simplifies the final part of the decoding.
- Each row must have Hamming weight $w = 3$. This is the key requirement for our proposal. The result is that each parity bit is obtained during the encoding by XORing only two data bits, and each syndrome bit is calculated during the first part of the decoding by XORing three bits.

Thanks to the last two requirements, simple and fast hardware-implemented decoders can be implemented. Even, the logic depth of the circuits does not scale with the word length. This feature is very interesting because increasing the word length is a common trend in modern microprocessors.

The main concern about these SEC codes is the increase of parity bits required (pointed by the last requirement). These codes need $n–k = k$ bits, that is, the number of parity bits are the same as the number of data bits. As explained before, these codes are designed to such devices where redundancy is a minor problem.

### B. Examples

When building a parity check matrix, an easy method is to separate the columns assigned to parity bits and data bits. This allows representing these codes in a systematic form. The simplest SEC code designed according to the requirements presented in Section 4.A can be seen in Equation (3). It is a (6, 3) SEC code.

$$\mathbf{H} = \begin{bmatrix} 100 & 110 \\ 010 & 101 \\ 001 & 011 \end{bmatrix} \tag{3}$$

Similarly, parity check matrices can be found for $(2k, k)$ SEC codes for any value of $k > 2$. For example, Equation (4) shows a generation matrix for the (16, 8) SEC code, and Fig. 3 illustrates its encoder circuit. As it can be observed, the delay introduced by the circuit is the latency of a 2-input XOR gate. As stated above, this delay does not depend on the word length.

$$\mathbf{H} = \begin{bmatrix} 10000000 & 11000000 \\ 01000000 & 10100000 \\ 00100000 & 01010000 \\ 00010000 & 00101000 \\ 00001000 & 00010100 \\ 00000100 & 00001010 \\ 00000010 & 00000101 \\ 00000001 & 00000011 \end{bmatrix} \quad (4)$$

The encoding formulas for this code are:

| $b_0$ | $b_1$ | $b_2$ | $b_3$ | $b_4$ | $b_5$ | $b_6$ | $b_7$ | $b_8$ | $b_9$ | $b_{10}$ | $b_{11}$ | $b_{12}$ | $b_{13}$ | $b_{14}$ | $b_{15}$ | *Encoding formulas* |
|---|---|---|---|---|---|---|---|---|---|---|---|---|---|---|---|---|
| | | | | | | | | $u_0$ | $u_1$ | $u_2$ | $u_3$ | $u_4$ | $u_5$ | $u_6$ | $u_7$ | |
| 1 | 0 | 0 | 0 | 0 | 0 | 0 | 0 | 1 | 1 | 0 | 0 | 0 | 0 | 0 | 0 | $b_0 = u_0 \oplus u_1$ |
| 0 | 1 | 0 | 0 | 0 | 0 | 0 | 0 | 1 | 0 | 1 | 0 | 0 | 0 | 0 | 0 | $b_1 = u_0 \oplus u_2$ |
| 0 | 0 | 1 | 0 | 0 | 0 | 0 | 0 | 0 | 1 | 0 | 1 | 0 | 0 | 0 | 0 | $b_2 = u_1 \oplus u_3$ |
| 0 | 0 | 0 | 1 | 0 | 0 | 0 | 0 | 0 | 0 | 1 | 0 | 1 | 0 | 0 | 0 | $b_3 = u_2 \oplus u_4$ |
| 0 | 0 | 0 | 0 | 1 | 0 | 0 | 0 | 0 | 0 | 0 | 1 | 0 | 1 | 0 | 0 | $b_4 = u_3 \oplus u_5$ |
| 0 | 0 | 0 | 0 | 0 | 1 | 0 | 0 | 0 | 0 | 0 | 0 | 1 | 0 | 1 | 0 | $b_5 = u_4 \oplus u_6$ |
| 0 | 0 | 0 | 0 | 0 | 0 | 1 | 0 | 0 | 0 | 0 | 0 | 0 | 1 | 0 | 1 | $b_6 = u_5 \oplus u_7$ |
| 0 | 0 | 0 | 0 | 0 | 0 | 0 | 1 | 0 | 0 | 0 | 0 | 0 | 0 | 1 | 1 | $b_7 = u_6 \oplus u_7$ |

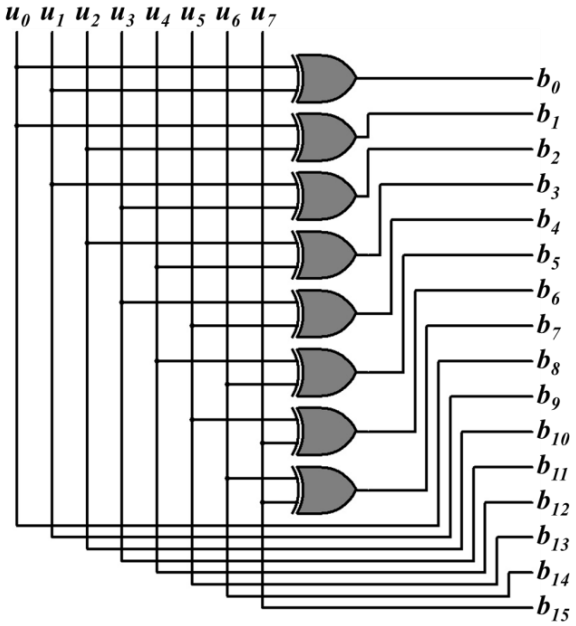


**Fig. 3.** Encoder circuit for the (16, 8) SEC code.

The formulas for syndrome calculation are:

| $r_0$ | $r_1$ | $r_2$ | $r_3$ | $r_4$ | $r_5$ | $r_6$ | $r_7$ | $r_8$ | $r_9$ | $r_{10}$ | $r_{11}$ | $r_{12}$ | $r_{13}$ | $r_{14}$ | $r_{15}$ | *Syndrome bits* |
|---|---|---|---|---|---|---|---|---|---|---|---|---|---|---|---|---|
| | | | | | | | | $u_0$ | $u_1$ | $u_2$ | $u_3$ | $u_4$ | $u_5$ | $u_6$ | $u_7$ | |
| 1 | 0 | 0 | 0 | 0 | 0 | 0 | 0 | 1 | 1 | 0 | 0 | 0 | 0 | 0 | 0 | $s_0=r_0\oplus r_8\oplus r_9$ |
| 0 | 1 | 0 | 0 | 0 | 0 | 0 | 0 | 1 | 0 | 1 | 0 | 0 | 0 | 0 | 0 | $s_1=r_1\oplus r_8\oplus r_{10}$ |
| 0 | 0 | 1 | 0 | 0 | 0 | 0 | 0 | 0 | 1 | 0 | 1 | 0 | 0 | 0 | 0 | $s_2=r_2\oplus r_9\oplus r_{11}$ |
| 0 | 0 | 0 | 1 | 0 | 0 | 0 | 0 | 0 | 0 | 1 | 0 | 1 | 0 | 0 | 0 | $s_3=r_3\oplus r_{10}\oplus r_{12}$ |
| 0 | 0 | 0 | 0 | 1 | 0 | 0 | 0 | 0 | 0 | 0 | 1 | 0 | 1 | 0 | 0 | $s_4=r_4\oplus r_{11}\oplus r_{13}$ |
| 0 | 0 | 0 | 0 | 0 | 1 | 0 | 0 | 0 | 0 | 0 | 0 | 1 | 0 | 1 | 0 | $s_5=r_5\oplus r_{12}\oplus r_{14}$ |
| 0 | 0 | 0 | 0 | 0 | 0 | 1 | 0 | 0 | 0 | 0 | 0 | 0 | 1 | 0 | 1 | $s_6=r_6\oplus r_{13}\oplus r_{15}$ |
| 0 | 0 | 0 | 0 | 0 | 0 | 0 | 1 | 0 | 0 | 0 | 0 | 0 | 0 | 1 | 1 | $s_7=r_7\oplus r_{14}\oplus r_{15}$ |

A single error in a data bit will always trigger two syndrome bits (all data columns have Hamming weight $w = 2$), simplifying the detection part of the decoder. The formulas for calculating the decoded data bits are shown in Equation (5), and Fig. 4 illustrates the decoder circuit for this code.

$$\begin{aligned} u_0 &= (s_0 \cdot s_1) \oplus r_8 \\ u_1 &= (s_0 \cdot s_2) \oplus r_9 \\ u_2 &= (s_1 \cdot s_3) \oplus r_{10} \\ u_3 &= (s_2 \cdot s_4) \oplus r_{11} \\ u_4 &= (s_3 \cdot s_5) \oplus r_{12} \\ u_5 &= (s_4 \cdot s_6) \oplus r_{13} \\ u_6 &= (s_5 \cdot s_7) \oplus r_{14} \\ u_7 &= (s_6 \cdot s_7) \oplus r_{15} \end{aligned} \tag{5}$$

It is also remarkable that the logic depth is always the same, independently of the word length.

## 5 Conclusions

We have presented a method to construct SEC codes that reduce the decoding and encoding delay by decreasing the logic depth of these circuits. Nevertheless, this reduction is accomplished by an increasing of the redundancy. In this way, only data bits errors are corrected. It is remarkable that the delays added by the encoder and decoder circuits do not depend on the data word length.

The SEC codes presented are an interesting option for designs where redundancy is not the main concern, but fast encoding and decoding is important. For example, microprocessor registers require fast encoding and decoding operations. As this component use a small silicon area, the spatial overhead introduced in this case will not be significant. On the other hand, as registers are updated frequently and the input data come from other circuit elements, correction of parity bits in registers has little interest.

In the future, we want to study with detail the correction of burst errors using interleaving. Also, a deeper analysis about codes with lower redundancy while maintaining a low delay is planned.

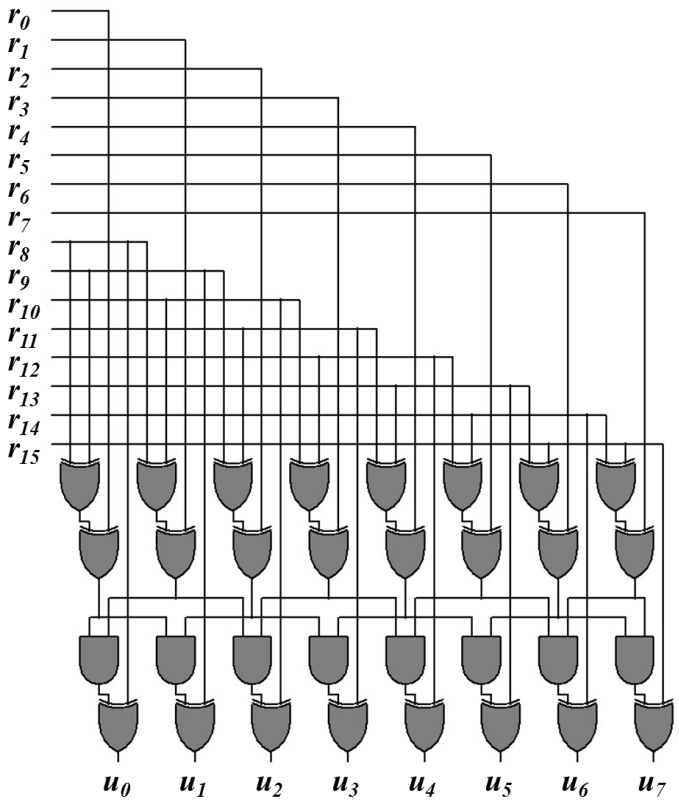


**Fig. 4.** Decoder circuit for the (16, 8) SEC code.

**Acknowledgement**. This work has been partially funded by the Universitat Politècnica de València under the Research Project DesTT (SP20120806), and the Spanish Government under the Research Project ARENES (TIN2012-38308-C02-01).

## References


1. J. Gracia, D. Gil, L. Lemus and P.J. Gil, “Studying Hardware Fault Representativeness with VHDL Models”, Procs. XVII Conference on Design of Circuits and Integrated Systems (DCIS 2002), pp. 33-38, November 2002.
2. P. Shivakumar, M. Kistler, S. Keckler, D. Burger and L. Alvisi, “Modeling the Effect of Technology Trends on Soft Error Rate of Combinational Logic”, Procs. 2002 International Conference on Dependable Systems and Networks (DSN-2002), pp. 389-402, June 2002.
3. E. Fujiwara, Code Design for Dependable Systems, John Wiley & Sons, 2006.
4. L.J. Saiz-Adalid, P.J. Gil-Vicente, J.C. Ruiz, D. Gil-Tomás, J.C. Baraza, and J. Gracia-Morán, "Flexible Unequal Error Control Codes with Selectable Error Detection and Correction Levels", in Proc. of Intl. Conf. on Computer Safety, Reliability and Security (Safecomp), pp. 178-189, September 2013.
5. R.W. Hamming, “Error detecting and error correcting codes,” Bell System Technical Journal, vol. 29, pp. 147 – 160, 1950.
6. L.J. Saiz-Adalid, P. Reviriego, P. Gil, S. Pontarelli, and J.A. Maestro, “MCU Tolerance in SRAMs Through Low-Redundancy Triple Adjacent Error Correction,” IEEE Transactions on Very Large Scale Integration (VLSI) Systems, in press. Available online at http://dx.doi.org/10.1109/TVLSI.2014.2357476.
7. J.A. Blome, S. Gupta, S. Feng, S. Mahlke and D. Bradley, “Cost-efficient soft error protection for embedded microprocessors,” in CASES ’06, pp. 421–431, 2006.
8. R. Baumann, “Soft errors in advanced computer systems”, IEEE Design and Test of Computers, 22(3):258–266, May-June 2005.
9. P. Reviriego, S. Pontarelli, J.A. Maestro, and M. Ottavi, “A Method to Construct Low Delay Single Error Correction (SEC) Codes for Protecting Data Bits Only,” IEEE Transactions on Computer-Aided Design of Integrated Circuits and Systems, Vol. 32, No 3, pp. 479-483, March 2013.
10. P. Gil et al., “Fault Representativeness”, Deliverable ETIE2 of Dependability Benchmarking Project (DBENCH), IST-2000-25245, July 2002.
11. M.G. Walker, “Modelling the Wiring of Deep Submicron ICs”, IEEE Spectrum, 27(3):65-71, March 2000.
12. D. Sylvester and K. Keutzer, “Rethinking Deep-Submicron Circuit Design”, IEEE Computer, pp. 25-33, November 1999.
13. C. Constantinescu, “Trends and challenges in VLSI circuit reliability,” IEEE Micro., vol. 23, no. 4, pp. 14–19, 2003.
14. D. Gil-Tomás, J. Gracia-Morán, J. C. Baraza-Calvo, L.J. Saiz-Adalid, and P.J. Gil-Vicente, “Studying the effects of intermittent faults on a microcontroller,” Microelectronics Reliability, vol. 52, no. 11, pp. 2837-2846, Nov. 2012.

# Development and validation of an electrophysiological characterization system for isolated perfused porcine heart model

Ramón Albert[1], Andreu M. Climent[2], Miguel Rodrigo[1] and María S. Guillem1[1]

[1] BIO-ITACA, Universitat Politécnica de Valencia, Valencia, Spain.
Phone: +34-963-877-968; e-mail: ramalmar@epsa.upv.es
[2] Cardiology Department, Hospital General Universitario Gregorio Marañón, Madrid, Spain

**Abstract.** Hypertension plays an important role in the initiation and maintenance of atrial fibrillation. In the present work a set of electronic and mechanical equipment for electrophysiological characterization of isolated perfused porcine hearts and for aortic pressure handling was developed and validated. This assembly keeps alive porcine hearts outside the body and allows the aortic pressure control through the peristaltic pump flux. An optical mapping system able to record the cardiac electrical activity was included as well as a system for physiological parameters measurement such as temperature and pH. The whole system was integrated into a single control software and was designed to be used in a wireless lab environment. The system performance was evaluated during isolated perfused porcine heart experiments and the proper operation of its components was assessed. The developed equipment represents a major advance in the automation of basic research on the relationship between hypertension and AF.

## 1 Introduction

Some studies argue that hypertension plays an important role in the onset of fibrillatory episodes [1- 5]. According to these authors, high atrial pressure levels are associated with structural changes in the atrial tissue which predispose to atrial fibrillation (AF) initiation and perpetuation. These changes include left atrial mechanical function changes, such as altered electrophysiology and increased ectopic activity, so the higher the atrial pressure the greater AF induction probability [6-7]. The analysis of the changes caused by a pressure increase in the atrial electrophysiological properties is of main importance for the full understanding of the maintaining mechanisms of AF and for developing novel therapies.

To learn more about the AF mechanisms, many efforts are directed towards animal experimentation. Some experimental techniques have been developed in order to study the atrial electrophysiology behavior under controlled situations. The most used experimental technique is the Langerdoff preparation, where an isolated animal heart can be preserved under physiological conditions by perfusion of a liquid with all the needed nutrients [8]. This technique allows controlling some physiological conditions of the heart, such as the temperature, the pH or the atrial pressure [9]. Besides, optical



C.Fernandez-Llatas and M.Guillen (Ed.):
Workshop on Innovation on
Information and Communication Technologies
(ITACA-WIICT 2015)

ISBN 978-84-608-4139-5

recordings of the atrial electrical activity can be carried out by using the optical mapping technique. This recording technique allows obtaining the atrial electrical activity from the luminescent activity of an injected photometric dye [10-12] with much higher spatial resolution than electrical recordings.

Nevertheless, these assemblies are difficult to manage due to the number of variables that can affect the reliability of the experiment. Until the present study, these experiments were performed using prototypes not adapted to the laboratory environment, with lower reliability and lower functionality, and sometimes putting safety on risk due to the high amount of wires. The lack of a commercial equipment to suit the needs of this experimental set was the aim of this work, but also the benefit of having our own system for experimentation with a lower cost and higher versatility.

In the present work a set of electronic and mechanical equipment for electrophysiological characterization of isolated porcine hearts and handling the aortic pressure is presented. The system has to accomplish the next conditions: to manage the perfusion pump flux of the isolated heart preparation for controlling the atrial pressure, to apply programmed electrical stimulation protocols, to control the LED lights for optical mapping recording and to measure the temperature and pH of the perfusion liquid. The system will be designed to be managed from a single computer program and to be used in a wireless lab environment.

## 2 Methods

Figure 1 shows a general diagram of the designed system, where the role of each function module can be observed. The system was divided into 3 function modules: the physiological variables control, the illumination control for optical mapping and the pacing system, all of them interconnected through a wireless network. A SCADA (Supervisory Control and Data Acquisition) software was programmed to intuitively control and monitor the different modules. The designed system was modular, so its function modules were able to operate without connection with the PC or the connection with other modules.

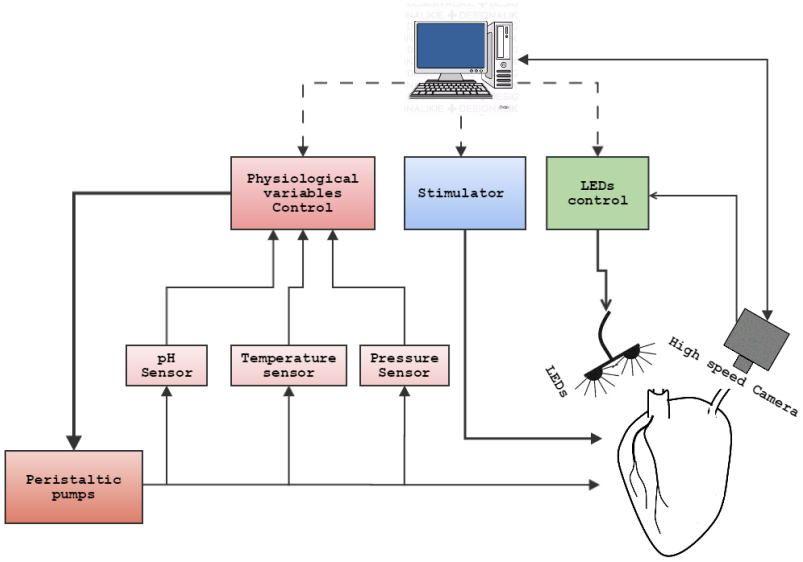


**Fig. 1.** System diagram

### 2.1 Control of physiological variables

This module controls the caudal provided by the peristaltic pumps which perfuse the isolated heart with the nutrient liquid and performs the measurement over the physiological variables: temperature, atrial pressure and pH. It consists in a microcontroller based on the Arduino architecture and the electronic instrumentation of the sensors and actuators.

By measuring the atrial pressure and controlling the pump flux, the system is able to automatically set a desired value to the atrial pressure. Moreover, the microcontroller constantly sends the physiological measurements to the PC through the wireless connection based on the ZigBee protocol to be displayed in the SCADA. In addition, this module includes an external LCD 32-characters screen which displays the measurements.

### 2.2 Stimulator system

In order study the atrial electrophysiology on the isolated porcine hearts, the atrial muscle is subjected to external electric stimuli. These electrical impulses allow to provoke controlled activation rhythms of the atrial muscle and to investigate the electrical behavior under these controlled conditions. Besides, the atrial tissue stimulation allows inducing AF episodes.

A 4-channel electro stimulator controlled by PC and connected wirelessly was implemented in order to apply programmable stimulation protocols and to facilitate the AF induction. It was managed by an Arduino microcontroller, and the wireless connection was based on the ZigBee protocol. The systems allowed operating without the SCADA supervision: in case of disconnection between the PC and the stimulation module, the stimulation module continues applying the last programmed stimulation protocol. This system was capable of establishing stimulation protocols with configurable pulse width, frequency and amplitude, with an output voltage range from 4V to 40V and a maximum output current of 1A.

### 2.3 LED control

During an optical mapping experiment the atrial muscle needs to be illuminated with an LED in order to excite the photometric dyes whose light reflection is used to measure the electrophysiological activity of the heart. In those cases in which two photometric dyes are used to simultaneously measure the membrane potential and the intracellular $Ca^{2+}$ concentration, two LED light sources are needed. However, as they share part of their light spectrum, they have to be alternatively switched in order to coincide with alternating frame captures of the camera. The synchronization of the light switching has to be very fast and reliable, since the high resolution camera works at 1000 frames per second. This system provides an element able to switch the two sets of LEDs to match their lighting with the capture of alternative frames from the high speed camera. Specifically, the module is able to support four sets of two LEDs. This device was capable of controlling the power of the LEDs for fine adjustment and calibration in every scenario, and was controlled also by the SCADA through a ZigBee wireless network.

### 2.4 Langendorff preparation with controlled pressure

After anesthesia and sedation the porcine heart was surgically extracted and immersed into cardioplegic solution. All blood vessels except the aorta and the inferior vena cava were sealed and a transeptal puncture was performed for connecting both atria. The heart was then connected to the Langendorff system for its survival through a cannula at the aorta [13-14]. Since the aorta valve remained closed, the oxygenated solution with all the nutrients (Tyrode's solution) was diverted to the coronary arteries due to the perfusion peristaltic pump flux (see Fig. 2). The nutrient solution then flowed into the right atrium through the coronary sinus after irrigating all the heart muscle, filling both atria through the transeptal puncture, and filling both ventricles too. Tyrode's solution drainage was carried out by a cannula placed in the inferior vena cava. Due to the sealing of all blood vessels, the flow rate of the perfusion and drain by using a peristaltic pump allowed to control the pressure of the nutrient liquid against the walls of the atrium.

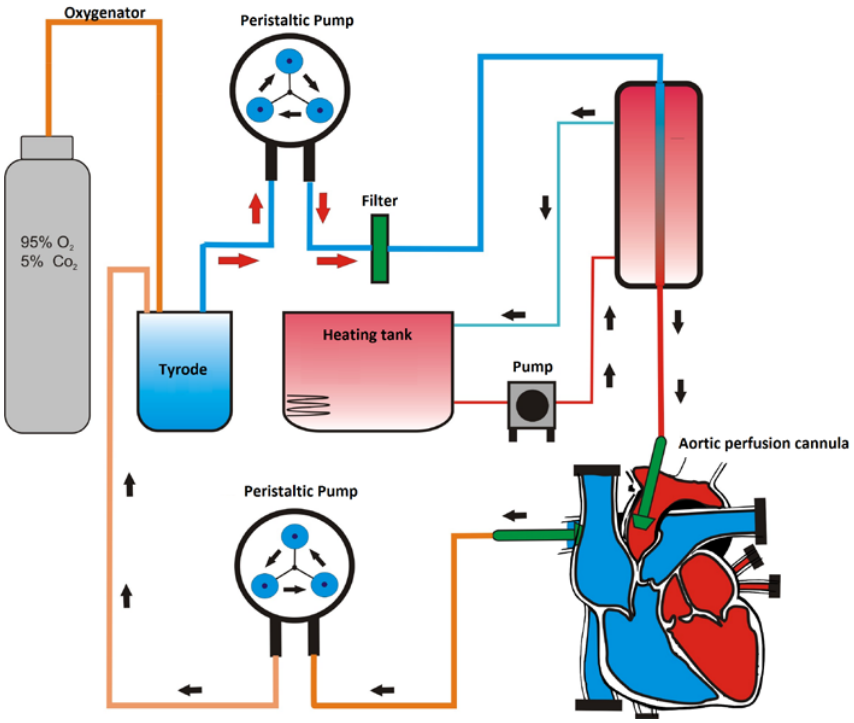


**Fig. 2.** Langendorff system with controlled pressure

Once the porcine heart remained stable, 800 mL of photometric dye Di-4 ANEPPS sensitive to transmembrane potential were introduced into the heart. Electric pacing was applied to the cardiac surface by using the stimulator system in order to generate controlled atrial rhythms. After the heart was activated with different pacing protocols, an AF episode was induced by increasing the frequency of the electrical stimulus. The electrical activity of the atrium was recorded during the entire experiment by optical mapping technique using the LED control system and the Evolve 128 high-speed camera, with a 128x128 pixels CCD sensor working at 1000 frames per second.

## 3 Results

With the purpose of validating the system performance, several measurements were carried out using the developed equipment. First, the aortic pressure was measured by using the physiologic variables module for different perfusion pump flows (see Figure 3). Flow increments were applied in the range from 150 ml to 300 ml / min using the perfusion peristaltic pump. This resulted in an increase in aortic pressure from 66mgH to 105 mmHg, showing the direct relationship between the inward perfusion flow and the intracavitary pressure.

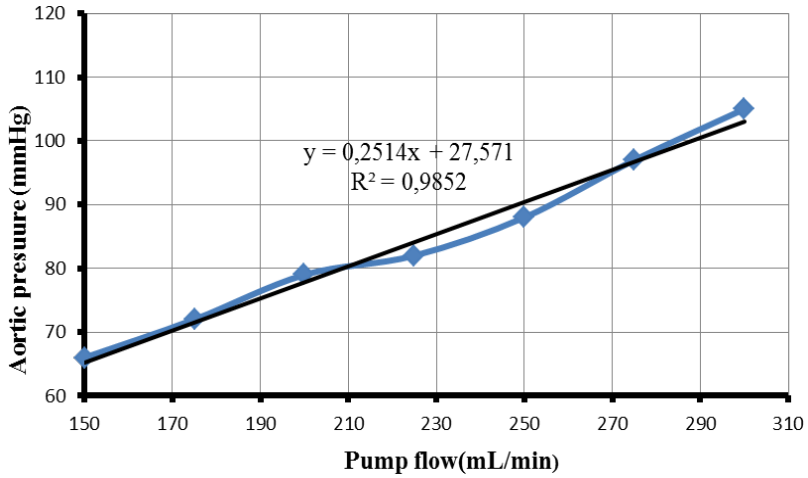


**Fig. 3.** Aortic pressure relative to pump flow

The LED light intensity for the proper optical mapping recordings was studied. The LED light was powered with voltages from 2.7 V to 3.5 V and the amplitude of the optical mapping signals was analyzed (see Figure 4). As expected, increasing the voltage levels of the LEDs provoked an increase of the signal amplitude received by the camera, and power voltages lower than 3 V did not provide signal amplitudes higher than the existing noise.

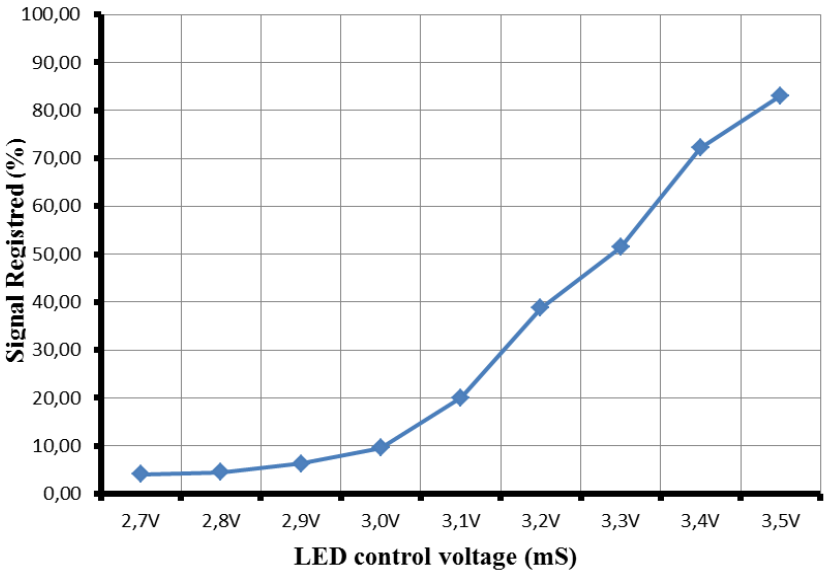


**Fig. 4.** Level of signal amplitude depending on the control voltage of LEDs

Several optical mapping videos were recorded during different stimulation protocols with increasing stimulation periods. The recorded signals were then band-pass filtered between 1 and 20 Hz and the action potential duration at 50% of its amplitude (APD50) was measured (see Figure 5). As expected, the increase of the stimulation period provoked larger APD50 values, as it has been described in the literature.

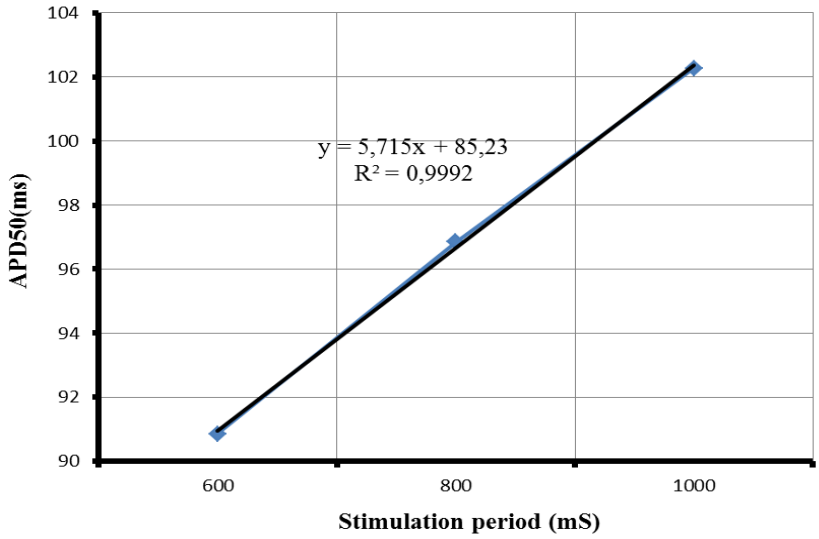


**Fig. 5.** Action potential duration at 50% of its amplitude (APD50) as a function of the stimulation period

An example of an optical mapping recording is shown in Figure 6. During this video, the stimulation catheter was placed at the left side of the field view and the stimulation period was 500 ms. At the left panel the isochronal map calculated from this video recording is depicted. The isochronal map depicts the activation time of each cardiac region (i.e. the instant when each pixel passes from resting state to its depolarization) according to a color map. The propagation pattern is clearly depicted in this map: the earliest region to be electrically activated is the left part of the heart, where the pacing catheter was placed, and the rest of the tissue is then progressively activated in a left-to-right pattern during 120ms. This pattern can be shown in the individual signals (right panel) extracted from the positions marked in the left panel. Signal from point #1 shows an earlier activation than signal #2 and #3, and signal #3 depicts the later activation around 100 ms after signal #1.

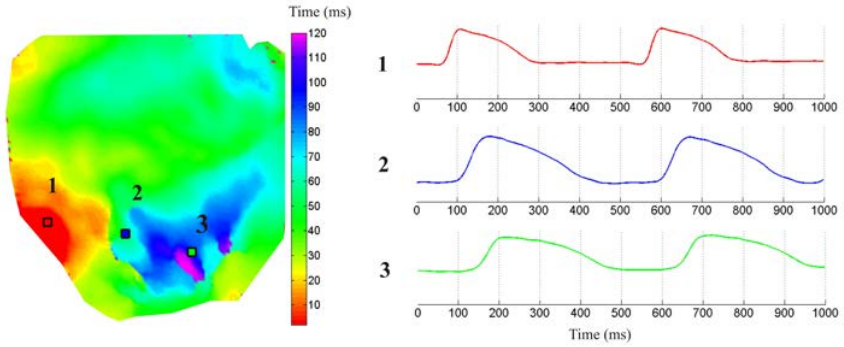


**Fig. 6.** Isochronal map (left) and individual pixel measurements (right) from an optical mapping recording during electrical pacing. Position of signals (right) are marked on the isochronal map (left).

Finally, an AF episode was induced after electrical stimulation with a period of 180 ms. Figure 7 shows the isochronal map and the action potential for 3 positions during the AF episode recorded with the optical mapping system. The isochronal map illustrates the chaotic nature of the fibrillatory episodes, where several propagation waves can be identified. This chaotic pattern can be also observed at the individual signals, where the activation times and action potential shape are difficult to identify.

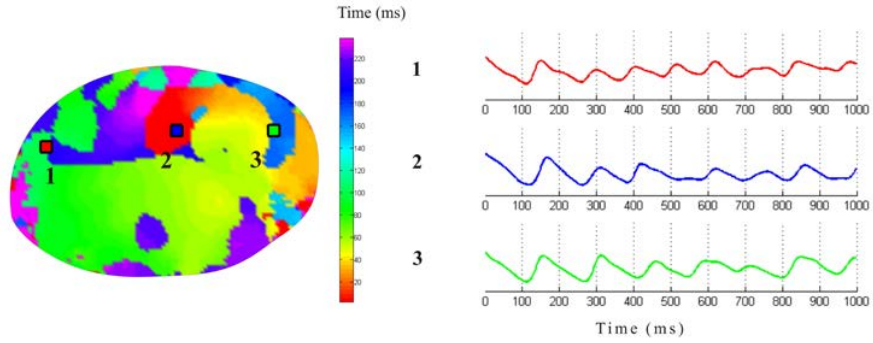


**Fig. 7.** Isochronal map (left) and individual pixel measurements (right) from an optical mapping recording during AF. Position of signals (right) are marked on the isochronal map (left).

## 4 Discussion

In this paper, an electronic control system for cardiac experimentation has been developed and tested. This system allows to control the atrial pressure through the perfusion pump flow, to electrically stimulate the cardiac muscle, synchronize the LED lights with the optical mapping camera and measure the temperature and the pH of the

Tyrode solution. The modules developed have demonstrated their proper performance during isolated heart experiments.

Some advantages have been achieved in the presented system respect to the previous prototypes and respect to commercial systems. First of all, this is the first system than includes in the same software the management of all the modules coexisting in an electrophysiology laboratory. Moreover, the wireless connection and the designed packaging for laboratory environments allowed using the modules in the same work space in which the experiment is carried out and provides more safe experiments. The automation of certain tasks such as control of pumps or LED lights allows the researcher to focus on more important tasks during the experiment and the independence of the different modules avoid stopping the experiment in case of interruption of the PC intercommunication. Finally, this is the first control equipment for Langendorff perfusion systems that allows automatic control of the aortic pressure by pump flux.

A limitation in our current model is the inability to control some of the variables under study, such as the temperature or the pH of the Tyrode solution. One improvement could be the temperature automatic control, by managing the Tyrode heater. The handling of the Tyrode pH is harder to solve as it would require the manipulation of the composition of the Tyrode. Another future line is to add another pair of peristaltic pumps to create a control technique called working heart. This technique allows independent control of the left and right cardiac circuits. In this case, the electrical stimulator is synchronized with the peristaltic pumps, provoking a higher flow rate at the time of stimulation and allowing higher similarity of working conditions of a heart in a body.

## 5 Conclusion

At the present work a modular control system for isolated and perfused porcine heart with controlled pressure has been presented. The automatic pressure control was achieved by the perfusion pump flux management. Besides, the system included the automatic measurements of physiological parameter such as temperature or pH.

System improvements respect to previous prototypes were included in the new assembly, such as the ZigBee wireless connections, and all the management system was joined in a single control software. Finally, this equipment was installed and validated in the laboratory, giving a satisfactory result.

## References


1. Miller J.T., O'rourke R.A., Crawford M.H.: Left atrial enlargement: an early sign of hypertensive heart disease. Am. Heart. J. 116 (1988) 1018-1051
2. Healey J.S., Connolly S. J.: Atrial fibrillation: Hypertension as a causative agent, Risf Factor for complications and potential therapeutic Target. Am J Cardiol. 91 (2003) 9G–14G
3. Dunn F.G., Chandraratna P., Dacarvalho J.G.R., Basta L.L., Frohlich E.D.: Pathophysiologic assessment of hypertensive heart disease with echocardiography. Am. J. Cardiol. 39 (1977) 789-795

4. Tarazi R.C., Miller A., Frohlich E.D., Dustan H.P.: Electrocardiographic changes reflecting left atrial abnormality in hypertension. Circulation. 34 (1966) 818-822
5. Frolich E.D., tarazi R.C., Dustan H.P.: Clinical-physiological correlations in the development of hypertensive heart disease. Circulation. 44 (1971) 446-455
6. Pearson A.C., Gudipati C., Nagelhout D., Sear J., Cohen J.D., Labovitz A.J.: Echocardiographic evaluation of cardiac structure and function in elderly subjects with isolated systolic hypertension. J. Am. Coll. Cardiol. 17 (1991) 422-430
7. Kannel W.B., Wolf P.A., Benjamin E.J., Levy D.: Prevalence, incidence, prognosis, and predisposing conditions for atrial fibrillation: population-based estimates. Am. J. cardiol. 82 (1998) 2N-9N
8. Langendorff O.: Untersuchungen am überlebenden Säugetierherzen Investigation of the living mammalian heart. Pflügers. 61 (1895) 291
9. Chorro Gascó F.J., Such-Belenguer L., López-Merino V.: Modelos animales de enfermedad cardiovascular, Revista Española De Cardiología. 62 (2009) 69
10. Lee P., Yan P., Ewart P., Taghavi F., Yan P., Ewart P., Ashley E.A., Loew L.M., Kohl P., Bollensdorff C., Woods CE.: In Situ Optical Mapping of Voltage and Calcium in the Heart. 7 (2012) e42562. doi:10.1371/journal.pone.0042562
11. Encheva E,m., Kostov Y., Tchernev E., Tung L.: Fluorescence imaging of electrical activity in cardiac cells using an all-solid state system. IEE trasnBiomed. 51 (2004) 333-41
12. Efimov IR., Vladimír P,. Nikolski., Salama G.: Optical Imaging of the Heart of the Heart Circ Res. 94 (2004) 21-33
13 Filgueiras-Rama D., Martins R.P., Ennis S.R., Mironov S., Jiang J., Yamazaki M., Kalifa J., Jalife J., Berenfeld O.: Optical Mapping in a Sheep Model of Stretch-Induced Atrial Fibrillation. J Vis Exp. 29 (2011) 3103. doi: 10.3791/3103
14. Ravelli F., Allessie M.: Effects of Atrial Dilatation on Refractory Period and Vulnerability to Atrial Fibrillation in the Isolated Langendorff-Perfused Rabbit Heart. Circulation. 96 (1997) 1686-1695

The ITACA-WIICT'15 is a meeting forum for scientifics, technicians and other professionals who are dedicated to Information and communication technologies study and research. Its fundamental scope is to promote the contact among scientific and professionals, improving the cooperation as well as the technological transfer among professionals.

ISBN 978-84-608-4139-5

Institute ITACA
Information and Communication Technologies